

# Northumbria Research Link

Citation: Roythorne, Ashleigh (2014) Exploring the Role of Topoisomerase II Beta in Macrophage Maturation and Pro-inflammatory Cytokine Production. Doctoral thesis, Northumbria University.

This version was downloaded from Northumbria Research Link:  
<http://nrl.northumbria.ac.uk/id/eprint/21412/>

Northumbria University has developed Northumbria Research Link (NRL) to enable users to access the University's research output. Copyright © and moral rights for items on NRL are retained by the individual author(s) and/or other copyright owners. Single copies of full items can be reproduced, displayed or performed, and given to third parties in any format or medium for personal research or study, educational, or not-for-profit purposes without prior permission or charge, provided the authors, title and full bibliographic details are given, as well as a hyperlink and/or URL to the original metadata page. The content must not be changed in any way. Full items must not be sold commercially in any format or medium without formal permission of the copyright holder. The full policy is available online: <http://nrl.northumbria.ac.uk/policies.html>

**Exploring the Role of Topoisomerase II  
Beta in Macrophage Maturation and  
Pro-inflammatory Cytokine Production**

Ashleigh Roythorne

PhD

2014

# **Exploring the Role of Topoisomerase II Beta in Macrophage Maturation and Pro-inflammatory Cytokine Production**

Ashleigh Roythorne

A thesis submitted in partial fulfilment of the requirements of the  
University of Northumbria for the degree of Doctor of Philosophy

**July 2014**

## Abstract

---

Although it is known that DNA topo II $\beta$  is required for the regulation of transcription during neural development and differentiation, it is not clear whether the enzyme is required during differentiation of human monocytes into macrophages and/or the subsequent transcription of cytokine genes. To test this, a robust model of differentiation of monocyte-like cells into macrophage-like cells using U937 and HL-60 cells treated with phorbol 12-myristate 13-acetate (PMA) and Lipopolysaccharide (LPS) was validated. Differentiation was determined by morphological and growth characteristics and CD11b surface antigen expression as determined by flow cytometry. qRT-PCR was also used to measure mRNA transcript levels of key genes known to be up-regulated during monocyte differentiation and the secretion of pro-inflammatory cytokines produced by differentiated cells were measured using ELISA.

siRNA topo II $\beta$  knockdown did not hinder monocyte-like cells from undergoing differentiation, however experiments revealed a correlation between topo II $\beta$  knockdown and secreted TNF $\alpha$ , with the latter decreasing when topo II $\beta$  was reduced. This pattern was also noted when measuring IL-1 $\beta$  secretion. Similar results were seen using a Murine transgenic fibroblast cell line lacking topo II $\beta$ , which when stimulated with LPS secreted significantly lower levels of IL-6 compared to the wild type cells. Thus topo II $\beta$  expression is necessary for secretion of normal levels of the cytokines, TNF $\alpha$ , IL-1 $\beta$  and IL-6 in response to LPS at certain time points. In addition in the macrophage-like state of the two cell lines, the relative levels of the  $\beta$  isoform (mRNA and protein) were shown to be significantly increased compared to  $\alpha$ , further outlining the importance of topo II $\beta$  in the differentiated state. Chromatin immuno-precipitation followed by qPCR showed however that topo II $\beta$  was not associated at three defined proximal promoter regions of either the TNF $\alpha$  and IL-1 $\beta$  genes, although further studies are required to rule out a direct association of topo II $\beta$  with these and other regions of the genes.

Down regulation of topo II $\beta$  protein using the inhibitor ICRF-193 did not hinder monocyte-like cells from undergoing differentiation either. However, contrary to the knockdown results, a 6 h pre-treatment with 1 nM ICRF-193 increased TNF $\alpha$  levels in these cells, both at the mRNA and the protein level, along with a slight increase in secreted TNF $\alpha$ . NF- $\kappa$ B, EGR2, TLR4 and TLR2 transcript levels were also increased under these conditions. Thus further studies are required to determine if these increases are due to additional cellular effects of the drug or whether topo II $\beta$  may play an inhibitory effect on transcription.

Thus it is clear that topo II $\beta$  plays an important role in expression of cytokines and understanding the exact nature of this requires further research that may yield potential new avenues for treatment of disease.

## Table of Contents

<b>TITLE PAGE .....</b>	<b>II</b>
<b>ABSTRACT .....</b>	<b>III</b>
<b>TABLE OF CONTENTS .....</b>	<b>IV</b>
<b>LIST OF FIGURES .....</b>	<b>IX</b>
<b>LIST OF TABLES .....</b>	<b>XV</b>
<b>LIST OF ABBREVIATIONS .....</b>	<b>XVIII</b>
<b>ACKNOWLEDGMENTS .....</b>	<b>XXI</b>
<b>AUTHOR'S DECLARATION.....</b>	<b>XXII</b>
<b>CHAPTER 1: INTRODUCTION.....</b>	<b>1</b>
1.1 TOPOISOMERASES – AN OVERVIEW .....	1
1.2 THE CATALYTIC EFFECTS OF TOPOISOMERASE ON DNA TOPOLOGY .....	2
1.3 CLASSIFICATION OF TOPOISOMERASES.....	2
1.4 STRUCTURE OF TOPOISOMERASES .....	4
1.4.1 Structure of type II topoisomerases .....	4
1.5 CATALYTIC CYCLE OF TOPOISOMERASE II .....	8
1.5.1 DNA binding.....	8
1.5.2 DNA cleavage.....	9
1.5.3 Strand Passage and DNA re-ligation .....	10
1.6 THE ROLE OF TOPOISOMERASE II.....	11
1.6.1 Replication and Transcription.....	11
1.6.2 Chromosome structure and mitotic function.....	13
1.7 MAMMALIAN TOPOISOMERASE II .....	13
1.7.1 An overview.....	13
1.7.2 Cell Cycle Distribution .....	14
1.7.3 Cellular Distribution .....	14
1.8 TOPOISOMERASE II DRUGS.....	16
1.8.1 An overview.....	16
1.8.2 Topoisomerase II poisons .....	16
1.8.3 Topoisomerase II inhibitors .....	19
1.8.4 Processing of cleavable complexes.....	20
1.8.5 Factors involved in drug sensitivity .....	23
1.9 ROLE OF TOPOISOMERASE II $\alpha$ .....	24
1.9.1 Replication, chromosome structure and mitotic function .....	24
1.9.2 Apoptosis .....	25
1.9.3 Protein-protein interactions.....	25
1.9.4 Transcription.....	26
1.10 ROLE OF TOPOISOMERASE II $\beta$ .....	26
1.11 PROTEIN ASSOCIATION AND POST-TRANSLATIONAL MODIFICATIONS OF TOPO II .....	29
1.12 THE INNATE IMMUNE SYSTEM .....	30
1.12.1 Macrophage Differentiation.....	31
1.12.2 Inflammation .....	35
1.12.3 Toll-Like Receptors .....	35
1.12.4 Activation of NF- $\kappa$ B .....	36

1.13 CYTOKINES .....	39
1.13.1 TNF $\alpha$ .....	39
1.13.2 Interleukin 1 .....	41
1.13.2.1 Interleukin-1 $\beta$ .....	41
1.13.2.2 Interleukin-1 $\alpha$ .....	43
1.13.3 Interleukin 6.....	44
1.14 CHRONIC INFLAMMATORY DISORDERS AND CANCER .....	45
1.15 AIMS .....	46
<b>CHAPTER 2: MATERIALS AND METHODS .....</b>	<b>48</b>
2.1 STERILISATION .....	48
2.2 TISSUE CULTURE CONSTITUENTS .....	48
2.3 CHEMICALS .....	48
2.4 DRUGS .....	48
2.5 BUFFERS.....	49
2.6 ANTIBODIES .....	50
2.7 qPCR CONSTITUENTS .....	50
2.8 CELL LINES.....	52
2.8.1 Characterisation of U937 cells and maintenance in culture .....	52
2.8.2 Characterisation of HL-60 cells and maintenance in culture .....	52
2.8.3 Characterisation of mouse embryonic fibroblasts (Wild Type and #5) and maintenance in culture .....	52
2.9 CELL HARVESTING .....	53
2.10 CELL COUNTING .....	53
2.11 PREPARATION OF LIQUID NITROGEN STOCKS .....	53
2.12 PERIPHERAL BLOOD MONOCYTES .....	54
2.13 CD14 SELECTION OF PBMCs .....	54
2.13.1 Background.....	54
2.13.2 Method.....	55
2.14 FLOW CYTOMETRY .....	55
2.14.1 Background.....	55
2.14.2 Quantitation of surface antigen expression using Flow cytometry.....	56
2.14.3 Cell cycle analysis using Flow cytometry.....	58
2.15 XTT ASSAY.....	58
2.15.1 Background.....	58
2.15.2 Method.....	58
2.16 QUANTIFYING PROTEIN EXPRESSION.....	59
2.16.1 Whole Cell Extraction.....	59
2.16.2 Quantification of total protein.....	59
2.16.3 Preparation of whole cell lysates for SDS-PAGE.....	60
2.16.4 SDS-PAGE .....	60
2.16.5 Wet Western Blotting .....	61
2.16.6 Coomassie staining .....	61
2.16.7 Probing.....	62
2.16.8 Densitometry.....	62
2.17 QUANTIFYING MRNA EXPRESSION.....	62
2.17.1 RNA extraction .....	62
2.17.2 Reverse Transcription .....	63
2.17.3 qPCR.....	64
2.18 ELISAs .....	66

2.18.1 ELISA to human TNF $\alpha$ .....	66
2.18.2 ELISA to human IL-1 $\beta$ .....	67
2.18.3 ELISA to mouse IL-6.....	67
2.18.4 ELISA to mouse IL-1 $\alpha$ .....	67
2.19 CHROMATIN IMMUNOPRECIPITATION .....	68
2.19.1 Crosslinking of chromatin.....	68
2.19.2 Cell Lysis and Sonication .....	68
2.19.3 Immunoprecipitation of crosslinked chromatin .....	69
2.19.4 Reverse Crosslinking .....	69
2.19.5 DNA Purification .....	69
2.19.6 qPCR .....	70
2.20 siRNA .....	71
2.21 STATISTICAL ANALYSIS .....	72
<b>CHAPTER 3: ESTABLISHING A ROBUST MODEL FOR THE QUANTITATIVE MEASUREMENT OF PMA INDUCED DIFFERENTIATION.....</b>	<b>74</b>
3.1 INTRODUCTION .....	74
3.2 AIM .....	75
3.3 MEASUREMENT OF CD11b EXPRESSION TO DETERMINE OPTIMAL CONDITIONS OF PMA EXPOSURE TO GENERATE DIFFERENTIATED U937 AND HL-60 CELLS. ....	76
3.4 EFFECTS OF PMA TREATMENT ON CELL GROWTH .....	81
3.5 CHARACTERISATION OF DIFFERENTIATION BY CHANGES IN MORPHOLOGY .....	84
3.6 SUMMARY .....	86
<b>CHAPTER 4: QUANTIFICATION OF TOPO IIA AND TOPO IIB IN PMA AND NON-PMA TREATED CELLS AND THE EFFECTS OF DIFFERENTIATION ON TOPO II DRUG SENSITIVITY INTRODUCTION .....</b>	<b>87</b>
4.1 INTRODUCTION .....	87
4.2 AIMS.....	88
4.3 QUANTIFICATION OF TOPOISOMERASE II A AND B MRNA IN NON-PMA AND PMA TREATED U937 AND HL-60 CELLS. ....	88
4.3.1 Determining the optimal reference gene to use for qPCR .....	88
4.3.2 Determining the efficiency of the qPCR reaction using topo II $\alpha$ and topo II $\beta$ . ....	91
4.3.3 Quantification of Topoisomerase II $\alpha$ and $\beta$ mRNA in non-PMA and PMA treated U937 and HL-60 cells. ....	93
4.3.4 Quantification of topo II $\alpha$ and topo II $\beta$ in Primary monocytes and M-CSF treated monocytes .....	103
4.3.5 Quantification of Topoisomerase II $\alpha$ and $\beta$ protein in U937 and HL-60 cells .....	107
4.4EFFECT OF TOPOISOMERASE II DRUGS IN CELL VAIBILITY, USING THE XTT ASSAY. ....	113
4.4.1.Effect of etoposide .....	113
4.4EFFECT OF TOPOISOMERASE II DRUGS IN CELL VAIBILITY, USING THE XTT ASSAY. ....	113
4.4.1.Effect of etoposide .....	113
4.4.2 Effect of ICRF-193 .....	121
4.4.3 Effect of ICRF-187 .....	125
4.5 SUMMARY .....	131
<b>CHAPTER 5: THE EFFECTS OF TOPOISOMERASE IIB INHIBITION ON MULTIPLE FACTORS ASSOCIATED WITH MACROPHAGE DIFFERENTIATION AND STIMULATION.....</b>	<b>132</b>
5.1 INTRODUCTION .....	132
5.2 AIMS .....	135

5.3 DETERMINING THE EFFECT OF DIFFERENT LENGTHS OF EXPOSURE TO 1 nM ICRF-193 ON TOPO II $\beta$ PROTEIN LEVEL IN U937 CELLS.....	135
5.4 EFFECT OF THE TOPOISOMERASE II INHIBITOR, ICRF-193 ON LEVELS OF MACROPHAGE CELL SURFACE ANTIGENS. ....	137
5.4.1 Effect of bacterial lipopolysaccharide on CD11b expression on PMA treated cells	138
5.4.2 Effect of ICRF-193 pre-treatment on CD11b expression .....	139
5.4.3 Effect of ICRF-193 pre-treatment on HLA-DR expression.....	142
5.4.4 Effect of ICRF-193 pre-treatment on TLR4 expression .....	145
5.5 EFFECT OF TOPOISOMERASE II INHIBITOR, ICRF-193 ON EXPRESSION OF MRNA IN A VARIETY OF TRANSCRIPTION FACTORS INVOLVED IN MACROPHAGE ACTIVATION .....	147
5.5.1 POLR2A .....	148
5.5.2 SP1 .....	149
5.5.3 Early Growth Response Protein 2 .....	152
5.5.4 NF- $\kappa$ B .....	153
5.5.5 Toll Like Receptors 2 and 4.....	154
5.5.6 TNF $\alpha$ .....	157
5.6 EFFECT OF A CO-TREATMENT OF ICRF-193, PMA AND LPS ON MRNA EXPRESSION AND PROTEIN SECRETION OF THE PRO-INFLAMMATORY CYTOKINES TNF $\alpha$ AND IL-1 $\beta$ . ....	168
5.6.1 TNF $\alpha$ .....	169
5.6.2 IL-1 $\beta$ .....	175
5.7 COMPARING CYTOKINE EXPRESSION OF WILD TYPE MOUSE EMBRYONIC FIBROBLASTS WITH TOPO II $\beta$ DEFICIENT MOUSE EMBRYONIC FIBROBLASTS (#5) .....	178
5.7.1 Comparing differences in IL-6 protein expression .....	178
5.7.2 Comparing differences in IL-1 $\alpha$ protein expression .....	182
5.8 KNOCKDOWN OF TOPOISOMERASE II $\beta$ IN U937 CELLS USING siRNA .....	183
5.8.1 Determination of appropriate oligonucleotide to use.....	183
5.8.2 Quantification of topoisomerase II $\beta$ protein post siRNA experiment .....	185
5.8.3 Effect of topoisomerase II $\beta$ knockdown on TNF $\alpha$ protein expression .....	188
5.8.4 Effect of topoisomerase II $\beta$ knockdown on IL-1 $\beta$ protein expression.....	189
5.9 SUMMARY .....	192
<b>CHAPTER 6: THE ASSOCIATION OF TOPOISOMERASE II<math>\beta</math> AT DISCRETE REGIONS OF INTEREST WITHIN THE TNF<math>\alpha</math> AND IL-1<math>\beta</math> GENES IN NON-LPS AND LPS TREATED CELLS.....</b>	<b>193</b>
6.1 INTRODUCTION .....	193
6.2 AIM .....	194
6.3 DESIGNING PRIMERS TO BE USED IN QPCR FOLLOWING CHIP .....	194
6.4 OPTOMISATION OF SONICATION STEP FOR CHIP .....	201
6.5 ANALYSIS OF CHIP-QPCR DATA .....	202
6.6 ASSOCIATION OF TOPO II $\beta$ at regions of the IL-1 $\beta$ GENE.....	205
6.7 ASSOCIATION OF TOPO II $\beta$ AT REGIONS OF THE TNF $\alpha$ gene .....	208
6.8 DISCUSSION OF RESULTS GENERATED BY CHIP-QPCR .....	209
<b>CHAPTER 7: CONCLUSIONS AND FURTHER WORK .....</b>	<b>212</b>
7.1 COMPARATIVE QUANTIFICATION OF TOPO IIA AND TOPOII $\beta$ IN NON-PMA AND PMA TREATED CELLS .....	212
7.2 THE EFFECT OF PMA TREATMENT ON THE CYTOTOXICITY OF THE TOPO II POISON, VP-16 AND AND THE INHIBITOR, ICRF-193.....	214
7.3 THE EFFECTS OF 1 nM ICRF-193 PRE-TREATMENT ON MRNA EXPRESSION OF PROTEINS INVOLVED IN DIFFERENTIATION AND STIMULATION .....	216



7.4 THE EFFECTS OF A CO-TREATMENT WITH ICRF-193, PMA AND LPS ON MRNA EXPRESSION AND PROTEIN SECRETION OF THE PRO-INFLAMMATORY CYTOKINES TNFA AND IL-1B.....	217
7.5 THE EFFECT OF TOPO II $\beta$ DIRECTED siRNA KNOCKDOWN ON THE PROTEIN SECRETION OF THE PRO-INFLAMMATORY CYTOKINES, TNFA AND IL-1B.....	219
7.6 TOPO II $\beta$ ASSOCIATION AT DISCRETE LOCATIONS PROXIMAL TO THE TNFA AND IL-1 $\beta$ PROMOTERS IN NON-LPS AND LPS STIMULATED PMA TREATED U937 CELLS .....	220
7.7 THE EFFECT OF AN ABSENCE OF TOPO II $\beta$ ON LPS INDUCED IL-6 EXPRESSION IN MOUSE EMBRYONIC FIBROBLASTS CELLS .....	221
7.8 CONCLUSION.....	223
<b>REFERENCE LIST .....</b>	<b>225</b>
<b>APPENDICES .....</b>	<b>268</b>
APPENDIX A .....	268
APPENDIX B .....	273
APPENDIX C .....	280

## List of Figures

<b>Chapter 1</b>		<b>Page</b>
Figure 1.1	Schematic Diagram of the action of DNA topoisomerases upon the topology of DNA	1
Figure 1.2	Amino acid sequence homology in Type II topoisomerases	5
Figure 1.3	Identification of amino acid and structural regions of topoisomerase II	7
Figure 1.4	Diagrammatic representation of the catalytic cycle of topoisomerase II	9
Figure 1.5	Schematic representation of topological changes induced by replication machinery	11
Figure 1.6	Interaction of Etoposide with Topo II	17
Figure 1.7	Schematic representation of the pathway of macrophage differentiation by M-CSF and PMA	33
Figure 1.8	Schematic diagram outlining the pathway of NF- $\kappa$ B activation by TLR ligation	38
<b>Chapter 2</b>		
Figure 2.1	Analysis of data obtained by flow cytometry	57
Figure 2.2	Diagrammatic representation of a sandwich enzyme linked immunosorbant assay (ELISA)	66
<b>Chapter 3</b>		
Figure 3.1	Flow cytometric analysis of CD11b expression on PMA treated U937 determining optimal PMA concentration	76
Figure 3.2	Flow cytometric analysis of CD11b expression on PMA treated HL-60 (a) and U937 (b) cells – determining optimal PMA time exposure	78
Figure 3.3	Comparison of CD11b expression on non PMA and PMA treated cells	80
Figure 3.4	Trypan Blue Proliferation Assay of HL-60 (a) and U937 (b) cells	83

Figure 3.5	Visual analysis of non-PMA and PMA treated U937 cell morphology	84
Figure 3.6	Flow cytometric analysis of non-PMA and PMA treated HL-60 cells	85
<hr/>		
<b>Chapter 4</b>		
<hr/>		
Figure 4.1	Determination of a suitable reference gene for use in qPCR when using non-PMA and PMA treated HL-60 cells, using the commercially available geNorm kit	90
Figure 4.2	Establishing the efficiency of qPCR – Calibration Curves	92
Figure 4.3	Comparing the relative levels of Topoisomerase II $\alpha$ and $\beta$ mRNA in Non-PMA vs PMA treated U937 cells	94
Figure 4.4	Comparing the relative levels of Topoisomerase II $\alpha$ and $\beta$ mRNA in Non-PMA vs PMA treated HL-60 cells	95
Figure 4.5	Cell cycle analysis of non-PMA U937 cells	98
Figure 4.6	Cell cycle analysis of PMA treated U937 cells	99
Figure 4.7	Comparing fold expression of topo II $\alpha$ and $\beta$ mRNA in non-PMA and PMA treated U937 cells	101
Figure 4.8	Comparing fold expression of topo II $\alpha$ and $\beta$ mRNA in non-PMA and PMA treated HL-60 cells	102
Figure 4.9	Comparison of relative levels of Topoisomerase II $\alpha$ mRNA in CD14 <sup>+</sup> monocytes from PBMC isolation compared to M-CSF treated cells of the same lineage	104
Figure 4.10	Comparison of relative levels of Topoisomerase II $\beta$ mRNA in CD14 <sup>+</sup> monocytes from PBMC isolation compared to M-CSF treated cells of the same lineage	105
Figure 4.11	Example of a BSA Standard Curve	107
Figure 4.12	Semi-Quantitation of topo II $\alpha$ and $\beta$ protein in non-PMA and PMA treated U937 cells	109
Figure 4.13	Semi-Quantitation of topo II $\alpha$ and $\beta$ protein in non-PMA and PMA treated HL-60 cells	110

Figure 4.14	Comparing the cytotoxic effect of VP-16 on non-PMA and PMA treated U937 cells	114
Figure 4.15	Comparing the cytotoxic effect of VP-16 on non-PMA and PMA treated HL-60 cells	115
Figure 4.16	Comparing the effects of VP-16 on PMA pre-treated cells and PMA/VP-16 co-treated cells	118
Figure 4.17	Comparing the cytotoxic effect of ICRF-193 on non-PMA and PMA treated U937 cells	122
Figure 4.18	Comparing the cytotoxic effect of ICRF-193 on non-PMA and PMA treated HL-60 cells	123
Figure 4.19	Comparing the cytotoxic effect of ICRF-187 on non-PMA and PMA treated U937 cells	126
Figure 4.20	Comparing the cytotoxic effect of ICRF-187 on non-PMA and PMA treated HL-60 cells	127
Figure 4.21	Comparison of topo II $\alpha$ and topo II $\beta$ protein levels in non-PMA treated HL-60 cells vs non-PMA treated U937 cells	130

---

## Chapter 5

---

Figure 5.1	Semi Quantification of topo II $\beta$ post treatment with 0.1% DMSO (v/v) (a) and 1 nM ICRF-193 (b) for varying lengths of exposure	136
Figure 5.2	Comparison of CD11b expression on LPS stimulated PMA treated cells and non LPS stimulated PMA treated cells	139
Figure 5.3	Determining the effects of ICRF-193 on expression of surface antigen, CD11b	141
Figure 5.4	Determining the effects of ICRF-193 on expression of surface antigen, HLA-DR	143
Figure 5.5	Determining the effects of ICRF-193 on expression of surface antigen, TLR 4	146
Figure 5.6	Determining the effects of 1 nM ICRF-193 on mRNA expression of POLR2A	148
Figure 5.7	Determining the effects of 1 nM ICRF-193 on mRNA expression	150

	of SP1	
Figure 5.8	Determining the effects of 1 nM ICRF-193 on mRNA expression of EGR2	152
Figure 5.9	Determining the effects of 1 nM ICRF-193 on mRNA expression of NF- $\kappa$ B	154
Figure 5.10	Determining the effects of 1 nM ICRF -193 on mRNA expression of TLR2 and TLR4	156
Figure 5.11	Determining the effects of 1 nM ICRF-193 on mRNA expression of TNF $\alpha$	158
Figure 5.12	An overview of some of the genes quantified following pre-treatment with 1 nM ICRF-193	159
Figure 5.13	Comparing the effects of different exposure times to 1 nM ICRF-193 prior to PMA and LPS treatment on TNF $\alpha$ protein secretion	162
Figure 5.14	Semi-quantification of TNF $\alpha$ protein expression from a whole cell lysate	165
Figure 5.15	Comparing the effects of different exposure times to 1 nM ICRF-193 prior to PMA and LPS treatment on TNF $\alpha$ protein secretion – raw data	166
Figure 5.16	Determining the effect of 1 nM and 150 nM ICRF-193, PMA, and LPS co-treatment on the expression of TNF $\alpha$ mRNA	170
Figure 5.17	Comparing the effects of different concentrations of 1 nM and 150 nM ICRF-193 when cells are co-treated with ICRF-193, PMA and LPS on TNF $\alpha$ protein secretion	171
Figure 5.18	Determining the effect 1 nM and 150 nM ICRF-193, PMA, and LPS co-treatment on the expression of IL-1 $\beta$ mRNA	175
Figure 5.19	Comparing the effects of different concentrations of ICRF-193 when cells are co-treated with ICRF-193, PMA and LPS on IL-1 $\beta$ protein expression	176
Figure 5.20	Determining the difference in levels of IL-6 protein in wild type mouse embryonic fibroblasts and a stable topo II $\beta$ MEF	180

	knockdown	
Figure 5.21	Quantification of topo II $\beta$ protein following transfection with siRNA oligonucleotides in non-PMA treated U937 cells	184
Figure 5.22	Quantification of topo II $\beta$ protein following transfection with siRNA oligonucleotides and subsequent addition of PMA and LPS in U937 cells	186
Figure 5.23	Determining the effect of topoisomerase II $\beta$ targeted siRNA transfection on expression of TNF $\alpha$ protein secretion – analysis of each independent data set	188
Figure 5.24	Determining the effect of topoisomerase II $\beta$ targeted siRNA transfection on expression of IL-1 $\beta$ protein secretion – analysis of each independent data set	189
Figure 5.25	Correlation of topo II $\beta$ expression with TNF $\alpha$ secretion (a) and IL-1 $\beta$ secretion (b)	191
<hr/> <b>Chapter 6</b> <hr/>		
Figure 6.1	Designing primers towards areas of interest within the IL-1 $\beta$ and TNF $\alpha$ genes	195
Figure 6.2	Tables containing published data on putative topoisomerase II binding sites	200
Figure 6.3	Determining the amount of sonication cycles to generate the correct size of DNA fragments	201
Figure 6.4	Calculating percentage of input using qPCR data	203
Figure 6.5	Determining if topo II $\beta$ association increases at sites proximal to the promoter region of the IL-1 $\beta$ gene when cells are PMA treated cells are stimulated with LPS	204
Figure 6.6	Determining if topo II $\beta$ association increases at sites proximal or within the promoter region of the TNF $\alpha$ gene when PMA treated cells are stimulated with LPS	207
<hr/> <b>Appendix A</b> <hr/>		
Figure A.1	Calculating the Efficiency of Primers	268

Figure A.2	Western blot probed for GAPDH as loading control- Figure 4.11a	272
Figure A.3	Western blot probed for GAPDH as loading control- Figure 4.11b	272
Figure A.4	Western blot probed for GAPDH as loading control- Figure 4.12a	272
Figure A.5	Western blot probed for GAPDH as loading control- Figure 4.12b	272
<hr/> <b>Appendix B</b> <hr/>		
Figure B.1	Western blot probed for GAPDH as loading control- Figure 5.1a	276
Figure B.2	Western blot probed for GAPDH as loading control- Figure 5.1b	276
Figure B.3	Western blot probed for Topoisomerase II $\beta$	276
Figure B.4	Western blot probed for Topoisomerase II $\beta$ – 72 h 1 nM ICRF-193 pre-treatment	277
Figure B.5	Western blot probed for GAPDH as loading control- Figure 5.14	277
Figure B.6	Western blot probed for GAPDH as loading control- Figure 5.21	277
Figure B.7	Western blot probed for GAPDH as loading control- Figure 5.22a	278
Figure B.8	Western blot probed for GAPDH as loading control- Figure 5.22b	278
Figure B.9	Western blot probed for TNF $\alpha$ (whole blot from Figure 5.14	278
Figure B.10	Western blot probed for TNF $\alpha$ - 72 h 1 nM ICRF-193 pre-treatment	279
Figure B.11	Western blot probed for GAPDH as loading control- Figure B.8	279
Figure B.12	Western blot probed for topoisomerase II $\beta$ - validating topo II $\beta$ -/- cell line	279
<hr/> <b>Appendix D</b> <hr/>		
Figure D.1	Scatter graphs for HL-60 cells (non-PMA treated) after flow cytometry using and antibody to CD11b	286
Figure D.2	Scatter graphs for HL-60 cells (PMA treated) after flow cytometry using and antibody to CD11b	287
<hr/>		

## List of Tables

<b>Chapter 1</b>		<b>Page</b>
Table 1.1	Classification of Type I topoisomerases	3
Table 1.2	Classification of Type II topoisomerases	3
<b>Chapter 2</b>		
Table 2.1	Chemical recipes for buffers used in experimental procedures	49
Table 2.2	Details of purchase and dilution of antibodies used in experimental procedures	50
Table 2.3	Details of Hydrolysis primers used for qPCR	51
Table 2.4	Consituents of 7.5% Polyacrylamide Gel	61
Table 2.5	Volume of components used to generate a master-mix for reverse transcription	64
Table 2.6	Reaction conditions for qPCR using Hydrolysis probes	65
Table 2.7	Purchase Details and Dilutions of Antibodies used in Immunoprecipitations	70
Table 2.8	Reaction conditions for qPCR of samples obtained by ChIP	71
Table 2.9	Details of siRNA oligonucleotides	72
<b>Chapter 4</b>		
Table 4.1	LD50 values for non-PMA treated U937 and HL-60 cells exposed to 72 h of treatment with the topo II poison, VP-16 and the topo II inhibitors, ICRF-193 and ICRF-187	127
<b>Chapter 6</b>		
Table 6.1	Location and sequences of DNase hypersensitivity regions within the IL-1 $\beta$ gene	197
Table 6.2	Location and sequences of DNase hypersensitivity regions within the TNF $\alpha$ gene	198



Table 6.3	Primer sequences for controls when investigating the IL-1 $\beta$ and TNF $\alpha$ genes	199
-----------	--	-----

---

### Appendix A

---

Table A.1	p values from Figure 4.3	269
Table A.2	p values from Figure 4.4	269
Table A.3	p values from Figure 4.7	269
Table A.4	p values from Figure 4.8	269
Table A.5	p values from Figure 4.9	269
Table A.6	p values from Figure 4.11	269
Table A.7	p values from Figure 4.12	269
Table A.8	p values from Figure 4.13	270
Table A.9	p values from Figure 4.14	270
Table A.10	p values from Figure 4.15a Co-treat vs non-PMA	270
Table A.11	p values from Figure 4.15a Co-treat vs PMA	270
Table A.12	p values from Figure 4.15b Co-treat vs non-PMA	270
Table A.13	p values from Figure 4.15b Co-treat vs PMA	270
Table A.14	p values from Figure 4.16	271
Table A.15	p values from Figure 4.17	271
Table A.16	p values from Figure 4.18	271
Table A.17	p values from Figure 4.19	271

---

### Appendix B

---

Table B.1	p values from Figure 5.3	273
Table B.2	p values from Figure 5.4	273
Table B.3	p values from Figure 5.5	273
Table B.4	p values from Figure 5.13	273
Table B.5	p values from Figure 5.6	274
Table B.6	p values from Figure 5.7	274

Table B.7	p values from Figure 5.8	274
Table B.8	p values from Figure 5.9	274
Table B.9	p values from Figure 5.10a	274
Table B.10	p values from Figure 5.10b	274
Table B.11	p values from Figure 5.11	274
Table B.12	p values from Figure 5.16	274
Table B.13	p values from Figure 5.17	274
Table B.14	p values from Figure 5.18	274
Table B.15	p values from Figure 5.19	274
Table B.16	p values from Figure 5.20a	275
Table B.17	p values from Figure 5.20b	275
<hr/> <b>Appendix C</b> <hr/>		
Table C.1	p values from Figure 6.5	280
Table C.2	p values from Figure 6.5	280
Table C.3	p values from Figure 6.5	280
Table C.4	p values from Figure 6.6	280
Table C.5	p values from Figure 6.6	281
Table C.6	p values from Figure 6.6	281
Table C.7	p values from Figure 6.6	281
Table C.8	p values from Figure 6.6	281

---

## List of Abbreviations

Ab	Antibody
AcH3	Acetylated Histone 3
ADAM	A Disintegrin And Metalloprotease
ADP	Adenosine 5'-diphosphate
APC	Allophycocyanin
APS	Ammonium Persulphate
ATP	Adenosine 5'-triphosphate
ATRA	All trans retinoic acid
BAF	Mammalian SWItch/Sucrose NonFermentable complex
BCA	Bicinchoninic acid
BRCT	BRCA1 C Termini domain
BSA	Bovine Serum Albumin
CAP	Catabolite Activator Protein
cDNA	Complementary DNA
ChIP	Chromatin Immuno-precipitation
Ct	Cycle threshold
CV	Coefficient of Variation
DAG	Diacylglycerol
DAMPs	Danger Associated Molecular Patterns
DMSO	Dimethylsulphoxide
DNA	Deoxyribonucleic acid
dNTPs	Deoxyribonucleotide Triphosphates
DTT	Dithiothreitol
ECL	Enhanced Chemi-Luminescence
ENCODE	Encyclopedia of DNA elements
ESC	Embryonic Stem cell
<i>E.coli</i>	<i>Escherichia Coli</i>
ELISA	Enzyme-Linked Immunosorbant Assay
FBS	Foetal Bovine Serum
FC	Flow Cytometry
FITC	Fluorescein isothiocyanate
g	Gram
GAPDH	Glyceraldehyde-3-phosphate dehydrogenase
GFP	Green Fluorescent Protein

HCl	Hydrochloric Acid
HDAC	Histone Deacetylase
HLA-DR	Major Histocompatibility complex DR
HRP	Horse-Radish Peroxidase
ICRF-187	Imperial Cancer Research Fund -187
ICRF-193	Imperial Cancer Research Fund -193
IFN $\gamma$	Interferon gamma
I $\kappa$ B	Inhibitor of kappa B
IKK	Inhibitor of kappa B kinase
IL-1 $\alpha$	Interleukin 1 alpha
IL-1 $\beta$	Interleukin 1 beta
IL-6	Interleukin 6
kDa	Kilo Dalton
L	Litre
LBP	Lipopolysaccharide binding protein
LPS	Lipopolysaccharide
M	Molar
MAC-1	Macrophage Antigen-1
mAMSA	N-(4'-(9-acridinylamino)-3-methoxy-phenyl) methane sulphonamide
M-CSF	Macrophage – Colony Stimulating Factor
MD-2	Lymphocyte antigen 96
MDC1	Mediator of DNA checkpoint activity protein
mg	Magnesium
ml	Millilitre
mM	Millimolar
mRNA	Messenger RNA
NaOH	Sodium Hydroxide
ng	nanograms
nM	nanomolar
NF- $\kappa$ B	Nuclear factor kappa B
ng	nanograms
PAMPs	Pathogen Associated Molecular Patterns
PBMC	Peripheral Blood Mononuclear Cells
PBS	Phosphate Buffered Saline
PCR	Polymerase Chain Reaction
Pen/Strep	Penicillin/Streptomycin
PKC	Protein Kinase C
PMA	Phorbol Myristate Acetate

PMS	Phenazine methosulphate
PMSF	Phenylmethanesulphonyl fluoride
PRR	Pathogen recognition receptor
qRT-PCR	Quantitative reverse transcription polymerase chain reaction
RA	retinoic acid
RNA	ribonucleic acid
ROS	reactive oxygen species
rpm	Revolutions per minute
SDS	Sodium Dodecyl Sulphate
SDS PAGE	Sodium Dodecyl Sulphate Polyacrylamide Gel Electrophoresis
siRNA	small interfering RNA
SV40	Simian Virus 40
TACE	TNF $\alpha$ Converting Enzyme
TBS	Tris Buffered Saline
TEMED	N,N, N', N'-tetramethylethylene diamine
TLR	Toll Like Receptor
TLR2	Toll Like Receptor 2
TLR4	Toll Like Receptor 4
TNF $\alpha$	Tumour Necrosis Factor alpha
Topo I	Topoisomerase I
Topo II	Topoisomerase II
Topo II $\alpha$	DNA Topoisomerase II alpha
Topo II $\beta$	DNA Topoisomerase II beta
Tris	Tris(hydroxymethyl)aminomethane
TSA	Trichostatin A
T test	Student T-test
TTBS	Tween- tris –buffered- saline
Tween-20	Polyoxyethylene (2) sorbitan monolaurate
$\mu$ g	Micrograms
$\mu$ M	Micromolar
v/v	Volume/Volume
VP-16	Etoposide
WHD	Winged Helix Domain
XTT	(sodium 3'-[1-(phenylaminocarbonyl)-3,4-tetrazolium] –bis (4-methoxy-6-nitro) benzene sulfonic acid hydrate)

## Acknowledgments

This is possibly the hardest part of my thesis to write, there have been so many people integral in this process; those who encouraged me to pursue an education in science and those who have supported and helped me over the past three and a half years. Far too many people to mention, but to all I am very grateful!

First and foremost I would like to thank my supervisor, Dr Kay Padget, a truly lovely person, with a big generous heart. I cannot express how much I appreciate the opportunity she has given me, let alone how grateful I am for all the support, advice and encouragement she has provided throughout the project. It has been an absolute pleasure to work with her and an honour to be her first PhD student.

I'd also like to thank Prof Steve Todryk, for his expertise and advice on the Immunology aspects of this project. Steve has often asked me questions that seem simple to him, but what I describe to 'blow my mind!' He has been a constant source of encouragement and often brings many a laugh to the lab!

I would like to extend my thanks to Dr Hannah Walden and Dr Robert Finn for all their advice with regards to qPCR. In addition I would like to thank Dr John Taylor and Dr Katrin Jaedicke for providing me with samples and probes for use in my work.

I would also like to express my gratitude to the members of the lab, both fellow students and technicians; Louise Brown, Rachael Dack, Kirsty Graham, Catherine Bowe, Zoe Gotts, Jen Wright, Dawn Bruce, Vivien Brindley, Deborah Pettit, Sam Jameson and Robyn Wilkinson for their friendship, support, advice and encouragement – I'm a high maintenance kind of girl and you all deserve medals for being friends with me!

On a more personal note, I would like to thank my Mam, Dad and Grandparents for their love and support with everything I have undertaken, especially my Granda, who has always had faith in me and who I strive to make eternally proud. Finally I'd like to thank my boyfriend, Chris, for his patience, support and love over the past three years. I love you all very much.

I would also like to acknowledge Northumbria University for funding this project.

### **Author's Declaration**

I declare that the work contained in this thesis has not been submitted in the past, or is to be submitted at any other University for any other award and that it is all my own work. I also confirm that this work fully acknowledges opinions, ideas and contributions from the work of others. When necessary, permission was requested for the reuse of figures in the printed and electronic copies of this thesis that are subject to copyright. This project has had full ethical approval (RE27-09-1164).

The word count of this thesis is 46,187 words.

Name:

Signature:

Date:

# Chapter 1

## Introduction

---

### 1.1 Topoisomerases – an overview

DNA topoisomerases are ubiquitous enzymes found in all nucleated cells (Kunze *et al.*, 1991). The double helical structure of DNA, where two strands are wound round one another gives rise to many problems in events such as replication, recombination and transcription where the strands require separation. In events such as this DNA can become tangled, intertwined or over-wound. DNA topoisomerases are a family of enzymes that are capable of unknotting and decatenating DNA and relaxing supercoils in order to maintain DNA in an under-wound and untangled state (Figure 1.1) (McClenndon *et al.*, 2005; Deweese *et al.*, 2008; Nitiss, 2009; Liu *et al.*, 2009).

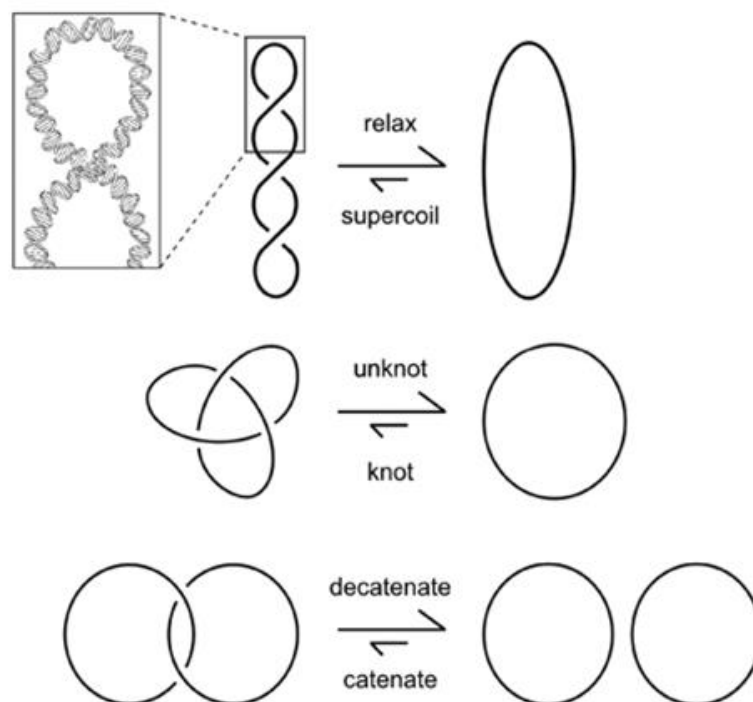


**Figure 1.1 Schematic Diagram of the action of DNA topoisomerases upon the topology of DNA (Liu *et al.*, 2009)**

Each single line is representative of one double strand of DNA. Topoisomerases act to relax supercoiled DNA, unknot knotted DNA and decatenate catenated DNA. Bacterial gyrase and archaeal reverse gyrase, however, have been shown to introduce negative supercoils into DNA.



Topoisomerases use two strategies to untangle DNA. They either create a strand break in the DNA catalysing the passage of another strand of DNA through the break before re-sealing, or they can perform a controlled rotation of one DNA strand around another. However the mechanism that they employ is dependent on the type of topoisomerase, this will be discussed further in Section 1.3.

## **1.2 The catalytic effects of topoisomerase on DNA topology**

Topoisomerases can alter DNA topology by changing the linking number of DNA (Lk). Linking number is determined by the twist and writhe of the DNA. Twist is the number of times one DNA strand wraps around the other whereas writhe is a measure of how many times the axis of the double helix crosses over itself to form a supercoil. The sum of twist and writhe represents the number of times one strand wraps around the other and is called the linking number (Lk). A positive linking number indicates that the DNA is positively supercoiled (left-handed supercoils) and over-winding of the DNA, whereas a negative linking number corresponds with negative supercoiling (right-handed supercoils) and under-winding of the DNA.

The catalytic activity of topoisomerases can relieve torsional stress caused by either over-winding or under-winding of DNA. It achieves this by changing the linking number of the DNA. Type I topoisomerases alter the linking number by 1, i.e., remove one supercoil in one catalytic cycle (Kunze *et al.*, 1991), and type II topoisomerases change the linking number by 2, i.e., remove two supercoils in one catalytic cycle (Garcia-Rubio *et al.*, 2012). Presently DNA gyrase is the only enzyme capable of introducing negative supercoiling into DNA (Papillon *et al.*, 2013).

## **1.3 Classification of Topoisomerases**

DNA topoisomerases are classified by differences in their structure and biochemical activities.

Type I topoisomerases act by creating a single strand break in duplex DNA, and either pass another intact single strand of DNA through the break or catalyse the controlled rotation of the strand breakage around the intact strand (Kunze *et al.*, 1991; Stewart *et*

*al.*, 1998). Type I topoisomerases are further sub-classified into type IA and type IB topoisomerases (Table 1.1). Type IA topoisomerases form a 5'-phosphotyrosyl linkage with one target DNA strand (Changela *et al.*, 2001), in comparison, type IB topoisomerases create a 3' phosphotyrosyl linkage to one target DNA strand (Stivers *et al.*, 1997).

**Table 1.1 Classification of Type I topoisomerases**

Class A	Class B
Eubacterial Topo I & III	Eubacterial Topo V
Yeast Topo III	Vaccinia Topo
Eubacterial & Archaeal Reverse DNA Gyrase	Human Topo I (I & Imitochondrial)
Eubacterial Reverse Gyrase	
Human Topo III ( $\alpha$ & $\beta$ )	

Type II topoisomerases act by creating a transient double strand break in a DNA duplex, they then catalyse the passage of another intact double strand of DNA through the break before resealing it (Liu *et al.*, 1980; Roca & Wang, 1992; Roca *et al.*, 1996). Type II topoisomerases are further sub-classified into type IIA and type IIB topoisomerases (Table 1.2). Type IIA topoisomerases all share sequence homology at the amino acid level. Type IIB topoisomerases share very little amino acid sequence homology with type IIA topoisomerases, thus leading to a separate classification (Champoux, 2001).

**Table 1.2 Classification of Type II topoisomerases**

Class A	Class B
Prokaryotic DNA Gyrase	Archaeal DNA Topo VI
Prokaryotic Topo IV	
Yeast DNA Topo II	
Eukaryotic Topo II ( $\alpha$ & $\beta$ )	

## 1.4 Structure of topoisomerases

Type I topoisomerases act as monomeric enzymes (Das *et al.*, 2002), with the exception being that of the eubacterial reverse gyrase found in *Methanopyrus kandleri*, which is heterodimeric, consisting of a 42 kDa subunit that interacts with DNA, and a 138 kDa ATP binding subunit (Krah *et al.*, 1996).

Type II topoisomerases all act as either dimeric or tetrameric enzymes (Nitiss, 2009). Eukaryotic and yeast topoisomerase II enzymes act as homodimers ( $A_2$ ). The prokaryotic DNA gyrase and archaeal DNA topoisomerase VI act as  $A_2B_2$  tetramers. In contrast the prokaryotic DNA topoisomerase VI acts as a  $C_2E_2$  heterodimer (Champoux, 2001; Das *et al.*, 2002; Corbett & Berger, 2004; Wall *et al.*, 2004).

### 1.4.1 Structure of type II topoisomerases

Type II topoisomerases are comprised of three distinct regions as determined by limited digestion with *Staphylococcus aureus* V8 (SV8) protease (Lindsley & Wang, 1991). The three distinct regions included the N terminal domain, the central domain and the C terminal domain.

The tertiary structure of yeast topoisomerase II was first reported by Berger *et al.* (1996). Berger *et al.* (1996) generated a crystal structure of the 92 kDa monomer of yeast topoisomerase II. They described the monomer as a flattened crescent structure that folds into 2 subunits, B' and A'. The subunits were shown to possess a high amino acid sequence homology with *E.coli* DNA gyrase. The B' subunit corresponded with amino acid residues 420-633 of the gyrB domain of DNA gyrase, whilst the A' subunit corresponded with amino acid residues 682-1178 of the gyrA domain of DNA gyrase (Figure 1.2). However the structure lacked an ATPase domain (residues 1-409) and a C terminal region (residues 1203-1429). Interestingly the monomer was still capable of cleaving DNA, however it was unable to facilitate transport of the duplex through the cleavage site. Once dimerised the crescent shaped monomers created a heart like structure that contained a large central hole, 55Å at the base, 25Å at the top and 60Å in height, a size capable of fitting a DNA duplex, thus suggesting this was the site of DNA cleavage (Berger *et al.*, 1996).

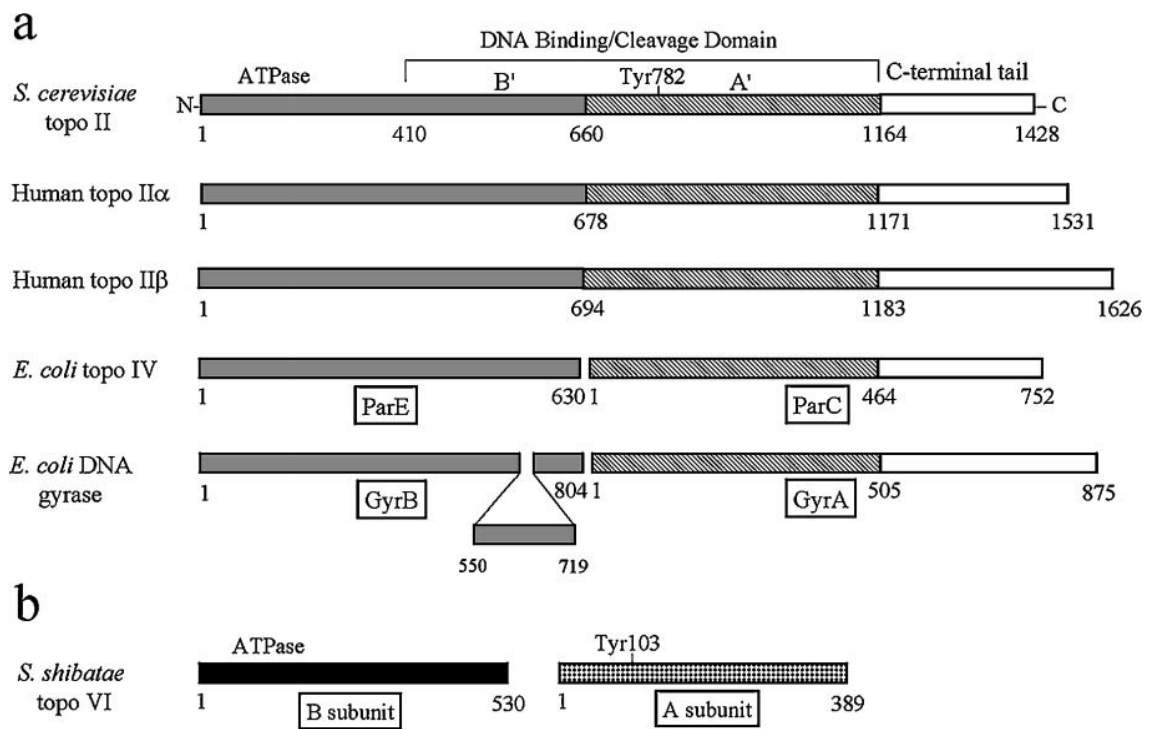


**Figure 1.2 Amino acid sequence homology in Type II topoisomerases.** Type IIA topoisomerase sequence homology is compared to that of *E.coli* DNA gyrase. GyrB of DNA gyrase, ParE of *E.coli* topo IV and B' (N-terminal) of eukaryotic topo II are shown in grey; this region is highly conserved in type IIA topoisomerases and contains the ATPase domain of the protein. GyrA, ParC and A' (C-terminal) are shown in a diagonal striped pattern. This region is moderately conserved between similar species. It is this domain that contains the active site tyrosine and DNA binding domain. The C-terminal tail of all type IIA topoisomerases is shown in white. This domain does not share a high amino acid sequence identity between type IIA topoisomerases (a). Type IIB topoisomerases, of which there is only one to date, *Sulfolobus shibatae* topo VI contains only two domains, with very little amino acid sequence identity to type IIA topoisomerases. The B subunit (in black) contains the ATPase domain and the A subunit (striped) contains the active site tyrosine (b) (Champoux, 2001).

Further work using *E.coli*, yeast and mammalian type II topoisomerases identified other regions of the topo II structure, including particular amino acid residues (Figure 1.3) involved in the catalytic cycle and the homology between species.

The N-terminal domain is the most highly conserved region of the type IIA topoisomerases. It contains the transducer domain that contains the ATPase region, capable of binding ATP or the analogue AMP-PMP (Champoux, 2001; Nitiss, 2009). The TOPRIM (topoisomerase primase) domain, a common domain found in DnaG-type primases, small-primase like proteins from bacteria and archaea, and type IA and type II topoisomerases (Aravind *et al.*, 1998), is involved in divalent cation binding, and is also found in the N-terminal region of type II topoisomerases (Nitiss, 2009). It adopts an  $\alpha/\beta$  fold and is positioned so that it physically interacts with cleaved DNA (Figure 1.3) (Aravind *et al.*, 1998).

The core domain, containing the DNA binding and cleavage site is highly conserved between closely related species. It is this domain that contains the active site tyrosine found in the catabolite activator protein (CAP) like fold, or winged helix domain (WHD) close to the N termini (Champoux, 2001, Nitiss, 2009). Berger *et al.*, (1996) describe a semi-circular groove in this core where the DNA duplex docks.

The C-terminal domain of the enzyme is the least conserved, displaying only 30% amino acid sequence identity (Austin & Marsh, 1998). Differences in the sequence are believed to participate in differential protein association, drug action and regulation of enzymatic activity (Schoeffler & Berger, 2008; Gilroy & Austin, 2011).

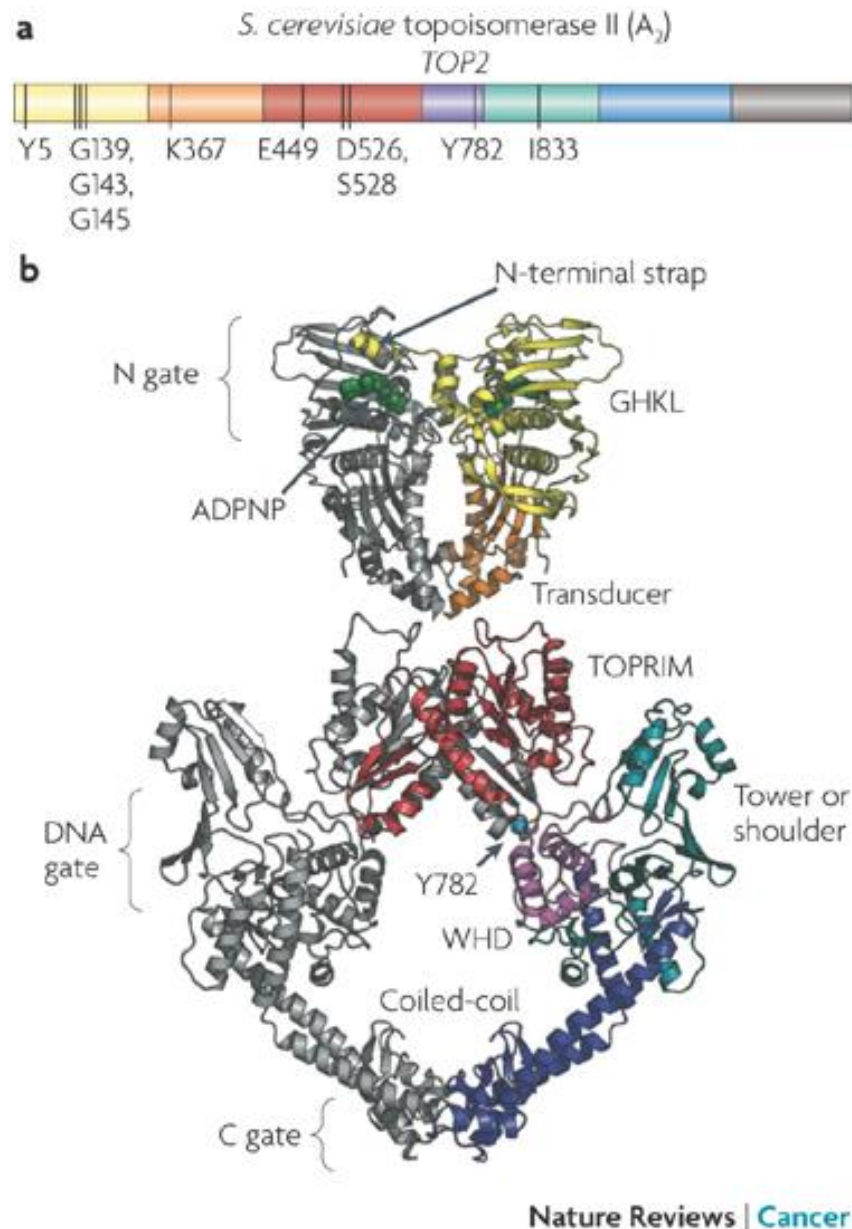


**Figure 1.3 Identification of amino acid and structural regions of topoisomerase II.**

Structural domains of *Saccharomyces cerevisiae* bound to ADPNP (5'-adenylyl- $\beta$ ,  $\gamma$  - imidodiphosphate) (a) Particular amino acid residues of importance are; G139, G143, and G145 of the ATP binding domain (yellow) K367 in the transducer, ATPase domain (orange), the acidic triad, E449, D526 and D528 of the TOPRIM domain (red), Y782 involved in the covalent attachment with DNA (purple), I833 of the tower domain involved in DNA interaction (green). The structure of the ATPase and breakage reunion domain of yeast topo II (b) The GHKL (gyrase, HSP90, histidine kinase, MutL) and the transducer domain are shown in yellow and orange respectively. The TOPRIM domain is shown in red. The WHD (or CAP like domain) is shown in purple, and the tower and coiled coil are shown in green and blue (Champoux, 2009).

## **1.5 Catalytic cycle of topoisomerase II**

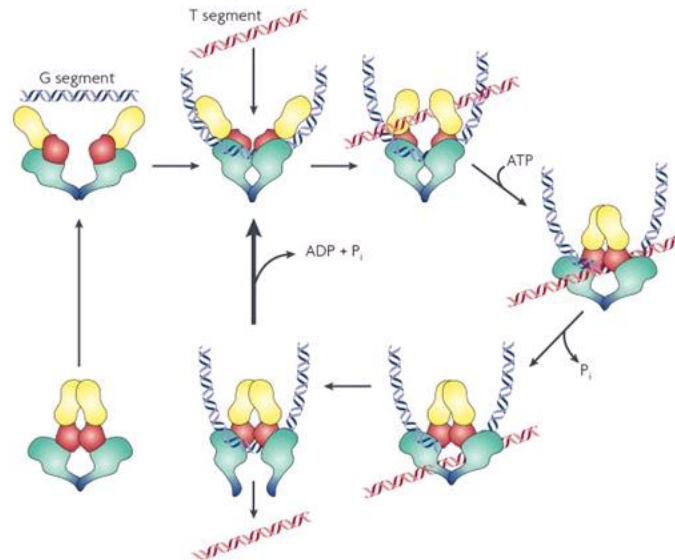
### **1.5.1 DNA binding**

Recognition of specific sites of the genome by topoisomerase has been a vast area of interest.

Topo II binds preferably to supercoiled DNA over linear, relaxed DNA (Crisona *et al.*, 2000). Investigations into site-specific binding have focused on primary and secondary DNA structure. Using specific topoisomerase II poisons and inhibitors (see section 1.8) short conserved nucleotide sequences have been established that reside at either side of the cleavage site, however these sequences appear to be species specific and dependent on the poison or inhibitor used. Investigations into secondary structure recognition revealed that topoisomerase II binds to and stabilizes DNA crossovers, associates with helix-helix juxtapositions and cleaves at inverse repeat sequences within DNA hairpins (Zechiedrich & Osheroff, 1990; Froeslich-Ammon, 1994; Roca *et al.*, 1993; West *et al.*, 1999).

Topo II initially begins its catalytic process by binding one DNA duplex (termed the G segment), this causes a conformational change in the enzyme structure, allowing the G segment to interact with the enzyme's cleavage domain. Upon binding of ATP (Figure 1.4), dimerisation of the N terminal domains of each monomer occurs. This then captures the second DNA duplex (termed the T segment) creating a closed clamp structure (Corbett & Berger, 2004).

A.



B.

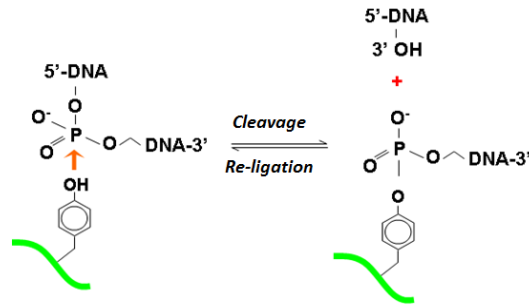


**Figure 1.4 Diagrammatic representation of the catalytic cycle of topoisomerase II.**

- A. The Topoisomerase II enzyme is shown in colour. The yellow, red and green structures represent the N terminal domain, core domain and C terminal domain, respectively (Nitiss, 2009). First the Topoisomerase II binds to a DNA duplex, referred to as the G-segment. The enzyme introduces a double strand break in this DNA in the presence of  $Mg^{2+}$ , forming a phosphotyrosine linkage between each single DNA strand and a tyrosine in each subunit (see part B). ATP binding causes the N-terminal domains to close which captures a second double DNA strand (T-segment) and also opens the cleaved DNA forming the 'gate'. One ATP is hydrolysed which facilitates the enzyme to pass the T segment through the gate in the first double stranded DNA. The G segment is then re-sealed. After passing through the break in the G segment, the T segment exits the enzyme through the bottom of the enzyme. The second ATP hydrolysis step (along with release of ADP and  $P_i$ ) allows the clamp to re-open, and allows release of the G segment. Alternately, the enzyme may initiate another catalytic cycle without dissociating from the G segment.
- B. The green line represents the topo II monomer. The hydroxyl group of the conserved tyrosine at the active site in the topo II monomer is responsible for the nucleophilic attack on the phosphodiester backbone of the DNA. This then creates a covalent phosphotyrosyl bond with the 5' of the DNA, leaving a hydroxyl moiety on the 3' end, and a site of DNA cleavage. Diagram adapted from Cowell & Austin. (2012).



### 1.5.2 DNA cleavage

Each monomer of topo II then initiates a transesterification reaction by nucleophilic attack by a conserved tyrosine on the phosphodiester backbone of separate strands of the DNA duplex of the G segment, thus resulting in two covalent phosphotyrosyl bonds between the protein and DNA. A bond is formed between the CAP (catabolite activator protein) domain of each of the monomers and the 5' end of the DNA, leaving a hydroxyl moiety on the remaining 3' end (Corbett & Berger, 2004). This results in a 4bp staggered cleavage site within the G segment (Shapiro *et al.*, 1999). The reaction requires the binding of the divalent cation,  $Mg^{2+}$  at the TOPRIM domain for successful cleavage to occur (Corbett & Berger, 2004). Although it is  $Mg^{2+}$  that is required *in vivo*, *in vitro* studies have revealed that  $Mn^{2+}$ ,  $Ca^{2+}$  and  $Co^{2+}$  actually increase levels of double strand cleavage (Deweese *et al.*, 2008).

### 1.5.3 Strand Passage and DNA re-ligation

Hydrolysis of bound ATP causes a conformational change in the enzyme and the T segment is then driven through the cleaved strand (Roca & Wang, 1992), however an electrostatic potential gradient has also been identified within the topo II structure that may also facilitate movement (Berger *et al.*, 1996). Once the T segment has passed through the cleaved strand it leaves through the carboxy termini of the enzyme (see Figure 1.4) (Roca *et al.*, 1996). The G segment is then re-ligated by a reverse transesterification reaction. The phosphorous of the phosphotyrosyl bond is attacked by the oxygen of the hydroxyl bond formed in the first transesterification reaction, thus breaking the bond and allowing the resealing of the DNA strands (Burden & Osheroff, 1998; Deweese *et al.*, 2008). Due to the nature of the covalent bonds created between the enzyme and the DNA strands, no recombination or rearrangement of the DNA occurs, leaving the integrity of nucleotide sequence intact. A second ATP hydrolysis step facilitates the reopening of the N terminal domain and release of the G segment, allowing the efficient turnover of the topo II enzyme.

A study by Ding *et al.* (2013) has postulated that the entire catalytic cycle of topo II lasts 0.84 s. A diagrammatic representation of the full catalytic cycle of topo II is shown in Figure 1.4.

## 1.6 The Role of Topoisomerase II

### 1.6.1 Replication and Transcription

Genomic DNA is globally under-wound, thus enabling greater access to the DNA templates by replicative machinery (Gentry *et al.*, 2011). Semi-conservative replication involves the separation of the DNA duplex in order for new strands to be synthesised (Figure 1.5A). This separation creates torsional stress in the form of positive supercoiling ahead of the replication fork (Figure 1.5B). As the replication machinery rotates around and travels along the template strand building up positive supercoils ahead, compensatory negative supercoils are formed behind the machinery in the newly replicated daughter molecules in an effort to nullify the positive supercoils (Figure 1.5C). These are referred to as precatenanes (Lucas *et al.*, 2001; McClendon *et al.*, 2005).

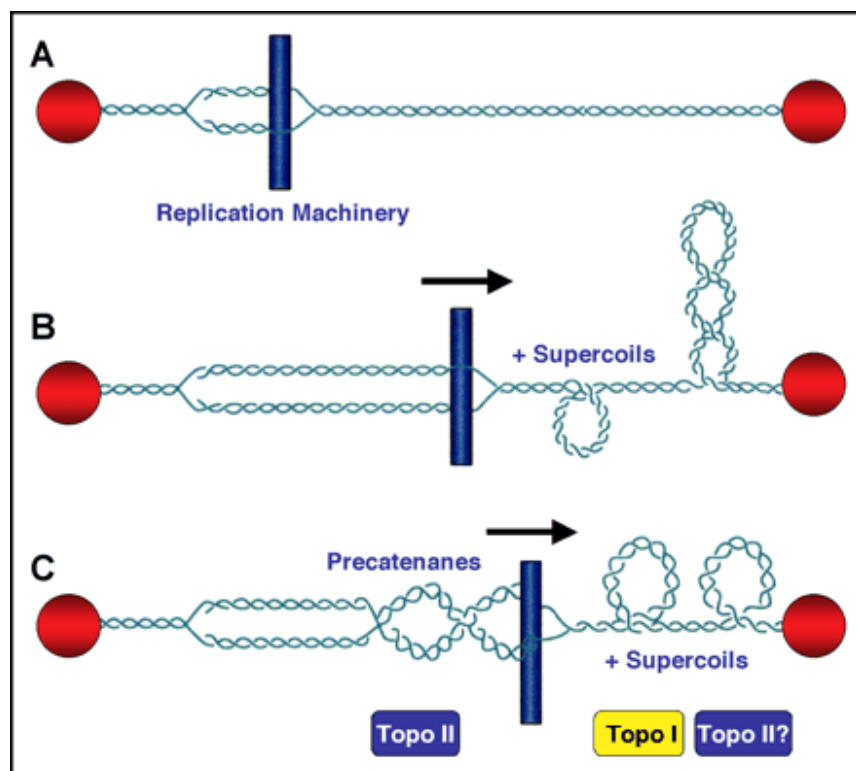


**Figure 1.5 Schematic representation of topological changes induced by replication machinery.**

(A) Replication machinery requires the separation of DNA strands in order to undergo semi-conservative replication of the DNA. (B) Replication results in positive supercoils ahead of the replication fork. (C) precatenanes are formed from newly synthesised DNA behind the replication fork. Topo II acts to resolve the catenanes. Topo I and Topo II are both capable of relaxing positive supercoils (McClendon *et al.*, 2005).

Resolution of such detrimental topology attributed distinct roles to type I and type II topoisomerases. Topo I, due to its ability to relieve torsional stress caused by positive supercoiling was believed to work ahead of the replication fork. Resolution of precatenanes was attributed to the catalytic activity of topoisomerase II. However there is now evidence to suggest that indeed topo II works ahead of the replication fork in addition to behind it (McClendon *et al.*, 2005). This is supported by evidence suggesting that topo II $\alpha$ , a specific mammalian isoform of topo II favours positive supercoiling.

One of the first studies to suggest that topo I and II were required for DNA replication was that of Nelson *et al.* (1986) who, using the topoisomerase II targeting drug teniposide, and 3H-thymidine pulse-labelled topo II, showed that newly replicated DNA in rat prostatic adenocarcinoma cells interacted with topo II near the replication fork. Furthermore, Yan *et al.* (1987) showed that inhibition of topo I and II resulted in a decrease in DNA synthesis by 15-20 fold. A further study has also shown that mutation of the gene encoding Topo I slows the growth rate of yeast but is not lethal, suggesting that topo II can compensate for the activities of topo I (Levin *et al.*, 1993).

Interestingly depletion and catalytic inactivation of topo II has been shown to result in DNA damage at different time points during the cell cycle, however both depletion and inhibition are lethal to the cell. A study using budding yeast cells showed depletion of topo II by mutation of the gene with a restrictive promoter prevented decatenation during S phase, however cells still proceeded at the same rate through mitosis. DNA damage was induced when the cell underwent cytokinesis during the latter stages of mitosis. In contrast catalytic inhibition of topo II by mutating the active tyrosine residue, results in DNA damage in late S phase of the cell cycle and G2/M arrest of the cell (Baxter & Diffley, 2008).

Supercoiling can also occur due to the actions of transcription (Liu & Wang, 1987). It has been established that a hindrance to the rotational movement of transcriptional machinery around its template, or movement of DNA around its axis can lead to formation of positive and negative supercoils at the same rate ahead and behind of the transcriptome, respectively (Fernandez *et al.*, 2014). Indeed research has shown that an increase in Z DNA is found near the promoter of actively transcribed genes and this is quickly resolved by the actions of topoisomerases (Rich & Zhang, 2003).

## **1.6.2 Chromosome structure and mitotic function**

Topoisomerase II also facilitates chromosome condensation and segregation. Yan *et al.* (1987) reported that simian virus 40 purified DNA required the isolated nuclei of HeLa cells in order for successful segregation of newly synthesised daughter chromatids to occur. Further to this, studies in yeast using temperature sensitive topo II mutations revealed a lack of chromosome separation even when spindles had formed; additionally condensed chromosomes were shown to fragment during separation when topo II was unavailable. Further to this, the study also showed that cell viability was lost when cells underwent mitosis in the absence of topoisomerase II (Uemura *et al.*, 1987).

The role of topoisomerase II in chromosome condensation remains controversial however, as there is high variability between studies when using different inhibitors, mutants, antibodies or RNAi. Some studies suggest that topo II is necessary for successful chromosome condensation, however others saw little difference when topo II was inhibited. For example using chicken erythrocyte nuclei, Adachi *et al.* (1991) showed that low levels of topo II contained in the nuclei correlated with an inability to condense chromosomes; upon addition of purified topo II, chromosome condensation occurred normally. In contrast, Lavoie *et al.* (2002) showed that topo II was not required for rDNA condensation establishment and maintenance in budding yeast.

## **1.7 Mammalian topoisomerase II**

### **1.7.1 An overview**

Mammalian topoisomerase II, a 170 kDa protein was first discovered by Miller *et al.* (1981). A larger 180 kDa protein, possessing a similar structure but slightly different antigenicity was later discovered (Drake *et al.*, 1987). Thus mammals were seen to possess two distinct topoisomerase II isoforms, later termed  $\alpha$  and  $\beta$ . The genes for the isoforms have been mapped to q12-21 on chromosome 17 and p24 on chromosome 3, respectively (Tan *et al.*, 1992). In humans the isoforms are structurally similar, possessing 68% amino acid sequence identity, with 77% of that being in the conserved N terminal domain (Austin *et al.*, 1993). They also appear to be biochemically similar, sharing the same catalytic cycle.

### 1.7.2 Cell Cycle Distribution

Levels of topo II protein are highest in exponentially growing cells (Hsiang, 1988) and decrease during differentiation (Zwelling *et al.*, 1990). This is reflected in levels of topo II during the cell cycle, however protein expression of the isoforms during the cell cycle differs greatly. Serum starved NIH 3T3 and BALB/c 3T3 cells appear to have undetectable levels of topo II $\alpha$  protein until late S phase; levels of topo II $\alpha$  then peak in G2/M phase before slowly declining into negligible amounts in G0 (Woessner *et al.*, 1991; Chow & Ross, 1987). This pattern of topo II $\alpha$  was reflected in mRNA levels in a later study in HeLa cells, and attributed to changes in mRNA stability; mRNA in G1 had a half-life of 30 mins, in contrast mRNA in late S phase had a half-life of over 4 h (Goswami *et al.*, 1996). Interestingly levels of topo II $\beta$  during the cell cycle are described in many publications as remaining constant throughout the cell cycle (Kobayashi *et al.*, 1998; de Campos-Nebel *et al.*, 2010), despite multiple reports on the contrary (Woessner *et al.*, 1991; Turley *et al.*, 1997; Padget *et al.*, 2000). For example work by Woessner *et al.* (1991) and Padget *et al.* (2000) using NIH-3T3 and Raji cells respectively report a decline in topo II $\beta$  protein expression as cells become confluent or enter G0, although in contrast to topo II $\alpha$ , topo II $\beta$  protein remains detectable at this time. Furthermore, Aoyama *et al.* (1998) showed that levels of topo II $\beta$  increase during retinoic acid induced differentiation of HL60 cells from a promyelocytic cell type to a granulocytic cell morphology. Additionally McNamara *et al.* (2010) report that when NB4-MR2 cells are treated with phorbol-12-myrsitate-13-acetate (PMA) for two hours they display an increase in topo II $\beta$  expression, this is in contrast to Zwelling *et al.* (1990) who showed HL-60 cells induced to differentiate into macrophage like cells by 24 h of treatment with PMA displayed a decrease in topo II protein expression, but they did not report on isoform specificity. However there is too much variation in experimental procedure to compare the results effectively.

### 1.7.3 Cellular Distribution

The opinion of where both topo II isoforms differentially localise within the cell differs from one publication to another. Petrov *et al.* (1993) reported that topo II $\alpha$  was seen exclusively in the nucleolus, whilst topo II $\beta$  appeared in the nucleolus, the nucleoplasm and at the periphery of heterchromatin. Zini *et al.* (1994) supported this report partially

by showing that they also found topo II $\alpha$  in the nucleolus, but also in the nucleoplasm, however they only saw topo II $\beta$  at a nucleolar level, with a notable absence in the heterochromatin and euchromatin. Chaly & Brown (1996) reported that distribution of topo II $\alpha$  was similar during interphase and mitosis, however the distribution of topo II $\beta$  appeared variable during interphase, they also suggested that small amounts of topo II $\beta$  associated with internucleolar chromatin. Later work by Cowell *et al.* (1998) showed using isoform specific anti sera and an epitope tagging approach that topo II $\beta$  localised to the nucleus but not the nucleolar compartment. Further to this, later studies showed that topo II $\alpha$  was actually concentrated in the heterochromatin in mid to late S phase, supporting its requirement for chromosome segregation. Topo II $\beta$  was shown to be associated with the periphery of heterochromatic regions in fixed and living cells. Interestingly treatment of cells with a histone deacetylase inhibitor revealed that topo II $\beta$  re-localised from heterochromatin to euchromatin (Cowell *et al.*, 2011). Adachi *et al.* (1997) revealed that localisation of topo II $\alpha$  in the mitotic nucleus was lost in interphase whilst conversely topo II $\beta$  was upregulated during interphase and that the C terminal domain of the enzymes was required for this nuclear localisation. Interestingly Kellner *et al.* (1997), report that topo II $\alpha$  is localised in the nucleus during interphase. The discrepancies between reports may be attributed to differences in sample preparations, for example earlier studies (Petrov *et al.*, 1993; Zini *et al.*, 1994) did not appear to account for potential differences in cell cycle distribution. It may also be due to differences between species or particular cell lines, for example Adachi *et al.* (1997) used mouse topo II $\alpha$  protein expressed in yeast, whilst Kellner *et al.* (1997) used the human cell line HL-60 to investigate localisation. Additionally, although in all studies immunofluorescence microscopy was used, the antibodies used may have had different efficiencies and specificities, indeed Kellner *et al.* (1997) was the only study to generate and investigate the specificity of multiple monoclonal antibodies. Taken together, the differences in experimental procedure may account for the variation in topo II cellular distribution recorded in the literature.

## **1.8 Topoisomerase II targeting drugs**

### **1.8.1 An overview**

The nature of eukaryotic topoisomerase II and its catalytic actions in essential cell functions leaves it an attractive target for antineoplastic compounds. Many topoisomerase II drugs are readily available in the clinic treating a multitude of cancers including non-Hodgkin's lymphoma, leukaemia and Kaposi's sarcoma to name but a few. Etoposide (VP-16) is now the anti-cancer drug of choice for a number of human cancers including; testicular cancer, small-cell lung cancer and lymphoma (Bender, *et al*, 2008; Soubeyrand, *et al*, 2010; Tanaka, *et al*, 2007). Topoisomerase II drugs are split into two distinct categories; poisons and inhibitors. Classification is based on the mode of action of the drug and its interaction with topoisomerase II.

### **1.8.2 Topoisomerase II poisons**

Topo II poisons act by stabilising the topo II cleavable complex, inhibiting the re-ligation of the double strand break created by the enzyme (Germe & Hyrien, 2005). Recognition of the double strand break by the cell is required in order for apoptosis to occur; this will be discussed later in the chapter. Topo II poisons may be additionally subdivided into non-DNA intercalators and DNA intercalators.

In 1965, aldehyde condensation of the non-purified root of the Indian plant, *Podophyllum* yielded products displaying anti-tumour properties. These products were further isolated to obtain the agent, demethylepipodophyllotoxin (DEPBG). DEPBG when applied to cells resulted in an inhibition of mitosis (Hande, 1998). Etoposide (VP-16) and teniposide (VM-26), analogues of DEPBG were then synthesised and the Food and Drug Administration (FDA) approved them for clinical use in 1983 and 1993, respectively.

Addition of etoposide to cell cultures induced single and double strand breaks. However, addition of etoposide to purified DNA yielded no single or double strand breaks. Interestingly addition of the drug to isolated cell nuclei saw the single and double strand breaks seen in whole cells return (Loike & Horwitz, 1976; Wozniak & Ross, 1983). This then led to the discovery that etoposide induced DNA damage was mediated by the nuclear enzyme, topo II.

Etoposide and teniposide belong to the non-intercalating group of topo II drugs, the epipodophyllotoxins. Epipodophyllotoxins stabilise the topo II cleavage complex by binding to cleaved strands of DNA, preventing re-ligation. It has been shown the two molecules of etoposide are required for successful stabilisation; one at each scissile bond. Bromberg, (2003) propose a two-drug model of etoposide action. They revealed two molecules of etoposide were required for the stabilisation of a strand specific nick rather than a double strand break at each scissile bond. The work also suggested that in the presence of etoposide, there was no communication between the topoisomerase II protomers.

Etoposide and teniposide have both been shown to preferentially target one topoisomerase II isoform over another, indeed etoposide and teniposide have both been shown to preferentially target topo II $\alpha$  (Fernandes *et al.*, 1995). However neither drug targets this isoform exclusively (Willmore *et al.*, 1998). The specific residues of topo II that etoposide has been shown to target are shown in Figure 1.6

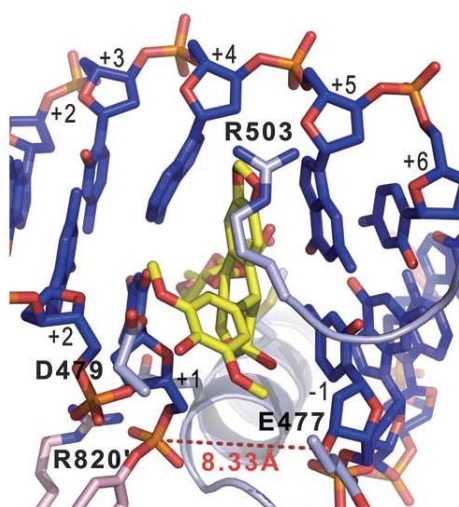


**Figure 1.6 Interaction of Etoposide with Topo II**

DNA is shown in blue, etposide is shown in yellow, two topo II $\beta$  monomers are shown in this diagram, they are coloured pink and light purple. Key residues involved in drug interaction are labelled. The one that belongs to the second, pink monomer is flagged with a prime (Wu *et al.*, 2011).



Elucidating the binding properties of etoposide with topo II has led to the development of analogues of the drug with both increased effectiveness and fewer side effects. Furthermore, it has also aided in elucidating reasons for certain cell line resistance to etoposide. For example mutations in key residues of the enzyme lead to a decrease in binding activity of the drug, thus decreasing its ability to form cleavage complexes, and in turn decreasing its cytotoxicity. In addition, mutations at other sites of the enzyme may lead to a decrease in the binding affinity of the enzyme with the DNA or decrease the catalytic activity of the enzyme by hindering communication between the ATPase domain and the TOPRIM domain, thus reducing the capability of the drug to induce cleavage complexes (Wu *et al.*, 2011).

Other topo II poisons that act through intercalation of DNA to prevent re-ligation of the cleavable complex include the anthracyclines. First isolated from *Streptomyces peucetius*, the analogues; doxorubicin and daunorubicin were shown to have anti-cancer properties by targeting topoisomerase II. The ring structure of these compounds capable of intercalating DNA is important in their ability to stabilise the topoisomerase II cleavable complex (Fan *et al.*, 2007). Other topo II poisons include the acridine, mAMSA and the anthracenedione, mitoxantrone. They also intercalate DNA, and during the cytotoxic response of cells to these drugs, topo II $\beta$  is preferentially targeted (Errington *et al.*, 1999). Interestingly, a mAMSA derivative has been shown to intercalate at specific sites of topo II cleavage (Capranico *et al.*, 1998). Furthermore, a specific amino acid residue in yeast topo II has been identified as mAMSA sensitive suggesting that mAMSA may also elicit a poisoning effect by directly binding to topo II in addition to intercalating DNA (Nitiss, 2009).

Although used regularly in many chemotherapeutic regimens, the anthracyclines produce a certain amount of cardiotoxicity. For example reduction of doxorubicin by NADH dehydrogenase results in the formation of superoxide radicals. In addition formation of doxorubicin-iron complexes are shown to catalyse the Fenton reaction thus producing reactive oxygen species (ROS). An accumulation of free radicals induces a great amount of oxidative stress on cardiomyocytes which can result in heart failure (Volkova & Russel, 2011). When administered clinically, anthracyclines are often given synergistically with the topo II inhibitor ICRF-187 which also possesses iron chelating capabilities and therefore can reduce the generation of iron related ROS (Grausland *et al.*, 2007).

Additionally, a rare side effect of treatment with topo II poisons is therapy related acute leukemia, in particular therapy related acute myeloid leukemia. This is associated with a translocation involving MLL locus, and it is hypothesised that this occurs due to repair of topo II poison induced adducts in such close proximity that the translocation occurs (Cowell & Austin, 2012). Thus it is important to investigate thoroughly the possible side effects of topo II poisons in order to be able to potentially combat them and/or determine the susceptibility of patients to the side effects potentially using the information to alter their chemotherapeutic regimen accordingly.

### **1.8.3 Topoisomerase II inhibitors**

Topo II inhibitors act by inhibiting the catalytic activity of topo II, thus hindering its action in essential cell mechanisms. Several types exist including Merbarone, a thiobarbituric acid derivative which inhibits the catalytic action of topo II by preventing topo II mediated cleavage of DNA (Fortune & Osheroff, 1998). However the types of topo II inhibitors used in this study are a family known as the bisdioxopiperazines. These are a group of topo II inhibitors that non-competitively bind to topo II to prevent the hydrolysis of ATP, thus inhibiting their catalytic abilities. Drugs included in this group include ICRF-154, ICRF-187, and ICRF-193. Classen *et al.* (2003) showed that one molecule of bisdioxopiperazine was required to stabilize the ATPase region by binding both protomers simultaneously, thus creating a bridge and hindering the binding of ATP. Mutation of specific amino acid sequences in the ATPase domain have led to topo II inhibitor resistance thus supporting the mechanism proposed (Hu *et al.*, 2002). However other site mutations in the N terminal and C terminal domains also confer resistance suggesting that ICRF-193 may bind to multiple sites (Larsen *et al.*, 2003), possibly inducing a conformational change in the enzyme preventing ATP hydrolysis.

The action by which the bisdioxopiperazines exert their cellular effects is still largely unknown. It is postulated that by inhibiting the catalytic cycle, and thus preventing enzyme turnover the cellular effects, such as an inability of cells to complete chromosome segregation, may be one action. Rattner *et al.* (1996) propose that in particular ICRF-193 inhibits the translocation of topo II $\alpha$  to the centromere to aid with formation of solid kinetochores, indeed upon treatment of cells with ICRF-193 kinetochores became visibly more fragile. Huang *et al.* (2001) used the protein

denaturant guanidinium chloride (GuHCL) in place of the traditional denaturant sodium dodecyl sulphate (SDS) to reveal, topo II cleavable complexes in the presence of ICRF-193, thus suggesting that ICRF-193 may also act as a topo II poison. Interestingly they also report that using this method that ICRF-193 preferentially targets topo II $\beta$ . Taken together these studies suggest that ICRF-193 may have a dual action as a poison and inhibitor, however due to resistance being mediated through mutant ATPase regions it would be sensible to assume that it acts mainly as an inhibitor. Additionally treatment with ICRF-193 has been shown to result in entangled mitotic chromosomes, in contrast to the fragmented chromosomes caused by treatment with topo II poisons (Larsen *et al.*, 2003). In addition, the work of Isik *et al.* (2003) supports the work by Huang *et al.* (2001) with regards to the preferential targeting of topo II $\beta$  by ICRF-193. They report that treatment with ICRF-193 causes an increase in sumoylation of topo II $\beta$  leading to its selective degradation by the proteasome.

ICRF-193 has also been shown to exert a p53 independent delay in G2/M cells (Ishida *et al.*, 1994) often resulting in cell death. Interestingly, as this checkpoint is not ATM dependent it most likely is not a DNA damage checkpoint but a decatenation checkpoint (Deming *et al.*, 2001). Progression of cells through G2/M cells in the presence of ICRF-193 results in multiploid cells due to incomplete chromosome segregation (Iwai *et al.*, 1997), leading to activation of caspase-3 and apoptotic cell death (Larsen *et al.*, 2003).

The crystallisation of domains of the human topo II ATP domain has led to a better understanding of its structure, and therefore has facilitated the development of other topo II inhibitors, for example quinolone aminopurine 1 (QAP1) that has been shown to bind competitively to the ATP domain of the human topo II enzyme (Chene *et al.*, 2009).

#### **1.8.4 Processing of cleavable complexes**

The action by which topo II poisons and inhibitors lead to apoptosis has been the focus of much research and speculation. Indeed how does the cell recognise and process reversible double strand breaks induced by topo II when the double strand break is shielded by the topo II protein itself? Previous studies have shown that the stabilisation of transient cleavage complexes is not enough to induce cytotoxicity (Kaufmann *et al.*, 1998). This suggests that processing of the complex by another mechanism is required

to elicit a cytotoxic effect. Furthermore, removal or dilution of the drug results in the resealing of the staggered cuts by the enzyme, of which there is evidence in both *in vitro* (Tewey *et al.*, 1984; Chen *et al.*, 1983; Pommier *et al.*, 1985) and *in vivo* models (Hsiang and Liu, 1989; Caldecott *et al.*, 1990; Borgnetto *et al.*, 1996; Binaschi *et al.*, 1997). For example studies using etoposide show that upon removal of the drug 50% of topo II $\alpha$  and topo II $\beta$  mediated cleavage complexes are disassociated within 40 and 20 minutes of drug removal respectively (Errington *et al.*, 2004). However as cytotoxicity is still observed some of the remaining cleavage complexes must be processed to lethal lesions (Caldecott *et al.*, 1990). Using the gamma H2AX assay these lethal lesions were induced approximately 1 to 2 h following drug exposure (Sunter *et al.*, 2010).

Studies using the topo II poison, teniposide (VM-26) have shown that the replication fork arrests when it comes into contact with the cleavable complex (Catapano *et al.*, 1997), indicating that replicational machinery could be physically colliding with the topoisomerase II enzyme, resulting in its physical disassociation from the DNA thus revealing the double strand break. Furthermore non-topo II associated double strand breaks have also been reported at sites proximal to the replication fork arrest, induction of these double strand breaks has been suggested to be the result of recombination nucleases in an effort to repair and restart the replication fork (Barbour and Xiao, 2003; Andreassen *et al.* 2006). Thus taken together treatment of cells with topo II poisons can lead to the indirect generation of double strand breaks, this is termed the 'collateral damage' model (Caldecott *et al.*, 1990; Hong and Kreuzer, 2003; Polhaus and Kreuzer, 2005).

Further work has suggested that the cytotoxicity of topo II poisons is not exclusively reliant on the mechanism of replication. Indeed studies have shown using the replication inhibitor aphidicolin prior to cellular exposure to topo II poisons that it actually has no protective effect (3T3 fibroblasts, Chow and Ross, 1987; mouse mastocytoma cells, Schneider *et al.*, 1988 & 1989) or a very little 2 fold protective effect (V79 cells, D'Arpa *et al.*, 1990; L1210 cells, Chow *et al.*, 1988). In addition, work using a mouse carcinoma cell line revealed that treatment with aphidicolin only reduced the cytotoxicity of VP-16, teniposide and mAMSA but not daunorubicin, doxorubicin, idarubicin, epirubicin or mitoxantrone (Haldane *et al.*, 1993). The difference in cytotoxicity between cell lines and different topo II poisons may be due to the varying longevity of topo II poison induced cleavage complex that still may have remained when replication was recovered.

Xiao *et al.* (2003) showed that transcriptional arrest caused by treatment of HL-60 cells with teniposide was responsible for activation of 26S proteasome degradation of topo II $\beta$  specifically, leading to a DNA damage signal. Further work has shown using the transcription inhibitor, 5,6 dichlorobenzimidazole riboside that cells exposed to the topo II poisons, teniposide, VP-16 and mAMSA were more resistant to their cytotoxic effects (D'Arpa *et al.*, 1990; Mao *et al.*, 2001). Further to this cells were also shown to be more protected when transcription was inhibited during G1 phase rather S phase thus suggesting that certain cell cycle associated mechanisms may also contribute to drug sensitivity.

When both replication and transcription are inhibited a synergistic protective effect against topo II poisons is observed, however cell killing also persists (D'Arpa *et al.*, 1990; Kaufmann, 1991), thus suggesting other cellular mechanisms are involved in the processing of cleavage complexes to lethal lesions.

Further studies have shown that inhibition of protein synthesis using cyclohexamide results in a 8-fold protection to the cytotoxic effects of mAMSA (Schneider *et al.*, 1989). This is in support of previous work that has shown protection of cells against topo II poisons during replication when protein synthesis is reduced (Chow *et al.*, 1988; Hromas *et al.*, 1983).

Studies have also shown that deletion of key proteins involved in the repair of topo II – DNA complexes increase the sensitivity of cells to topo II drugs, one such protein is a TRAF and TNF receptor associated protein (TTRAP) with tyrosyl phosphodiesterase activity, specifically a 5' tyrosyl phosphodiesterase activity, named TDP2 (Cortes-Ledesma *et al.*, 2009; Zeng *et al.*, 2011). Further studies also identified a nuclease protein that removed topo II $\alpha$  from genomic DNA *in vitro*, and also showed that inhibition of MRE11 led to an increase in topo II $\alpha$  and  $\beta$  – DNA complex formation in the absence of topo II poisons such as VP-16 (Lee *et al.*, 2012).

Taken together, replication, transcription, protein synthesis and repair of topo II-DNA complexes are all required for the processing of cleavage complexes to induce a cytotoxic effect mediated by topo II poisons. However these mechanisms do not act exclusively and other important cellular mechanisms such as DNA repair and chromatin remodelling may also play a part in mediating topo II poison induced cytotoxicity.

### 1.8.5 Factors involved in drug sensitivity

The factors that govern sensitivity to topoisomerase II poisons and inhibitors are multi variable; the drug used, the cells treated and the time course of exposure used.

Many studies have focused on quantification of topoisomerase II $\alpha$  and  $\beta$  to predict drug sensitivity of particular cells, with the aim to possibly generate personalised chemotherapeutic regimens (Dingemans *et al.*, 1999; Depowski *et al.*, 2000). Drug resistant cell lines such as that of the p388 leukaemia amsacrine resistant cell line displayed a significant deficiency in topo II (Per *et al.*, 1987). Conversely an increase in topo II $\beta$  expression resulted in increased sensitivity to etoposide. In addition this increase in topo II $\beta$  expression was also correlated with chromatin remodelling at the topo II $\beta$  promoter.

In addition to a decrease in topo II conferring resistance to topo II drugs, a decrease in catalytic activity of topo II also affects drug sensitivity. Eijdemans *et al.* (1995) showed that the mAMSA resistance exhibited by SW-1573 cells did not correlate with topo II $\alpha$  protein or mRNA levels, but did correlate with a decrease in topo II $\alpha$  catalytic activity and they further proposed this to be due to an unknown post-translational modification. Gilroy *et al.* (2006) further demonstrated that a mutation in topo II $\beta$  decreased the affinity for ATP and ATP hydrolysis by 3 fold, thus conferring mAMSA resistance.

Truncated forms of topo II have also been implicated in drug sensitivity; Feldhoff *et al.* (1994) revealed that the etoposide resistant small cell lung cancer cell line H209/V6 possessed a truncated form of topo II $\alpha$  with a molecular weight of 160 kDa (which was later attributed to a partial deletion in exon 34 of the TOP2A allele (Mirski *et al.*, 2000). The truncation did not affect the catalytic activity of topo II, however it did affect the cellular localisation, with the majority of it being found in the cytoplasm, this is in contrast to the 170 kDa form which is found in the nucleus (Feldhoff *et al.*, 1994).

Thus cellular distribution of topo II also displays an influence on drug efficacy. Cowell *et al.* (2011) report that upon treatment of cells with the HDAC inhibitor, trichostatin A (TSA), topo II $\beta$  was redistributed from heterochromatin to euchromatin, thus treatment with TSA prior to VP-16 resulted in a more relevant target for VP-16 to exert its actions.

Errington *et al.* (2004) showed that the half-life of cleavable complexes also contributed to drug sensitivity. A study using a doxorubicin resistant HL-60 cell line revealed a change in the phosphorylation states of topo II $\alpha$  and  $\beta$ . Topo II $\alpha$  became hypo-phosphorylated and topo II $\beta$  became hyper-phosphorylated at specific sites not seen in the wild type (Grabowski *et al.*, 1999).

High concentrations of the anthracycline and DNA intercalator, doxorubicin is shown to change the structure of DNA leading to the inhibition of topo II binding, and therefore a reduction in the formation of cleavable complexes (Vejpongsa & Yeh, 2014).

The treatment length of cells to topo II poisons and inhibitors also affects the sensitivity of the cells to the drug. Indeed only a prolonged period of exposure to bisdioxopiperazines for long periods results in DNA damage, conversely a short exposure results in no DNA damage. This is not seen when using topo II poisons, which are shown to elicit DNA damage within a matter of minutes (Jensen *et al.*, 2004).

## **1.9 Role of topoisomerase II $\alpha$**

### **1.9.1 Replication, chromosome structure and mitotic function**

As described previously topo II has been shown to play a role in DNA replication. Interestingly topo II $\alpha$ , unlike topo II $\beta$  prefers to exert its actions on positive supercoil substrates. As shown in Figure 1.5, positive super-coiling is generated ahead of the replication fork, therefore it is suggested that topo II $\alpha$  is the main isoform involved in replication (McClendon *et al.*, 2005).

Extensive research has been undertaken to elucidate the role of topo II in chromosome condensation. Isoform specific studies have revealed that topo II $\alpha$  accumulates at the centromeres of condensed chromosomes during metaphase thus suggesting that topo II $\alpha$  is the main isoform involved in chromosome condensation (Rattner *et al.*, 1996). Additionally a regulated down-regulation of topo II $\alpha$  transcription by doxycycline results in 99% of chromosome condensation but with slower kinetics and an increased amount of partially condensed chromosomes (Carpenter *et al.*, 2004). Furthermore Johnson *et al.* (2009) report that treatment of chicken DT40 cells with short hairpin RNA targeting chicken topo II $\alpha$  resulted in longer and thinner chromosomes. Interestingly, Grue *et al.* (1998) showed that topo II $\beta$  does not display the same chromatin binding properties as that of topo II $\alpha$  and actually showed that topo II $\beta$

diffused away from the chromatin during mitosis, thus supporting previous work demonstrating the important role of topo II $\alpha$  in chromosome condensation.

The role of topo II $\alpha$  in mitotic events is suggested to be essential for cell survival. Carpenter and Porter (2004) reported that synthesis of a topo II $\alpha$  knockout cell line, HTETOP, revealed that cells underwent mitosis but not anaphase or cytokinesis, thus leading to cell death. Interestingly when trying to create a topo II $\alpha$  knockout mouse model, embryonic cells failed to complete nuclear division and underwent a forced cytokinesis resulting in cell death (Akimitsu *et al.*, 2003).

### **1.9.2 Apoptosis**

Mammalian topo II $\alpha$  has also been shown to have a possible role in chromatin degradation. Varecha *et al.* (2012) used fluorescence resonance energy transfer (FRET) analysis of HeLa and SK-NSH cells to show that endonuclease G, an enzyme released from mitochondria that participates in chromatin degradation in apoptosis, interacts with topo II $\alpha$  to degrade chromatin during apoptosis. This work is in support of a previous study that showed topo II $\alpha$  was required for the caspase-independent apoptotic pathway induced by staurosporine in NB-2a neuroblastoma cells (Solovyan, 2007).

### **1.9.3 Protein-protein interactions**

Various studies have also demonstrated that topoisomerase II $\alpha$  requires interaction with various proteins in order to promote its decatenation activity. De Haro *et al.* (2010) show that interaction of metnase, an enzyme containing methylase and nuclease domains with topo II $\alpha$  promotes topo II $\alpha$  dependent chromosome decatenation. Using HeLa, U2OS, WI38 and HCT116 cells lines, Ramamoorthy *et al.* (2012) describe a direct interaction with the helicase, RECQ15 with topo II $\alpha$  and its ability to increase topo II $\alpha$  mediated decatenation. Additionally work by Dykehuizen *et al.*, (2013) propose that topo II $\alpha$  physically interacts with the BAF complex (mammalian SWItch/Sucrose Non Fermentable complex) and the ATPase activity of one of its subunits, Brg1 is required for the binding of topo II $\alpha$  to the genome. Indeed the ability of topo II $\alpha$  to bind to DNA was decreased in Brg1 mutants.



The activity of topo II $\alpha$  has also been shown to be a requirement for the G2 decatenation checkpoint (Bower *et al.*, 2010). More specifically phosphorylation of topo II $\alpha$  at serine 1524 acts as a binding site for the BRCT domain (BRCA1 C-Termini domain) of MDC1 (Mediator of DNA Checkpoint Activity protein) and binding of MDC1 is required for successful G2 decatenation checkpoint activity. This is supported by work showing the mutant serine 1524 correlates with a defective G2 decatenation checkpoint (Luo *et al.*, 2009). However topo II $\alpha$  has not been shown to be required for DNA damage checkpoint activation (Luo *et al.*, 2009; Bower *et al.*, 2010).

#### **1.9.4 Transcription**

Interestingly a recent study by Thakurela *et al.* (2013) report that topo II $\alpha$  binds to promoter regions in embryonic stem cells (ESCs) that are marked with the active histone mark, H3K4me2, and their association with developmental silent genes in ESCs could be involved in creating accessible chromatin for later activation.

#### **1.10 Role of topoisomerase II $\beta$**

It is now widely reported that topoisomerase II $\beta$  plays a role in the regulation of transcription in mammalian cells, particularly in differentiating cells (Yang *et al.*, 2000; Tsutsui *et al.*, 2001; Chikamori *et al.*, 2006; Ju *et al.*, 2006; Lyu *et al.*, 2006; Tiwari *et al.*, 2012).

Aoyama *et al.* (1998) reported that differentiation of HL-60 cells into granulocytic cells with retinoic acid caused an increase in protein and phosphorylation levels of topo II $\alpha$  and  $\beta$ . This effect persisted for 96 h with retinoic acid treatment and levels of topo II $\beta$  were still elevated 96 h after retinoic acid had been removed. A persistent elevation in topo II $\beta$  levels could be attributed to the decrease in the degradation rate of the protein. Using 35S-methionine, the degradation rate of topo II $\beta$  in retinoic acid (RA) treated cells was 2 fold slower than those that had not been exposed (Aoyama *et al.*, 1998). This then suggests that topo II $\beta$  is required for the transcription of genes involved in RA induced differentiation. This is supported by a further study using the same cell line that showed that topo II $\beta$  associated with a gene required for RA induced differentiation, the RAR $\alpha$  gene (McNamara *et al.*, 2008).

Conversely McNamara *et al.* (2008) using a topo II $\beta$  targeting inhibitor, ICRF-193 showed that down-regulation of topo II $\beta$  resulted in the increase in expression of genes in response to RA suggesting that normally topo II $\beta$  negatively modulates the expression of RA induced genes. However the study used the NB4 cell line, which contains the RAR $\alpha$  gene fused to the promyelocytic leukaemia gene (PML) to form PML/RAR $\alpha$ . This fusion may then change the association and therefore the role of topo II $\beta$  at this gene.

The catalytic activity of topo II $\beta$  has also been shown to be important in neuronal development. Topo II $\beta$  knockout mice proved to be non-viable due to defects in neuronal development; motor neurons did not innervate the diaphragm muscle and there was an absence of sensory projections in the spinal cord (Yang *et al.*, 2000). A more detailed inspection of murine brain development in a topo II $\beta$  knockout mouse model revealed an aberrant lamination pattern in the developing cerebral cortex (Lyu *et al.*, 2003). Further investigation revealed that topoisomerase II $\beta$  was actually responsible for the up and down regulation of 30% of all developmentally regulated genes, predominantly in the latter stage of neuronal development (Lyu *et al.*, 2006). This was supported by work by Tiwari *et al.* (2012) who reported a switch from topo II $\alpha$  to II $\beta$  during neuronal differentiation. They also found that topo II $\beta$  binds to DNA sites that are transcriptionally active as determined by an increase in methylation at lysine 4 of histone 3 during this time, and that topo II $\beta$  prefers to bind to promoter regions of gene targets involved in the progression of neuronal progenitor to neuron. An absence of topo II $\beta$  revealed a change in transcription due to alterations in accessibility to target genes, leading to premature death of post-mitotic neurons. Thus suggesting the role of topo II $\beta$  may be in chromatin rearrangement, leading to an 'open' chromatin assembly, facilitating transcription of target genes. Also it has been shown that DNA superhelicity can facilitate the formation of transcription pre-initiation complexes on eukaryotic genes (Mizutani *et al.*, 1991).

A novel mechanism by which topo II $\beta$  facilitates transcription has been proposed by Ju *et al.* (2006). Stimulation of the breast cancer cell line, MCF-7 with 17 $\beta$ -estradiol resulted in an increased association in topo II $\beta$  and PARP-1, along with CBP co-activator at the ps2 promoter. This was followed subsequently by recruitment of RNA polymerase II. Further investigation using co-ChIP revealed that PARP-1, DNA-PK, Ku86 and Ku70 were also found on the same strand of DNA, and it was proposed that they may function as part of a multi-protein complex. Interestingly a strand break was

discovered in the ps2 promoter, and the authors inferred that this was generated by topo II $\beta$ , this inference was supported by work showing that inhibition of topo II $\beta$  resulted in no strand break and no exchange of histone H1 with HMGB1/2 at nucleosome 3 resulting in suppression of ps2 gene expression. Further to this, Ju *et al.* (2006) also investigated the promoter of other hormone responsive genes, one such gene was the TPA (PMA) responsive gene, AP-1, an important transcription factor involved in macrophage differentiation. Again they showed an increase in topo II $\beta$ , PARP-1, Ku86 and Ku70 at the promoter of this gene following 10 min, 30 min and 60 min of treatment with TPA. Taken together these results suggest that a topo II $\beta$  mediated double strand break is required for rearrangement of local chromatin architecture leading to recruitment and exchange of proteins involved in active transcription. This work is supported by work by Haffner *et al.* (2010) who reported that androgen signalling resulted in the recruitment of the androgen receptor and topo II $\beta$  to sites of the TMPRSS2 genomic breakpoint and that this triggered topo II $\beta$  generated double stranded breaks, furthermore they also reported that detectable *de novo* transcripts of the TMPRSS2 gene required topo II $\beta$  and other components of the double strand repair machinery. Further work investigating the role of topo II $\beta$  at the ps2 promoter in response to estrogen suggests that estrogen induced H3K9 demethylation leads to the generation of hydrogen peroxide and subsequent oxidation of bases. The repair of this oxidative DNA damage results in the removal of the oxidised bases result in single stranded nicks in the DNA. Interestingly, topo II $\beta$  is suggested to be recruited to these transient nicks, causing chromatin to bend allowing the RNA initiation complex to access the DNA and thus facilitating transcription (Perillo *et al.*, 2008).

Further to this, proteasomal degradation by the 26S proteasome of topo II $\beta$  upon treatment of cells with ICRF-193 is due to transcriptional arrest rather than DNA damage (Xiao *et al.*, 2003). It is possible that the transcriptional arrest is occurring because topo II $\beta$  is unable to act due to inhibition with ICRF-193, thus supporting the increasing evidence base that topo II $\beta$  is required for transcriptional regulation.

### **1.11 Protein association and post-translational modifications of topo II**

Investigations into the cell cycle distribution of the topo II isoforms revealed an interesting change in the molecular weight of topo II $\beta$ . Kimura *et al.* (1994) showed a

10 kDa increase in the molecular weight of topo II $\beta$  in HeLa cells when cells entered metaphase. In addition they also reported a return of topo II $\beta$  to 180 kDa when cells exited metaphase. They postulated that this increase in molecular weight could be due to phosphorylation of topo II $\beta$ . Indeed an earlier study showed that phosphorylation of topo II $\alpha$  increased as cells reached M phase (Sayor *et al.*, 1992). Burden *et al.* (1994) suggested that hyper-phosphorylation of topo II $\beta$  in mitosis may be involved in the stabilisation of the enzyme during nucleolar disassembly. This work was supported by Aoyama *et al.* (1998) who showed that phosphorylation of topo II $\beta$  was increased in retinoic acid treated cells and this correlated with a decreased rate of degradation of the enzyme, thus suggesting an increase in stability. In addition McNamara *et al.* (2010) speculate that the increase in topo II $\beta$  protein expression displayed upon Phorbol Myristate Acetate (PMA) stimulation is due to an increase in stability caused by phosphorylation of the protein by Protein Kinase C (PKC).

Post-translational modifications of topo II are also involved in the degradation of the enzyme upon treatment with topo II poisons and inhibitors. Mao *et al.* (2001) reported that ubiquitination of topo II in HeLa cells treated with VM-26 lead to a 26S proteasome mediated degradation of topo II. Interestingly, topo II $\beta$  was preferentially degraded over topo II $\alpha$ . Previously they had shown that SUMO-1 physically interacts with topo II, and an increase in SUMO-1/topo II conjugate was observed when HeLa cells were treated with VM-26, ICRF-193 and heat shock. They also suggested that the conformational change in topo II caused by VM26 and ICRF-193 may trigger binding of SUMO-1 (Mao, 2000). A later study revealed that modification of topo II $\beta$  by SUMO 2/3 and polyubiquitination occurred after cells had been treated with ICRF-193, resulting in the degradation of topo II $\beta$ . Additionally knock down of the SUMO conjugating enzyme Ubc9 resulted in a lack of topo II $\beta$  degradation (Isik *et al.*, 2003).

Both isoforms of topo II have also been shown to physically interact with HDAC 1/2. Topo II $\beta$  was shown to interact specifically with MTA2, a component of the NurrD complex of HDAC1, and as discussed earlier. Inhibition of HDAC causes the redistribution of topo II $\beta$  from heterochromatin to euchromatin (Cowell *et al.*, 2011). Further co-localisation experiments revealed that HDAC2 and topo II $\alpha$  were associated with each other in the nucleoplasm (Tsai *et al.*, 2000).

Cowell *et al.* (2000) used the cell line MCF7 to co-immunoprecipitate topo II $\alpha$  and topo II $\beta$  with p53. They also revealed using the yeast system *Sacchomyces cerevisiae* that

topo II $\beta$  interacts specifically with the C terminal domain of p53. Interestingly, prior to this, p53 was shown to repress the gene expression of topo II $\alpha$  (Wang *et al.*, 1997).

Nakano *et al.* (1996) proposed a mechanism by which CD3 $\epsilon$  may regulate the action of topo II $\beta$ . Using the murine hybridoma cell lines 2B4 and DO11.10 and a  $^{32}\text{P}$ -labelled GST fusion protein they revealed that upon T cell activation CD3 $\epsilon$  translocates to the nucleus and associates with topo II $\beta$ . This supports work with expression libraries that revealed topo II $\beta$  clone sequences bind to CD3 $\epsilon$ . Treatment of the same cells with topo II inhibitors causes a super induction of Interleukin-2, a similar effect is witnessed when Cd3 $\epsilon$  binds to topo II $\beta$  suggesting that it may regulate topo II $\beta$  by hindering its catalytic action.

It is now widely accepted that topo II $\beta$  is involved in the regulation of transcription, particularly so in the regulation of genes involved in neuronal development and differentiation. Both these cellular events require multiple changes in gene expression, and thus topo II $\beta$  is required for such changes, including activation and repression. However differentiation events are not solely limited to cells of a neuronal lineage; in fact the innate immune system gives rise to regular differentiation events, which also require changes in gene expression for commitment of cell fate.

In addition levels of topo II $\beta$  are also increased in the serum of patients suffering with hepatitis B induced liver inflammation, thus indicating a role for topo II $\beta$  in inflammation, indeed it is postulated that an inflammation induced up-regulation of topo II $\beta$  may represent an initial marker of inflammation related malignancy (He *et al.*, 2003).

### **1.12 The innate immune system**

The innate immune system is the first line of defence against infection. Its actions are immediate, non-specific and with no immunological memory. Along with recognition and destruction of potentially pathogenic infections it also acts to present foreign molecules to cells of the adaptive immune system (Mogenson, 2009). Cells of the innate immune system largely comprise leukocytes, and in particular a family of phagocytes that include, monocytes, macrophages, dendritic cells and neutrophils (Janeway & Medzhitov, 2002). Recognition of potentially pathogenic microbes is via conserved

regions of the microbe, termed pathogen associated molecular patterns (PAMPs). PAMPs are distinctively different from any host molecules. Mononuclear phagocytes recognise PAMPs through pattern recognition receptors (PRRs) (Janeway, 1989). PRRs of particular importance are termed the Toll like receptors (TLR) due to their high homology with the *Drosophila* receptor, Toll (Seong & Matzinger, 2004) that also recognise pathogens.

### **1.12.1 Macrophage differentiation**

Hematopoietic differentiation leads to the generation of various different cell types originating from a single progenitor, the hematopoietic stem cell. From here, the hematopoietic stem cell differentiates into a multipotent progenitor and then into a dyspoietic progenitor including the common lymphoid and common myeloid progenitors. Further differentiation of these progenitors leads to commitment into mature cells including B cells, T cells, natural killer (NK) cells and dendritic cells, macrophages and granulocytic cells respectively (Seita & Weissman, 2010). Monocytes are specifically derived from CD34<sup>+</sup> progenitor cells in the bone marrow, they are then released into the peripheral blood where they circulate for several days before entering the tissues to replenish any tissue macrophages lost to apoptosis (Gordon, 2005).

Differentiation occurs *in vivo* via stimulation of monocytes by macrophage colony stimulating factor (M-CSF). *In vitro* models of monocyte differentiation use phorbol esters such as Phorbol 12-Myristate 13-Acetate (PMA) to differentiate monocyte derived cell lines into cells that display a macrophage like phenotype. Previous work utilising this differentiating agent was done so in order to elucidate the transcriptional and post-translational mechanisms involved in differentiation and stimulation of monocytes and macrophages (Suzan *et al.*, 1991; Ghosh *et al.*, 2010). For example, Shelley *et al.* (2002) reported that an up-regulation of the CD11c integrin on the cell surface of cells undergoing differentiation was due to binding of the transcription factor Pur $\alpha$  to the CD11c promoter. The cell model used in this investigation was the monocytic cell line U937 that can be stimulated with PMA. U937 cells are of a monocytic lineage and express the gene encoding TNF $\alpha$  and secrete TNF $\alpha$  in response to PMA and LPS (Sundstrom & Nilsson, 1976). Differentiation with PMA also allows the investigation of the inflammatory response (Carruba *et al.*, 2003). For example, Infantino *et al.* (2010) reported that stimulation of PMA treated U937 cells with LPS leads to an up-regulation of citrate carrier mRNA and protein expression and suggest

that the mitochondrial citrate carrier plays an important role in the inflammatory response.

Differentiation of monocytes into macrophages is accompanied by changes in cell morphology and cell growth. Terminally differentiated macrophages lose their ability to proliferate (Takashiba *et al.*, 1999), this is reflected by the G2/M arrest observed in various PMA treated cells (Kosaka *et al.*, 1996; Barboule *et al.*, 1999, Oliva *et al.*, 2008). During differentiation, cells become more granular, and Daigneault *et al.* (2010) attributed this to an increase in membrane bound organelles. Additionally an increase in intracellular organelles may also be observed due to an increase in the amount of mitochondria and lysosomes present within the macrophages (Valledor *et al.*, 1999).

PMA induces differentiation of monocytes to macrophages by activation of the protein kinase C (PKC) pathway (Johnson *et al.*, 2002). This is the major pathway of activation. The PKC family is divided into three distinct subsets; conventional, novel and atypical. Conventional PKCs include  $\alpha$ ,  $\beta$ I,  $\beta$ II and  $\gamma$ , and this subset of PKCs require  $\text{Ca}^{2+}$ , diacylglycerol (DAG) and the co factor phosphatidyl for activation. Novel PKCs include  $\delta$ ,  $\epsilon$ ,  $\theta$ ,  $\eta$ , and  $\mu$ . This subset of PKCs unlike the conventional PKC subset do not require,  $\text{Ca}^{2+}$  for activation. The atypical PKCs include  $\zeta$  and  $\text{I}/\lambda$  and require  $\text{PIP}_3$ , ceramide and phosphatidic acid for activation (Valledor *et al.*, 1999).

A detailed outline of PKC mediated macrophage differentiation is described in Figure 1.7.

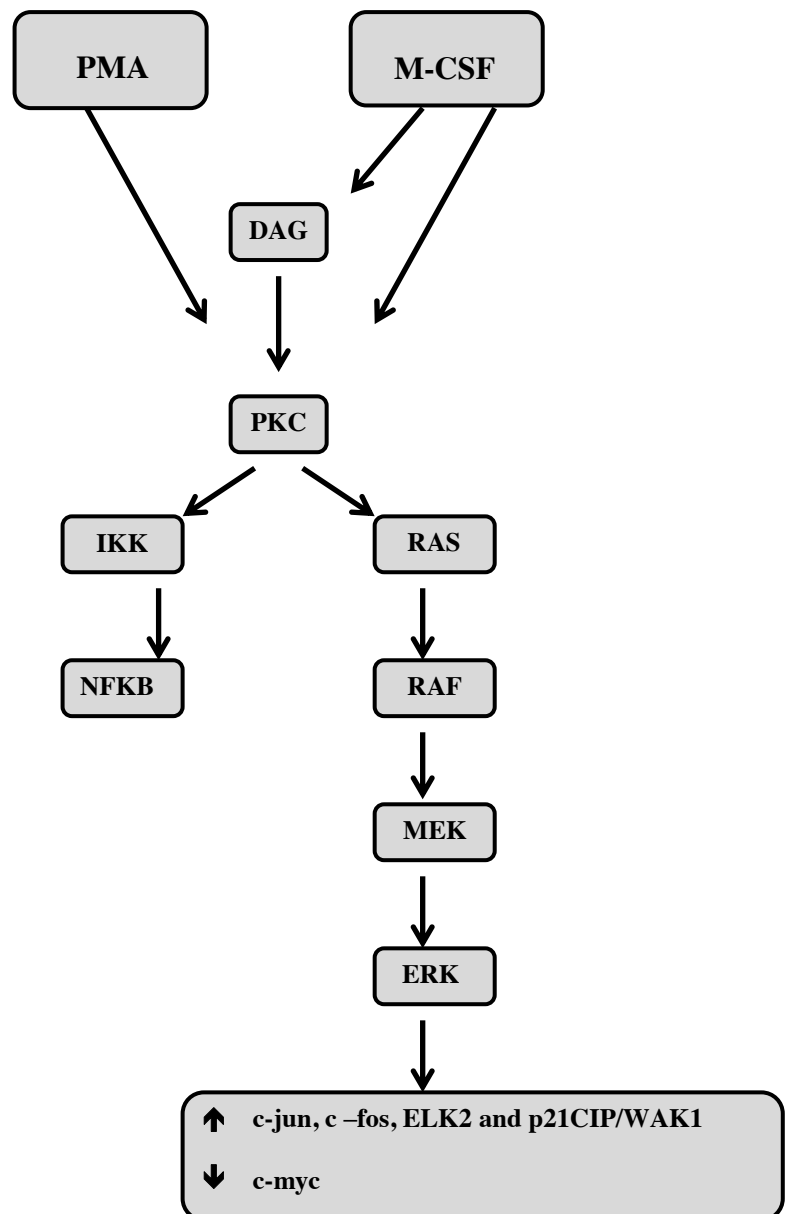


**Figure 1.7 Schematic Representation of the pathways of macrophage differentiation by M-CSF and PMA.**

Binding of M-CSF to the tyrosine residue of the FMS receptor results in its autophosphorylation which in turn leads to the activation of phospholipase C and cleavage of phosphatidyl-inositol biphosphate creating DAG and release of  $\text{Ca}^{2+}$ . DAG and  $\text{Ca}^{2+}$  along with the co factor phosphatidyl activate conventional protein kinases, which then lead to activation of the GTPase switch, Ras. This in turn activates Raf-1, a serine/threonine protein kinase. This phosphorylates and activates MEK-1, which then induces the phosphorylation and activation of ERK 1 and 2. Activation of ERK 1 and 2 leads to an up-regulation of transcription factors involved in early macrophage differentiation and a decrease in transcription factors involved in driving differentiation to a neutrophil like lineage. PMA is homologue of DAG and so acts through the same PKC dependent pathway. Conventional ( $\alpha$ ), novel ( $\epsilon$ ) and atypical ( $\delta$ ) PKCs have been implicated in the activation of NF- $\kappa$ B either by phosphorylation of IKK or by increasing NF- $\kappa$ B DNA binding (Valledor *et al.*, 1999; Lee *et al.*, 2003).



The primary transcription factor involved in monocyte to macrophage differentiation is Pu.1. Studies involving generation of Pu.1 knockout mice report death of the mice within 48 hr due to severe bacterial septicaemia, resulting from a lack of mature anti-bacterial macrophages (McKercher *et al.*, 1996). In order for differentiation to occur, monocytes must successfully respond to signalling by the macrophage-colony stimulating factor (M-CSF) via the macrophage colony stimulating factor receptor. The M-CSF receptor is the protein product of the *c-fms* gene. Pu.1 has been shown to bind to purine rich sites in the promoter of the *c-fms* gene, facilitating its transcription. Additionally Pu.1 has been shown to cause the up-regulation of adhesion molecules including CD11b, CD18 and CD14, which are all concomitant with macrophage differentiation (Valledor *et al.*, 1998). Furthermore, Oshuri & Natoli (2013) propose that in addition to actively promoting gene expression, binding of Pu.1 to distal genomic regions causes nucleosome depletion and deposition of H3K4me1, resulting in sites of accessible chromatin thus facilitating the binding of multiple other transcription factors. Other transcription factors involved in the commitment to macrophage lineage include Sp1, EGR2, HOXB7 and NF-Y and members of the proto-oncogene families Jun/Fos (Valledor *et al.*, 1998). Interestingly other transcription factors, for example EGR-1, have been shown to block the differentiation of cells towards a granulocytic lineage, therefore driving macrophage differentiation (Krishnaraju *et al.*, 1998). Furthermore, loss of proliferation associated with a macrophage phenotype has been attributed to repression of the *c-Myb* and *c-Myc* genes early in the differentiation process (Valledor *et al.*, 1998).

Macrophages are a highly heterogeneous population of cells, found in all areas of the body. Microglia are macrophages that are found in the brain, alveolar macrophages are found in the lung; histiocytes are found in interstitial connective tissue and Kupffer cells in the liver. However differences in macrophage populations does not rely solely on location in the body. The various populations of macrophages are activated differently; these populations are broadly grouped into, classically activated (M1) and alternatively activated (M2) macrophages.

Classically activated macrophages require a type I cytokine environment including interferon gamma (IFN $\gamma$ ) and cytokine stimuli (TNF $\alpha$ , IL-1 $\beta$ ) in order to be activated. Conversely a type II cytokine environment, comprising IL-4 and IL-13 inhibits classically activated macrophages (Ghassabeh *et al.*, 2006). M1 macrophages also display an IL-12<sup>high</sup>, IL-23<sup>high</sup>, IL-10<sup>low</sup> phenotype (Manotovani, 2006).

Alternatively activated macrophages are activated in a type II cytokine environment, and are inhibited in a type I cytokine environment (Namagala *et al.*, 2001). It was first postulated that this type of macrophage was the result of IL-4 antagonism of classically activated macrophages, however identification of a mannose receptor (MC1) which was up-regulated upon IL-4 stimulation along with an increase in expression of MHC class II molecules supported the distinction of this type of macrophage from a classically activated one (Gordon, 2003). Alternatively activated macrophages also display a distinguishable IL-12<sup>low</sup>, IL-23<sup>low</sup>, IL-10<sup>high</sup> phenotype (Manotovani, 2006).

### **1.12.2 Inflammation**

Inflammation is characterised by five symptoms; swelling, redness, pain, fever and loss of function (Punchard *et al.*, 2004). Inflammation in response to activation of the innate immune response by pathogenic stimuli, results in stimulation of resident tissue macrophages that then signal for the recruitment of leukocytes to the site of infection and their subsequent activation (Granger *et al.*, 2010). Activation of macrophages occurs via stimulation by IFN $\gamma$ , M-CSF, TNF $\alpha$  and lipopolysaccharide (LPS). Macrophages play a pleotropic role in inflammation including, phagocytosis, antigen presentation and immunomodulation (Fujiwara *et al.*, 2005). Deactivation of macrophages requires secretion of anti-inflammatory cytokine such as IL-10 and TGF $\beta$  by resting macrophages, thus leading to inhibition of inflammation that is necessary in order to allow repair of the affected site (Mosser *et al.*, 2003). A dysregulation of the inflammatory response is associated with many disease states such as Rheumatoid Arthritis, Type II Diabetes and cancer (Coussens *et al.*, 2002; Pickup *et al.*, 2004; Moelants *et al.*, 2013).

### **1.12.3 Toll Like Receptors**

There are 13 known Toll like receptors found in mammals, each recognising a distinct pattern associated with different pathogens either directly or indirectly (Shubolet *et al.*, 2007). Characterisation of Toll like receptors is based on the leucine rich repeat in the extracellular domain and the TIR domain in the intracellular domain (Takeda *et al.*, 2003). Toll like receptor 2 recognises and binds to a specific PAMP found in lipotechoic acid that makes up the wall of Gram-positive bacteria, and it has also been shown to recognise components of the herpes simplex virus. TLR3 has been shown to

recognise and bind viral double-stranded RNA. Toll like receptor 4 indirectly recognises lipopolysaccharide (LPS) found in the membrane of gram-negative bacteria. LPS firstly binds to LPS binding protein, which is in turn bound to the cell surface antigen, CD14, this then associates with the extracellular domain of TLR4. TLR5 has been shown to recognise bacteria flagellin, whilst TLR9 recognises unmethylated CpG sites on bacterial DNA (Moresco *et al.*, 2011).

Recognition of foreign material by TLRs causes a cascade of intracellular signalling leading to activation of NF- $\kappa$ B and thus expression of genes involved in the innate immune response (Zhang *et al.*, 2001).

#### **1.12.4 Activation of NF- $\kappa$ B**

NF- $\kappa$ B is a family of transcription factors that contain a Rel homology domain (RHD) which bind to discrete sequences of DNA termed  $\kappa$ B sites.  $\kappa$ B sites are often found in promoter or enhancer regions of various genes including those that encode pro-inflammatory cytokines. There are five members of the NF- $\kappa$ B family identified to date, including RelA (p65), Rel B, C-Rel, p100 and p105. NF- $\kappa$ B exists as a heterodimer or homodimer of these components. It is synthesised and stored within the cell in its inactive form; bound to a member of the inhibitor of kappa B (I $\kappa$ B) family. The I $\kappa$ B family are a group of inhibitor proteins including I $\kappa$ B $\alpha$ , I $\kappa$ B $\beta$ , I $\kappa$ B $\gamma$ , I $\kappa$ B $\epsilon$ , Bcl-3, I $\kappa$ B $\zeta$ , I $\kappa$ BM (Oeckingham & Ghosh, 2009; Lawrence 2009). It has been demonstrated that I $\kappa$ B $\alpha$ , I $\kappa$ B $\beta$ , I $\kappa$ B $\gamma$  and I $\kappa$ B $\epsilon$  inhibit the translocation of NF- $\kappa$ B to the nucleus, thus inhibiting its actions as a transcription factor (Anratha *et al.*, 1999). The remaining I $\kappa$ B's are believed to interact with NF- $\kappa$ B in the nucleus to regulate transcription (Yamazaki *et al.*, 2001). Stimulation of TLRs leads to phosphorylation of serine residues within the I $\kappa$ B by the IKK complex (a complex including the catalytic domains IKK $\alpha$  and IKK $\beta$ , along with the regulator NF- $\kappa$ B essential modifier, NEMO). Phosphorylation of I $\kappa$ B leads to its polyubiquitination and subsequent degradation by the 26S proteasome (Chen *et al.*, 2005; Krappman *et al.*, 2005). This then releases the NF- $\kappa$ B, allowing its translocation to the nucleus. A more detailed pathway of activation is described in Figure 1.8.

Interestingly a comparatively new area of investigation with regards to NF- $\kappa$ B is the activation of it in response to DNA damage. In particular, elucidating the mechanism of

recognition of DNA damage including double strand breaks and the subsequent activation of NF- $\kappa$ B. Studies have shown that ataxia telangiectasia mutated (ATM) protein, a protein kinase activated by DNA damage is indispensable for the activation of NF- $\kappa$ B in response to irradiated radiation and topoisomerase poisons that are able to induce double strand breaks. Indeed it has been suggested that ATM does not recognise these double strand breaks through direct binding but through alterations in high-order chromatin as a result of the double strand break (Janssens & Tschopp, 2006). Activation of ATM then phosphorylates NEMO, a component of the IKK signalosome. Phosphorylation then leads to the zinc finger dependent ubiquitination of NEMO. Both the phosphorylation and ubiquitination of NEMO are required for NF- $\kappa$ B activation. Upon ubiquitination of NEMO, a small amount of ATM is re-localised to the cytoplasm where it activates TAK1. Activation of TAK1 leads to association and activation of multiple proteins and protein complexes, however the exact mechanism still remains unclear. These interactions ultimately lead to activation of the conserved IKK thus leading to activation of NF- $\kappa$ B (McCool & Miyamoto, 2012).

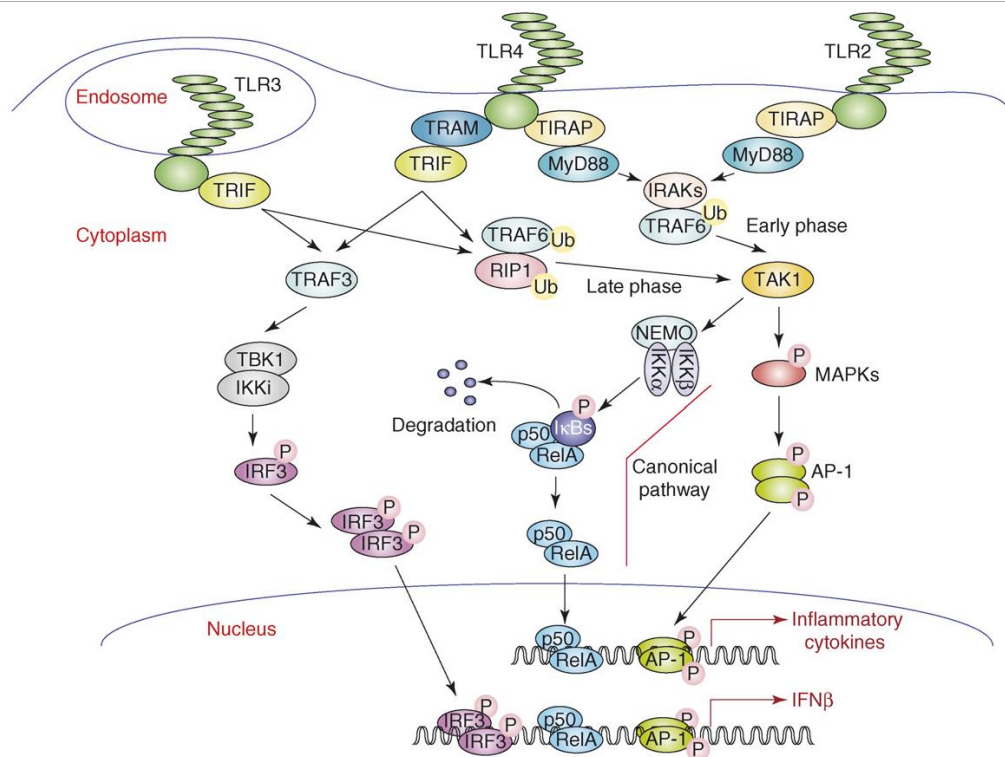


**Figure 1.8 Schematic diagram outlining the pathway of NF- $\kappa$ B activation by TLR ligation (Kawai & Akira, 2007)**

Ligation of TLR leads to activation of the myeloid differentiation primary response gene 88 (MyD88) dependent pathway and the TRIF dependent pathway. For successful transcription of pro-inflammatory cytokines induced by NF- $\kappa$ B, activation of both the TRIF and MyD88 pathway are required post stimulation of TLR4. Activation of MyD88 and TRIF is via TIR domain containing adaptors, TIRAP and TRAM respectively. The death domain of MyD88 then associates with the death domain of the protein kinases IRAK1 and IRAK4. Activation of IRAK4 leads to phosphorylation of IRAK1, thus causing the dissociation from MyD88. IRAK1 and 4 then interact with TRAF6, a ring domain E3 ubiquitin ligase, this then associates with Ubc13, E2 and UeV1a to ubiquitinate itself, leading to the recruitment of TAK1. This then activates the IKK and MAPK pathways. Activation of IKK leads to phosphorylation and subsequent degradation of I $\kappa$ B leading to the release and translocation of NF- $\kappa$ B to the nucleus. Activation of MAPK leads to the phosphorylation and activation of another transcription factor involved in the transcription of pro-inflammatory cytokines, AP-1.

The TRIF pathway of activation is similar to that of MyD88, however it binds directly to TRAF6 via the TRAF6 binding motif in its N terminal domain.

### 1.13 Cytokines

Cytokines are proteins released by the cell in response to a variety of stimuli, including UV radiation, heat shock and activation of the MAPK pathway via toll like receptor activation or binding of external cytokines. Cytokines possess no conserved amino acid sequence motifs or 3D structure similarity; instead they are identified and grouped according to their biological activity. Historically, cytokine is a general term used to describe these proteins, more specific terms used are; lymphokines, cytokines released by lymphocytes; monokines, cytokines released by monocytes; chemokines, cytokines that have chemotactic activity and interleukins, cytokines that are produced by and activate leukocytes. For the purposes of this work the general term, cytokine will be used. Cytokines are produced by all nucleated cells, however the largest source of cytokine production are T helper cells and macrophages (Epstein *et al.*, 1998; Dinarello, 2000). Different cell types may release the same cytokine; in addition these cytokines may act pleotropically, activating different cell types (Zhang *et al.*, 2007). Cytokines are loosely grouped into those that induce a pro-inflammatory effect and those that have an anti-inflammatory effect, although some cytokines for example IL-6 (Schiller *et al.*, 2011) may have both a pro and anti-inflammatory effect depending on the environment they are acting in.

The most abundant pro-inflammatory cytokines found at sites of inflammation are TNF $\alpha$ , IL-1 (specifically IL-1 $\beta$ ) and IL-6 (Cavaillon, 1993). Thus they have proven to be an attractive target of investigation.

#### 1.13.1 TNF $\alpha$

Tumour necrosis factor alpha (TNF $\alpha$ ) is a type II transmembrane protein. It exists as a 51 kDa homotrimer (Idris *et al.*, 2000). The 17 kDa monomers consist of antiparallel  $\beta$  pleated sheets along with antiparallel  $\beta$  strands to form a beta structure (Eck & Sprang, 1989). TNF $\alpha$  is constitutively produced by a variety of cells including, macrophages, mast cells, endothelial cells and fibroblasts. The actions of TNF $\alpha$  are pleotropic, capable of inducing apoptosis, cell proliferation and cytokine production (Horiuchi *et al.*, 2010).

TNF $\alpha$  is inactive in its membrane bound form, cleavage and release of the homotrimer from the membrane by TNF $\alpha$  converting enzyme (TACE) allows the release of TNF $\alpha$  into the extracellular environment. Reactive oxygen species are shown to mediate the

LPS induced catalytic activity of TACE indirectly through activation of the p38 signalling pathway (Scott *et al.*, 2011).

Activation of cells is via TNF receptors, TNF-R1 and TNF-R2. TNF-R1, a 55 kDa protein is ubiquitously expressed on most cells (Shen & Pervaiz, 2006), whilst the 75 kDa protein TNF-R2 is expressed in low levels on cells of immune lineage (Idris *et al.*, 2000). Both receptors can bind membrane bound and soluble TNF $\alpha$ , however TNF-R2 is only fully activated by binding of membrane bound TNF $\alpha$ . Binding of TNF $\alpha$  to TNF-R1 and TNF-R2 results in the activation of the NF- $\kappa$ B survival pathway.

Interestingly extracellular domains of TNF-R1 and R2 can be cleaved to form soluble fragments that have been shown to neutralise soluble TNF $\alpha$ . It has been shown that TNF-R2 is also cleaved by TACE, however the enzyme responsible for the cleavage of TNF-R1 remains unknown. Studies have shown that inhibiting the cleavage of TNF-R1 results in a disease state similar to that of an auto-inflammatory disease, thus suggesting that the neutralising actions of TNF-R1 fragments are required for regulation of the TNF $\alpha$  driven inflammatory response (Horiuchi *et al.*, 2010).

Signalling of TNF $\alpha$  through TNF-R1 and R2 leads to the translocation and activation of NF- $\kappa$ B (Poyet *et al.*, 2000), which in turn leads to further transcription of cytokines. Thus TNF $\alpha$  is able to perpetuate the pro-inflammatory response, whilst creating a positive feedback loop leading to further transcription of the TNFA gene.

TNF-R1 contains a death domain that is required for the recruitment of the death domain containing TRADD protein. The subsequent TNF-R1-TRADD complex then creates a physical platform to enable the binding of TRAF2 to the receptor interacting kinase (RIP). TNF-R2 in comparison is able to directly recruit TRAF2, leading to gene expression (Wajant *et al.*, 2003).

Activation of both TNF-R1 and TNF-R2 in the presence of HIV infected T cells and peripheral blood lymphocytes has been shown to induce apoptosis of the infected cells and initiation of this was via cooperative signalling of TNF-R1 and TNF-R2 (Lazdins *et al.*, 1997). This suggests that TNF $\alpha$  signalling through binding of transmembrane TNF $\alpha$  is more important than first thought, thus an increasing amount of studies are focusing on the role of transmembrane TNF $\alpha$ .

Studies using transmembrane TNF $\alpha$  knock-in mice that are unable to secrete soluble TNF $\alpha$  are capable of controlling *Leishmania* infection (Allenbach *et al.*, 2008). Previous work showed that interaction of transmembrane TNF $\alpha$  on CD4<sup>+</sup> on *Leishmania* infected macrophages resulted in the inhibition of intracellular *Leishmania* (Birkland *et al.*, 1992).

The requirements for the transcription of TNF $\alpha$  appear to differ in variations of macrophages. Means *et al.*, (2000) report that transcription of TNF $\alpha$  in response to LPS in alveolar macrophages requires ERK signalling, in contrast inhibition of ERK in non-pulmonary macrophages cells did not affect the LPS induced transcription of TNF $\alpha$ . In addition they also identified MAPK dependent and independent elements in the TNF $\alpha$  promoter, and proposed that use of them was cell type specific.

Transcription of TNF $\alpha$  also appears to be dependent on the type of stimulus it is activated by. Trede *et al.*, (1995) showed that stimulation treatment of the monocytic THP-1 cells with Staphylococcal enterotoxin A caused an up-regulation of NF- $\kappa$ B binding to specific kappa 3 site in the TNF $\alpha$  promoter.

Additionally post-transcriptional regulation has been attributed to TNF $\alpha$  regulation. Inhibition of p38 lead to a decrease in translation of the TNF $\alpha$  transcript, implying that p38 may stabilise TNF $\alpha$  mRNA (Lee *et al.*, 1999).

### **1.13.2 Interleukin 1**

Interleukin 1 is a family of cytokines including IL-1 $\alpha$  and IL-1 $\beta$ . They share only 26% amino acid sequence homology, however they have been grouped together as they both share the same receptor, IL-1R1 (Kohira *et al.*, 1993; Hacham *et al.*, 2002). IL-1 $\alpha$  and  $\beta$  exist as precursor proteins, pro-IL-1 $\alpha$  and pro-IL-1 $\beta$  (Fettelschoss *et al.*, 2011).

### **1.13.3 Interleukin-1 $\beta$**

Pro-IL-1 $\beta$  is a 31 kDa precursor protein, which is then cleaved by the enzyme caspase-1 to create the 17 kDa, mature, active IL-1 $\beta$  (Hailey *et al.*, 2009). The mature IL-1 $\beta$  protein is a  $\beta$  trefoil fold formed by 12  $\beta$  strands (Chavez *et al.*, 2006). IL-1 $\beta$  is



primarily produced by monocytes and macrophages, however it is also produced in smaller quantities in neutrophils, keratinocytes, epithelial cells and fibroblasts. The role of IL-1 $\beta$  in the innate immune system is to promote the recruitment of inflammatory cells, increasing the amount of adhesion molecules on endothelial cells and inducing stromal cells to release chemokines.

In order for caspase-1 to cleave and thus activate IL-1 $\beta$ , it must first be activated. This is regulated via the actions of the inflammasome (NALP3), a multi-protein complex comprised of caspase-1, the adaptor protein, ASC and the NOD like receptor, and NLR (Agostini *et al.*, 2004; Gabay *et al.*, 2010). Studies have also shown that pro-IL-1 $\beta$  can also be cleaved by extracellular proteases to yield active IL-1 $\beta$  (Fantuzzi *et al.*, 1999). Interestingly, NF- $\kappa$ B in addition to activating the transcription of IL-1 $\beta$  has also been shown to inhibit caspase-1 dependent IL-1 $\beta$  cleavage by increasing the expression of anti-apoptotic genes (Greten *et al.*, 2007).

Binding of IL-1 $\beta$  to IL-1R1 leads to recruitment of the IL-1R accessory protein, IL-1RAcP. The IL-1-IL-1R1-IL1RAcP complex induces the recruitment of MyD88 which then as described previously (section 1.12.4), leads to activation of NF- $\kappa$ B, p38, and the JNK, ERK 1/2 and MAPK pathways (Gabay *et al.*, 2010).

Transcription of IL-1 $\beta$  also relies on the actions of specific transcription factors involved in the regulation of cytokine expression, for example, SP-1, AP-1 and NF- $\kappa$ B. However, like TNF $\alpha$ , variability in actions of transcription factors may be environment dependent. Exposure of cells to fibronectin, a protein produced by injured tissues led to an up-regulation of IL-1 $\beta$  mRNA expression. An increased binding of the transcription factor, AP-1 was observed at the IL-1 $\beta$  promoter, however there was no change in NF- $\kappa$ B binding. Fibronectin was shown to bind to the cell surface integrin  $\alpha$ 5 $\beta$ 1 which then activated the MAPK pathway leading to the increased binding of AP-1 (Roman *et al.*, 2000). Furthermore, a chronic stimulation of chondrocytes with inflammatory cytokines led to an increase in expression of IL-1 $\beta$ . This was associated with an increase in demethylation of specific CpG sites in the IL-1 $\beta$  proximal promoter (Hashimoto *et al.*, 2013).

#### 1.13.4 Interleukin-1 $\alpha$

Pro-IL-1 $\alpha$  is a 31 kDa precursor protein. Removal of the N terminal amino acids by the protease calpain results in the 18 kDa mature form of IL-1 $\alpha$ . IL-1 $\alpha$  is mainly produced by macrophages and neutrophils but can also be expressed by cells of non-hematopoietic lineage including keratinocytes and fibroblasts (Rider *et al.*, 2013). IL-1 $\alpha$  is active in both its soluble and membrane bound form. It has been hypothesised that phosphorylation of pro-IL-1 $\alpha$  leads to a conformational change resulting in surface anchoring via lectin binding (Beuscher *et al.*, 1988; Brody *et al.*, 1989). Active membrane bound IL-1 $\alpha$  has been shown to allow physical cell – cell signalling, important for activation of neighbouring cells. Activation of membrane bound IL-1 $\alpha$  relies solely on activation of NF- $\kappa$ B. However activation of soluble IL-1 $\alpha$  requires activation of NF- $\kappa$ B, the inflammasome and caspase-1. Interestingly, secretion of IL-1 $\alpha$  requires the action of IL-1 $\beta$  as a shuttle to enter the extracellular environment (Fettelschoss *et al.*, 2011). IL-1 $\alpha$  signals through the same receptor ligand as IL-1 $\beta$ , leading to a cascade of intracellular signalling as described in Section 1.13.3 (Hacham *et al.*, 2002)

IL-1 $\alpha$  may also have a dual role within the cell. IL-1 $\alpha$  contains a functional nuclear localisation sequence that allows translocation to the nucleus where it has been shown to bind to histone acetyltransferases thus facilitating the expression of pro-inflammatory cytokines, furthermore it is able to do this independently of IL-R1 binding at the cells surface (Rider *et al.*, 2013).

Little is known with regards to the transcriptional regulation of IL-1 $\alpha$  compared to other pro-inflammatory cytokines. Kameda & Sato (1994) demonstrated an up-regulation of IL-1 $\alpha$  mRNA expression in keratinocytes stimulated with LPS, PMA and TNF $\alpha$  independently. Further to this Bailly *et al.* (1996) found using an electromobility shift assay an LPS induced AP-1 binding region in the IL-1 $\alpha$  promoter, however no NF- $\kappa$ B binding sites were identified in the IL-1 $\alpha$  promoter or first intron.

IL-1 $\alpha$  has also been shown to play a role in the stimulation of osteoclastogenesis; a dysregulation of which can result in osteosarcoma. Cao *et al.* (2008) used a mouse cell line K7M2 to show that under normal circumstances the osterix zinc finger transcription factor binds to an SP-1 binding site at the IL-1 $\alpha$  promoter leading to suppression of IL-1 $\alpha$  transcription.

### 1.13.5 Interleukin 6

Interleukin 6 (IL-6) is a cytokine with both pro and anti-inflammatory capabilities. It is a 28 kDa protein constructed as a 4 helix bundle, consisting of four long helices structured in an up-down topology. IL-6 is secreted by immune cells and non-immune cells, such as osteoblasts and keratinocytes (Ishimi *et al.*, 1990; Neuner *et al.*, 1991; Scheller *et al.*, 2011). There are many roles attributed to the action of IL-6 including regulation in inflammation, metabolic control and bone metabolism. More specifically IL-6 trans-signalling leads to the recruitment of monocytes during infection. It has been shown to reduce neutrophil attracting chemokines, whilst up-regulating monocyte recruiting chemokines. It has also been shown to up-regulate adhesion molecules, such as Intercellular Adhesion Molecule-1 (ICAM-1) and Vascular Cell Adhesion Molecule-1 (VCAM-1) on endothelial cells and increase M-CSF receptor expression resulting in a drive towards macrophage differentiation.

IL-6 contains three receptor-binding sites; a recognition site for the receptor IL-6R, a contact site for the gp130 domain and a contact domain for Ig-like molecules (Scheller *et al.*, 2011). IL-6R is a transmembrane glycoprotein belonging to the family of membrane bound  $\alpha$  receptors. Binding of IL-6 to membrane bound IL-6R leads to association with two molecules of the 150 kDa type 1 transmembrane protein, gp130. Creation of the IL-6R-gp130 homodimer leads to activation of the JAK/STAT, ERK and P13K pathways. However only macrophages, neutrophils, some T cells and hepatocytes express membrane bound IL-6R on their cell surface (Scheller *et al.*, 2011). These cells are able to shed IL-6R, creating soluble IL-6R. This, along with IL-6 is able to bind gp130 that conversely is found on the surface of most cell types therefore activating cell types that do not constitutively express membrane bound IL-6R (Rose-John *et al.*, 2007; Scheller & Rose-John, 2006). Cleavage of membrane bound IL-6R to soluble IL-6R is via the catalytic actions of the  $\text{Zn}^{2+}$  - metalloproteinase family, a disintegrin and metalloprotease (ADAM) (Mullberg *et al.*, 1994; Matthews *et al.*, 2003; Chalaris *et al.*, 2010). ADAM-10 is involved in the constitutive slow cleavage of membrane bound IL-6R to soluble IL-6R (Matthews *et al.*, 2003). ADAM-17 in contrast, is activated by IL-1 $\beta$ , TNF $\alpha$  and the synthetic phorbol ester, PMA to actively cleave IL-6R (Mullberg *et al.*, 1993). Interestingly soluble IL-6R has also been shown to be synthesised as a result of alternatively spliced IL-6R mRNA (Lust *et al.*, 1992). Alternative splicing of gp130 has also been shown to result in soluble gp130 (Daimant

*et al.*, 1997). It has been hypothesised that binding of soluble gp130, soluble IL-6R and IL-6 can lead to extracellular inhibition of IL-6 (Rose-John, 2012).

Transcriptional regulation of IL-6 appears to be cell type dependent. A study examining the transcription of IL-6 in murine macrophages identified a Notch binding motif that overlapped with a NF- $\kappa$ B binding site (Wongchana & Palaga, 2012). Additionally, up-regulation of IL-6 in this cell line required the cooperative actions of Notch and NF- $\kappa$ B. Conversely, Xiao *et al.*, 2004 report that sites of AP-1 and C/EBP in a prostate cancer cell line were the most important transcription factors for IL-6 expression. Using a luciferase reporter assay they showed that, although there is indeed a NF- $\kappa$ B binding site and NF- $\kappa$ B is recruited, NF- $\kappa$ B may be dispensable for IL-6 expression. Furthermore Zhang *et al.*, (2013) suggest that LPS-mediated TLR4 activation leads to binding of c-Jun to activating transcription factor 4 at the promoter of the IL-6 gene and this is required for TLR4-mediated IL-6 expression.

#### **1.14 Chronic Inflammatory disorders and cancer.**

Rheumatoid Arthritis is a chronic inflammatory disease that affects approximately 1% of the population of Great Britain as reported by the National Institute for Health and Care Excellence (NICE). The susceptibility to Rheumatoid Arthritis is proposed to be due to a combination of environmental and genetic factors leading to the onset of the disease (Moelants *et al.*, 2013).

Pain, stiffness and inflammation of the synovial membrane of diarthrodial joints are the main symptoms of those patients suffering with Rheumatoid Arthritis (Brennan *et al.*, 2008). Unsurprisingly, activated macrophages are numerous in the inflamed synovial membranes of affected joints, characterised by an overexpression of MHC class II and release of pro-inflammatory cytokines (Kinne *et al.*, 2000). TNF $\alpha$  in particular is present in the majority of synovial biopsies, studies have shown that TNF $\alpha$  induces leukocyte activation, pain receptor sensitization, angiogenesis and bone loss due to inhibition of osteoclast differentiation (McInnes & Schett, 2007; Moelants *et al.*, 2013). Inhibition of TNF $\alpha$  has also been shown to suppress the symptoms in various arthritis models, thus it is an attractive target in the treatment of Rheumatoid Arthritis (Brennan *et al.*, 2008).

A further consequence of chronic inflammatory disorders is the increased risk of developing a multitude of cancers. Chronic inflammation has been shown to have pro-tumourgenic effects possibly caused by a promotion in cell survival due to an increase in the release of the cytokines  $\text{TNF}\alpha$ , IL-1 and IL-6. Patients with Rheumatoid Arthritis have been shown to be two-fold more likely to develop lymphoma and leukemia, whilst they are at 20-50% increased risk of developing respiratory tract cancers (Beyaert *et al.*, 2013).

Other chronic inflammatory illnesses include Crohn's disease, ulcerative colitis and systemic lupus erythematosus. Crohn's disease and ulcerative colitis make up two of the main groups of inflammatory bowel diseases, and sufferers are at a higher risk of developing colorectal cancer. Further to this, systemic lupus erythematosus is associated with a higher risk of development of non-Hodgkin's lymphoma (Beyaert *et al.*, 2013).

Thus elucidating the mechanisms that regulate the immune responses orchestrating inflammation are important in order to generate new therapies to treat such conditions, and therefore lowering the risk to inflammatory derived cancers.

### **1.15 Aims**

Topo II $\beta$  is required for neuronal differentiation, more specifically it is shown to be required for both the up and down regulation of genes required for the early stages of neuronal development (Yang *et al.*, 2000; Lyu *et al.*, 2006). Levels of topo II $\beta$  protein also increase during neuronal differentiation thus reflecting its essential requirement in this process (Tiwari *et al.*, 2012). Other work has investigated the role of topo II in retinoic acid induced granulocytic differentiation, suggesting that topo II $\beta$  may negatively regulate the expression of essential transcription factors required for differentiation to occur (Aoyama *et al.*, 1998; McNamara *et al.*, 2008). However there is nothing in the literature to date that shows that topo II $\beta$  is required for macrophage differentiation.

The overall aim of this project was to determine if topo II $\beta$  is required for macrophage differentiation and/or for pro-inflammatory cytokine production.

To achieve this, a reliable model of differentiation was created. Levels of both topo II $\alpha$  and topo II $\beta$  mRNA and protein were measured in macrophage-like cells compared to monocyte-like cells.

The effect of down-regulating topo II $\beta$  on various markers of differentiation and cytokine production was measured. Various methods of topo II $\beta$  down-regulation were employed, including siRNA, stable topo II $\beta$  knock-out cell lines and usage of the topo II $\beta$  specific inhibitor, ICRF-193.

Chromatin Immunoprecipitation was also used to elucidate any topo II $\beta$  interaction at specific sites of interest.

## **Chapter 2**

### **Materials and Methods**

---

#### **2.1 Sterilisation**

Sterilisation was performed by autoclaving; buffers and pipette tips were heated to 121°C for 16 minutes at 0.14 MPa and left to cool before using.

Sterilisation of drugs was performed by passing the solution through a 0.22 µm filter.

All tissue culture work was performed inside a laminar flow hood (Microflow class II biological safety cabinet) to ensure sterility.

#### **2.2 Tissue Culture Constituents**

Tissue culture constituents including media, foetal calf serum and penicillin/streptomycin were purchased from GIBCO, Life Technologies.

Plastic ware including 25 cm<sup>3</sup> and 75 cm<sup>3</sup> culture flasks, multi-well plates and graduated pipettes for use in tissue culture were purchased from Greiner.

#### **2.3 Chemicals**

All chemicals were purchased from Sigma-Aldrich unless otherwise stated.

#### **2.4 Drugs**

Topoisomerase II drugs including ICRF-187, ICRF-193 and etoposide (VP-16) were purchased from Sigma-Aldrich. Dilutions of the drugs were made in dimethylsulphoxide (DMSO) also purchased from Sigma-Aldrich, and sterilised as described in Section 2.1.

## 2.5 Buffers

See Table 2.1

**Table 2.1. Chemical recipes for buffers used in experimental procedures.**

Buffers	Ingredients
Whole Cell Extraction Buffer	2% (w/v) SDS, 2 µg/ml pepstatin, 2 µg/ml leupeptin, 1 mM DTT, 1 mM benzamidine, 1 mM PMSF
4 x SDS PAGE Loading buffer	20% (v/v) glycerol, 4% (w/v) SDS, 25% (v/v) stacking gel buffer, 10% (v/v) β-mercaptoethanol, 5% (v/v) H <sub>2</sub> O, 0.004% (w/v) bromophenol blue
SDS-PAGE stacking gel buffer	0.25 M Tris-HCl (Melford) pH 6.8
SDS- PAGE separating buffer	0.75 M Tris-HCl (Melford) pH 8.8
10 X SDS-PAGE running buffer	250 mM Tris (Melford), 1.92 M Glycine (Melford), 1% (w/v) SDS
5 X Tris Buffered Saline (TBS)	100 mM Tris-HCl (Melford) pH 7.5, 2.5 M NaCl
TTBS (Probing of western blots)	1 x TBS, 0.05% (v/v) Tween20
Wet Western Transfer Buffer	25 mM Tris HCl (Melford) pH 8.3, 192 mM glycine (Melford), 10% (v/v) Methanol, 0.1% (w/v) SDS
Phosphate buffered saline (PBS)	1.37 M NaCl, 0.027 M KCl, 0.1 M Na <sub>2</sub> HPO <sub>4</sub> , 0.02 M NaH <sub>2</sub> PO <sub>4</sub>
Coomassie Blue Stain	45% (v/v) Methanol 45 % (v/v) H <sub>2</sub> O 10% Glacial acetic acid (v/v) 0.004% (w/v) Brilliant Blue R
Coomassie Blue de-stain	45% (v/v) Methanol 45% (v/v) H <sub>2</sub> O, 10% (v/v) Glacial Acetic Acid
ELISA Wash Buffer	1 X PBS 0.05% (v/v) Tween20



## 2.6 Antibodies

**Table 2.2. Details of purchase and dilution of antibodies used in experimental procedures.**

Antibody	Details	Concentration used
Anti-Topoisomerase II $\alpha$	Rabbit polyclonal IgG (Sigma AV04007) Western Blotting	1.25 $\mu$ g/ml
Anti-Topoisomerase II $\beta$	Mouse Polyclonal (BD Bioscience 611493) Western Blotting	1/500
Anti-GAPDH	Rabbit polyclonal IgG (abcam ab9485) Western Blotting	1 $\mu$ g/ml
Anti-TNF $\alpha$	Mouse monoclonal (abcam ab9485) Western Blotting	1/5000
Anti- rabbit –HRP conjugated	Goat polyclonal IgG (abcam ab6721) Western Blotting	1/1000
Anti-mouse –HRP conjugated	Rabbit polyclonal IgG (DAKO P0260) Western Blotting	1/1000
Anti-CD11b –APC conjugated	(eBioscience 17-0118-41) Flow Cytometry	1/10
Anti-HLA-DR –FITC conjugated	(eBioscience 11-9956-73) Flow Cytometry	1/10
Anti-TLR4 –PE conjugated	Serotech Flow Cytometry	1/10

## 2.7 qPCR Constituents

Mastermix for use in qPCR with hydrolysis primer-probes was purchased from Primer-Design (Precision-iC 2X qPCR mastermix).

Mastermix for use in qPCR with non-probe bound primers was purchased from BIO-RAD (iQ- SYBR green supermix 170-886)

**Table 2.3. Details of Hydrolysis primers used for qPCR.**

Primer	Details	Sequence
Homo sapiens topoisomerase (DNA) II $\alpha$	Taqman Primer Design	Forward: TGGATTTGGATTCAGATGAAGATTT Reverse:CTAAGTTTTGGGGAAGTTTTGGT
Homo sapiens topoisomerase (DNA) II $\beta$	Taqman Primer Design	Sense:ATATGTCTCTGTGGTCTCTTACTAAA Anti-sense:GCCGCTAAATCCTCTTTCCAA
TLR2*	Life technologies Hs00152932_m1	Sequence not provided
TLR4*	Life technologies Hs00152939_m1	Sequence not provided
SP1*	Life technologies Hs02786711_m1	Sequence not provided
NF $\kappa$ B*	Life technologies Hs00765730_m1	Sequence not provided
IL-1 $\beta$	Life technologies Hs01555410_m1	Sequence not provided
POLR2A*	Life Technologies Hs00172187_m1	Sequence not provided
EGR2*	Life Technologies Hs00166165_m1	Sequence not provided
TNF $\alpha$	Life Technologies Hs01113624_g1	Sequence not provided
18S*	Life Technologies Hs99999901_s1	Sequence not provided

\* Primer Probes kindly donated by Dr J Taylor, Newcastle University

## **2.8 Cell Lines**

### **2.8.1 Characterisation of U937 cells and maintenance in culture**

U937 cells were purchased from the American Type Culture Collection (ATCC) and are originally derived from a 37 year old Caucasian male suffering from histiocytic lymphoma. Cells were obtained originally from a pleural effusion and are characterised as being monocytic. U937 are suspension cells, they were maintained at a cell density between  $1 \times 10^5$  and  $6 \times 10^5$  cells/ml in RPMI-1640 medium supplemented with 10% (v/v) FCS, 45.5 units/ml Penicillin, 45.5  $\mu$ g/ml streptomycin and 2 mM glutamine. Cells were cultured in T25 or T75 flasks and incubated at 37°C, 5% (v/v) CO<sub>2</sub> in a humidified atmosphere.

### **2.8.2 Characterisation of HL-60 cells and maintenance in culture**

HL-60 cells were purchased from the American Type Culture Collection (ATCC) and are originally derived from a 36 year old Caucasian female suffering from acute promyelocytic leukaemia. Cells were originally obtained from peripheral blood leukocytes by leukopheresis and are characterised as promyeoblasts. HL-60 are suspension cells, they were maintained at a cell density between  $1 \times 10^5$  and  $6 \times 10^5$  cells/ml in RPMI-1640 medium supplemented with 10% (v/v) FCS, 45.5 units/ml penicillin, 45.5  $\mu$ g/ml streptomycin and 2 mM glutamine. Cells were cultured in T25 or T75 flasks and incubated at 37°C, 5% (v/v) CO<sub>2</sub> in a humidified atmosphere.

### **2.8.3 Characterisation of Mouse Embryonic Fibroblasts (Wild Type and #5) and maintenance in culture**

Wild type and stable topo II $\beta$  knock-out mouse embryonic fibroblasts (MEFs) were kindly provided by Prof C. A. Austin, Newcastle University. Cells were grown to confluency in Dulbecco's Modified Eagle Medium (DMEM), supplemented with 10% (v/v) FCS, containing 45.5 units/ml penicillin, 45.5  $\mu$ g/ml streptomycin and 2 mM glutamine. Cells were cultured in T25 or T75 flasks and incubated at 37°C, 5% (v/v) CO<sub>2</sub> in a humidified atmosphere. Passage of cells required the detachment of cells from the culture flask. Media was removed from the flask (T25) and cells were washed with 5 ml of 1 x PBS (Table 2.1). 1.5 ml of 0.25% (v/v) Trypsin was then added to the flask and cells were incubated for 1 min at 37°C. 4 ml of fresh media was then added to the flask to stop the reaction. The flask was then gently agitated to facilitate the detachment

of the cells. The cells were then harvested and centrifuged at 500 x g for 3 min. Media containing trypsin was removed and the cells were washed in 5 ml of 1 x PBS, as described previously. Cells were centrifuged again at 500 x g for 3 min. PBS was removed and cells were re-suspended in 10 ml of fresh media, and added to a new culture flask.

## **2.9 Cell Harvesting**

Non-adherent U937 and HL-60 cells were removed from the culture flask and centrifuged for 5 min at 1500rpm. Media was then removed and fresh media was added to the cells. Cells were then placed into a fresh culture flask. If U937 and HL-60 had been treated with Phorbol-Myristate acetate and thus adhered to the culture flask, media was first gently removed from the flask and removed. 5 ml (for T25) 10 ml (for T75) of 1 X PBS was then added to the flask. A 18 mm cell scraper (Fisher) was then used to gently detach the cells from the culture flask. Cells were then centrifuged for 5 min at 500 x g. The PBS was removed and cells were re-suspended in fresh media.

## **2.10 Cell Counting**

Cell counts were performed using an Improved Neubauer hemocytometer (0.1 mm, 1/400 mm<sup>2</sup>). Briefly, a steamed cover slip was applied on top of the chambers. The presence of newton rings implied successful application. 12 µl of cell suspension was then added to each chamber and cells in the four large corner squares of each were counted. Each large square represented 10<sup>4</sup> cells/ml. By counting the cells seen in the 1 mm<sup>2</sup> squares, and taking the dilution factor into account the number of cells in the original suspension can be calculated using the equation below;

$$\text{Mean cell count per } 1\text{mm}^2 \text{ square} \times \text{dilution factor} = \text{cells/ml} \times 10^4$$

If Trypan Blue Exclusion was to be performed, a 1:1 mix of cell suspension to Trypan Blue was performed immediately before counting.

## **2.11 Preparation of liquid nitrogen stocks**

Cells were counted as previously described (Section 2.8) and washed twice in PBS. 2 x 10<sup>6</sup> cells/ml were then suspended in 1 ml of freezing solution (FCS containing 10% DMSO) and transferred to a cryovial (Nunc). Cryovials were then stored in a Mr Frosty

(Thermo-scientific) container and placed in an -80°C freezer for 24 h before being transferred to a liquid nitrogen container (Statebourne bio 36).

## **2.12 Peripheral Blood Mononuclear Cell Isolation**

Peripheral blood mononuclear cell (PBMC) isolation was used to obtain primary monocytes. A qualified phlebotomist obtained 50 ml of venous blood from consenting healthy volunteers (Project Reference SUB86\_AJ\_0511 with regards to Ethical Approval)

Specialised leucosep tubes (Greiner) were used to separate whole blood into plasma, buffy coat (leukocytes and platelets) and erythrocytes. The tubes were prepared prior to addition of whole blood by addition of 15 ml of lymphoprep (Axis-Shield). The tubes were then centrifuged briefly to ensure the lymphoprep was below the filter in the leucosep tube. Whole blood was then added to the leucosep tube and was centrifuged for 12 min at 700 x g with no deceleration.

The plasma fraction was contained above the filter in the leucosep tube. This was carefully removed and discarded. The buffy coat layer was then transferred into a sterile 50 ml falcon tube. The fraction containing the erythrocytes was also discarded. 50 ml of FCS free-RPMI-1640 was then added to the buffy coat in the tube, and the tube was centrifuged at 600 x g for 10 min with maximum deceleration.

The supernatant was then discarded and the remaining cells were re-suspended in 2 ml of FCS free -RPMI-1640. A cell count was then performed using a Casy® Counter.

## **2.13 CD14 selection of PBMCs**

### **2.13.1 Background**

Isolation of CD14<sup>+</sup> cells from freshly isolated PBMCs was performed using magnetic cell sorting of human leukocytes (MACS) (Miltenyi Biotec). This method involves the addition of a mouse monoclonal anti-human CD14 antibody conjugated to magnetic microbeads. The antibodies then bind to CD14<sup>+</sup> cells, and when the sample is applied to a magnetic field, these cells are attracted to the magnetic field and become firmly

attached to the side of the tube. Thus cell that are not antibody bound are flushed from the sample, leaving only CD14<sup>+</sup> remaining.

### **2.13.2 Method**

Freshly isolated PBMCs were centrifuged at 500 x g for 5 min.  $1 \times 10^7$  cells were then re-suspended in 50 µl of buffer (2 mM EDTA/PBS pH 7.2, 0.5% (v/v) FCS). 20 µl of CD14 Microbeads (Miltenyi Biotec) were then added to the suspension of cells, which were then mixed and incubated for 15 min at 4°C. 1.5 ml of buffer (as previous) was then added to the suspension of cells, this was followed by centrifugation at 1500rpm for 5 min. The supernatant was removed and cells were re-suspended in 500 µl of buffer (as previous). At this time a MACS MS<sup>+</sup>/RS<sup>+</sup> column was applied to the MACS separator (magnetic field) and washed with 500 µl of buffer (as previous). The cell sample was then added and any flow through was discarded. The column was then washed a further 3 times with 500 µl of buffer (as previous). The column was then removed from the MACS separator and 1 ml of buffer was used to flush out the CD14<sup>+</sup> cells.

## **2.14 Flow cytometry**

### **2.14.1 Background**

Flow cytometry was used to measure levels of various cell surface antigens. When a sample is processed by flow cytometry it is hydro-dynamically focused using sheath fluid to pass through a very small nozzle which then takes single cells past the laser light. The cells when passed across the path of the laser light cause the light to scatter. Detectors in front of the laser measure the forward scatter, which corresponds to the size of the cell and detectors to the side of the laser measure the side scatter that corresponds to the granularity of the cell. Thus cells in a sample containing multiple cell types can be identified by their size and granularity.

If the cells have been treated with a fluorochrome-conjugated antibody raised to bind to a particular extracellular antigen then once the sample is excited at a particular wavelength, the fluorochrome will emit detectable light. For example FITC conjugated antibody labelled samples when excited at 519 nm will emit a detectable light. This then allows the detection and quantification of extracellular antigens.

#### **2.14.2 Quantitation of surface antigen expression using Flow cytometry**

Cells were harvested as appropriate (Section 2.9) and washed twice with PBS containing 0.1% FCS (see Table 2.1). Cells were then transferred to a FACs tube (Sarstedt) and centrifuged at 1000rpm for 5 min. PBS was removed and cells were re-suspended in 20  $\mu$ l of fresh PBS containing 0.1% (v/v) FCS. 2  $\mu$ l of antibody (see Table 2.2 for antibodies used) was then added. One sample did not have antibody added to it, this acts as the unstained control. Cells were gently mixed and allowed to incubate for 30 min out of visible light. Samples were then washed twice with 1 ml PBS and re-suspended in 300  $\mu$ l PBS. Flow cytometry was then performed.

Method of analysis of flow cytometry data is described in Figure 2.1.

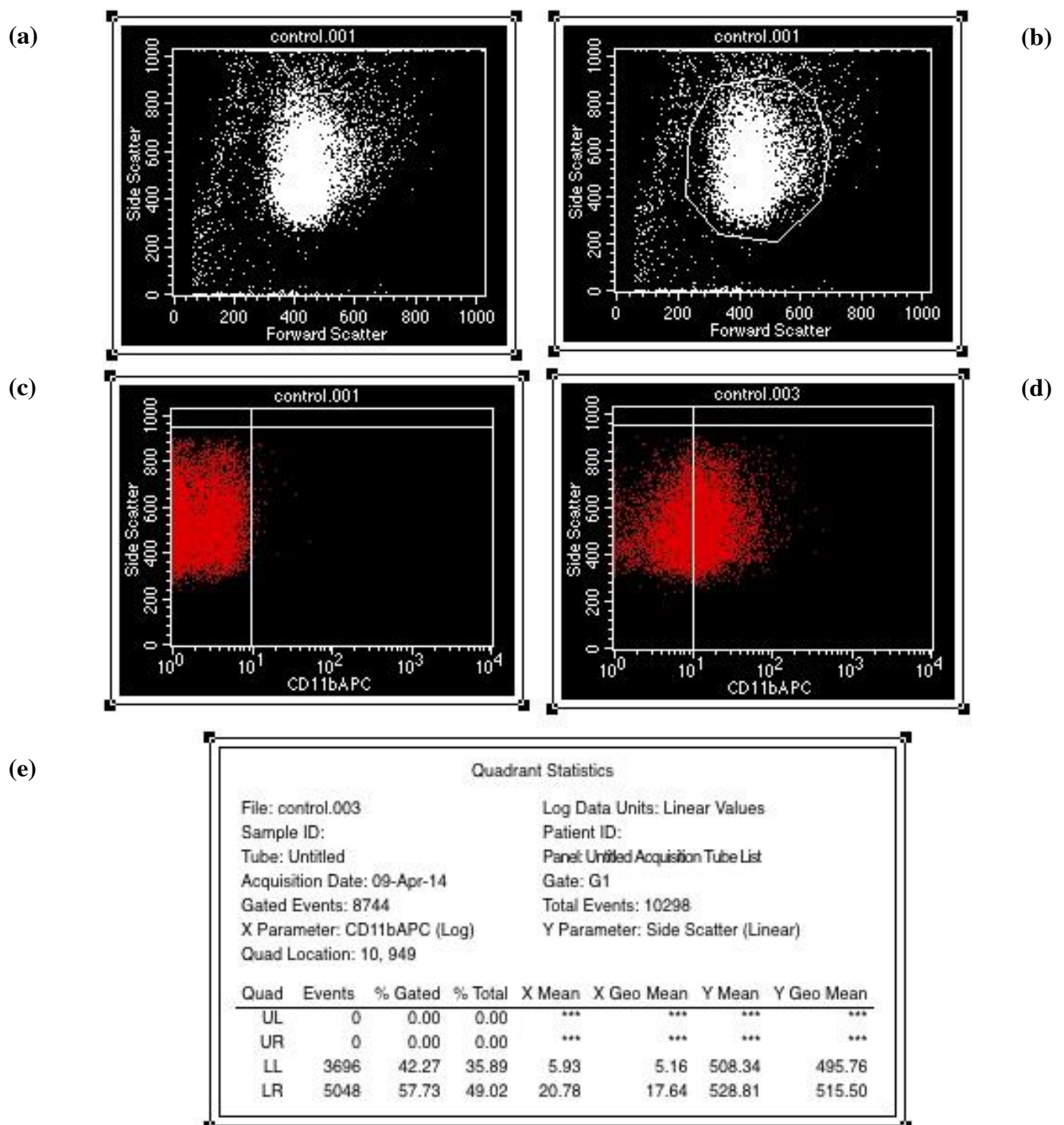


**Figure 2.1 Method of analysis of data obtained by flow cytometry.** The first scatter graph obtained plots the side scatter against the forward scatter, thus the size and granularity of cells can be determined. A single acquired cell is represented as a dot on the scatter graph (a). The cell population was then gated and the gate applied to any future analysis (as shown by white polygon surrounding large cell population (b)). The forward scatter on the X axis is then changed to represent the channel detecting the conjugate on the antibody bound to each cell. The first sample processed should be an unstained control, thus any auto-fluorescence produced by the cell can be gated out (as shown by the quadrant) (c). Samples that have been stained with antibody can then be analysed; applying the gate determined in (b) and then the quadrant determined in (c). Therefore only cells in the lower right quadrant are considered positive for the surface antigen investigated (d). Statistics can then be determined for each quadrant including the mean fluorescent intensity captured from the cells in each particular quadrant (e). It is important to note that if mean fluorescent intensity is reported that the quadrants are not employed. Cells used in this example were 0.1% DMSO (v/v) treated U937 cells.



### **2.14.3 Cell cycle analysis using Flow cytometry.**

Cells were harvested (Section 2.9) and washed twice with PBS. Cells were then resuspended in 200 µl PBS and added drop-wise to 2ml of ice cold 70% (v/v) Ethanol in PBS. Cells were fixed for 30 min at 4°C. The fixative was then removed and the cells were resuspended in 1 ml of PBS containing 0.2 µg/ml RNase A and 10 µg/µl propidium iodide. Cells were then incubated for 30 min at 37°C. Flow cytometry was then performed.

## **2.15 XTT Assay**

### **2.15.1 Background**

The XTT assay uses (2,3 -Bis- [2-methoxy-4-nitro-5-sulfophenyl] -2H-tetrazolium-5-carboxyanilide salt (XTT) to measure cell viability. Living cells actively metabolise, thus the mitochondria in these cells produce NADH. NADH reduces the yellow tetrazolium salt, XTT into a soluble orange formazan dye in the presence of an electron-coupling agent, PMS. The resulting colour formation can then be measured spectrophotometrically. As the amount of NADH directly correlates with cell viability, then the amount of reduced XTT is a reliable measure of cell viability (Berridge *et al.*, 2005).

### **2.15.2 Method**

The XTT was stored at -20°C in 2.5 ml aliquots at a concentration of 1 mg/ml in RPMI-1640. PMS was stored at -20°C in 15 µl aliquots at a concentration of 5 mM in PBS. Before use the XTT was defrosted in a water-bath at 50°C in order to dissolve any visible precipitate. PMS was defrosted at room temperature, 12.5 µl of PMS was then added to 2.5 ml XTT just before use. 50 µl of the XTT/PMS reagent was then added to each 200 µl cell sample (in a 96 well plate). The plate was then incubated at 37°C, 5% (v/v) CO<sub>2</sub> in a humidified atmosphere for 4 hrs. The endpoint absorbance was then read at 450nm on a spectrophotometer (Synergy). A further endpoint absorbance read was at 630nm in order to be able to eliminate any smudges on the plate that may affect the end result.

The value obtained for the plate read at 630nm was then subtracted from the value obtained for the 450nm value on the corresponding wells. The value for the well

containing media only was also subtracted from the values of all wells. An average of the experimental replicates was determined, and percentage cell viability was determined by calculated as follows:

$$\frac{\text{Specific absorbance of test sample}}{\text{Specific absorbance of control sample}} \times 100$$

## **2.16 Quantifying protein expression**

### **2.16.1 Whole Cell Extraction**

Cells were washed in 5 ml of PBS containing protease inhibitors in order to reduce protein degradation (leupeptin, pepstatin, DTT, benzamidine, and PMSF, see Table 2.1). Lysis buffer containing 2% (w/v) SDS in PBS and inhibitors (leupeptin, pepstatin, DTT, benzamidine, and PMSF) was heated to 68°C before addition to cells. Cells were incubated for 5 min at 68°C in the lysis buffer before being passed through a fine gauge needle 10 times in order to shear DNA.

### **2.16.2 Quantification of total protein**

Quantification of total protein in whole cell lysates was performed using the BCA Protein Assay kit (Thermo-scientific). This assay uses a two-step reaction to quantify protein levels. Initially addition of the bicinchoninic acid (BCA) substrate to the protein samples causes reduction of the cuprous ions (in the substrate) to cupric ions by the peptide bonds in the protein. The resulting cupric ions then chelate with the BCA in the substrate, creating a purple coloured complex that can be measured spectrophotometrically at 562nm (Smith *et al.*, 1985).

Standard samples were prepared by diluting bovine serum albumin in PBS to create a range of concentrations (125, 250, 500, 750, 100, 1500 and 2000 ng/ml). Whole cell lysate samples were diluted 1/10 in PBS. 10 µl of sample was added to a well of a 96 well plate in triplicate. 200 µl of a 50:1 ratio of the BCA working reagents A and B was then added to each well. The plate was then incubated at 37°C for 30 min before the endpoint absorbance was measured at 562nm (BMG labtech).

Absorbance values were then plotted against the concentration of standard samples and linear regression of the line was used to determine concentration of protein in unknown samples. Results were multiplied by 10 in order to adjust for the dilution.

### **2.16.3 Preparation of whole cell lysates for SDS- PAGE**

Lysates were prepared for separation by SDS-PAGE by addition of 2 x loading buffer (Table 2.1) at a 2:1 dilution. Samples were then heated for 3 min at 68°C. Heating above this temperature has been shown to affect levels of topoisomerase II (Woessner *et al.*,1990).

### **2.16.4 SDS- PAGE**

Sodium dodecyl sulphate polyacrylamide gel electrophoresis (SDS-PAGE) was used to separate proteins in order of size. SDS-PAGE was performed using a 7.5% (v/v) gel. The gels made were 13 cm long, 18 cm wide and 1.55 mm thick, with a stacking gel of 2 cm in depth. The gels were made using the recipe shown in Table 2.4. After addition of the resolving gel to the plates, 70% (v/v) isopropanol was layered on top to prevent the formation of bubbles. This was washed off with water after the gel had set and before the addition of the stacking gel. The gel was placed into a mini PROTEAN Tetra system (BIO-RAD) with SDS-PAGE running buffer (Table 2.1) Samples were loaded onto the gel along with a pre-stained molecular weight marker (BIO-RAD) and proteins were separated for 1 h at 100 V using a power pac 200 (BIO-RAD).

**Table 2.4 Constituents of 7.5% Polyacrylamide Gel**

Resolving Gel		Stacking Gel	
Separating buffer (Table 2.1)	7.5 ml	Stacking buffer (Table 2.1)	6 ml
30% (w/v) Acrylamide	3.75 ml	30% (w/v) Acrylamide	2 ml
H <sub>2</sub> O	3.45 ml	H <sub>2</sub> O	3.7 ml
10% (w/v) SDS	150 µl	10% (w/v) SDS	120 µl
10% (w/v) APS	100 µl	10% (w/v) APS	120 µl
TEMED	50 µl	TEMED	10 µl

**2.16.5 Wet Western blot**

Wet Western blotting was used to transfer proteins vertically from the SDS-PAGE gel as described in Section 2.16.4 onto a 0.45 µm nitrocellulose membrane (BIO-RAD). Protein was transferred from the gel onto nitrocellulose using wet Western blotting. Sponges, filter paper (Whatmann) and nitrocellulose were soaked in wet Western buffer for 10 min prior to assembly of the plates. A sponge was placed on the black plate, followed by filter paper (cut to the size of the gel) and the gel. Nitrocellulose also cut to the size of the gel was placed on the gel and any bubbles underneath were removed. A second sheet of filter paper was placed on the nitrocellulose followed by the second sponge, that plates were closed and placed into the mini trans-blot electrophoretic transfer cell (BIO-RAD) along with wet western buffer (Table 2.1) prior to electrophoresis at 100 V, 500 mA for 1 hr.

**2.16.6 Coomassie staining**

Following wet Western transfer gels were stained with Coomassie blue stain (Table 2.1) overnight at room temperature with gentle agitation. Coomassie blue stain was then removed and gels were allowed to soak in de-stain (Table 2.1) until the gels became transparent. The gels were then inspected for any blue bands thus indicating any remaining protein and an inefficient transfer.

### **2.16.7 Probing**

Blots were incubated overnight in 50 ml TTBS (see Table 2.1) with 3% (w/v) powdered skimmed milk at 4°C to block any non-specific protein binding sites. Blots were then washed 3 x 5 min in 50 ml TTBS. The primary antibody was then diluted as appropriate (see Table 2.2 for antibody information) in 3% (w/v) powdered skimmed milk in TTBS; the blot was then submerged in the diluent containing antibody and allowed to incubate for 2 h at room temperature with gentle agitation. The primary antibody sera was then removed and the blot was washed 3 x 5 min in 50 ml TTBS. The secondary antibody was then diluted as appropriate (Table 2.2) in 3% (w/v) powdered skimmed milk in TTBS. The blot was then submerged into the antibody containing diluent and allowed to incubate for 1 h at room temperature with gentle agitation. The antibody diluent was then removed and the blot was washed again 3 x 5 min in 50 ml TTBS. Detection of protein was then performed using an enhanced chemiluminescent substrate (45 µl coumaric acid (1.5% (w/v) in DMSO), 100 µl luminol (4.4% (w/v) in DMSO) in 10 ml 100 mM Tris-HCl pH 8.5 combined with 6 µl hydrogen peroxide in 10 ml 100 mM Tris-HCl pH 8.5). The blot was submerged in the ECL substrate for 1 min before exposure and capture using the G-box chemiluminescent detection system (Syngene).

### **2.16.8 Densitometry**

Densitometry was performed using synergy genetools software. Bands were adjusted for background noise by subtracting the arbitrary unit given for the background away from the arbitrary unit given for the protein band.

## **2.17 Quantifying mRNA expression**

### **2.17.1 RNA Extraction**

RNA extraction was performed using the High Pure RNA Isolation kit (Roche). Cells were pelleted and all supernatant was removed. 1 ml of Tri Reagent reagent was added to the cells and incubated for 5 min at room temperature to allow complete dissociation of nucleoprotein complexes. 200 µl of chloroform was then added to each sample and the tubes were mixed vigorously by hand for 15 sec. Samples were then left to incubate for 2 min at room temperature. Samples were then centrifuged for 15 min at 13000 x g

and 4°C. Following this, 400 µl of the colourless upper fraction of the sample was transferred to a new RNase free tube. 400 µl of 70% (v/v) ethanol was then added to the tube and the sample was then vortexed to ensure thorough mixing. 700 µl of sample was then transferred to a spin cartridge with a collection tube and was centrifuged for 15 sec at 13000 x g. The sample flow through was then discarded from the collection tube. 350 µl of wash buffer I (Roche) was then added to the spin cartridge and the sample was centrifuged for 15 sec at 13000 x g. The flow through and collection tube was then discarded and the spin cartridge inserted into a fresh collection tube. 80 µl of DNase mixture (8 µl of the provided 10x DNase reaction buffer, 10 µl of the provided DNase, 62 µl RNase free water) was then added to each sample to digest any contaminating DNA in the sample. Samples were left to incubate with the DNase mixture for 15 min at room temperature before 350 µl of the provided wash buffer I was added and the tubes centrifuged for a further 15 sec at 13000 x g. Sample flow through was then discarded and 500 µl of wash buffer I was added to the tube followed by centrifugation at 13000 x g for 15 sec. Sample flow through was then discarded and the step using wash buffer II (Roche) was repeated. The spin cartridge was then centrifuged for 1 min at 13000 x g to dry the membrane with the bound RNA. The cartridge was then inserted into a recovery tube and 30 µl of RNase free water was added to it and left to incubate for 1 min at room temperature. The spin cartridge/recovery tube was then centrifuged at 13000 x g for 1 min. The spin cartridge was then discarded and the recovery tube containing the sample was stored at -80°C until required.

### **2.17.2 Reverse Transcription**

Synthesis of cDNA from RNA was performed using the Precision nanoscript reverse transcription kit (PrimerDesign). Annealing was performed by the addition of RNA to a 0.2 ml thin walled PCR tube, along with 1 µl of the provided random nonamer primer and nuclease free water in order to obtain a reaction volume of 10 µl. The resulting sample was then heated at 65°C for 5 min. An ice water bath was used to immediately cool the sample.

Extension was performed by the addition of 10 µl of reverse transcription mastermix (Table 2.5) followed by incubation at 25°C for 5 min. A control sample was also performed at this time, where all components of the mastermix were added with the exception of the nanoscript enzyme (the transcriptase). This was performed for each

sample. The sample was then incubated for a further 15 min at 55°C. Heat inactivation of the sample was then performed by incubation at 75°C for 15 min. Samples were then stored at -20°C until used.

**Table 2.5. Volume of components used to generate a master-mix for reverse transcription.**

Reverse transcription component	Volume required (final volume 10µl)
Nanoscript 10X buffer (provided)	2.0 µl
dNTP mix 10 mM (each)	1.0 µl
DTT 100 mM	2.0 µl
RNase/ DNase Free water	4.0 µl
Nanoscript enzyme (provided)	1.0 µl

### 2.17.3 qPCR

qPCR was performed using the C1000 Thermal Cycler BIO-RAD CFX96 Real time system. For each hydrolysis probe to be analysed a mastermix was made up; this contained 1 µl primer/probe, 10 µl mastermix (Precision-iC 2X qPCR mastermix) and 4 µl of RNase/DNase free water per sample. 15 µl of this mastermix was added to each well of a 96 well PCR plate (BIO-RAD, HSP-945). 5 µl of 5 ng/µl of sample cDNA was added in triplicate to the plate. A no template control (RNase/DNase free water) was added in duplicate to the plate for each probe used. In addition the reverse transcription control (without enzyme – see Section 2.17.2) was also added to the plate in duplicate. This was necessary to determine if any genomic DNA is present in the samples. The conditions for qPCR are outlined in Table 2.6.

Analysis was performed using the comparative  $\Delta\Delta C_t$  method (Livak & Schmittgen, 2001) to determine relative fold expression compared to the control sample.

For example;

$$\Delta Ct = \text{Sample Ct value} - \text{Reference Ct value}$$

$$\Delta Ct \text{ expression} = 2^{-\Delta Ct}$$

$$\Delta\Delta Ct \text{ expression} = \frac{\text{Test } \Delta Ct \text{ expression}}{\text{Control } \Delta Ct \text{ expression}}$$

$$\Delta\Delta Ct \text{ expression} \times 100 = \text{Percentage fold expression}$$

**Table 2.6. Reaction conditions for qPCR using Hydrolysis probes.**

PCR step	Conditions
1. Enzyme Activation	95°C 10:00
2. Denaturation	95°C 0:15
3. Data collection	50°C 0:30
4. Extension	72° 0:15
Go to step 2	(x50 times)



## 2.18 ELISAs

All ELISA kits were purchased from eBiosciences as part of the 'Ready-set-go' range. Figure 2.2 illustrates the principle of the sandwich enzyme linked immunosorbant assay.

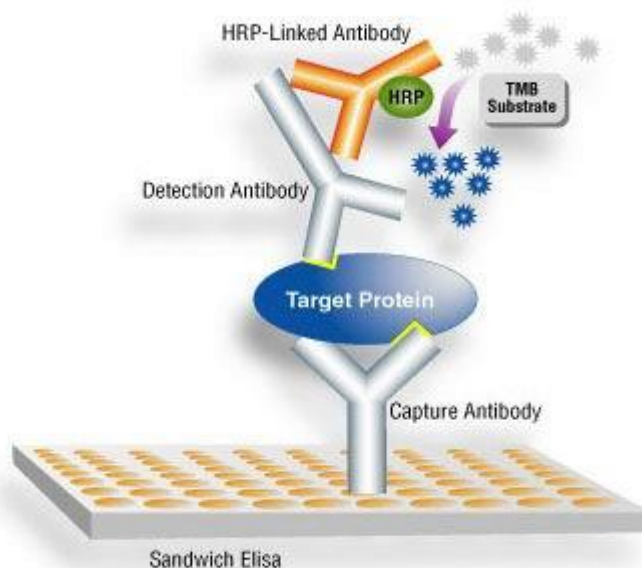


**Figure 2.2 Diagrammatic representation of a sandwich enzyme linked immunosorbant assay (ELISA) diagram taken from EIAab News.**

This method indirectly detects the presence of the target protein. The capture antibody is coated onto a 96 well ELISA plate, the sample containing the target protein is added to the plate where it will bind to the capture antibody. A second antibody capable of detecting the target protein is then added and binds to the protein. In order to allow detection of the bound detection antibody, a horse-radish peroxidase (HRP) conjugated antibody that recognises and binds to the detection antibody is added. A 3, 3', 5,5' Tetramethylbenzidine (TMB) substrate is then added, and the (HRP) causes the oxidation of the substrate and thus a measurable colour change can be observed.

### 2.18.1 ELISA to human TNF $\alpha$

Quantification of TNF $\alpha$  released into the supernatant was performed using the Ready-Set-Go ELISA kit to human TNF $\alpha$  (eBioscience). A 96 well ELISA plate was coated with a TNF $\alpha$  capture antibody. 48  $\mu$ l of capture antibody was diluted in 12 ml of the supplied coating buffer, 100  $\mu$ l was then added to each well. The plate was then sealed and incubated overnight at 4°C. The wells were then aspirated and washed by

submerging the plate into a bath containing ELISA wash buffer (Table 2.1). This was repeated 5 times. The top TNF $\alpha$  standard was prepared by adding 6  $\mu$ l of 1.65  $\mu$ g/ $\mu$ l recombinant TNF $\alpha$  to 20 ml of the supplied assay diluent. A serial dilution was performed using assay diluent and 100  $\mu$ l of standard samples and experimental samples (diluted  $\frac{1}{2}$ ) were then added to the plate in triplicate. The plate was then incubated for 2 h at room temperature. The wells were then aspirated and washed 3 times in ELISA wash buffer (Table 2.1). TNF $\alpha$  detection antibody was diluted 48  $\mu$ l in 12 ml in the supplied assay diluent and 100  $\mu$ l of this was added to each well of the 96 well plate. The plate was incubated for a further hour at room temperature. Wells were again aspirated and washed 5 times in ELISA wash buffer (Table 2.1). The avidin –HRP enzyme was diluted 48  $\mu$ l in 12 ml of assay diluent and 100  $\mu$ l of this was added to each well of the 96 well plate. The plate was then incubated for 30 min at room temperature before the wells were aspirated and washed 7 times in ELISA wash buffer. 100  $\mu$ l of substrate solution was then added to each well and the plate was left to incubate for a further 15 min. 50  $\mu$ l of 2M H<sub>2</sub>SO<sub>4</sub> was then added to each well to stop the reaction. The plate was then read at 450 nM and 570 nM on a spectrophotometer (synergy).

#### **2.18.2 ELISA to human IL-1 $\beta$**

Quantification of IL-1 $\beta$  released into the supernatant was performed using the Ready-Set-Go ELISA kit to human IL-1 $\beta$  (eBioscience). This was performed using the same methodology as 2.18.1. However the topo IL-1 $\beta$  standard was prepared by adding 10  $\mu$ l of 1  $\mu$ g/ $\mu$ l recombinant IL-1 $\beta$  to 20 ml of the supplied assay diluent.

#### **2.18.3 ELISA to mouse IL-6**

Quantification of IL-6 released into the supernatant was performed using the Ready-Set-Go ELISA kit to mouse IL-6 (eBioscience). This was performed using the same methodology as 2.18.1. However the topo IL-6 standard was prepared by adding 10  $\mu$ l of 1  $\mu$ g/ $\mu$ l recombinant IL-6 to 20 ml of the supplied assay diluent.

#### **2.18.4 ELISA to mouse IL-1 $\alpha$**

Quantification of IL-1 $\alpha$  released into the supernatant was performed using the Ready-Set-Go ELISA kit to mouse IL-1 $\alpha$ . This was performed using the same methodology as

2.18.1. However the topo IL-1 $\alpha$  standard was prepared by adding 10 $\mu$ l of 1  $\mu$ g/ $\mu$ l recombinant IL-1 $\alpha$  to 20 ml of the supplied assay diluent.

## **2.19 Chromatin Immunoprecipitation.**

### **2.19.1 Crosslinking of chromatin**

Chromatin Immunoprecipitation was performed to determine the association of topo II $\beta$  with regions of interest within the IL-1 $\beta$  and TNF $\alpha$  genes.

A Magna -EZ ChIP kit (Millipore) was kindly donated by Prof C. A Austin, Newcastle University.

Media from adherent cells was removed and replaced with 30 ml of fresh media. 1.1 ml of fresh formaldehyde (0.925 g paraformaldehyde, 4.8 ml H<sub>2</sub>O, 35 $\mu$ l 1N KOH) was then added and cells were left to incubate for 10 min at room temperature. 2 ml of glycine was then added, the flask was agitated, and then allowed to incubate for a further 5 min. Media was then removed and replaced with cold PBS. Cells were washed twice in PBS. 2 ml of PBS containing protease inhibitors (2  $\mu$ g/ml pepstatin, 2  $\mu$ g/ml leupeptin, 1 mM DTT, 1 mM benzamidine, 1 mM PMSF) was then added and cells scraped and pelleted by centrifugation at 500 x g for 5 min. All PBS was then removed and the cell pellet was frozen at -80°C until used.

### **2.19.2 Cell Lysis and Sonication**

Once the cell pellet was thawed, 0.5 ml of the supplied cell lysis buffer containing 1 x protease inhibitor cocktail (Millipore) was then added. The cells were left to incubate for 15 min and vortexed every 5 min in that time. The suspension was then centrifuged at 800 x g for 5 min at 4°C. The supernatant was then removed and 0.5 ml of the supplied Nuclear Lysis buffer containing 2.5  $\mu$ l of the provided 1 x protease inhibitor cocktail (Millipore) was then added to the lysed cells. The suspension was then left on ice and sonication was used to shear the cross-linked DNA. Sonication cycles were performed at 25% power for 15 sec. Following sonication cells were centrifuged at 10000 x g for 10 min at 4°C.

### **2.19.3 Immuno-precipitation of cross-linked chromatin**

Protein A Magnetic beads (Millipore) and antibody were then prepared. Antibody was added to the upper liquid of 25  $\mu$ l of Protein A Beads (see Table 2.7 for dilution details). The suspension was then mixed and left to incubate for 30 min at room temperature to allow binding of the antibody to the beads.

Chromatin suspension (the sample after sonication) was then diluted 1/10 in the supplied dilution buffer (with 17.5  $\mu$ l of 1 x protease inhibitors added) and split into 500  $\mu$ l aliquots. The aliquots were then added to the Protein A Magnetic beads/antibody suspensions. The samples were then left to incubate for 18 h at 4°C with rotation.

Protein A Magnetic beads were then separated from the rest of the sample using a magnetic separator. The antibody/chromatin complex was then washed by re-suspending it in 0.5 ml in a series of wash buffers provided in the Magna EZ ChIP kit; Low salt Immune Complex Wash buffer, High Salt Immune Complex Wash buffer, LiCl Immune Complex Wash buffer and TE Buffer (all Millipore), allowing 5 minutes for incubation for each wash.

### **2.19.4 Reverse crosslinking**

100  $\mu$ l of the supplied ChIP Elution buffer (with 1  $\mu$ l Proteinase K) was added to all samples including the 'Input' sample and left to incubate for 3 h at 62°C with rotation. The samples were then heated to 95°C for 10 min. Samples were then cooled to room temperature. The beads were then removed from the sample using a magnet.

### **2.19.5 DNA Purification**

DNA was purified by adding 0.5 ml of Bind reagent A (Millipore) to each 100  $\mu$ l DNA sample (including 'INPUT'). The sample was then transferred to spin column (with filter) in a collection tube. The column was then centrifuged for 30 sec at 10,000 x g. The flow through was then discarded and the column placed back into the collection tube. 500  $\mu$ l of Wash Reagent 'B' (Millipore) was then added to the spin filter and the sample was centrifuged for a further 30 sec at 10000 x g. The flow through was again discarded and the spin filter placed back into the collection tube. The spin column was centrifuged again at 10000 x g for 30 sec, and the flow through along with the collection tube was discarded. The spin filter was placed into a fresh collection tube and 50  $\mu$ l of

Elution buffer 'C' (Millipore) was added to the centre of the filter. The spin column was centrifuged for 30 s at 10000 x g and the sample in the collection tube was retained and stored at -20°C until analysis.

**Table 2.7. Purchase Details and Dilutions of Antibodies used in Immunoprecipitations**

Antibody	Details	Dilution
Anti-topoisomerase II $\beta$	Cambridge Research Biochemicals. Custom made; raised in rabbit to CTD peptide of topoisomerase II $\beta$	1/12.5
Anti -AcH <sub>3</sub>	Millipore magna –EZ kit	1/5
Anti-GFP	Santa Cruz #SC-8334	1/5

### 2.19.6 qPCR

qPCR was performed using primer pairs (see Chapter 6, Figure 6.1) and purchased from Integrated DNA Technologies. The GAPDH primer pair for use with the AcH<sub>3</sub> positive control samples was part of the Magna –EZ kit. For each primer pair under investigation a large master mix was made up, this contained (per sample); 12.5  $\mu$ l of iQ-SYBR green supermix (BIO-RAD), 0.1  $\mu$ l Forward Primer, 0.1  $\mu$ l Reverse Primer, 9.3  $\mu$ l H<sub>2</sub>O. 22  $\mu$ l of this mastermix was added to each well of a 96 well PCR plate (BIORAD 223-9441). 3  $\mu$ l of sample DNA was then added in triplicate to the appropriate wells to make a final reaction volume of 25  $\mu$ l. A no template control (RNase/DNase free water) was added in triplicate to the plate for each primer pair used. qPCR was performed using the reaction conditions outlined in Table 2.8. Melting curve analysis was also performed when running the qPCR in order to check for primer-dimer artifacts and reaction specificity. Analysis of qPCR data is outlined in Chapter 6, Figure 6.4.

**Table 2.8. Reaction conditions for qPCR of samples obtained by ChIP**

PCR step	Conditions
1. Initial Denaturation	95°C 4:00
2. Denaturation	95°C 0:15
3. Annealing	62°C 0:25
4. Plate read	-
5. Extension	72° 0:25 72°C 5:00
Go to step 2	(x39 times)
6. Extension	72°C 5:00
7. Melt curve	65°C - 95°C at 0.5°C 0:05
8. Plate read	-

## 2.20 siRNA

Cells were seeded at  $1 \times 10^5$  cells/ml and allowed to incubate for 24 hr. 12  $\mu$ l of siRNA oligonucleotide (Table 2.9, Qiagen) was then added to 88  $\mu$ l of Optimem (Life Technologies) in a 1.5 ml microfuge tube. In a separate microfuge tube 2  $\mu$ l of lipofectamine (Life Technologies) was added to 98  $\mu$ l of Optimem. Both tubes were then mixed and left to incubate for 5 min. The contents of both tubes were then mixed together and left to incubate for a further 20 min. The siRNA/lipofectamine mixture was then added to 2 ml of cells to obtain a final siRNA concentration of 10 nM. Cells were left to incubate for 4 h before media was changed. Experiments using siRNA treated cells were carried out 48 h after media was last changed.

**Table 2.9. Details of siRNA oligonucleotides.**

siRNA oligonucleotide	siRNA oligonucleotide sequence	Final concentration
Hs_TOP2B_5 (SI02780736)	TCGGGCTAGGAAAGAAGTAAA	10 nM
Hs_TOP2B_6 (SI02781135)	CAGCCGAAAGACCTAAATACA	10 nM
Hs_TOP2B_3 (SI00021560)	GTGGATTATGTGGTAGATCAA	10 nM
Hs_TOP2B_7 (SI03109596)	TACGATTAAGTTATTACGGTT	10 nM
Ambion Silencer Select Negative Control #1 (4390843)	Sequence not provided	10 nM

## 2.21 Statistical Analyses

The mean and standard error of the mean were calculated when all experimental replicates were complete. This was calculated as;

$$\text{standard error of the mean} = \frac{\text{standard deviation } (\sigma)}{\sqrt{n}}$$

$\sigma$  is the standard deviation from the mean, and n is the number of data sets.

The unpaired t-test (student t-test), linear regression, correlation coefficient, coefficient of variation, the analysis of variation (ANOVA) and Kolmogorov-Smirnov were all performed using Graphpad (Prism) software. The student t-test was used to test the difference of two means from two small sample populations. When data is presented as percentage of control, all controls are set as 100% when performing the student t-test. Standard error of the mean with regards to the control is to show the spread of data within control samples themselves.

Linear regression was used to draw a trend-line or 'line of best fit'. The correlation coefficient was used to determine the strength of the linear correlation. The coefficient of variation was used to determine the extent of variation in a sample set. An ANOVA was used to determine differences between groups and the Kolmogorov-Smirnov was used to determine Gaussian distribution and thus to indicate whether to use parametric or non-parametric statistical analysis. All data however followed a Gaussian distribution and therefore only parametric statistical analysis was performed.



## Chapter 3

### Establishing a Robust Model for the Quantitative Measurement of PMA Induced Differentiation.

---

#### 3.1 Introduction

Peripheral blood monocytes, originally derived from myeloid progenitor cells produced during hematopoiesis, are the precursors to tissue macrophages (Martinez, 2006; Valledor, 1998). Circulating monocytes display a significant level of heterogeneity, once believed to be distinguished from other circulating cells by their high level of CD14 expression, a membrane bound surface antigen that interacts with Toll Like Receptor 4 (TLR4), Lymphocyte antigen 96 (MD-2) and Lipopolysaccharide binding protein (LBP) to recognise bacterial LPS (Akashi *et al.*, 2003). There actually appears to be three subsets; classical CD14<sup>+</sup>CD16<sup>-</sup>, intermediate CD14<sup>++</sup>CD16<sup>+</sup> and non-classical CD14<sup>+</sup>CD16<sup>++</sup> (Huber *et al.*, 2014).

Monocytes can be stimulated to differentiate into macrophages by various factors; by changes in the microenvironment, for example presence of infection, or an up-regulation of Macrophage colony stimulating factor (M-CSF) (Krause *et al.*, 2000; Daigneault *et al.*, 2010). They may also be stimulated to differentiate to maintain homeostasis by replenishing resident macrophages lost by apoptosis (Rey-Giraud *et al.*, 2012). Upon stimulation monocytes adhere to the wall of the blood vessel, once in the cell wall they then differentiate into a phenotype consistent with that of a macrophage (Ley *et al.*, 2011). Macrophages are also considered to display a high level of heterogeneity, this is a result of diversity in the differentiation programme as consequence of variations in the environment (Daigneault *et al.*, 2010). Despite their heterogeneity all macrophages express the cell surface antigen, CD11b. CD11b is a subunit of the integrin heterodimer, Macrophage Antigen -1 (MAC-1) (Bullard *et al.*, 2005; Ahn *et al.*, 2010). MAC-1 plays a role in cellular adhesion and leukocyte recruitment (Moreland *et al.*, 2002; Gomes *et al.*, 2010). This is in contrast to monocytes that express very low levels of CD11b in comparison (Garcia *et al.*, 1999). Thus CD11b represents an excellent cellular marker for monocyte to macrophage differentiation.

There are many factors that contribute to the difficulties in working with primary macrophages. They can be obtained from peripheral blood but not only is this method invasive, the number of macrophages obtained is small and they do not survive long in culture thus making it difficult to perform extensive research on them (Wetzka *et al.*, 1997; Li *et al.*, 2007). Additionally, the variability of cells between donors can also hinder any explorative research (Maeb *et al.*, 2014). Therefore in order to determine if topoisomerase II $\beta$  plays a role in differentiation and/or a role in cytokine expression, the continuous human cell lines, U937 and HL-60 cells were used (see Materials and Methods, Section 2.8). U937 cells possess monocyte morphology and HL-60 are characterised as being promyeloblast. Both cell lines have been shown to differentiate into different cell types when treated with various chemical agents (Padilla *et al.*, 2000; Passmore *et al.*, 2001; Jacob *et al.*, 2002; Tagliafico *et al.*, 2002). Thus these cell lines represent a viable model system for exploring macrophage development and cytokine production. One such differentiating agent is Phorbol-Myristate Acetate (PMA), a synthetic phorbol ester that has been shown to differentiate both HL-60 and U937 cells into macrophage like cells (Padilla *et al.*, 2000; Ciubotaru *et al.*, 2005; Jerke *et al.*, 2009). PMA acts via activation of various protein kinases, which in turn lead to a signalling cascade resulting in an alteration in gene expression (Obara & Nakahata, 2002) (See Introduction 1.8.1). The conditions using PMA differ greatly amongst publications. For example a range of concentrations between 2 – 200 nM, for durations between 24 hours and 120 hours has been reported (Melhem *et al.*, 1991; Takashiba *et al.*, 1999). Conditions used for exposure to PMA also appear to be cell line specific (Liu *et al.*, 2009).

### **3.2 Aim**

In order to determine the effects of topo II $\beta$  inhibition on differentiation it was necessary to carry out a series of experiments to define optimum conditions for macrophage production for the model system that would enable the robust measurement of differentiation in these cell lines.

Three variables were chosen to identify mature macrophages, these were; expression of the surface marker CD11b, changes in cell morphology and changes in cell proliferation.

### 3.3 Measurement of CD11b expression to determine optimal conditions of PMA exposure to generate differentiated U937 and HL-60 cells.

The literature suggests that differentiation of monocytes will occur using concentrations of PMA between 1 - 125 ng/ml approximately (Melhem *et al.*, 1991; Takashiba *et al.*, 1999; Padilla *et al.*, 2000; Jerke *et al.*, 2009; Liu *et al.*, 2009).

In order to determine the optimal concentration of PMA to differentiate U937 and HL-60 monocytes, cells were exposed to varying concentrations of PMA for 72 h and levels of the cell surface antigen, CD11b were measured using flow cytometry. A 72 h exposure was chosen initially as many papers showed successful differentiation using this length of exposure (Ciuboaru *et al.*, 2005; Jerke *et al.*, 2009; Liu *et al.*, 2009; Quattrorii *et al.*, 2012). The results are shown in Figure 3.1.

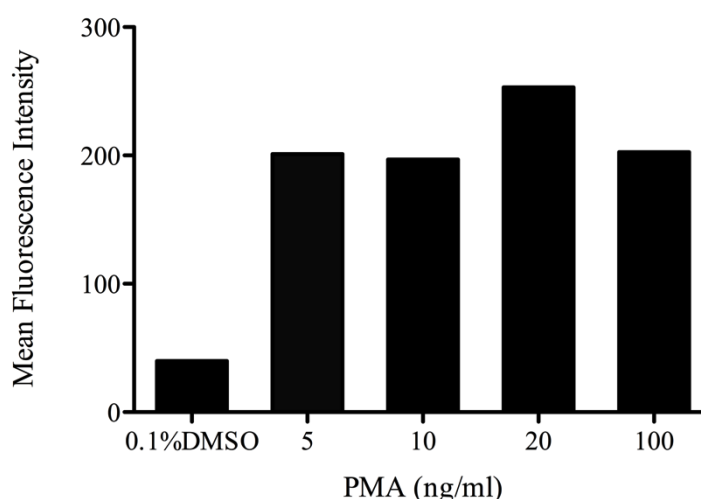


**Figure 3.1 Flow cytometric analysis of CD11b expression on PMA treated U937 determining optimal PMA concentration.**

Cells were seeded at a density of  $3 \times 10^5$ /ml in a 12 well tissue culture plate in complete media (detailed in materials and methods) with 5, 10, 20 and 100 ng/ml PMA. Cells were allowed to incubate for 72 h. Cells were then labelled with anti-human CD11b-APC conjugated antibody. Flow cytometry was performed using the Becton Dickinson flow cytometer (detailed in materials and methods). Results are presented as the mean fluorescence intensity of  $1 \times 10^5$  acquired cells.

Mean Fluorescence Intensity was plotted rather than percentage CD11b positive cells as this gave a more quantitative measurement of CD11b surface antigen. From Figure 3.1 it is clear that cells treated with PMA, for 72 h, at all concentrations expressed higher

levels of CD11b than the DMSO control. However there was little difference in CD11b expression when comparing the different concentrations of PMA used.

The length of exposure of cells to PMA required for differentiation is also considerably variable between publications (24 – 120 h) (Takashiba *et al.*, 1999, Melhem *et al.*, 1991). Although a 72 h exposure was used initially, it was decided to investigate whether differentiation could be achieved using shorter exposures to PMA. For this experiment, 5 ng/ml of PMA was utilised as there was no great difference observed in CD11b expression at higher concentrations of PMA, in comparison. Cells were exposed for 24, 48 and 72 h before CD11b surface antigen expression was measured using flow cytometry. The results are shown in Figure 3.2.

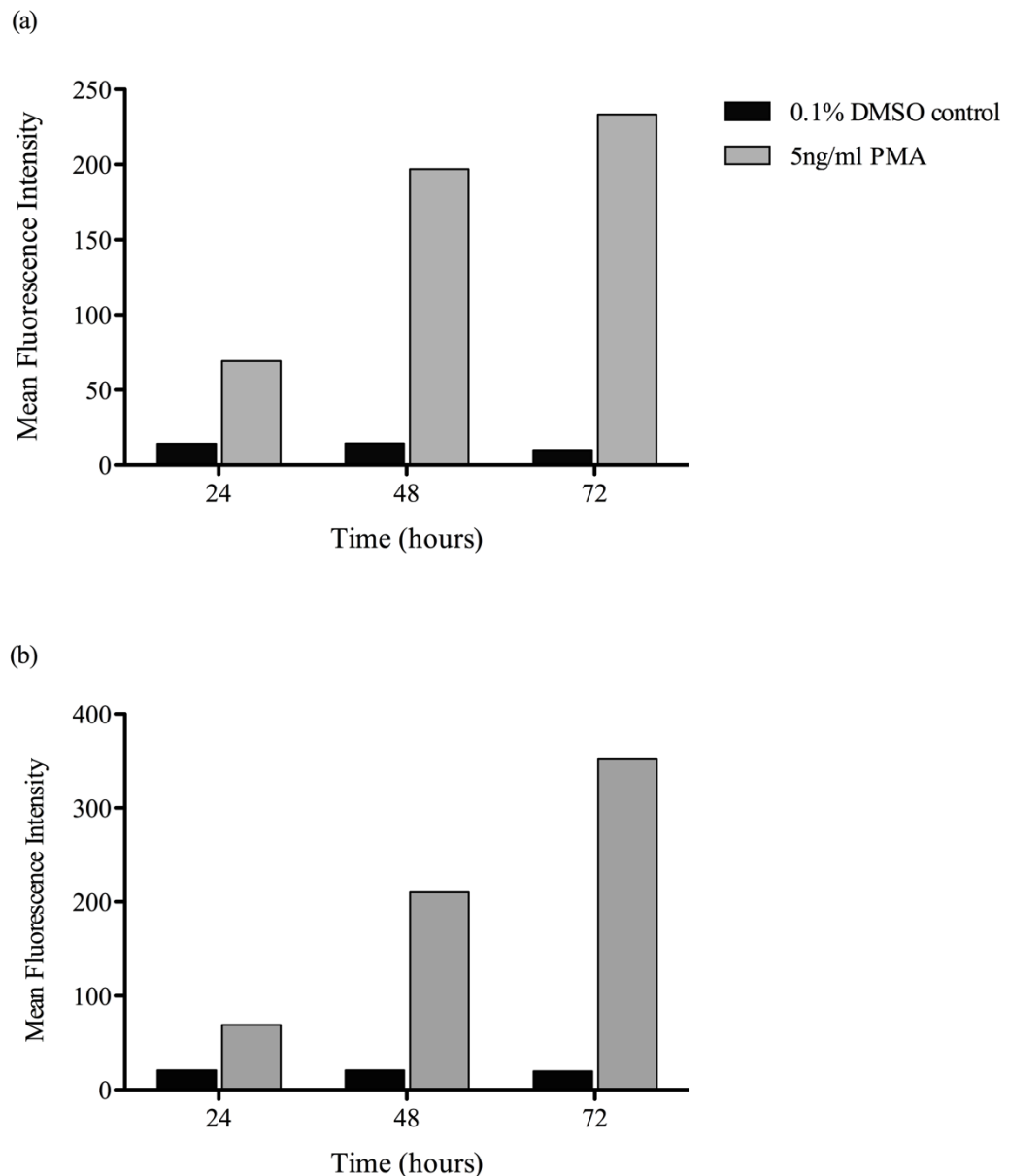


**Figure 3.2 Flow cytometric analysis of CD11b expression on PMA treated HL-60 (a) and U937 (b) cells – determining optimal PMA time exposure.**

Cells were seeded at a density of  $3 \times 10^5$ /ml in a 12 well tissue culture plate in complete media (detailed in materials and methods) with 5 ng/ml PMA (grey) or 0.1% (v/v) DMSO (black). Cells were allowed to incubate for 24, 48 and 72 h. Cells were then harvested by cell scraping and were then labelled with anti-human CD11b-APC conjugated antibody. Flow cytometry was performed using the Becton Dickinson flow cytometer (detailed in materials and methods). Results are presented as the mean fluorescence intensity of  $1 \times 10^5$  captured cells.

Figure 3.2 shows an increase in CD11b expression between 24 and 48 h, 48 h and 72 h, and 24 and 72h. This is in agreement with Jerke *et al.* (2009) who saw a consistent increase in CD11b expression when cells were treated every 24 h for 72 h with PMA. However whilst this study used THP-1, a different monocytic cell line, the study was also carried out using 2 nM PMA, a much lower concentration than has been used in Figure 3.2. These differences in procedure may explain why the results do not correlate. Thus for all future experiments using both cell lines, a 72 h exposure to 5 ng/ml PMA was used to generate macrophage-like cells. In addition for all such experiments a sample of cells was taken and CD11b expression was analysed to verify successful macrophage differentiation.

To verify that these conditions would generate macrophages consistently and reproducibly, flow cytometry was used to quantify CD11b on non-PMA and PMA treated U937 and HL-60 cells from three independent experiments. The results are shown in Figure 3.3.

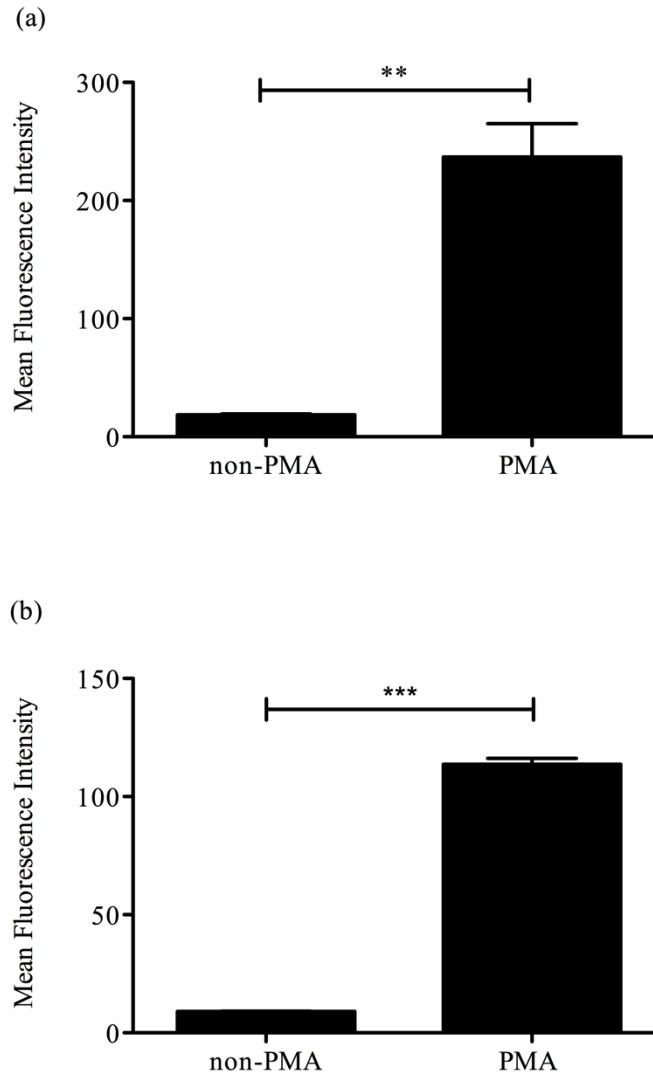


**Figure 3.3 Comparison of CD11b expression on non-PMA and PMA treated cells.**

U937 (a) and HL-60 (b) cells were seeded at a density of  $3 \times 10^5$  cells/ml and incubated with the vehicle control 0.1% (v/v) DMSO (non-PMA) or 5 ng/ml PMA for 72 h. Cells were then labelled with anti-human CD11b-APC conjugated antibody. Flow cytometry was performed using the Becton Dickinson flow cytometer (detailed in materials and methods). Results are presented as the mean fluorescence intensity of  $1 \times 10^5$  acquired cells. The means of three independent experiments are shown  $\pm$  standard error. \*\*\* =  $p < 0.001$ , \*\* =  $p < 0.01$

Results from Figure 3.3 showed that there was a significant difference (Figure 3.3a,  $p = 0.0015$ , student t test. Figure 3.3b,  $p < 0.0001$ , student t test) in expression of CD11b on the cell surface of non-PMA treated cells compared to PMA treated cells. Indeed

CD11b surface antigen expression increased in response to PMA treatment in both U937 (Figure 3.3a) and HL-60 cells (Figure 3.3b). This is in agreement with previous studies that demonstrate an increase in CD11b post PMA treatment (Zhao *et al.*, 2004; Basoni *et al.*, 2005; Baek *et al.*, 2009).

### **3.4 Effects of PMA treatment on cell growth**

U937 and HL-60 cells are both cancer derived cell lines; histiocytic lymphoma and acute promyelocytic leukaemia, respectively. Therefore a characteristic both cell lines possess is a dysregulation in cell division, causing an up-regulation in cell proliferation. This does not reflect the behaviour of monocytes and promyelocytic cells *in vivo*, which generally do not divide unless stimulated (van Furth *et al.*, 1979; Okabe & Yasukawa, 1990). Baek *et al.* (2009) report that once U937 and HL-60 cells have undergone differentiation they lose their ability to proliferate. This then allows another method for establishing differentiation.

In order to test whether 5 ng/ml PMA for 72 h prevented proliferation as expected, a cell proliferation assay was carried out. Proliferation was assayed by counting viable cell numbers using trypan blue exclusion. In this assay viable cells that possess an intact cell membrane, and thus exclude the trypan blue dye are counted. Conversely, non-viable cells, which do not possess an intact plasma membrane are flooded with the dye, and are excluded from the count.

HL-60 and U937 cells were exposed to the drug vehicle control 0.1% (v/v) DMSO or 5 ng/ml PMA for 72 h. Cell proliferation was measured and the results are shown in Figure 3.4.

Two counts were performed on PMA-treated cells; cells that were in suspension in the well were counted, and cells that had adhered to the bottom of the well were also counted. Results from both cell lines demonstrated a significant difference in the proliferation of cells treated with 0.1% (v/v) DMSO compared to 5 ng/ml PMA ( $p = < 0.000$ , ANOVA). A decrease in suspension cells and increase in adherent cells can be observed up until 48 h. The amount of adherent cells then plateaus until 72 h where it then decreases gradually. This was observed in both cell lines (Figure 3.4a + b). As stated previously (Section 3.1) CD11b is a component of the  $\beta 2$  integrin CD11b/CD18. The role of CD11b/CD18 *in vivo* is to mediate adhesion of cells to the endothelial lining and to components of the extracellular matrix (Lundahl *et al.*, 1996). Therefore it may be assumed that an up-regulation of CD11b surface expression may correlate with an



increase in cellular adhesion. Indeed when taken together adherence data in Figure 3.4a & b and Figure 3.3 do correlate; after 72 h of treatment with PMA, CD11b surface expression is at its highest and this is accompanied with a plateau in the number of adherent PMA treated cells. This data is in support of previous work that has shown that treatment of U937 cells, HL-60 cells and peripheral blood monocytes with PMA results in an up-regulation of CD11b surface expression and an increase in cellular adherence (Baek *et al.*, 2009; McIntire, 2004; Lundahl *et al.*, 1996). Collation of the data thus confirms that 5 ng/ml PMA exposure for 72 h causes differentiation of monocytes into macrophage like cells, which can be used as a reliable model in future experiments.

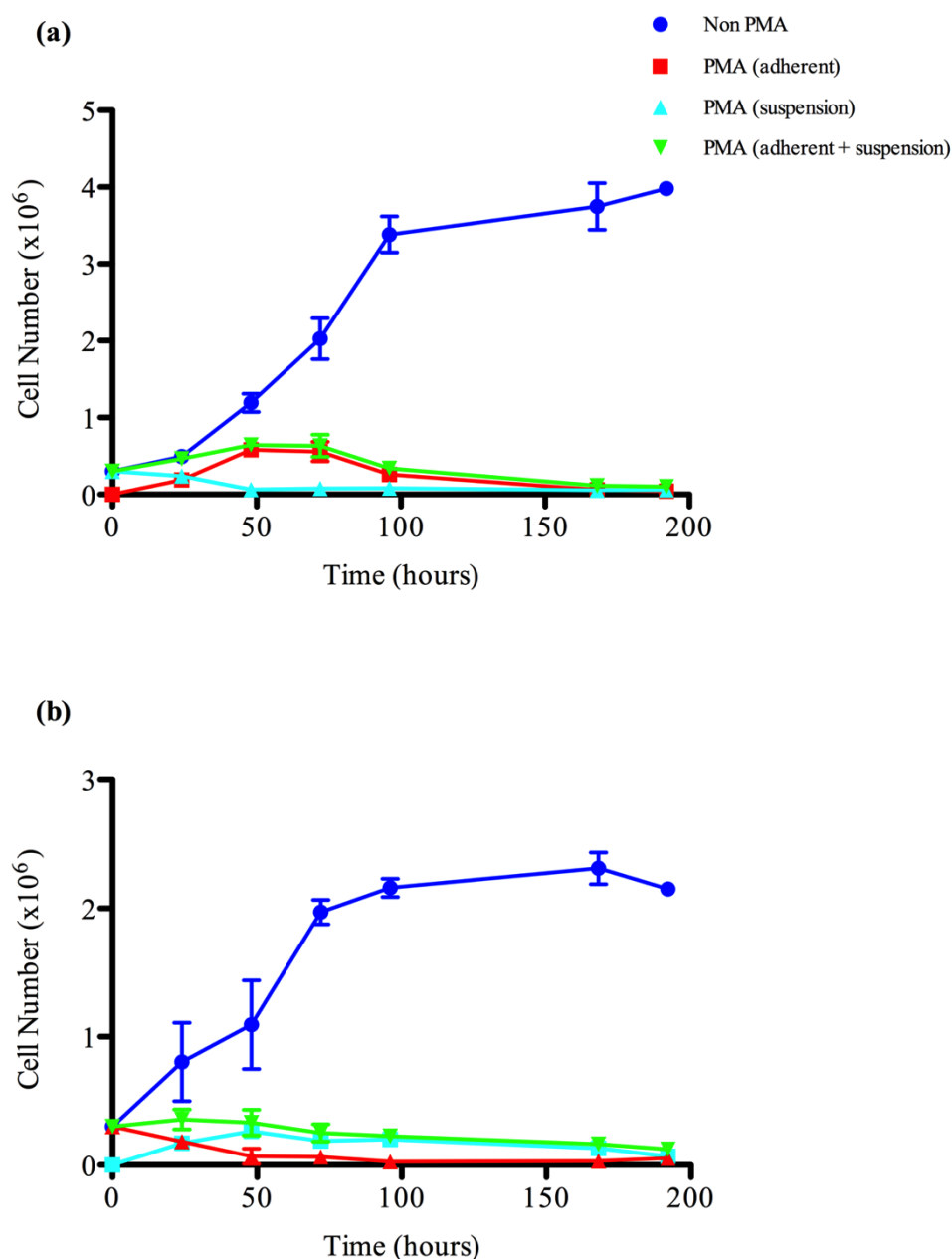


**Figure 3.4 Trypan Blue Proliferation Assay of HL-60 (a) and U937 (b) cells.**

Cells were seeded at a density of  $3 \times 10^5/\text{ml}$  in a 12 well tissue culture plate in complete media (detailed in materials and methods) either containing 0.1% DMSO (v/v) or 5 ng/ml PMA. Cell number was then measured after 24, 48, 73, 96, 168 and 196 h. Cells exposed to 0.1% (v/v) DMSO are represented as (blue). For cells exposed to PMA, both the adherent (red) and the cells remaining in suspension (cyan) were counted. The total number of PMA treated cells is also shown on the graph (green). The means of three independent experiments are shown  $\pm$  standard error.

### 3.5 Characterisation of differentiation by changes in morphology

Monocytes *in vivo* exhibit a high level of heterogenicity (Gordon, 2005; Auffray *et al.*, 2009; Tsujioka *et al.*, 2009), in comparison U937 and HL-60 cell lines appear more uniform (Figure 3.5a). This is due to the derivation of the cell lines from cancer, essentially the cell lines are clones (Sundstrom & Nilsson, 1976; Collins *et al.*, 1977). However cell morphology between monocytes and macrophages is even more striking when utilising clonally derived cell lines such as HL-60 and U937 (ATCC) rather than primary monocytes, which may be partially differentiated and thus display a high level of heterogenicity (Gordon, 2005; Auffray *et al.*, 2009; Tsujioka *et al.*, 2009).

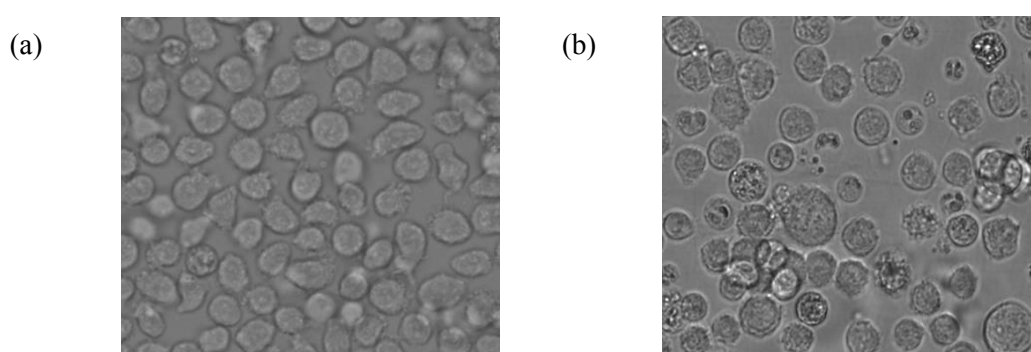


**Figure 3.5 Visual analysis of non-PMA and PMA treated U937 cell morphology.**

Cells were seeded at  $3 \times 10^5$  cells/ml with 0.1% (v/v) DMSO (a) or 5 ng/ml PMA (b) in a 75 cm<sup>3</sup> tissue culture flask and allowed to incubate for 72 h. Images were then captured using an x20 objective on a Zeiss Axiovert 25 light microscope with attached Nikon Coolpix camera.

U937 and HL-60 cells grow in suspension and once differentiated with PMA, observation of morphology revealed the resulting cells became adherent (Figure 3.5). In addition these cells could only be harvested from their culture vessel by cell scraping or trypsinization. This finding is in agreement with previous work that showed using HL-60 and U937 cells, PMA treatment resulted in an increase in adherence (Lu & Pitha, 2001). An increase in adherence to culture flasks and other cells to form clusters is the result of an increase in the expression of various surface antigens including CD11b that are involved in adhesion and up-regulated in response to PMA treatment (McKercher *et al.*, 1996; Deszo *et al.*, 2000).

PMA differentiated cells also display a higher level of granularity. This is determined by an increase in side scatter as measured by flow cytometry (Figure 3.6b) compared to non-PMA treated cells (Figure 3.6a). Additionally Figure 3.6b also shows an increase in forward scatter in a proportion of cells treated with PMA, thus reflecting an increase in the size of cells. Daigneault *et al.* (2010) describe an increase in granularity upon treatment of THP-1 cells with PMA. An increase in granularity is due to an increase in membrane bound organelles in response to PMA treatment. Furthermore an increase in intracellular organelles can also be observed in PMA treated cells (Figure 3.5b) Daigeneault *et al.* (2010) also used immunohistochemistry to identify an up-regulation of mitochondria and lysosomes in PMA-treated THP-1 cells. An increase in mitochondria and lysosomes reflects the functional activities of macrophages in the cell. Indeed macrophages may require more energy generated by mitochondria in order to successfully phagocytose foreign material. Also an increase in lysosomes is required to fulfil the role of macrophages in releasing lysosomal enzymes for particle digestion (Hakala *et al.*, 2003).

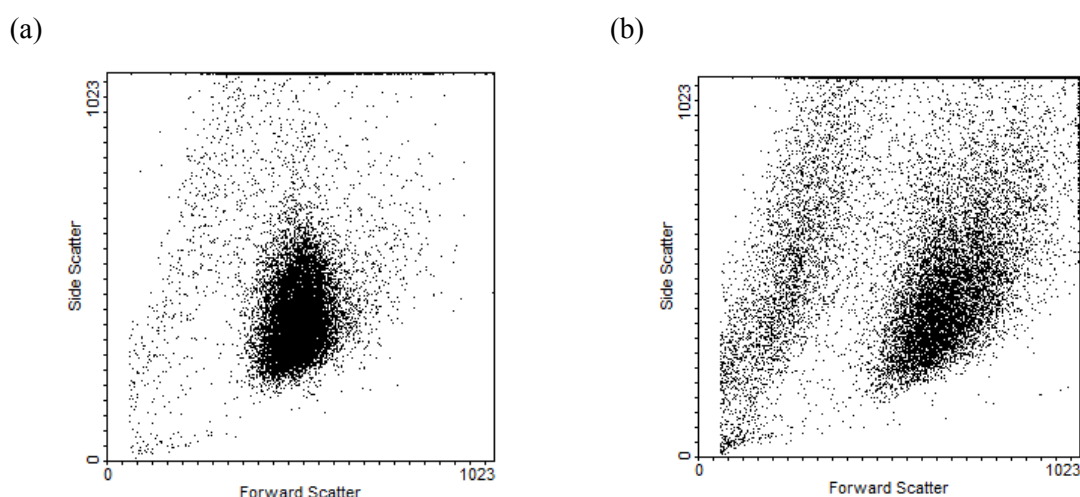


**Figure 3.6 Flow cytometric analysis of non-PMA and PMA treated HL-60 cells.**

Cells were seeded at  $3 \times 10^5$  cells/ml with 0.1% DMSO (v/v) (a) or 5 ng/ml PMA (b) in a  $75\text{cm}^3$  tissue culture flask and allowed to incubate for 72 h. Cells were harvested and flow cytometry was performed using the Becton Dickinson flow cytometer (detailed in materials and methods). Results are presented as side scatter (y axis) vs forward scatter (x axis). Results presented are representative of  $2 \times 10^5$  cells acquired cells.

The morphological changes during PMA induced differentiation seen in Figure 3.5 have all been described previously (Hansen, 1990; Garrelds, 1999; McIntire, 2004) and are

useful visual signs that the cells have been successfully differentiated. Subsequent experiments using PMA-treated cells were visually assayed using light microscopy to ensure differentiation had occurred.

### **3.6 Summary**

A robust model of differentiation has been achieved, which generates some of the features seen in monocyte to macrophage differentiation. Conditions for the treatment of U937 and HL-60 cells to PMA has been thoroughly investigated. This has resulted in a standardised method of differentiation, 5 ng/ml PMA for 72 h. Three independent methods of validation have also been identified; loss of ability to proliferate (Figure 3.5) changes in morphology (Figure 3.6) and an increase in CD11b expression (Figure 3.3). The latter also allows for the quantitative measurement of differentiation.

## Chapter 4

### Quantification of Topo II $\alpha$ and Topo II $\beta$ in PMA and non-PMA treated cells and the Effects of Differentiation on Topo II Drug Sensitivity

---

#### 4.1 Introduction

Quantification of topo II $\alpha$  and topo II $\beta$  has revealed a difference in the protein expression of the two isoforms during the cell cycle. Woessner *et al.* (1991) showed that levels of topo II $\alpha$  protein were negligible in serum starved cells but when re-entering the cell cycle levels of topo II $\alpha$  appeared to increase during late S phase and peaked in G2/M phase before slowly declining and becoming undetectable in G0. Similarly Padget *et al.* (2000) also showed that exponentially growing Raji cells contained more topo II $\alpha$  protein than confluent Raji cells, whilst peripheral blood lymphocytes in G0 contained no detectable topo II $\alpha$  protein. Levels of topo II $\beta$  protein during the cell cycle are described in many publications as remaining constant (Kobayashi *et al.*, 1998; de Campos-Nebel *et al.*, 2010), however multiple studies have shown a decline in levels of topo II $\beta$  when cells become confluent or enter G0 (Woessner *et al.*, 1991; Turley *et al.*, 1997; Padget *et al.*, 2000), thus suggesting that levels of topo II $\beta$  also vary during the cell cycle. Interestingly levels of topo II $\beta$  appear to change during differentiation. Tsutsui *et al.* (2001) report than an increase in the protein level of topo II $\beta$  can be observed during neuronal differentiation in cerebellar Purkinje cells and granule cells. The requirement for an up-regulation of topo II $\beta$  during neuronal differentiation has been attributed to the requirement of topo II $\beta$  in the regulation of transcription of genes in the later stages of neuronal development (Lyu *et al.*, 2006). Additionally Aoyama *et al.* (1998) also demonstrated an up-regulation of topo II $\beta$  protein expression when HL-60 cells were differentiated into granulocytic like cells using retinoic acid.

In order to determine whether topo II $\beta$  is the predominant isoform in differentiated cells of the immune system, topo II $\alpha$  and topo II $\beta$  mRNA and protein were quantified in non-PMA and PMA treated cells. In order to verify the differences in the levels of the two isoforms, a topo II poison and topo II inhibitors that differentially target the two isoforms were used. The topo II poison, etoposide (VP-16) acts by trapping the topo II enzyme in the DNA cleavage part of its catalytic cycle, termed the cleavable complex (Montaudon *et al.*, 1997; Willmore *et al.*, 1998). Processing of cleavable complexes

causes generation of double strand breaks, which in a high enough quantity will eventually result in apoptosis (Li & Lui., 2001). This particular poison has been shown to preferentially target topo II $\alpha$  (Errington *et al.*, 2004; Bandele & Osheroff, 2008). Toyoda *et al.* (2008) using mutant Nalm-6 cell lines, one of which was heterozygous for topo II $\alpha$  (TOP2 $\alpha^{+/-}$ ) and the other homozygous null for topo II $\beta$  (TOP2 $\beta^{-/-}$ ) showed that TOP2 $\alpha^{+/-}$  cells were more resistant to VP-16 than the wild-type but that TOP2 $\beta^{-/-}$  remained just as sensitive to VP-16 as the wild-type, thus supporting previous evidence to suggest that VP-16 preferentially targets the  $\alpha$  isoform. In contrast topo II inhibitors act differently to topo II poisons. The topo II inhibitor, ICRF-193 acts by hindering the binding and hydrolysis of ATP; leaving topo II unable to complete its catalytic cycle (Roca *et al.*, 1994). This ultimately causes an excess of DNA supercoiling that results in the inhibition of essential cellular processes such as replication and transcription. ICRF-193 has been shown to preferentially target topo II $\beta$  (Patel *et al.*, 2000).

If topo II $\alpha$  is reduced it would be expected that there would be a decrease in VP-16 sensitivity, conversely if topo II $\beta$  is reduced it would be expected that there would be a decrease in ICRF-193 sensitivity. In addition another topo II $\beta$  inhibitor, ICRF-187 was also used.

## **4.2 Aim**

To quantify the protein and mRNA levels of topo II $\alpha$  and topo II $\beta$  in non-PMA and PMA treated HL-60 and U937 cells.

To determine if a difference in levels of topo II $\alpha$  and topo II $\beta$  between non-PMA and PMA treated cells affects the efficacy of the topo II poison, etoposide and the topo II inhibitors, ICRF-193 and ICRF-187.

## **4.3 Quantification of Topoisomerase II $\alpha$ and $\beta$ mRNA in non-PMA and PMA treated U937 and HL-60 cells**

### **4.3.1 Determining the optimal reference gene to use for qPCR**

Quantitative real time PCR was used to generate reliable measurements of mRNA. Reference genes that have previously been used such as GAPDH and beta actin are now considered to be unreliable due to their variability in tissues and changes in the

regulation of their transcription during certain experimental procedures (Radonic *et al.*, 2004).

The Minimum Information for Publication of Quantitative Real-Time PCR Experiments (MIQE) guidelines requires a suitable reference gene be used in order to generate reliable results. MIQE guidelines were introduced in order to standardise the qPCR method (Bustin, 2009). Therefore in order to identify a suitable reference gene to quantify to topo II $\alpha$  and  $\beta$  in PMA and non-PMA treated cells, the geNORM kit (PrimerDesign) was utilised. This enabled the variability of multiple housekeeping genes to be measured between non-PMA and PMA treated cells.

The geNORM kit contained hydrolysis probes for 11 genes including; GAPDH, ACTB, SDHA, RPL13A, UBC, B2M, TOP1, EIFA2, YWHAZ, ATP5B and CYC1. These are considered to be the most widely used reference genes. Levels of each of the genes were quantified by qPCR using cDNA generated from non-PMA and PMA treated HL-60 samples in order to identify a suitable reference gene that did not change during PMA induced differentiation.

Figure 4.1a is a box and whisker diagram presenting the variation in Ct values of the reference genes in non- PMA and PMA treated samples. Figure 4.1b shows the coefficient variance of the Ct values that were calculated to identify the gene with the least variability between samples. TOP1 was seen to have the lowest coefficient variance, and therefore this gene was the reference gene in qPCR measurements in HL-60 cells. Interestingly, GAPDH, one of the most common reference genes used in western blotting (Chen *et al.*, 2014; Li *et al.*, 2006; Zhang *et al.*, 2011; De Boo *et al.*, 2009) displays the highest coefficient variance, these results support previous findings that GAPDH is not a suitable reference gene in qPCR (Glare *et al.*, 2002).

18S RNA was used as a reference gene for U937 cells as this had previously been shown to be suitable (Zhao *et al.*, 2013).



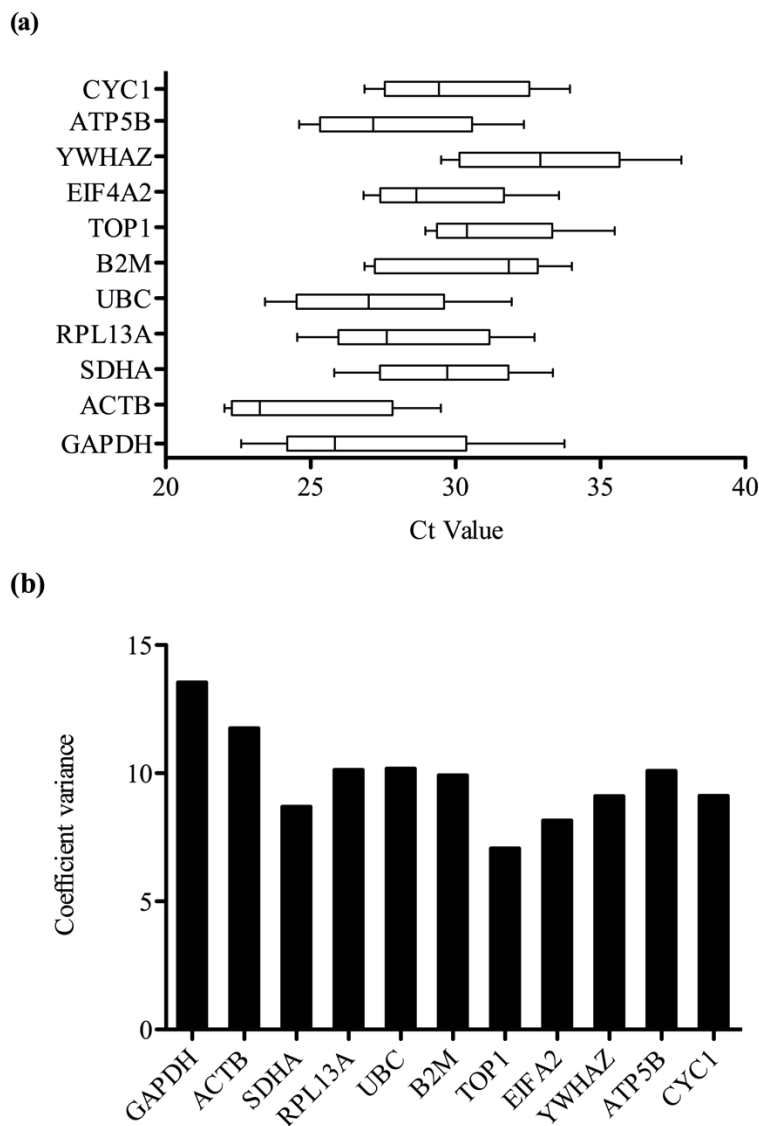


**Figure 4.1 Determination of a suitable reference gene for use in qPCR when using non-PMA and PMA treated HL-60 cells, using the commercially available geNorm kit.**

HL-60 cells were seeded at cell density of  $3 \times 10^5$  cells/ml with 5 ng/ml PMA or 0.1% (v/v) DMSO and left to incubate for 72 h before cells were harvested and RNA extracted (see Section 2.17.1). cDNA was then synthesised (Section 2.17.2) and qPCR was performed using PerfectProbe hydrolysis probes for GAPDH, ACTB, SDHA, RPL13A, UBC, B2M, TOP1, EIFA2, YWHAZ, ATP5B and CYC1. qPCR conditions can be found in Section 2.17.3. Results shown are the mean Ct of five independent experiments (a). Coefficient variance using data from (a) was calculated to determine amount of variability of Ct values between the non-PMA and PMA treated samples (b).

#### **4.3.2 Determining the efficiency of the qPCR reaction using topo II $\alpha$ , topoII $\beta$ and 18S hydrolysis probes.**

Hydrolysis probes obtained for the quantification of topo II $\alpha$  and  $\beta$  arrived optimised ready for use. The efficiency of these probes within the qPCR assay was required in order to make a comparison between genes.

An efficiency of 90- 105% is deemed acceptable. Genes that are to be compared to one another must have similar efficiencies in order for an accurate comparison to be made (Bustin, 2009).

The calibration curve for the calculation of the efficiency of the topo II $\alpha$ , topo II $\beta$  and 18S probes is displayed in Figure 4.2. A 1:2 dilution of cDNA was used to generate samples for the calibration curve. 5  $\mu$ l of each sample was used in a 20  $\mu$ l reaction volume, complete reaction conditions are documented in Materials and Methods Section 2.16.3.

Efficiency calculations were performed using the equation shown in Appendix Figure A.1, based on qPCR algorithms described in Rutledge & Côté (2003). The assay using the topo II $\alpha$  specific (TOP2A) hydrolysis probe was calculated to have an efficiency of 99.1%. The efficiency of the assay using the topo II $\beta$  (TOP2B) hydrolysis probe was calculated to be 104.2%, and the efficiency of the 18S probe was calculated to be 91%. The efficiencies of these assays are similar enough to be able to compare the two different genes being investigated (Bustin, 2009). It was expected that the hydrolysis probes would yield an acceptable efficiency as all gene assay kits are fully validated by the manufacturer (PrimerDesign) thus guaranteeing an efficiency within the acceptable range. Therefore efficiency for the TOP1 hydrolysis was not performed, as it was originally part of a fully validated kit especially designed for a comparative assay.

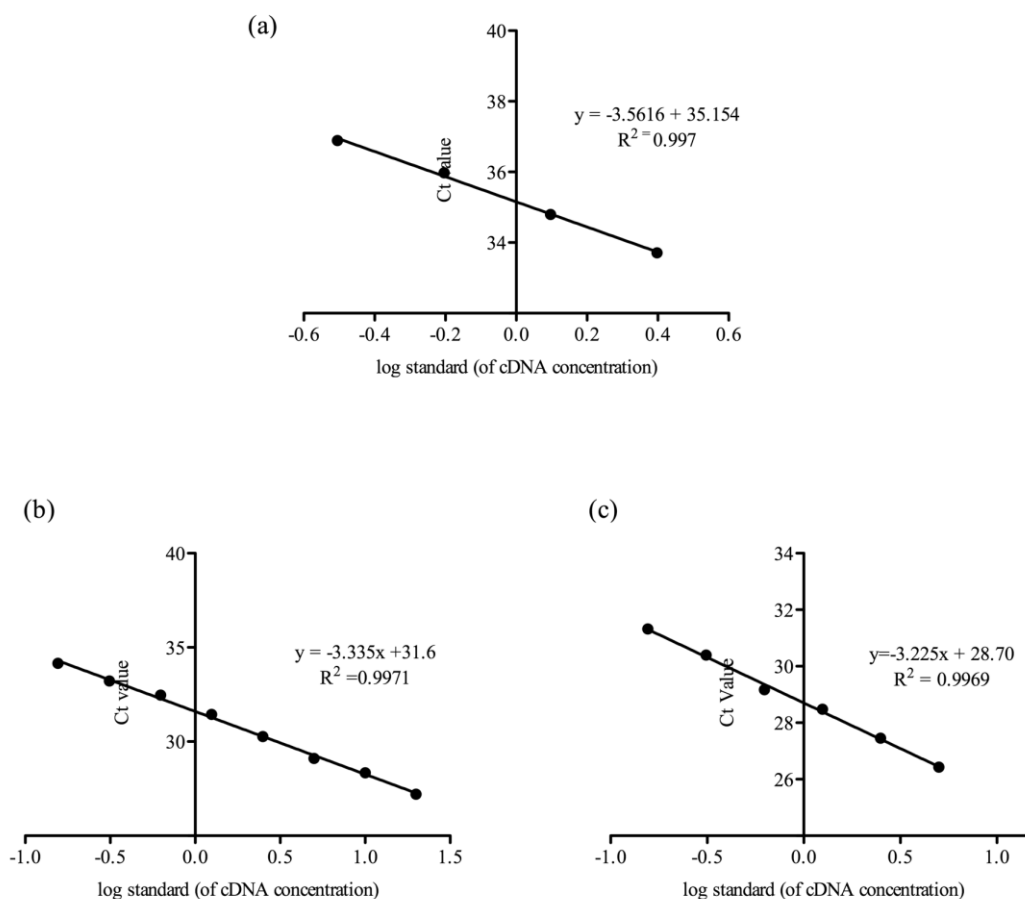


**Figure 4.2 Establishing the efficiency of qPCR – Calibration Curves.**

RNA was extracted from non-PMA treated U937 cells and quantified using the nanodrop. cDNA was then synthesised and concentration was determined from amount of RNA used in the reverse transcription reaction. cDNA was then serially diluted from 20 to 0.156 ng/μl. qPCR was then performed using Taqman hydrolysis probes to TOP2A, TOP2B and 18S (see Section 2.17.3 for qPCR conditions). Concentration of cDNA was converted into a logarithmic value and plotted against Ct value. Calibration curves were then generated for 18S (a), TOP2A (b) and TOP2B (c). A line of best fit was then added and the equation of the line generated using graphpad prism software.

#### **4.3.3 Quantification of Topoisomerase II $\alpha$ and $\beta$ mRNA in non-PMA and PMA treated U937 and HL-60 cells.**

Following determination of the efficiency of both topo II $\alpha$  and topo II $\beta$  hydrolysis probes, the probes were then used to quantify levels of topo II $\alpha$  and topo II $\beta$  mRNA in U937 and HL-60 PMA and non-PMA treated cells. To ensure only differentiated cells were to be analysed, any suspension cells in the PMA treated flasks were disposed of, and the remaining adherent cells were gently harvested using a cell scraper. To ensure differentiation had occurred, the levels of CD11b receptor expression for every sample to be analysed, was measured by flow cytometry (data not shown). Levels of topo II $\alpha$  and topo II $\beta$  mRNA were then quantified using qPCR. Analysis was performed using the comparative  $\Delta\Delta C_t$  method to measure fold expression. Samples taken from U937 cells were normalised to values obtained using the 18S reference gene, samples taken from HL-60 cells were normalised to values obtained using the TOP1 reference gene. The results are shown in Figures 4.3 and 4.4. Amplification efficiencies of both the target and reference genes were calculated and found to be approximately the same, falling within the acceptable range of amplification efficiency (see Figure 4.2)

This is the first time under these conditions a comparison of both topo II $\alpha$  and topo II $\beta$  has been made between monocytic cells and macrophage like cells at both the relative levels of mRNA and protein.

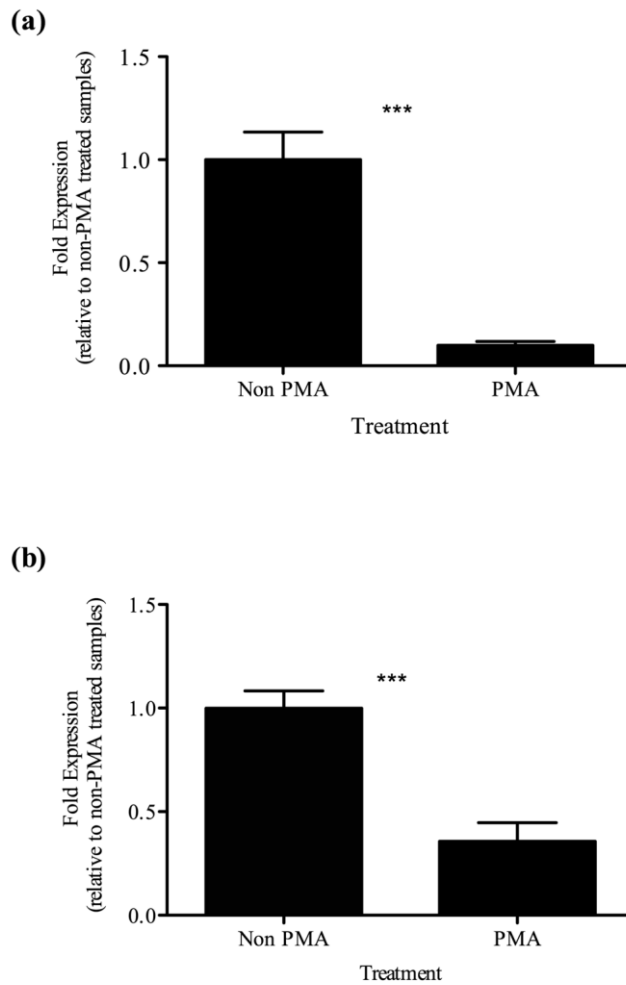


**Figure 4.3 Comparing the relative levels of Topoisomerase II $\alpha$  and  $\beta$  mRNA in Non-PMA vs PMA treated U937 cells.**

U937 cells were seeded at a density of  $3 \times 10^5$  cells/ml with 5 ng/ml PMA or 0.1% DMSO (v/v) (Non-PMA) and allowed to incubate for 72 h before harvesting. RNA was then extracted and cDNA synthesised (Section 2.16). qPCR was then performed using Taqman hydrolysis probes to TOP2A (a) and TOP2B (b). 5 $\mu$ l of 5ng/ $\mu$ l cDNA was used for each reaction. Samples were performed in experimental triplicate. Results were normalised to 18S and the  $\Delta\Delta C_t$  method was used to calculate fold expression. Results shown are the mean of five independent experiments  $\pm$  standard error. \*\*\* =  $p < 0.001$ . See Appendix Table A.1 for p values.

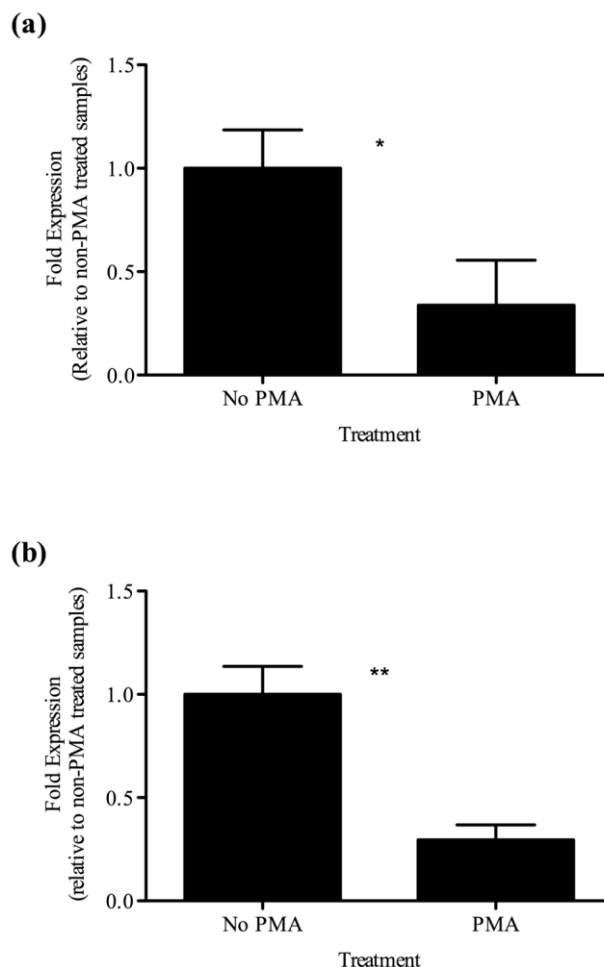


**Figure 4.4 Comparing the relative levels of Topoisomerase II $\alpha$  and  $\beta$  mRNA in Non-PMA vs PMA treated HL-60 cells.**

HL-60 cells were seeded at a density of  $3 \times 10^5$  cells/ml with 5 ng/ml PMA or 0.1% DMSO (v/v) (Non-PMA) and allowed to incubate for 72 h before harvesting. RNA was then extracted and cDNA synthesised (Section 2.16). qPCR was then performed using Taqman hydrolysis probes to TOP2A (a) and TOP2B (b). 5 $\mu$ l of 5ng/ $\mu$ l cDNA was used for each reaction. Samples were performed in experimental triplicate. Results were normalised to TOP1 (as determined by the geNorm kit, Figure 4.1) and the  $\Delta\Delta C_t$  method was used to calculate fold expression. Results shown are the mean of five independent experiments  $\pm$  standard error. \* =  $p < 0.05$ , \*\* =  $p < 0.01$ . See Appendix Table A.2 for p values.

Significant decreases in both the levels of topo II $\alpha$  and topo II $\beta$  mRNA were observed in both U937 and HL-60 PMA treated cells compared to non-PMA treated cells. An average 91% decrease in TOP2A was observed in PMA treated U937 cells (Figure

4.3a), compared to an average 66% decrease in PMA treated HL-60 cells (Figure 4.4a). Contrary to that expected, on average a 65% decrease in TOP2B in PMA treated U937 cells was measured. A similar 70% average decrease was observed in PMA treated HL-60 cells.

The large decrease in topo II $\alpha$  expression when cells are treated with PMA (Figure 4.3a and 4.4a) is in agreement with other studies that have reported similar findings. Loflin *et al.* (1996) demonstrated a down regulation of topo II $\alpha$  mRNA when K562 cells were treated with PMA. Additionally Lim *et al.* (1998) reported a decrease in topo II $\alpha$  mRNA expression and decatenation activity after 24 h of PMA treatment in HL-60 cells.

Along with the decrease in levels of topo II $\alpha$  and topo II $\beta$  mRNA upon treatment of cells with PMA as shown in Figure 4.3 and Figure 4.4 a change in distribution of cells at certain phases in the cell cycle can also be observed upon treatment with PMA. Non-PMA and PMA treated U937 cells were fixed, and stained with the nucleic acid stain, propidium iodide; analysis by flow cytometry was then performed. Approximately 58% of the exponentially growing, non-PMA treated cells were found to be in G0/G1, ~15% in S phase and ~5% in G2/M, this reflects previous studies that show that logarithmically growing cells follow this pattern during cell cycle analysis (Wang *et al.*, 2006; Otte *et al.*, 2011) (Figure 4.5c). In contrast, ~52% of cells that have been treated with PMA appear to be arrested in G2/M phase, with ~18% in S phase and ~2% in G0/G1 (see Figure 4.6b). This is in agreement with multiple other studies that found PMA arrested human umbilical vein endothelial cells, non-small lung cancer cells and MCF-7 cells in G2/M phase (Kosaka *et al.*, 1996; Oliva *et al.*, 2007; Barboule *et al.*, 1999). In normal, exponential growing cells levels of topo II $\alpha$  mRNA increases during S phase, peaks at G2/M and declines as cells enter G0 (Woessner *et al.*, 1991). However the results in Figures 4.3a and 4.4a do not support this, as levels of topo II $\alpha$  mRNA are down regulated during PMA induced G2/M arrest. The retinoblastoma tumour suppressor protein (Rb protein) has been shown to repress the expression of genes encoding proteins that are crucial for cell cycle progression through mitosis such as cdc2 and topo II $\alpha$  (Siddiqui *et al.*, 2003). Interestingly Rb protein has been shown to be hypo-phosphorylated and therefore activated when IEC-18 cells were treated with PMA for 6 h (Frey *et al.*, 1997). Indeed this PMA induced activation of Rb may lead to the repression of topo II $\alpha$  gene expression, leading to a down-regulation of topo II $\alpha$  mRNA as observed in Figures 4.3a and 4.4a. Additionally existing mRNA may not be detected

after 72 h treatment with PMA as topo II $\alpha$  mRNA stability has been shown to possess a finite half-life of 4 h during S phase (Goswami *et al.*, 1996).

There is a large difference in the percentage decrease of topo II $\alpha$  mRNA between U937 and HL-60 cells. It has previously been reported that PMA causes an up-regulation of p53. In turn, p53, a tumour suppressor protein, has been shown to cause a decrease in the expression of topo II $\alpha$  mRNA (Wang *et al.*, 1997). HL-60 cells are considered p53 null thus this pathway would not be activated, however it may explain why there is an average 66% decrease in TOP2A in HL-60 cells compared to an average 91% decrease in p53 positive U937 cells.

The decrease in topo II $\beta$  mRNA levels upon treatment with PMA is in disagreement to work by Tiwari *et al.* (2012) who showed that topo II $\beta$  mRNA expression was up-regulated during murine neuronal development. However the requirement of topo II $\beta$  during growth development has been shown to be stage specific. Lyu *et al.* (2006) showed that topo II $\beta$  was required for late but not early neuronal development. The decrease in topo II $\beta$  mRNA seen in Figure 4.3b and 4.4b is only reflective of one particular stage of differentiation. Thus an up-regulation of topo II $\beta$  may occur at a different stage.

Topo II $\beta$  has been shown to be involved in the regulation of transcription of various genes, for example Ju *et al.* (2006) reported that a topo II $\beta$  double strand break was required for the recruitment of co-activator proteins to the pS2 promoter in response to 17 $\beta$ -estradiol for transcription to occur. It has also been shown to play a role in gene silencing, for example Huang *et al.* (2011) reported that inhibition of topo II using a variety of topo II drugs including the topo II $\beta$  targeting ICRF-193 caused un-silencing of the dominant allele Ube3a in Ube3a-yellow fluorescent protein knock-in mice. A previous study has shown that knockdown of topo II $\beta$  in NB4 cells caused the up-regulation of retinoic acid induced gene expression (McNamara *et al.*, 2008). Therefore it may be postulated that a down regulation of topo II $\beta$  may lead to the un-silencing and activation of various genes; genes that may drive differentiation.



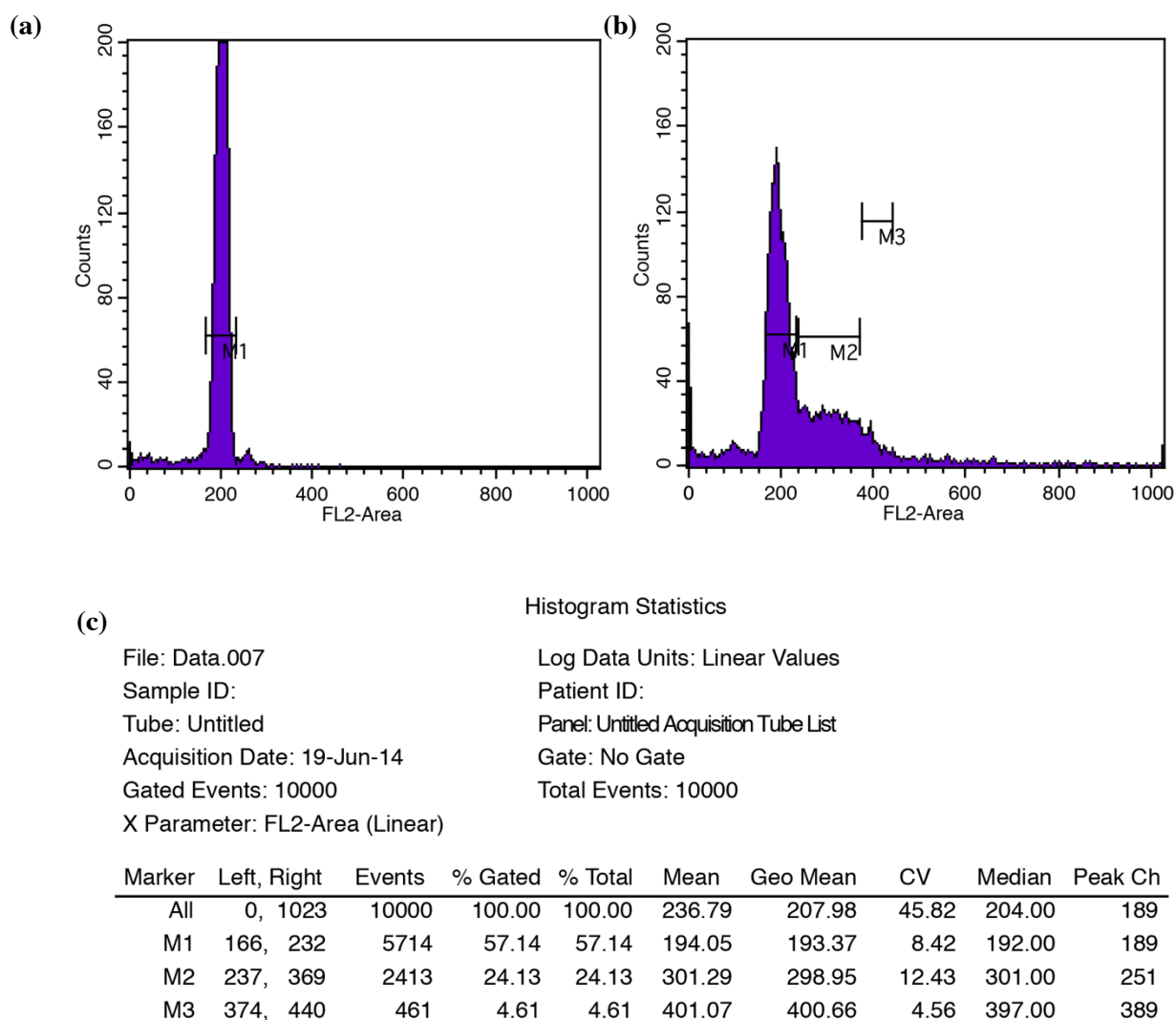


**Figure 4.5 Cell cycle analysis of non-PMA U937 cells.**

Cells were seeded at a cell density of  $3 \times 10^5$  cells/ml with 0.1% DMSO (v/v) (non-PMA) and allowed to incubate for 72 h at 37°C, 5% CO<sub>2</sub> in a humidified atmosphere. Flow cytometry was performed using propidium iodide. Propidium iodide stains DNA and therefore DNA content can be measured. Analysis was first performed using lymphocytes kindly donated by Prof S Todryk to calibrate the flow cytometer for cells in G1, G1 was identified at the arbitrary unit 200 (a). A histogram to show the spread of cells with different amount of DNA content was then performed using the test sample (b) G2/M was identified at the arbitrary unit 400 (as cells in this phase have double amount of DNA). Percentage of 10000 captured cells in each phase was then calculated (c).

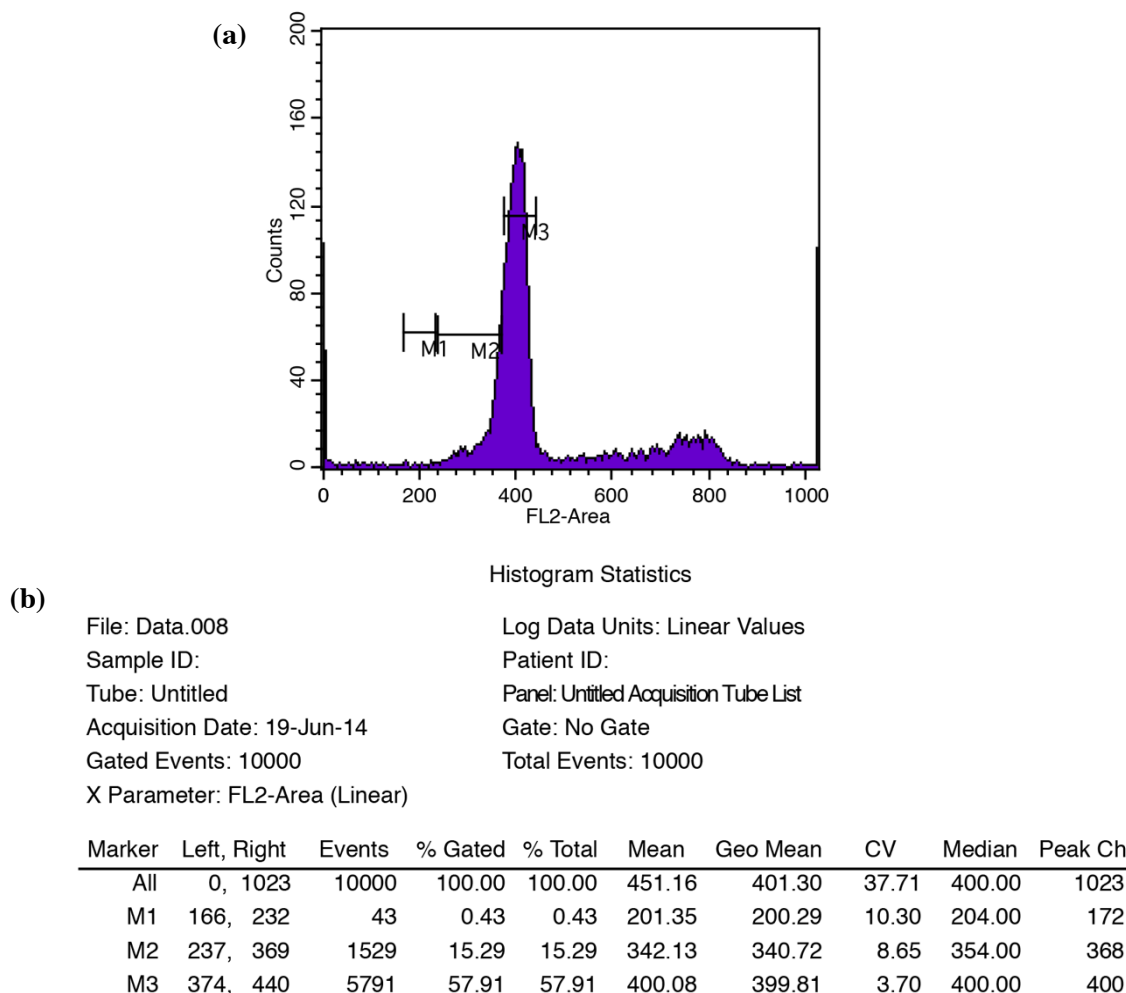


**Figure 4.6 Cell cycle analysis of PMA treated U937 cells**

Cells were seeded at a cell density of  $3 \times 10^5$  cells/ml with 5 ng/ml PMA and allowed to incubate for 72 h at 37°C, 5% CO<sub>2</sub> in a humidified atmosphere. Flow cytometry was then performed using propidium iodide. Propidium iodide stains DNA and therefore DNA content can be measured. Analysis was first performed using lymphocytes kindly donated by Prof S Todryk to calibrate the flow cytometer for cells in G1; G1 was identified at the arbitrary unit 200 (Figure 4.5a). A histogram to show the spread of cells with different amount of DNA content was then performed using the test sample (a) G2/M was identified at the arbitrary unit 400 (as cells in this phase have double amount of DNA). Percentage of 10000 captured cells in each phase was then calculated (b).

To determine if there was a change in the amount of topo II $\beta$  in relation to topo II $\alpha$  in non-PMA and PMA treated cell, fold expression of topo II $\beta$  mRNA was compared to topo II $\alpha$  mRNA using  $\Delta\Delta C_t$ . It is important to note that the efficiencies of both the topo II $\alpha$  and topo II $\beta$  probe were similar (see Section 4.3.3), and all samples were run on the same plate, therefore results for topo II $\alpha$  and topo II $\beta$  were normalised to the same set of 18S data.

Despite a decrease in both topo II $\alpha$  and topo II $\beta$  when cells are treated with PMA, indeed a change in the relative amount of topo II $\beta$  to topo II $\alpha$  mRNA was observed. In non-PMA treated cells there is no significant difference in levels of topo II $\beta$  mRNA to topo II $\alpha$  mRNA in both cell lines (Figures 4.7a and 4.8a). In PMA treated cells, there is 3.5 fold and 4.9 fold more topo II $\beta$  mRNA in U937 and HL-60 cells respectively. This then identifies topo II $\beta$  as the predominant message in PMA treated cells. Although the results do not correlate with previous studies with regards to a lack of increase in topo II $\beta$  during differentiation, it does support the findings the topo II $\beta$  is the predominant topo II isoform in differentiated cells (Tiwari *et al.*, 2012).

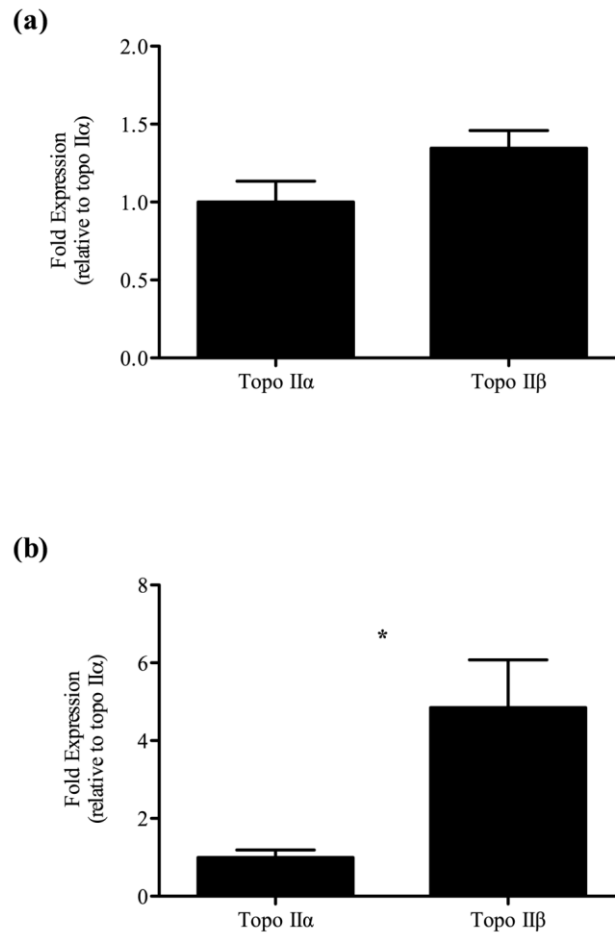


**Figure 4.7 Comparing fold expression of topo II $\alpha$  and  $\beta$  mRNA in non-PMA and PMA treated U937 cells.**

Data from Figure 4.3 was used to determine the fold expression of topo II $\beta$  to topo II $\alpha$  in non-PMA treated cells (a) and PMA treated cells (b).

Results shown are the mean of five independent experiments  $\pm$  standard error. \* =  $p < 0.05$ . See Appendix Table A.3 for p values.

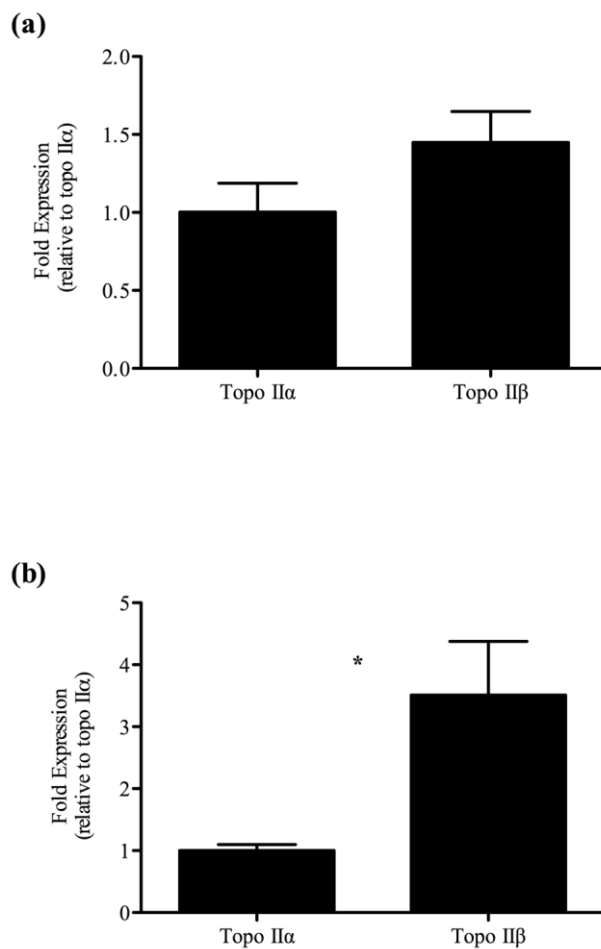


**Figure 4.8 Comparing fold expression of topo II $\alpha$  and  $\beta$  mRNA in non-PMA and PMA treated HL-60 cells.**

Data from Figure 4.4 was used to determine the fold expression of topo II $\beta$  to topo II $\alpha$  in non-PMA treated cells (a) and PMA treated cells (b).

Results shown are the mean of five independent experiments  $\pm$  standard error. \* =  $p < 0.05$ . See Appendix Table A.4 for p values.

#### **4.3.4 Quantification of topo II $\alpha$ and topo II $\beta$ mRNA in Primary monocytes and M-CSF treated monocytes**

In addition to quantifying topo II $\alpha$  and topo II $\beta$  in cell line models, primary monocytes were obtained and differentiated into macrophage like cells. Monocytes were isolated from peripheral blood by CD14<sup>+</sup> selection. CD14<sup>+</sup> monocytes are precursors of phagocytes such as macrophages (Kuwana *et al.*, 2003). Macrophage colony stimulating factor (M-CSF) was then used to differentiate the selected CD14<sup>+</sup> cells. It was decided M-CSF would be used rather than PMA in order to utilise a more biologically relevant model. M-CSF acts by indirectly activating Protein Kinase C (PKC) by inducing the production of diacylglycerol (DAG) (Valledor *et al.*, 1999). The activation of PKC causes a cascade of events leading to activation of transcription factors, and therefore transcription of genes involved in differentiation. This pathway of activation is very similar to that of PMA as PMA is analogous to DAG (Teixeira *et al.*, 2003), thus being able to stimulate PKC directly (see Introduction Section 1.12.1).

Levels of topo II $\alpha$  and topo II $\beta$  mRNA were then measured using qPCR. Analysis was performed using the comparative  $\Delta\Delta C_t$  method to measure fold expression. Samples taken from primary monocytes were normalised to values obtained using the 18S reference gene. The results are shown in Figure 4.9 and 4.10, respectively.

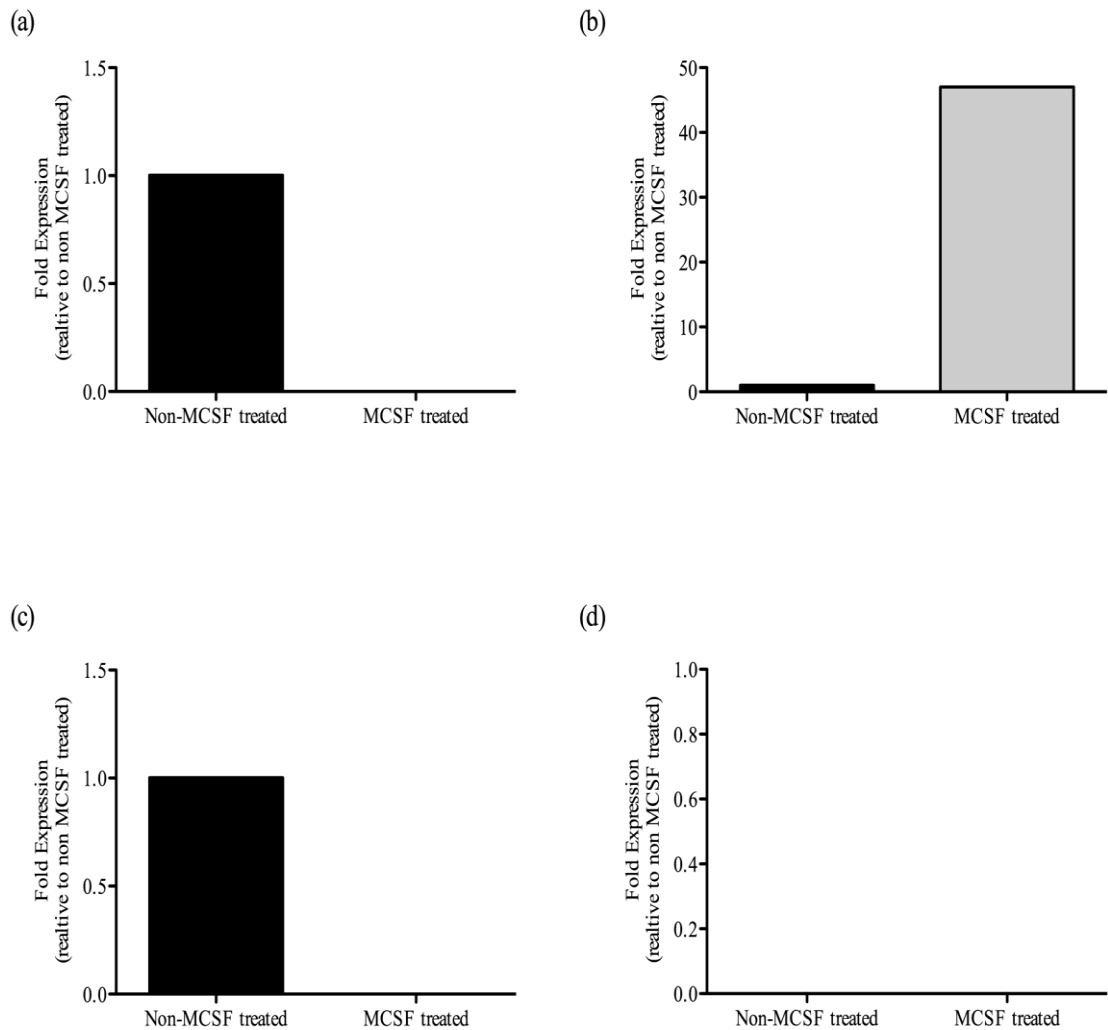


**Figure 4.9 Comparison of relative levels of Topoisomerase II $\alpha$  in CD14<sup>+</sup> monocytes from PBMC isolation compared to M-CSF treated cells of the same lineage.**

CD14<sup>+</sup> monocytes derived from peripheral blood were seeded at  $1 \times 10^6$ /ml in RPMI-1640 with 50 ng/ml M-CSF or 0.1% DMSO (v/v). Cells treated with 0.1% DMSO (v/v) were left to incubate for 24 h before harvesting. M-CSF treated cells were left to incubate for 7 days before harvesting. RNA was extracted and cDNA synthesised from the cells (Section 2.17). qPCR was performed using Taqman probes to TOP2A, and normalised to 18S (see Section 2.17.3 for qPCR conditions) 5  $\mu$ l of 3 ng/ $\mu$ l of cDNA was used for each reaction. Samples were performed in experimental triplicate. Results are shown comparing non-MCSF and MCSF treated CD14<sup>+</sup> monocytes from each individual donor (a –d).

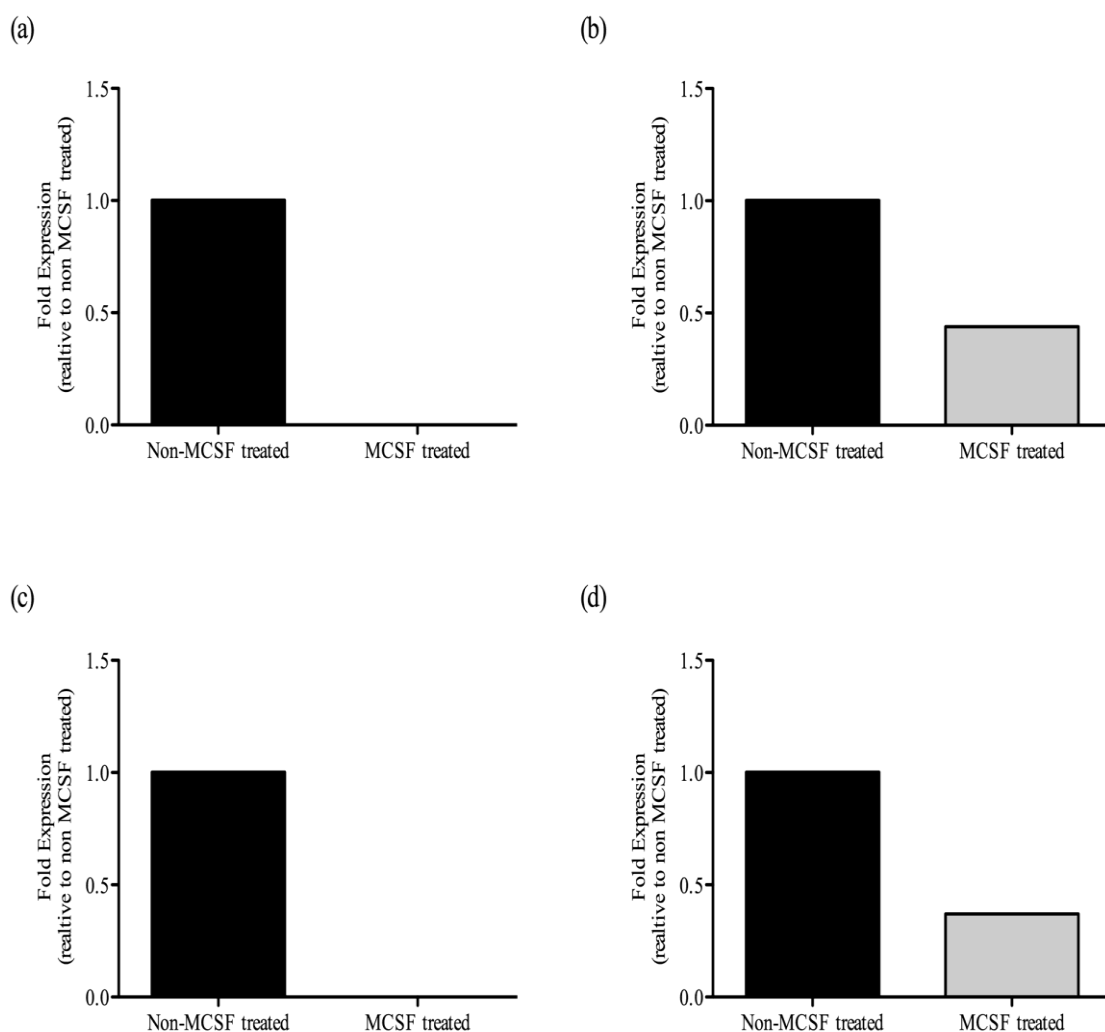


**Figure 4.10 Comparison of relative levels of Topoisomerase II $\beta$  in CD14<sup>+</sup> monocytes from PBMC isolation compared to M-CSF treated cells of the same lineage.**

CD14<sup>+</sup> monocytes derived from peripheral blood were seeded at  $1 \times 10^6$ /ml in RPMI-1640 with 50 ng/ml M-CSF or 0.1% DMSO (v/v). Cells treated with 0.1% DMSO (v/v) were left to incubate for 24 h before harvesting. M-CSF treated cells were left to incubate for 7 days before harvesting. RNA was extracted and cDNA synthesised from the cells (Section 2.17). qPCR was performed using Taqman probes to TOP2B, and normalised to 18S (see Section 2.17.3 for qPCR conditions) 5  $\mu$ l of 3 ng/ $\mu$ l of cDNA was used for each reaction. Samples were performed in experimental triplicate. Results are shown comparing non-MCSF and MCSF treated CD14<sup>+</sup> monocytes from each individual donor (a – d).

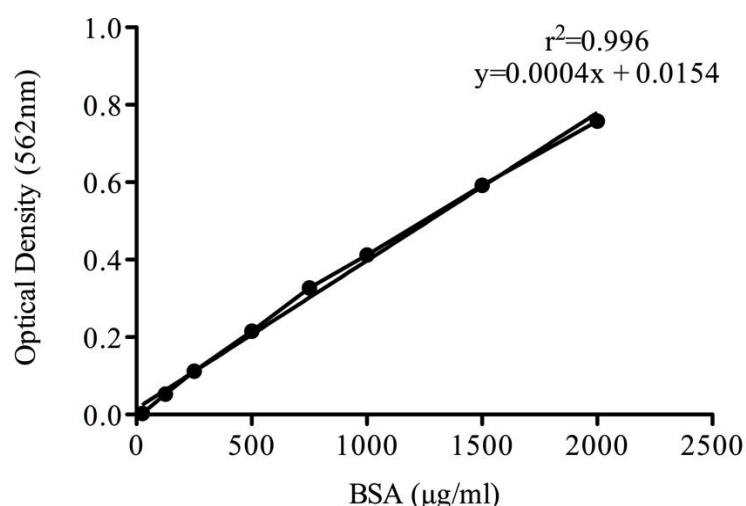


Figure 4.9 shows the mRNA levels of topo II $\alpha$  in non M-CSF and M-CSF treated CD14<sup>+</sup> cells from four different donors. The results show that levels of topo II $\alpha$  differ from donor to donor, indeed in two of the samples levels of topo II $\alpha$  mRNA appear to be higher in non M-CSF treated cells than M-CSF treated cells, this is demonstrated by a lack of amplification of topo II $\alpha$  suggesting that levels are so low they are undetectable (Figure 4.9a & c). In one sample set, no amplification was seen in non M-CSF and M-CSF treated cells (Figure 4.9d). In comparison in Figure 4.9b there appears to be more topo II $\alpha$  mRNA in M-CSF treated cells. The variance in data along with the heterogeneity of monocytes *in vivo* (ie. they may be at different stages of activation by various stimuli *in vivo*) makes it difficult to draw any firm conclusions, however Figure 4.9a & c do support previous data in this chapter, i.e., figure 4.3a and 4.4a show a decrease in topo II $\alpha$  mRNA expression in U937 and HL-60 cells differentiated with PMA. Unlike cancer derived cell lines, monocytes *in vivo* do not proliferate. Extensive research has shown that quiescent or cells in G0 (ie. non-proliferating) contain negligible levels of topo II $\alpha$  (Woessner *et al.*, 1991; Chow & Ross, 1987), however there are still detectable levels in non-proliferating differentiated cells (Figure 4.3a & Figure 4.4a), thus suggesting an unknown role for topo II $\alpha$  in differentiated cells. The results shown in Figure 4.9a & c are also in support of previous published work, Martinez, (2006) used transcriptome analysis to demonstrate a down regulation of topo II $\alpha$  mRNA when primary monocytes cells underwent differentiation with M-CSF.

Figure 4.10 shows the mRNA levels of topo II $\beta$  in non M-CSF and M-CSF treated CD14<sup>+</sup> cells from four different donors. The results show that levels of topo II $\beta$  mRNA decrease upon M-CSF treatment (Figure 4.10b & d), two of the data sets (Figure 4.10a & c) demonstrate this by a lack of amplification of topo II $\beta$  after treatment with M-CSF, suggesting that levels are so low they are undetectable. The results support previous work in this chapter that show that topo II $\beta$  mRNA levels decrease when cells are treated with PMA (Figure 4.3b and Figure 4.4b). Unlike the cell lines, the decrease in topo II $\beta$  mRNA is not due to a decreased in demand for this isoform due to a lack of cell replication, as CD14<sup>+</sup> monocytes do not proliferate (Clanchy *et al.*, 2006). The environment of the CD14<sup>+</sup> monocyte *in vivo*, however, may require transcription in response to stimuli in the micro-environment, therefore an up-regulation of topo II $\beta$  mRNA would be seen in CD14<sup>+</sup> monocytes.

#### 4.3.5 Quantification of Topoisomerase II $\alpha$ and $\beta$ protein in U937 and HL-60 cell lines.

Levels of topo II $\alpha$  and topo II $\beta$  protein were semi-quantified in samples from exponentially growing U937 and HL-60 cells (see Figure 3.4). These results were then compared to PMA treated U937 and HL-60 cells. To ensure only differentiated cells were to be analysed, any suspension cells in the PMA treated flasks were discarded, and the remaining adherent cells were gently harvested using a cell scraper. Following harvesting, whole cell extracts were performed (see Section 2.15) and total protein in each extract was quantified using the BCA Protein Assay kit (Thermo-scientific). A standard curve was then generated using bovine serum albumin; an example of which is demonstrated in Figure 4.11.



**Fig 4.11 Example of BSA Standard Curve.**

A 2mg/ml bovine serum albumin stock solution was used to generate dilutions of; 25, 125, 250, 500, 750, 1000, 1500 and 2000 µg/ml. Unknown protein samples were diluted 1/10 in PBS before all samples were added in triplicate to a 96 well plate, in addition to the samples PBS only was added in triplicate as the buffer control, and reagents from the BCA Protein Assay kit (Thermo-scientific) were added (Section 2.16.2) the plate was then incubated at 37°C for 30 min before endpoint absorbance was measured at 562 nm. The mean absorbance of the standard triplicate wells was then plotted against concentration. Unknown samples were determined by  $y = mx + c$  and adjusted for dilution.

Once quantified an equal amount of total protein was loaded onto SDS-PAGE gels and western blots were performed. The blots were then probed with antibodies specific to topo II $\alpha$  and topo II $\beta$  (see Section 2.16 for more information on methodology). Densitometry was then performed on the blots in order to semi-quantify the amount of topo II $\alpha$  and topo II $\beta$  present in the samples. The results are shown in Figures 4.12 and 4.13.

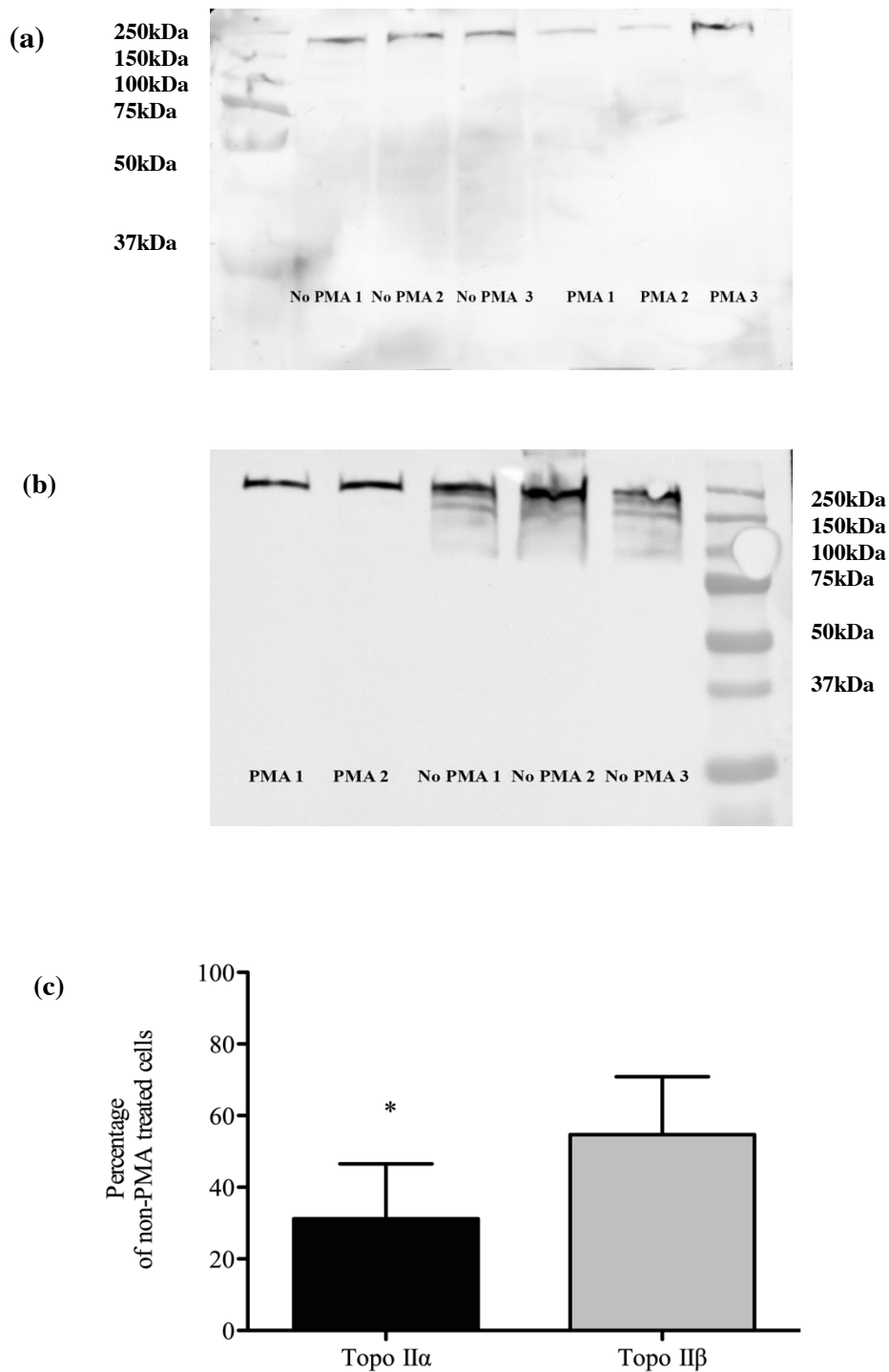


**Figure 4.12 Semi-Quantitation of topo II $\alpha$  and  $\beta$  protein in non-PMA and PMA treated U937 cells.**

Cells were seeded at  $3 \times 10^5$  cells/ml with 5 ng/ml PMA or 0.1% DMSO (v/v) in 75cm<sup>3</sup> culture flask and allowed to incubate for 72 h before harvesting. Whole cell protein was then extracted and quantified (Section 2.16). 185 $\mu$ g of total protein was then loaded onto a 7.5% SDS gel and SDS PAGE was then performed to separate the proteins out by size (Section 2.16.4) this was followed by protein transfer onto nitrocellulose paper by wet western blot (Section 2.16.5). Nitrocellulose blots were then probed with antibodies to topo II $\alpha$  (a) and topo II $\beta$  (b) (Section 2.16.7). Lanes are labelled with treatment and sample number (c) Quantification of protein was performed using the densitometry software, Syngene genetools, data is presented as amount of protein in PMA treated cells as a percentage of that in non-PMA treated cells. See Appendix Figure A.2 and A.3 for GAPDH loading control. Results shown are the mean of two independent sample  $\pm$  standard error. \* =  $p < 0.05$ . See Appendix Table A.5 for p values.

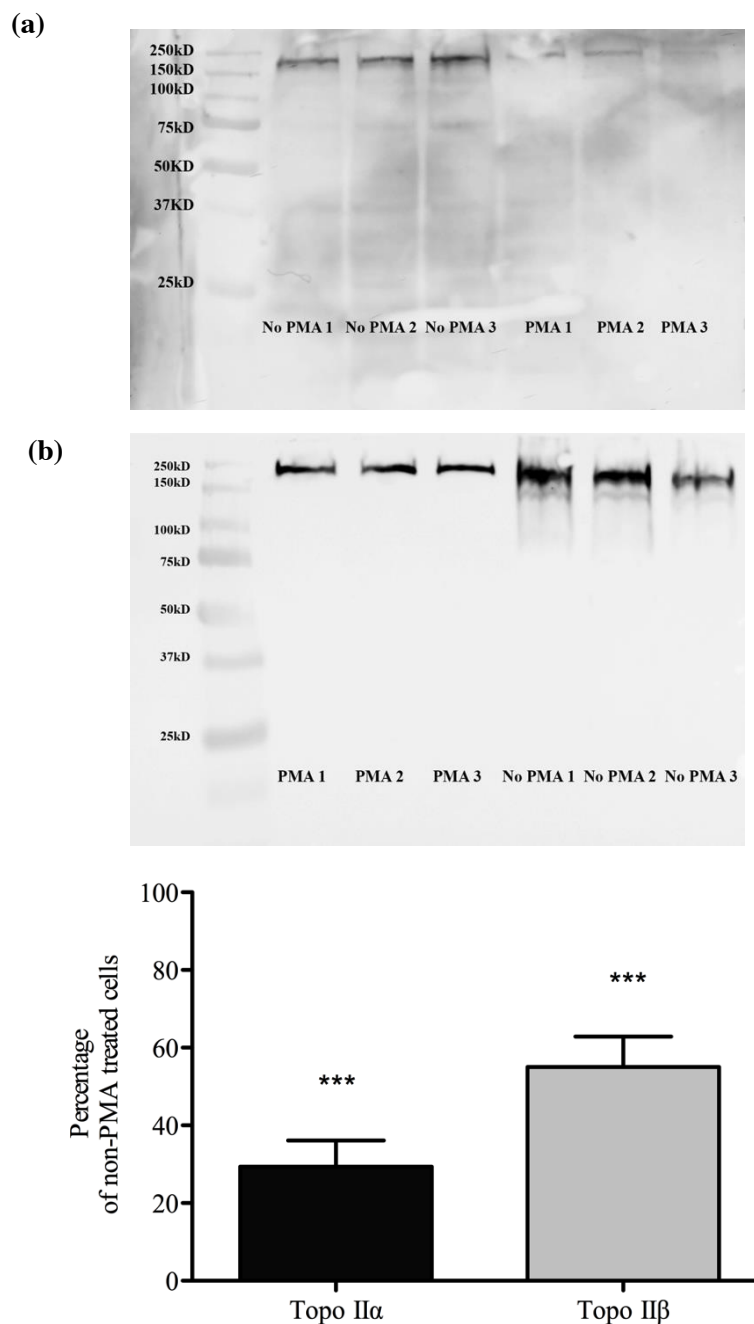


**Figure 4.13 Semi-Quantitation of topo II $\alpha$  and  $\beta$  protein in non-PMA and PMA treated HL-60 cells.**

Cells were seeded at  $3 \times 10^5$  cells/ml with 5 ng/ml PMA or 0.1% DMSO (v/v) in 75cm<sup>3</sup> culture flask and allowed to incubate for 72 h before harvesting. Whole cell protein was then extracted and quantified (Section 2.16.2). 185 $\mu$ g of total protein was then loaded onto a 7.5% SDS gel and SDS PAGE was then performed to separate the proteins out by size (Section 2.16.4) this was followed by protein transfer onto nitrocellulose paper by wet western blot (Section 2.16.5). Nitrocellulose blots were then probed with antibodies to topo II $\alpha$  (a) and topo II $\beta$  (b) (Section 2.16.7). Lanes are labelled with treatment and sample number (c) Quantification of protein was performed using the densitometry software, Syngene genetools, data is presented as amount of protein in PMA treated cells as a percentage of that in non-PMA treated cells. See Appendix Figures A.4 and A.5 for GAPDH loading control. Results shown are the mean of three independent samples  $\pm$  standard error. \*\*\* =  $p < 0.001$ . See Appendix Table A.6 for p values.

From the results (Figure 4.12 and 4.13) a decrease in both topo II $\alpha$  and topo II $\beta$  protein levels can be observed when both U937 and HL-60 cells are treated with PMA. This supports mRNA data in Figures 4.3 and 4.4. An average 69% decrease in topo II $\alpha$  protein was observed in PMA treated U937 cells compared to non-PMA treated cells, similarly an average 70% decrease in topo II $\alpha$  protein was seen in PMA treated HL-60 cells compared to the non-PMA treated cells. Interestingly an average 65% decrease in the level of topo II $\beta$  protein was observed when U937 cells were treated with PMA, whilst a 70% decrease in topo II $\beta$  protein was seen in PMA treated HL-60 cells compared to non-PMA treated cells. These findings are in agreement with Kauffman *et al.* (1991) who reported a decrease in levels of both topo II $\alpha$  and topo II $\beta$  protein when HL-60 cells underwent granulocytic differentiation. Constantinou *et al.* (1996) mirrored this finding, demonstrating a decrease in topo II catalytic activity followed by a decrease in phosphorylation and a subsequent decrease in protein levels when mouse erythroleukemic cells (MELs) were differentiated with hexamethylene bis-acetamide (HMBA). This was in support of work by Bodely *et al.* (1987) who demonstrated a decrease in topo II protein and activity in HMBA differentiated MELs.

As discussed previously (Section 4.2.1) down-regulation of topo II $\alpha$  may be the result of an arrest in the cell cycle. Figure 4.6a shows that when cells are treated with PMA, cells appear to arrest in late S phase, early G2/M. This is in agreement with previous studies that have also reported the same G2/M arrest (Kosaka *et al.*, 1996; Barboule *et al.*, 1999; Oliva *et al.*, 2008). Levels of topo II $\alpha$  protein have previously been shown to increase during S phase, peaking in G2/M (Woessner, 1991). This reflects the importance of the role of topo II $\alpha$  in the decatenation of sister chromatids during mitosis (Uemura *et al.*, 1987; Adachi *et al.*, 1991; Coelho *et al.*, 2003; Ramamoothy *et al.*, 2012). It may then be expected that levels of topo II $\alpha$  in PMA treated cells would be relatively high compared to cycling cells as the cells are arrested in G2/M. Taken together, the G2/M arrest seen in Figure 4.6a in PMA treated cells along with a lack of proliferation in PMA treated cells (Figure 3.4) it may be suggested that mitosis is not occurring, thus topo II $\alpha$  is not required. The half-life of topo II $\alpha$  has previously been reported to be 6.6 h. It then undergoes proteosomal degradation. A lack of progression through G2/M to enter the cell cycle again would result in normal degradation of topo II $\alpha$  and a lack of topo II $\alpha$  being synthesised. Thus this may explain the decrease in topo II $\alpha$  protein in PMA treated cells compared with cycling cells.

The decrease in topo II $\beta$  protein levels is however, in contrast with work by Aoyama *et al.* (1998) who reported that differentiation of HL-60 cells using *all-trans* retinoic acid resulted in an increase in topo II $\beta$  protein. However in an earlier study by Kauffman *et al.* (1991) using the same cell line, levels of topo II $\beta$  were shown to be reduced. The difference in topo II $\beta$  levels observed between the studies may be due to the differentiating agent used. Kauffman *et al.* (1991) used 1.3% DMSO to differentiate HL-60 into a granulocyte like cells, in contrast Aoyama *et al.* (1998) used 1 $\mu$ mol/L *all-trans* retinoic acid to induce granulocytic differentiation of HL-60 cells. Additionally McNamara *et al.* (2010) reported an up-regulation of topo II $\beta$  protein expression when NB4 and NB4-MR2 cells were treated with PMA for 2 h, and that an increase in protein expression correlated with an increase in PMA concentration. They also postulated that this up-regulation could be the result of an up-regulation of protein kinase delta (PKCD), which is stimulated by PMA and suggest that PKCD phosphorylates topo II $\beta$  leading to an increase in stability and a decreased rate of degradation. Inhibition of PKCD was also shown to result in a decrease in topo II $\beta$  protein level. The results are however in agreement with Padgett *et al.* (2000) who showed a higher abundance of both topo II $\alpha$  and topo II $\beta$  protein in exponentially growing Raji cells compared to the confluent counterparts, thus suggesting that levels of topo II $\beta$  may also be cell cycle dependent. Therefore the decrease in topo II $\beta$  protein demonstrated in Figure 4.12b and 4.13b may be due to similar scenario as that in the decrease of topo II $\alpha$ .

The difference between the levels of mRNA and protein expression with regards to quantification of both topo II $\alpha$  and topo II $\beta$  may be due to changes in the stability of the mRNA transcript or the stability of the protein via changes in translational modifications upon PMA treatment. Indeed phosphorylation of topo II $\alpha$  has previously been shown to increase the stability of the protein (Qi *et al.*, 2011) and PMA induced PKCD has been suggested to modulate the stability of topo II $\beta$  (McNamara *et al.*, 2010).

It was hypothesised that the changes in gene expression involved in the differentiation from monocyte to macrophage would require the actions of topo II $\beta$  in the regulation of transcription of lineage specific genes. Furthermore it was expected that an increase in the requirement of topo II $\beta$  may result in an up-regulation of its protein expression. However the results in Figures 4.9 and 4.10 do not support this hypothesis; levels of topo II $\beta$  are significantly less in differentiated cells than in cycling cells. McNamara *et al.* (2010) reported that topo II $\beta$  was increased 2 h after PMA treatment compared to a

non-PMA treated control. Indeed it may be suggested that the regulation of transcription of genes involved in differentiation occur very early on and the decrease in topo II $\beta$  after 72 h of PMA treatment may reflect a decrease in transcriptional activity within the cells. Certainly it is sensible to suggest that the transcriptional activity of differentiated cells may be less than cycling cells that require an increase in transcription in comparison for the synthesis of proteins for newly synthesised cells, and thus would contain a higher level of topo II $\beta$ .

#### **4.4 Effect of Topoisomerase II drugs on cell viability, using the XTT assay**

The cytotoxic assay, XTT was used to quantify the number of viable cells (see Section 2.15 for further detail) when non-PMA and PMA treated cells were exposed to the topoisomerase II drugs, etoposide (VP-16), ICRF-193 and ICRF-187.

Previous work has shown that efficacy of topo II drugs is directly related to the amount of topo II present in the cell (Depowski *et al.*, 2000). Therefore this assay will be used to verify the levels of topo II $\alpha$  and topo II $\beta$  determined in Section 4.2.

##### **4.4.1 Effect of etoposide**

Etoposide (VP-16) a topoisomerase II poison belongs to a group of non-intercalating drugs, the epipophyllotoxins. Etoposide acts by stabilising the topo II cleavable complex by forming a drug-DNA tertiary complex, thus preventing re-ligation of DNA strands. During the cell cycle the cleavable complexes are further processed and become permanent double strand breaks (Li & Lui, 2001). An accumulation of double strand breaks will eventually lead to apoptosis of the cell (Section 1.8.2).



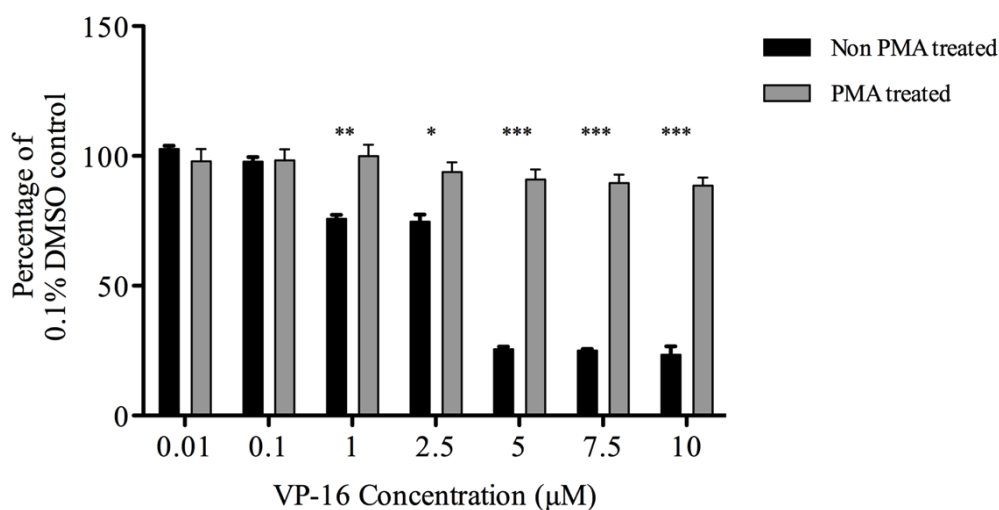


**Figure 4.14 Comparing the cytotoxic effect of VP-16 on non-PMA and PMA treated U937 cells.**

U937 cells were seeded at a density of  $3 \times 10^5$  cells/ml with 5 ng/ml PMA or 0.1% DMSO (v/v) and allowed to incubate for 72 h. Media was then replaced with the addition of varying concentrations of VP-16 (0.01, 0.1, 1, 2.5, 5, 7.5 and 10 μM) 0.1% DMSO (v/v) was used as the drug vehicle control. Cells were allowed to incubate for a further 72 h, after which an XTT assay was performed (Section 2.15).

Results are reported as percentage of 0.1% DMSO (v/v) vehicle control. Results shown are the mean of three independent experiments  $\pm$  standard error. \* =  $p < 0.05$ , \*\* =  $p < 0.001$ , \*\*\* =  $p < 0.001$ . See Appendix Table A.7 for p values.

Figure 4.14 shows the effects of various concentrations of VP-16 on U937 cells and PMA pre-treated U937 cells. When the concentration of VP-16 increases, there is a significant increase in cytotoxicity in non-PMA treated cells ( $p = < 0.0001$ ), reaching an average 75% decrease in viable cells at 5μM, a similar decrease is maintained when cells are treated with 7.5 and 10μM VP-16. In comparison, PMA treated cells maintain at least an average 85% cell viability up to the highest concentration of VP-16, 10μM. Thus pre-treatment of cells with PMA appears to have a protective effect against the cytotoxic affect of VP-16.

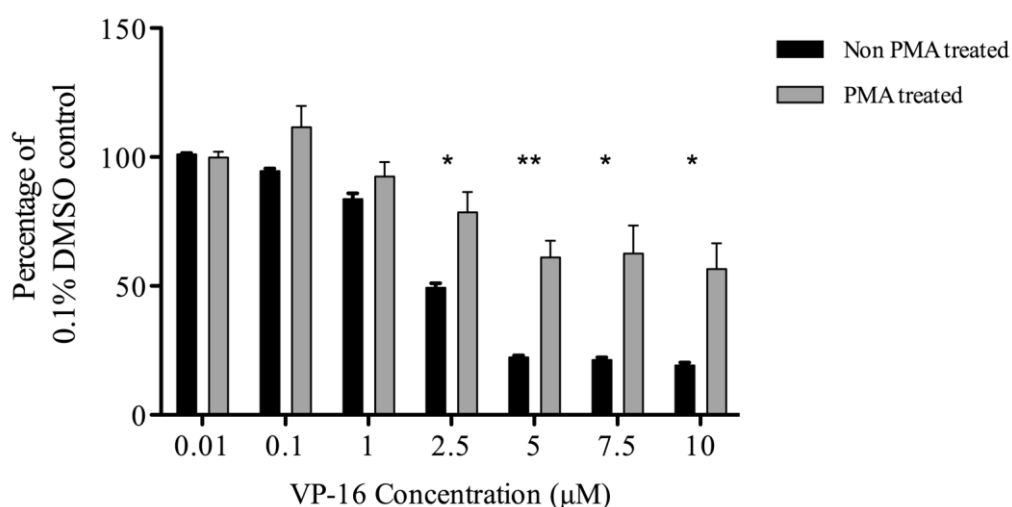


**Figure 4.15 Comparing the cytotoxic effect of VP-16 on non-PMA and PMA treated HL-60 cells.**

HL-60 cells were seeded at a density of  $3 \times 10^5$  cells/ml with 5 ng/ml PMA or 0.1% DMSO (v/v) and allowed to incubate for 72 h. Media was then replaced with the addition of varying concentrations of VP-16 (0.01, 0.1, 1, 2.5, 5, 7.5 and 10 μM) 0.1% DMSO (v/v) was used as the drug vehicle control. Cells were allowed to incubate for a further 72 h, after which an XTT assay was performed (Section 2.15).

Results are reported as percentage of 0.1% DMSO (v/v) vehicle control. Results shown are the mean of three independent experiments  $\pm$  standard error. \* =  $p < 0.05$ , \*\* =  $p < 0.01$ . See Appendix Table A.8 for p values.

A similar result is also observed in HL-60 cells (Figure 4.15); there is a significant decrease in cell viability in non-PMA treated cells as the concentration of VP-16 increases ( $p = > 0.0001$ ). When these cells are exposed to 10 μM of VP-16 they exhibit an average 82% decrease in cell viability. PMA treated cells, in contrast, again appear to be more protected against VP-16 with only a 43% average decrease in cell viability. This is in agreement with Jasek *et al.* (2008) who also saw a decrease in sensitivity to etoposide in PMA treated HL-60 cells.

The results of this assay (Figures 4.14 and 4.15) may be explained by analysis of the cell cycle in Figure 4.6a that demonstrates a G2/M cell cycle arrest when cells are differentiated with PMA. Sensitivity of cells to VP-16 induced apoptosis has been shown to require the transition of cells from G1 to S phase (Ferraro *et al.*, 2000). This is

supported by D'Arpa *et al.*, (1990) who reported that inhibition of nucleic acid synthesis rendered chinese hamster cells resistant to VP-16. Therefore an arrest in G2/M may lead to VP-16 resistance as seen in cells that undergo PMA pre-treatment (Figure 4.13 and 4.14) due to an inability to proceed through G1 and S phase.

Additionally, the cytotoxic action of VP-16 requires the processing of multiple cleavable complexes in order for enough double strand breaks to become visible to induce apoptosis (Li & Lui, 2001). The processing of cleavable complexes includes the physical collision of replication and/or transcriptional machinery with the cleavable complex, physically knocking topo II from the site to reveal the double strand break (Tammaro *et al.*, 2013). If replication is ceased, for example in cell cycle arrested or differentiated cells (Moore & Wang, 1994) then it is sensible to suggest the amount of cleavable complexes processed will be reduced, resulting in a decrease in cytotoxicity. Figure 4.5b shows the cell cycle distribution of 0.1% DMSO (v/v) treated and PMA treated U937 cells. 0.1% DMSO (v/v) treated cells display a typical cell cycle distribution of exponentially growing cells (Wang *et al.*, 2006), whilst PMA treated cells appear to accumulate in late S phase, G/M. This is in agreement with previous studies that have reported the same pattern of cell cycle distribution in PMA treated cells. Therefore from this data, along with the results from the growth curve in Chapter 3 (Figure 3.4) it can be inferred that PMA treated cells do not cycle. It may then be postulated that the decrease in sensitivity to VP-16 in PMA pre-treated cells compared to non-PMA treated cells is due to a reduction in the processing of cleavable complexes due to a decline in replication associated with cell cycle arrest. In addition, this cell cycle block may facilitate the reversal and/or repair of more drug-stabilised cleavable complexes (Branzai & Foiani, 2008). All of these scenarios are not mutually exclusive and would lead to a decrease in VP-16 sensitivity.

Furthermore Figures 4.3a, 4.4a 4.12a and 4.13a reveal a down-regulation of topo II $\alpha$  both at the mRNA and protein level when cells are treated with PMA for 72 h compared to non-PMA treated cells. Indeed it has already been established that VP-16 preferentially targets topo II $\alpha$ . A study by Errington *et al.* (2004) investigated the cytotoxic importance of each isoform, relating this to the stability of the topo II-drug complexes. They report that the longevity of topo II $\alpha$  – VP-16 complexes was greater than the topo II $\beta$  – VP-16 complexes. It may be postulated that a decrease in topo II $\alpha$  may render VP-16 ineffective due to a lack of topo II $\alpha$  target. This is in support of previous work that has shown that measurement of topo II levels can predict the

efficacy of chemotherapeutic drugs (Durbecq *et al.*, 2004; Deposki *et al.*, 2000; Schindlbeack *et al.*, 2010).

Once a difference in the efficacy of VP-16 on non-PMA and PMA treated cells was established, an investigation into the synergistic effect of PMA and VP-16 on cell viability was undertaken. This co-treatment would establish the effects of VP-16 on cells that were undergoing differentiation in contrast to when they were terminally differentiated (Figure 4.16).

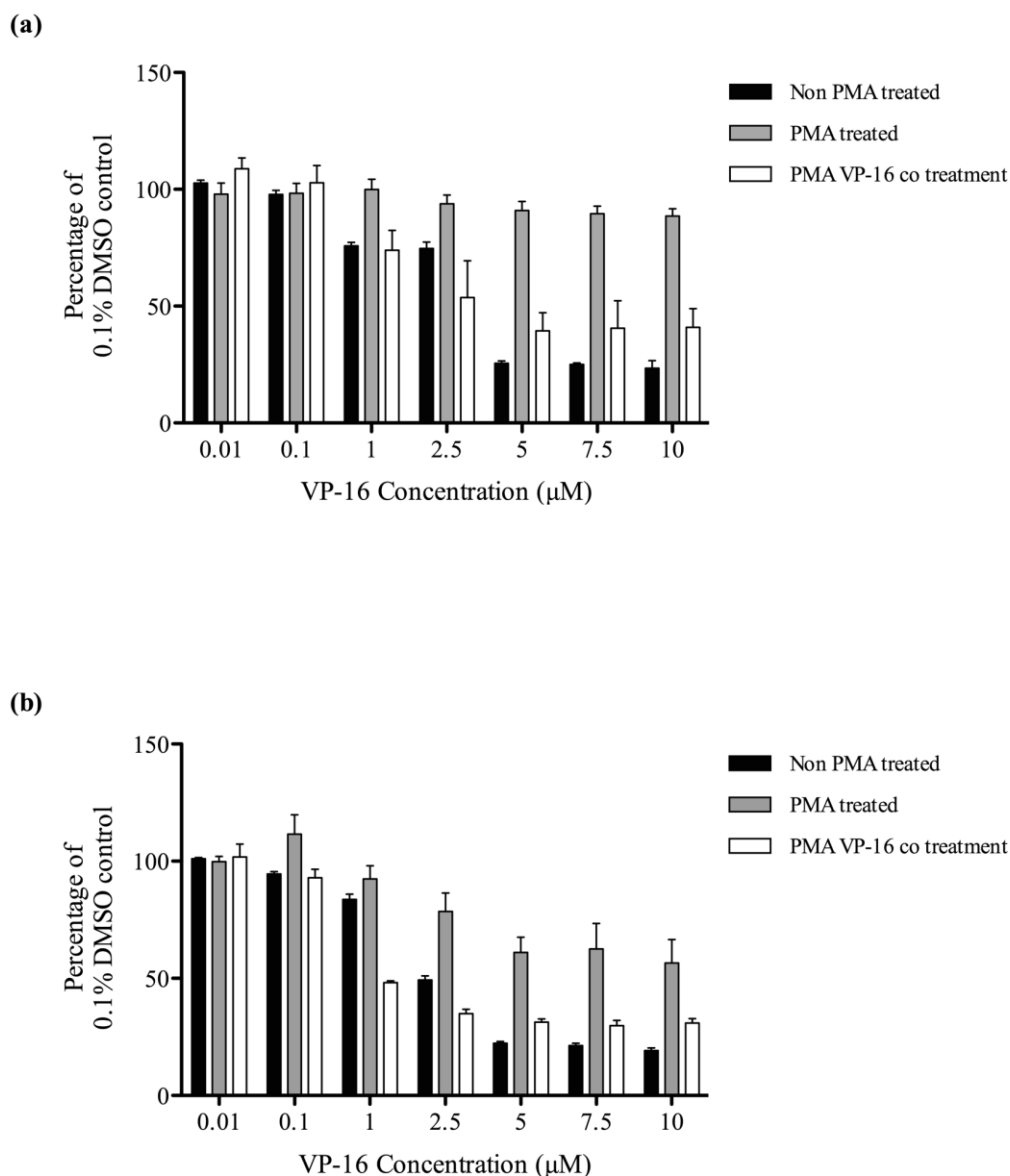


**Figure 4.16 Comparing the effects of VP-16 on PMA pre-treated cells and PMA/VP-16 co-treated cells.**

U937 cells (a) and HL-60 cells (b) were seeded at a density of  $3 \times 10^5$  cells/ml with 5 ng/ml PMA or 0.1% DMSO (v/v) and allowed to incubate for 72 h. Media was then replaced with the addition of varying concentrations of VP-16 (0.01, 0.1, 1, 2.5, 5, 7.5 and 10  $\mu$ M) 0.1% DMSO (v/v) was used as the drug vehicle control. At this time cells for VP-16 co-treatment were seeded at  $3 \times 10^5$  cells/ml with 5 ng/ml PMA and the various VP-16 concentrations. All cells were allowed to incubate for a further 72 h, after which an XTT assay was performed (See Section 2.15). Results are reported as percentage of 0.1% DMSO (v/v) control. Results shown are the mean of three independent experiments  $\pm$  standard error. See Appendix Tables A.9 to A.12 for p values.

At VP-16 concentrations of 5, 7.5 and 10  $\mu\text{M}$  U937 cells that had undergone PMA/VP-16 co-treatment are less sensitive to VP-16 than non-PMA treated cells, however they are more sensitive to VP-16 than PMA pre-treated cells. For example, Figure 4.16a shows U937 cells that have been co-treated with PMA/VP-16 at a concentration of 5  $\mu\text{M}$  VP-16. These cells display an average 60% reduction in cell viability. In comparison, non-PMA treated cells exposed to 5  $\mu\text{M}$  VP-16 display a 75% reduction in cell viability, these results are not significantly different (see Appendix Table A.9). Furthermore, cells pre-treated with PMA prior to treatment with 5  $\mu\text{M}$  VP-16 display an average 9% decrease in cell viability, this is significantly different from the co-treated cells ( $p=0.004$ ). This decrease in cell viability is mirrored in the results where 7.5  $\mu\text{M}$  and 10  $\mu\text{M}$  VP-16 were used (see Appendix Table A.10).

HL-60 cells exposed to the same conditions as U937 (Figure 4.16b) exhibit a similar pattern of response to co-treatment of PMA/VP-16 compared to PMA pre-treated samples and non-PMA treated samples. Again at VP-16 concentrations of 5, 7.5 and 10  $\mu\text{M}$  cells that had undergone co-treatment with PMA/VP-16 appeared more sensitive to VP-16 than PMA pre-treated cells as demonstrated by a larger decrease in cell viability. For example, Figure 4.16b shows HL-60 cells that have been co-treated with PMA/VP-16 at a concentration of 5  $\mu\text{M}$  VP-16. These cells display an average 69% reduction in cell viability. In comparison, non-PMA treated cells exposed to 5  $\mu\text{M}$  VP-16 display a 78% reduction in cell viability, which is significantly different from the co-treated cells ( $p=0.004$ ). Furthermore, cells pre-treated with PMA prior to treatment with 5  $\mu\text{M}$  VP-16 display an average 40% decrease in cell viability, again this is significantly different from the co-treated cells ( $p=0.01$ ). This decrease in cell viability is mirrored in the results where 7.5  $\mu\text{M}$  and 10  $\mu\text{M}$  VP-16 were used (see Appendix Table A.11).

Barry *et al.* (1993) showed that 30 minutes of treatment of HL-60 cells to VP-16 followed by varying lengths of incubation post treatment resulted in apoptosis of the cells within 8 h. A study using MCF-7 cells revealed that PMA induced G2/M arrest occurred between 6 to 9 h of PMA treatment (Barboule *et al.*, 1999). Taken together it may be postulated that results seen in Figure 4.15, where co-treatment of cells with PMA/VP-16 renders cells more sensitive to VP-16 than cells that had been pre-treated with PMA prior to VP-16 exposure may be due to DNA damage and apoptosis induced by VP-16 in the early stages of PMA treatment when cells are continuing to cycle. As described previously, the cytotoxic effects of VP-16 are shown to be reliant on the cellular processing of VP-16 induced cleavable complexes (Li & Lui, 2001). These

events include for example the physical interaction of replication machinery with the cleavable complex, knocking topo II from the site and thus revealing a double strand break (Tammaro *et al.*, 2013). As replication does not occur in non-cycling cells, such as those arrested in G2/M phase then it is sensible to suggest that the processing of the cleavable complexes is reduced. Pre-treated PMA cells are arrested in G2/M prior to treatment with VP-16 (Figure 4.6a), however co-treated VP-16/PMA cells have a 6-9 hour period of VP-16 exposure before G2/M arrest occurs (Barboule *et al.*, 1999). It may be that the co-treated cells are more sensitive to VP-16 than PMA pre-treated cells as they have a short period at the beginning of PMA treatment where cleavable complexes may be processed, subsequently triggering apoptosis.

Lower doses of VP-16 (0.001 – 0.1  $\mu$ M) appear to have little cytotoxic effect on non-PMA, PMA pre-treated and PMA/VP-16 co-treated cells. However in both U937 and HL-60 cells (Figure 4.16) cells co-treated with VP-16 at concentrations of 1 and 2.5  $\mu$ M along with PMA exhibit a higher sensitivity to the cytotoxic actions of VP-16 compared to PMA pre-treated cells (see Appendix Tables A.9-A.12 ).

Interestingly, low doses of VP-16 have been observed to up-regulate an early activation of PKC in HL-60 cells (Perez *et al.*, 1997). McNamara *et al.* (2010) reported that after 2 h of treatment with PMA, levels of PKCD increased and this correlated with an up-regulation of topo II $\beta$ , furthermore they suggest that this up-regulation of topo II $\beta$  is due to an increase in stability of the protein induced by its phosphorylation by PKCD. Therefore it may be possible that the results shown in Figure 4.16 with regards to the 1 and 2.5  $\mu$ M concentrations of VP-16 in the VP-16/PMA co-treated cells appearing more sensitive to VP-16 than non-PMA treated cells may be due to an attenuation effect of VP-16 and PMA resulting in an increased amount of PKCD resulting in an increase in topo II $\beta$  phosphorylation, a decreased rate of degradation, and therefore more target for VP-16 to act. This hypothesis is in agreement with work by Ritke *et al.* (1994) who showed that VP-16 resistant cells, K/VP.5 contained topo II that was 2.5 less phosphorylated than the K562 sensitive cells. Despite VP-16 preferentially targeting topo II $\alpha$  (Errington *et al.*, 2004; Bandele & Osherooff, 2008) it does also target topo II $\beta$  (Willmore *et al.*, 1998; Errington *et al.*, 2004). It may be that an early increase in topo II $\beta$  yields more target for VP-16 and therefore increases its cytotoxicity. Indeed it has been shown that levels of topo II can predict the efficacy of such drugs (Dingemans *et al.*, 1999).

The results shown in Figure 4.14 are in agreement with a study by Zwelling *et al.* (1988) who also showed that treatment of HL-60 cells with PMA prior to exposure to VP-16 led to decrease in sensitivity to the drug compared to non-PMA treated cells. Furthermore they show that PMA causes changes in chromatin architecture; such as changes in nuclease sensitivity and alterations in DNA linking number, and suggest that this may change the interaction of topo II with the DNA and VP-16 with the DNA. Additionally they also show that cells are more sensitive to the topo II poison and DNA intercalator, mAMSA than VP-16. They suggest that as a DNA intercalator, mAMSA may induce local changes in DNA structure therefore overcoming any hindering changes caused by PMA. This is in contrast to VP-16, which does not DNA intercalate and therefore cannot directly influence DNA structure. Zwelling *et al.* (1988) also suggest that PMA may induce the cellular re-distribution of topo II to non-DNA regions or non-cleavable DNA sites therefore protecting against VP-16. Indeed this hypothesis is plausible; Cowell *et al.* (2011) showed that treatment of cell cultures with the histone deacetylase inhibitor, trichostatin A (TSA) induced the re-distribution of topo II $\beta$  from heterochromatin to euchromatin and suggested that this redistribution then converts topo II $\beta$  to a more effective target of topo II poisons.

Taken together, the protective effect of PMA on VP-16 induced cytotoxicity appears to be multi-variant, and certainly deserves further investigation.

#### **4.4.2 Effect of ICRF-193**

ICRF-193, a topoisomerase II inhibitor from the bisdioxopiperazine family of drugs acts by non-competitively binding to topo II, preventing binding and hydrolysis of ATP. ATP hydrolysis is required for the release of the re-ligated DNA strand from the topo II dimer. Inhibition of ATP hydrolysis results in a closed clamp structure. The actions of ICRF-193 ultimately lead to prevention of enzyme turnover. Apoptosis of ICRF-193 treated cells is a result of an inability of cells to segregate chromosomes, leading to an accumulation of DNA damage post mitosis.

To investigate the effects of ICRF-193 on non-PMA and PMA pre-treated cells, cells were exposed to varying concentrations of ICRF-193 for 72 h.



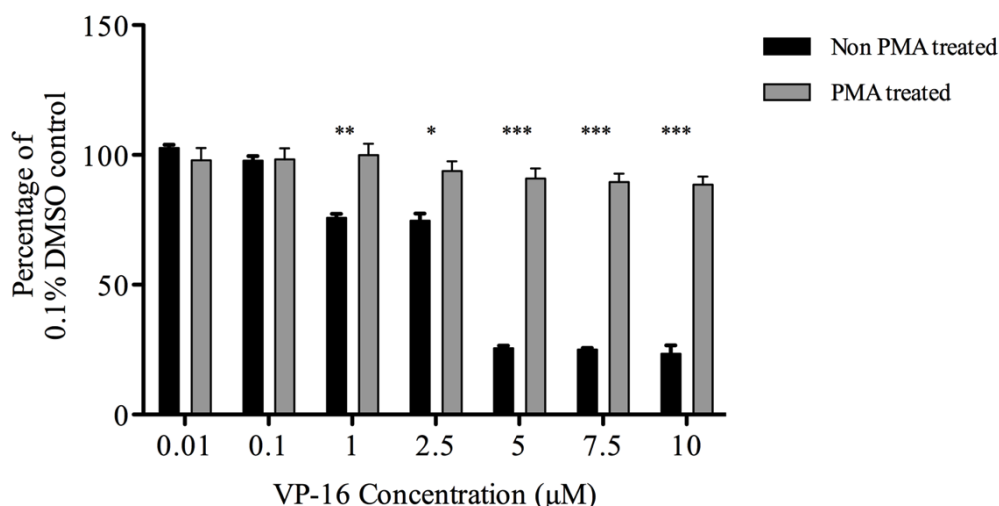


**Figure 4.17 Comparing the cytotoxic effect of ICRF-193 on non-PMA and PMA treated U937 cells.**

U937 cells were seeded at a density of  $3 \times 10^5$  cells/ml with 5 ng/ml PMA or 0.1% DMSO (v/v) and allowed to incubate for 72 h. Media was then replaced with the addition of varying concentrations of ICRF-193 (0.001, 0.01, 0.02, 0.04, 0.06, 0.08, 0.1, 2.5, 5 and 7.5  $\mu$ M) 0.1% DMSO (v/v) was used as the vehicle control. Cells were allowed to incubate for a further 72 h, after which an XTT assay was performed (Section 2.15).

Results are reported as percentage of 0.1% DMSO (v/v) vehicle control. Results shown are the mean of three independent experiments  $\pm$  standard error. \* =  $p < 0.05$ , \*\* =  $p < 0.01$ . See Appendix Table A.13 for p values.

The results in Figure 4.17 show that ICRF-193 exhibits a cytotoxic effect on non-PMA treated U937 cells from a concentration of 1  $\mu$ M. Non – PMA treated U937 cells exhibit an average 32% decrease in cell viability when treated with 1  $\mu$ M ICRF-193 for 72 h. This decrease in cell viability is similar when non-PMA treated cells are treated with higher concentrations of ICRF-193 including 2.5, 5 and 7.5  $\mu$ M. In comparison PMA treated U937 cells appear to be protected against the effects of ICRF-193 as the largest decrease in cell viability is on average, 11% seen when cells are treated with 1 and 5  $\mu$ M ICRF-193.

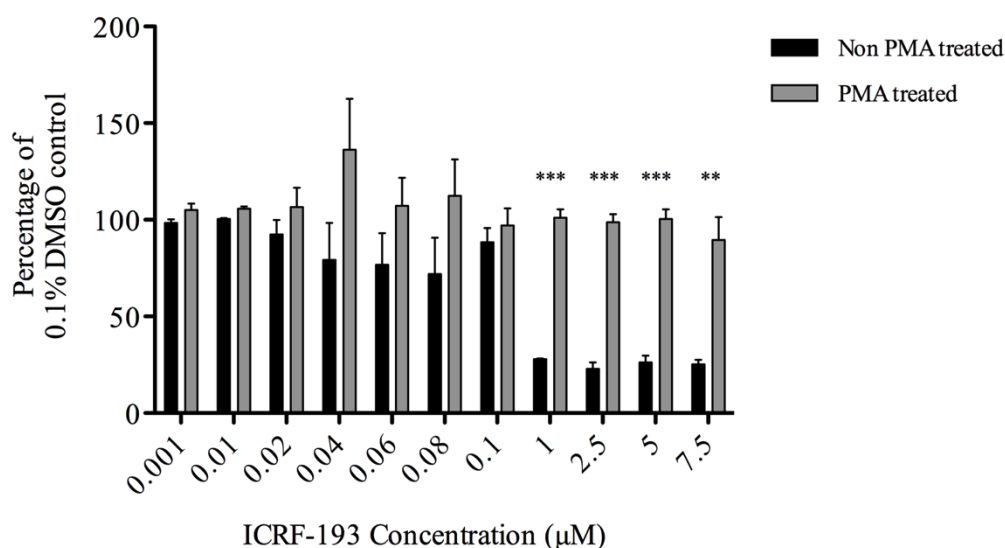


**Figure 4.18 Comparing the cytotoxic effect of ICRF-193 on non-PMA and PMA treated HL-60 cells.**

HL-60 cells were seeded at a density of  $3 \times 10^5$  cells/ml with 5 ng/ml PMA or 0.1% DMSO (v/v) and allowed to incubate for 72 h. Media was then replaced with the addition of varying concentrations of ICRF-193 (0.001, 0.01, 0.02, 0.04, 0.06, 0.08, 0.1, 2.5, 5 and 7.5 μM) 0.1% DMSO (v/v) was used as the vehicle control. Cells were allowed to incubate for a further 72 h, after which an XTT assay was performed (Section 2.15).

Results are reported as percentage of 0.1% DMSO (v/v) vehicle control. Results shown are the mean of three independent experiments  $\pm$  standard error. \*\* =  $p < 0.01$ , \*\*\* =  $p < 0.001$ . See Appendix Table A.14 for p values.

The results shown in Figure 4.18 reveal a similar pattern to that in Figure 4.17; ICRF-193 appears to have a cytotoxic effect on non-PMA treated HL-60 cells from a concentration of 0.04 μM, displaying an average decrease in cell viability of 21%. This effect on cell viability appears to peak at 1 μM ICRF-193 when non-PMA treated cells display an average decrease in cell viability of 72% upon exposure to the drug. This decrease in cell viability is similar when non-PMA treated cells are exposed to higher concentrations of ICRF-193, including 2.5, 5 and 7.5 μM. In contrast, PMA treated HL-60 cells appear to be protected against the effects of ICRF-193. At the highest

concentration of ICRF-193, 7.5  $\mu$ M, PMA treated cells only display an average decrease in cell viability of 11%.

The results of this assay reflect results presented in Figure 4.6a that demonstrated a G2/M arrest when cells were differentiated with PMA. The cytotoxic actions of ICRF-193 to induce apoptosis, like VP-16 require an active cell cycle (Iwai *et al.*, 1997; Li & Lui, 2001). However unlike VP-16, ICRF-193 requires progression through mitosis for DNA damage via accumulation of multiploid cells due to incomplete chromosome segregation (Iwai *et al.*, 1997). Further to this studies quantifying  $\gamma$ H2AX foci formation have shown that HeLa cells treated with ICRF-193 show an increase in  $\gamma$ H2AX foci formation in S phase, late mitosis and early G1 (Park and Avraham, 2006). Therefore it may be inferred that the decrease in ICRF-193 sensitivity in PMA treated cells compared to non-PMA treated cells may be due to the inability of ICRF-193 to exert its DNA damaging effects in cells that are not undergoing a cell cycle (Figure 4.6a).

In addition, as discussed in Section 4.2.1, Figures 4.3, 4.3, 4.11 and 4.12 show that differentiation of both U937 and HL-60 cells results in down-regulation of topo II $\alpha$  and topo II $\beta$  at both the transcript and protein level. ICRF-193 has been shown the target topo II $\beta$  preferentially (Isik *et al.*, 2003), however the specificity of it is under question as it has also been shown to interact with topo II $\alpha$  (Patel *et al.*, 2000). A down-regulation of topo II $\alpha$  and topo II $\beta$  protein would then decrease the amount of target available for ICRF-193 to bind. Therefore it may be possible that a down-regulation of topo II may render ICRF-193 ineffective as seen in Figures 4.17 and 4.18.

It is interesting to note that non-PMA treated HL-60 cells appear to be more sensitive to ICRF-193 than non-PMA treated U937 cells. When non-PMA treated HL-60 cells were exposed to 1  $\mu$ M ICRF-193 they displayed an average 72% decrease in cell viability (Figure 4.18); in comparison non-PMA treated U937 cells only displayed an average 32% decrease in cell viability when exposed to the same concentration of ICRF-193 (Figure 4.17). This pattern is also exhibited at higher concentrations of ICRF-193 (Figure 4.17 and 4.18).

HL-60 is a p53 null cell line. p53 is a tumour suppressor protein involved in the up-regulation of proteins involved in G1/S and G2/M checkpoint activation (Baus *et al.*, 2003). ICRF-193 has been shown to arrest or cause delay of cells in G2/M often leading

to cell death (Ishida *et al.*, 1994). Interestingly ICRF-193 resistant cell lines have been shown to exert their resistance by bypassing these checkpoints (due to mutations in checkpoint proteins), therefore continuing their cell cycle (Nishida *et al.*, 2001). However previous work has shown that HL-60 exerts its G2/M arrest in response to DNA damage via a p53 independent mechanism (Han *et al.*, 1995), thus a resistance to ICRF-193 is not observed in HL-60 cells.

#### **4.4.3 Effect of ICRF-187**

ICRF-187, like ICRF-193 is part of a group of synthetic compounds named the bispdioxopiperazines. ICRF-187 acts as a Topo II inhibitor in a similar way to ICRF-193, by creating a ‘closed clamp’ structure. Topo II therefore is unable to complete its catalytic cycle without the formation of a double strand break (Section 1.8.3). The cytotoxic effect of ICRF-187 was compared in non-PMA and PMA treated U937 and HL-60 cells.

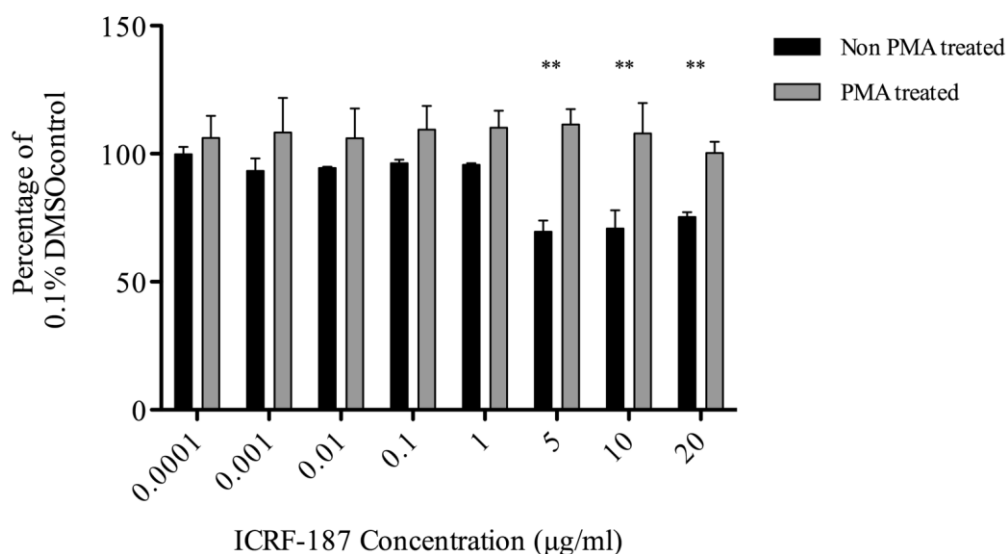


**Figure 4.19 Comparing the cytotoxic effect of ICRF-187 on non-PMA and PMA treated U937 cells.**

U937 cells were seeded at a density of  $3 \times 10^5$  cells/ml with 5 ng/ml PMA or 0.1% DMSO (v/v) and allowed to incubate for 72 h. Media was then replaced with the addition of varying concentrations of ICRF-187 (0.0001, 0.001, 0.01, 1, 5, 10 and 20 µg/ml) 0.1% DMSO (v/v) was used as the vehicle control. Cells were allowed to incubate for a further 72 h, after which an XTT assay was performed (Section 2.15).

Results are reported as percentage of 0.1% DMSO (v/v) vehicle control. Results shown are the mean of three independent experiments  $\pm$  standard error. \*\* =  $p < 0.01$ . See Appendix Tables A.15 for p values.

The results in Figure 4.19 show that ICRF-187 exhibits a cytotoxic effect on non-PMA treated cells from a concentration of 5 µg/ml. Non – PMA treated U937 cells exhibit an average 31% decrease in cell viability when treated with 5 µg/ml ICRF-187 for 72 h. This decrease in cell viability is similar when non-PMA treated cells are treated with higher concentrations of ICRF-187 including 10 and 20 µg/ml. In comparison PMA treated U937 cells appear to be protected against the effects of ICRF-187 as there appears to be no decrease in cell viability even at the highest concentration of ICRF-187.

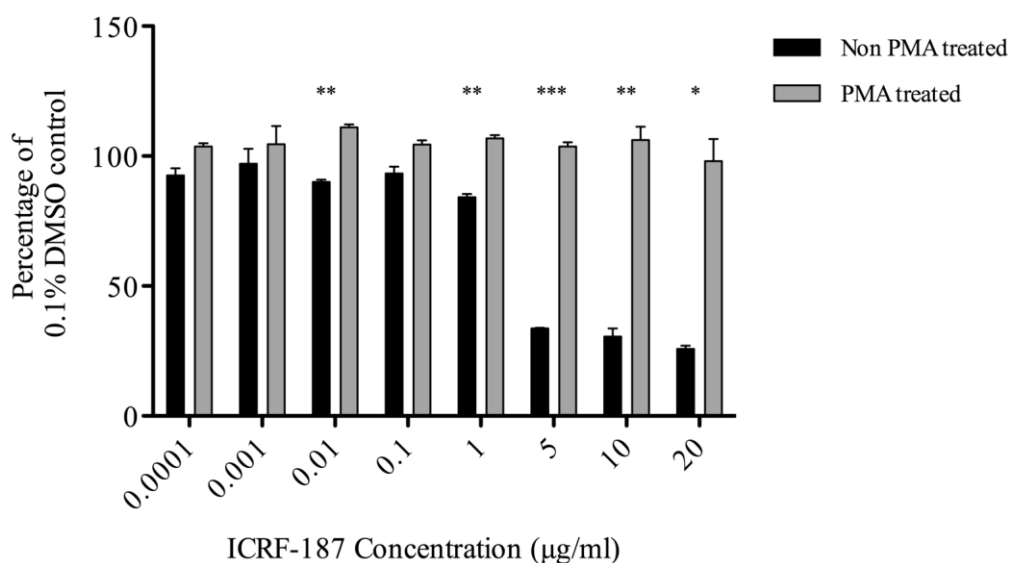


**Figure 4.20. Comparing the cytotoxic effect of ICRF-187 on non-PMA and PMA treated HL-60 cells.**

HL-60 cells were seeded at a density of  $3 \times 10^5$  cells/ml with 5 ng/ml PMA or 0.1% DMSO (v/v) and allowed to incubate for 72 h. Media was then replaced with the addition of varying concentrations of ICRF-187 (0.0001, 0.001, 0.01, 1, 5, 10 and 20 µg/ml) 0.1% DMSO (v/v) was used as the vehicle control. Cells were allowed to incubate for a further 72 h, after which an XTT assay was performed (Section 2.15).

Results are reported as percentage of 0.1% DMSO (v/v) vehicle control. Results shown are the mean of three independent experiments  $\pm$  standard error. \* =  $p < 0.05$ , \*\* =  $p < 0.01$ , \*\*\* =  $p < 0.001$ . See Appendix Table A.16 for p values.

The results in Figure 4.20 show that ICRF-187 exhibits a cytotoxic effect on non-PMA treated cells from a concentration of 0.01 µg/ml. Non – PMA treated HL-60 cells exhibit an average 10% decrease in cell viability when treated with 0.01 µg/ml ICRF-187 for 72 h. This decrease in cell viability increases as the concentration of ICRF-187 increases; at 5 µg/ml non-PMA treated cells display an average 67% decrease in cell viability upon treatment with the drug, a similar decrease in cell viability can be seen at higher concentrations of ICRF-187 including 10 and 20 µg/ml. In comparison PMA treated HL-60 cells appear to be protected against the effects of ICRF-187 as there appears to be no decrease in cell viability even at the highest concentration of ICRF-187.

As discussed previously in Section 4.2.1, Figures 4.3, 4.4, 4.11 and 4.12 show that differentiation of HL-60 and U937 cells with PMA results in a decrease of topo II $\alpha$  and topo II $\beta$  both at the mRNA and protein level. Indeed the protective effect that treatment of cells with PMA appears to elicit against the cytotoxic action of ICRF-187 (Figures 4.19 and 4.20) may be due to a lack of target for the inhibitor to act upon, however this hypothesis is controversial, Fattman *et al.* (1996) report that ICRF-187 activity is inversely proportional to levels of topo II, whilst Hasinoff *et al.* (1997) and Sehested *et al.* (1998) infer resistance of cells to ICRF-187 is due to a decrease in topo II protein levels.

Furthermore the exact mechanism by which ICRF-187 elicits its cytotoxic effects is still under investigation. Treatment of human leukemic CEM cells with ICRF-187 was shown to induce a G2/M decatenation checkpoint (Morgan *et al.*, 2000), suggesting that ICRF-187 may induce a DNA damaging effect similar to that induced by ICRF-193. As suggested previously, the cell cycle arrest observed in PMA treated cells (Figure 4.6a) may be stronger than the ICRF-187 induced checkpoint, indeed treatment of cells with an enantiomer of ICRF-187, ICRF-154 results in cell cycle arrest followed by cell death. Thus the cell cycle arrest induced by PMA may be protecting against the cell death induced effects of ICRF-187.

A difference in the potency of ICRF -193 and ICRF -187 was also observed in HL-60 cells. Table 4.1 shows the LD50 values when HL-60 and U937 cells are treated with VP-16, ICRF-193 and ICRF-187. As can be seen a dose of 0.2 $\mu$ M of ICRF-193 was required to kill 50% of HL-60 cells. In comparison, a dose of 7 $\mu$ M was required to kill 50% of HL-60 cells, thus suggesting that ICRF-193 is the more potent inhibitor. This is in agreement with previous work that has shown ICRF -193 is the most potent of the bispdioxopiperazines (Hasinoff *et al.*, 1995).

**Table 4.1** LD50 values for non-PMA treated U937 and HL-60 cells exposed to 72 h of treatment with the topo II poison, VP-16 and the topo II inhibitors, ICRF-193 and ICRF-187.

	<b>VP-16</b> ( $\mu\text{M}$ )	<b>ICRF-193</b> ( $\mu\text{M}$ )	<b>ICRF-187</b> ( $\mu\text{M}$ )
<b>U937</b>	3	N/A	N/A
<b>HL-60</b>	2	0.2	7

Interestingly LD50 values could not be calculated for U937 non-PMA treated cells exposed to ICRF-193 and ICRF-187 as at all concentrations of the inhibitors a decrease in cell viability did not reach or exceed 50% (Figure 4.17 and 4.19).

HL-60 cells appear to be more sensitive to the action of all three topo II drugs compared to U937 cells, as determined by LD50 values in Table 4.1. Indeed this may be due to a higher abundance of topo II within HL-60 cells compared to U937 cells, thus providing more target for the topo II drugs. Figure 4.21 compares the levels of topo II $\alpha$  and topo II $\beta$  protein in non-PMA treated HL-60 and U937 cells.



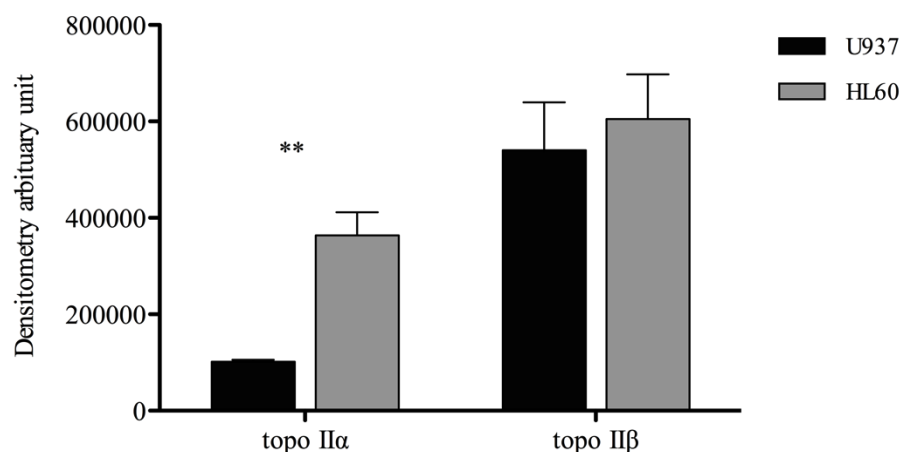


**Figure 4.21 Comparison of topo II $\alpha$  and topo II $\beta$  protein levels in non-PMA treated HL-60 cells vs non-PMA treated U937 cells.**

Densitometry data used to generate Figures 4.12 and 4.13 was used to compare levels of topo II $\alpha$  and topo II $\beta$  in non-PMA treated HL-60 cells vs non-PMA treated U937 cells.

Results reported use arbitrary units generated from analysis of western blots using the densitometry software Syngene genetools

Results shown are the mean of three independent experiments  $\pm$  standard error. \*\* =  $p < 0.01$

On average a significant increase ( $p=0.0055$ , student t-test) in the amount of topo II $\alpha$  protein can be observed in HL-60 cells compared to U937 cells. In addition, on average there is a small increase in topo II $\beta$  protein in HL-60 cells compared to U937 cells, however the difference is not significant.

A larger amount of topo II $\alpha$  and topo II $\beta$  protein in HL-60 cells compared to U937 cells may explain the increased sensitivity to all three topo II drugs. Despite VP-16 and ICRF-193 being clinically important in the targeting  $\alpha$  and  $\beta$  topo II isoforms respectively, there is an increased amount of both isoforms in non-PMA treated HL-60 cells, thus increasing the amount of target for each drug (Huang *et al.*, 2001; Cowell *et al.*, 2011). Again this data is in support of previous work that suggests the efficacy of topo II targeting chemotherapies can be measured by quantification of topo II protein levels (Dingemans *et al.*, 1999).

It could be argued that due to the mechanism of the XTT assay (Section 2.15) that essentially measures mitochondrial function; some of the cytotoxic effects observed whilst investigating topo II inhibitors could be a result of the iron chelating capabilities of the inhibitors impairing mitochondrial function (Grausland *et al.*, 2007). However very little cytotoxic effect was seen in PMA treated cells; who are shown to contain more mitochondria than monocytes (Monaco *et al.*, 1982) and that their function is increased in differentiated cells as reflected by an increase in mitochondrial citrate carrier (Infantino *et al.*, 2011) thus providing more target for the iron chelating capabilities of ICRF-193. This would then suggest that treatment with ICRF-193 is having little effect on mitochondrial function, and that the XTT assay is indeed an appropriate assay to use to measure the cytotoxic effects of ICRF-193.

#### **4.5 Summary**

The data in this Chapter reveals that levels of topo II $\alpha$  and  $\beta$  mRNA and protein are decreased when both HL-60 and U937 cells are differentiated with PMA. Moreover this result is also reflected when analysing mRNA levels of topo II $\alpha$  and  $\beta$  in CD14+ primary monocytes and in M-CSF differentiated CD14+ primary monocytes. Further to this, when comparing mRNA expression of topo II $\alpha$  to topo II $\beta$  in U937 and HL-60 cells, there appears to be no predominant isoform in non-PMA treated cells, with levels of mRNA expression between the two isoforms being similar, however in PMA treated cells levels of topo II $\beta$  message are much higher compared to levels of topo II $\alpha$  message, suggesting a role not yet known for topo II $\beta$  in PMA induced differentiation.

Cell cycle analysis of non-PMA and PMA treated cells demonstrated that upon differentiation with PMA cells experience a cell cycle block in G2/M phase. This is in support of previous studies that also report a G2/M block in PMA differentiated cells.

Investigation into the effect of PMA treatment on sensitivity to the topo II poison, VP-16 and topo II inhibitors, ICRF-193 and ICRF-187 revealed that PMA treated cells were protected from the cytotoxic effects of these drugs, and it is suggested that this may be due to the down-regulation of both topo II isoforms after PMA differentiation thus providing less target for the drug to induce its effects, or due to the PMA induced cell cycle blocking preventing processing of DNA damage.

## Chapter 5

### **The effects of topoisomerase II $\beta$ inhibition on multiple factors associated with macrophage differentiation and stimulation.**

---

#### **5.1 Introduction**

The vertebrate immune system is comprised of two distinct mechanisms; the innate immune system and the adaptive immune system (Flajnik & Pasquier, 2004).

The innate immune system provides immediate defence against sources of infection. It acts quickly, however it does not possess any immunological memory; it cannot mount a specialised response to a particular pathogen. Cells of the innate immune system include neutrophils, macrophages and dendritic cells (Janeway & Medzhitov, 2002; Bennouna *et al.*, 2003; Mitchell *et al.*, 2002).

The innate immune response is however capable of recognising particular molecular patterns common within similar pathogens, these are referred to as pathogen associated molecular patterns (PAMPs) (Kingston & Mills, 2011). Examples of these include bacterial lipopolysaccharide (LPS), found in the cell wall of Gram-negative bacteria, virally derived double stranded RNA and lipoteichoic acid found in Gram-positive bacteria (Tang *et al.*, 2012). Cells of the innate immune system are able to recognise these patterns via their pattern recognition receptors (PRRs); LPS for example, is recognised by Toll Like Receptor 4 (Mogensen, 2009). Binding of this PAMP to the PRR causes a cascade of intra-cellular signals, leading to the production of pro-inflammatory cytokines, generation of reactive oxygen species and activation of phagocytosis which are used to launch a cytotoxic attack against pathogens, subsequently engulfing them in order for them to be destroyed by lysosomes found in the macrophage (MacMicking *et al.*, 1997; BoseDasgupta & Pieter, 2014).

The adaptive immune system in comparison, acts much slower than the innate immune system (Alper *et al.*, 2007). It is often stimulated by the innate immune system, via actions of antigen presentation on the surface of antigen presenting cells such as macrophages. In contrast the adaptive immune system does possess immunological memory, and is the basis for vaccinations (Janeway *et al.*, 2002; Chandra, 1997).

Both the innate and adaptive immune system, as a whole rely upon a signalling network for communication in order to generate and regulate the immune response. Cytokines are an integral part of this. These are small proteins released by the cell in response to stress stimuli, with pleiotropic functions (Zhang *et al.*, 2007; Mosser & Edwards., 2008). Indeed some cytokines have both a pro-inflammatory effect and an anti-inflammatory effect (see Section 1.13) (Scheller *et al.*, 2011).

A dysregulation of the innate immune system can lead to an over production of cytokines leading to chronic inflammation. This is seen in autoimmune diseases such as atherosclerosis, asthma and Type 1 Diabetes that are associated with and the result of chronic inflammation (Cook *et al.*, 2004; Costa *et al.*, 2010). Interestingly, topoisomerase II autoantibodies are detectable in serum from patients with systemic sclerosis, Type 1 Diabetes and juvenile Rheumatoid Arthritis (Grigola *et al.*, 2000; Chang *et al.*, 1996; Zuklys *et al.*, 1991). The study by Grigola *et al.* (2000) identified autoantibodies specifically against topo II $\alpha$ , however it was not reported whether topo II $\beta$  had been investigated also, leaving their report of isoform specificity open to question. Studies by Chang *et al.* (1996) and Zuklys *et al.* (1991) did not investigate autoantibody specificity and thus report detection of autoantibodies to topo II generally.

Cytokine secretion in response to activation of the innate immune response relies on several important mechanisms; the transcription of the genes encoding the cytokine and/or their subsequent translation and secretion. The latter often relies on the cleavage of the cytokine by various proteases (that also require transcription) for activation and/or release into the extracellular environment (see Section 1.13) (Horiuchi *et al.*, 2010). It is the activation and up-regulation of transcription of these genes that is currently being investigated in cells of the innate immune system, specifically macrophages.

As stated previously (Section 4.1), topo II $\beta$  knockout mice die perinatally due to neuronal defects (Yang *et al.*, 2000; Lyu *et al.*, 2006) and topo II $\beta$  has been associated with the activation and repression of genes related to neuronal survival (Tiwari *et al.*, 2012). Activity of topo II $\beta$  has also been shown to repress the transcription of genes in granulocytes regulated by all-trans retinoic acid in a time dependent fashion (McNamara *et al.*, 2008). In addition studies have shown that topo II physically interacts with certain transcription factors, for example c-Jun and CREB (Kroll *et al.*,

1993; Takemori *et al.*, 2007) as well as HDAC 1 and 2, proteins involved in chromatin remodelling and gene silencing (Tsai *et al.*, 2000; Johnson *et al.*, 2001).

A mechanism by which topo II $\beta$  facilitates transcription was proposed by Ju *et al.* (2006). Cells stimulated with 17 $\beta$ -estradiol, a steroid hormone, revealed that activation of the pS2 promoter (a gene encoding a nuclear hormone receptor) required recruitment of topo II $\beta$ . They also showed using biotin d-UTP that DNA strand breaks were also present upon 17 $\beta$ - estradiol induction, and inferred that these were topo II $\beta$  generated. Induction of the strand breaks then appeared to facilitate the recruitment of numerous transcription factors, causing an alteration in local chromatin architecture. It has been widely documented that 17 $\beta$ -estradiol modulates the release of various pro-inflammatory cytokines (Rogers *et al.*, 2001; Kramer *et al.*, 2004). Taken together, the requirement of topo II $\beta$  activity in facilitation of gene expression in response to 17 $\beta$ -estradiol, and 17 $\beta$ -estradiol regulating the secretion of pro-inflammatory cytokines it may be hypothesised that topo II $\beta$  may required for the regulation of transcription of other pro-inflammatory cytokines. Interestingly Ju *et al.* (2006) also investigated other promoters that were responsive to external stimuli, MMP12 is an AP-1 regulated promoter, AP-1 is a transcription factor central to activation of genes involved in macrophage differentiation. Ju *et al.* (2006) showed that upon stimulation with TPA (PMA) topo II $\beta$  recruitment was increased at the MMP12 promoter, resulting in changes in local chromatin architecture, similar to that described previously. Thus topo II $\beta$  may be involved in the regulation of gene activation of many other genes regulated by PMA induced AP-1 recruitment.

## **5.2 Aims**

In order to investigate whether topo II $\beta$  plays a role in the transcription of genes associated with macrophage differentiation and stimulation, a range of experiments were designed and performed;

To determine the effects of down-regulation of topo II $\beta$ , using the topo II $\beta$  specific inhibitor ICRF-193 on surface antigen expression, expression of differentiation associated transcription factors and cytokine expression and secretion.

To investigate the effects of pre-treatment and co-treatment with ICRF-193 on cytokine expression and secretion in PMA treated cells.

To utilise siRNA technology to create a transient topo II $\beta$  knockout version of the U937 cell line; to examine the effects of this on TNF $\alpha$  and IL-1 $\beta$  expression.

To use wild-type mouse embryonic fibroblasts (WT MEFs) and topo II $\beta$  stable knockout mouse embryonic fibroblasts (#5 MEFs) to determine the difference in secretion of IL-6 and IL-1 $\alpha$  in response to various concentrations of LPS.

## **5.3 Determining the effect of different lengths of exposure to 1 nM ICRF-193 on topo II $\beta$ protein level in U937 cells.**

Previous studies have shown that exposure of cells to ICRF-193 leads to the 26S proteasome mediated degradation of topo II $\beta$ . Therefore in order to determine the effect of varying exposures of 1 nM ICRF-193 (2, 4, 6, 24, 48 and 72 h) on topo II $\beta$ , levels of the protein were quantified. The results are shown in Figure 5.1.

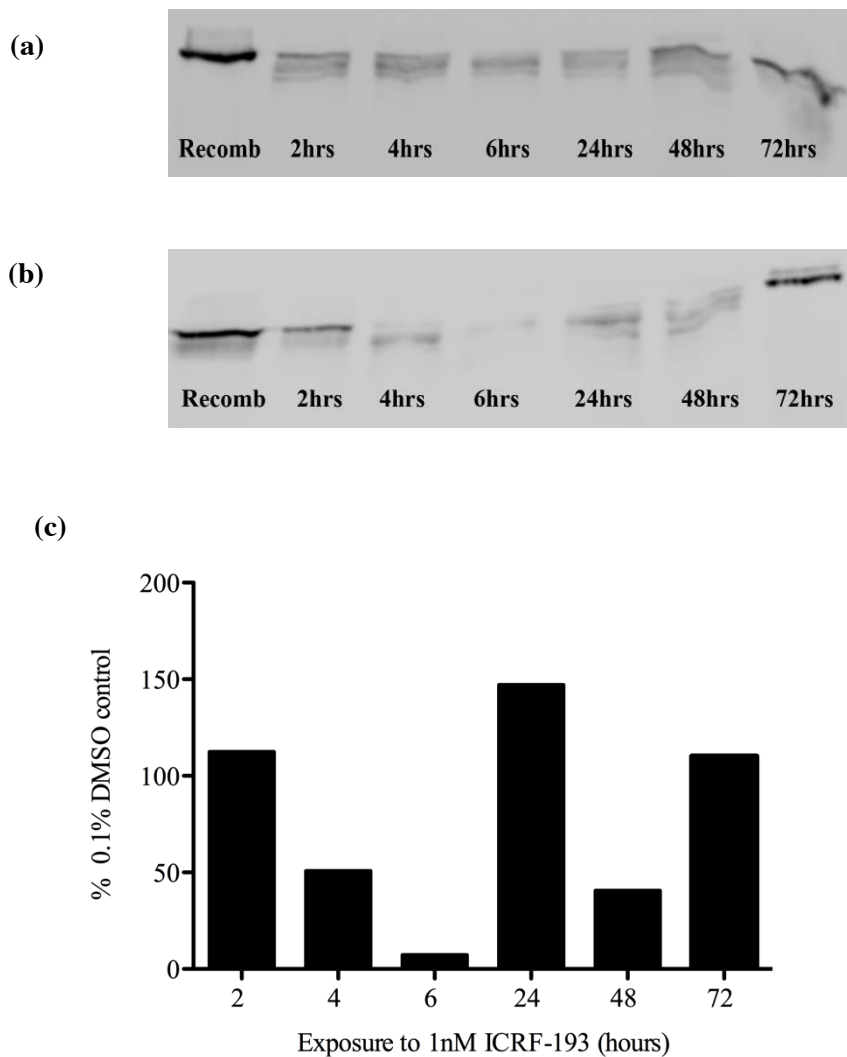


**Figure 5.1 Semi Quantification of topo II $\beta$  post treatment with 0.1% DMSO (v/v) (a) and 1 nM ICRF-193 (b) for varying lengths of exposure.**

Cells were seeded at  $3 \times 10^5$  cells/ml with 0.1% DMSO (v/v) (a) or 1 nM ICRF-193 and allowed to incubate for 2, 4, 6, 24, 48 or 72 h before harvesting. A whole cell protein extraction was then performed and quantified (see material and methods 2.15). 40.9 $\mu$ g of total protein was then loaded onto a 7.5% SDS gel and SDS PAGE was then performed to separate the proteins out by size (Section 2.16.4) this was followed by protein transfer onto nitrocellulose paper by wet western blot (Section 2.15.5). Nitrocellulose blots were then probed with an antibody to topo II $\beta$  (Section 2.16.7). Lanes are labelled with exposure time to 0.1% DMSO (v/v) (a) or 1 nM ICRF-193 (b) Recombinant topo II $\beta$  (40.9 $\mu$ g) was present in the lanes labelled 'Recomb' to act as a positive control. Quantification of protein was performed using the densitometry software, Syngene genetools See Appendix Figures B.1 and B.2 for GAPDH loading control. Results are expressed as percentage of 0.1% DMSO (v/v) treated samples (c).

The results in Figure 5.1 show that treatment of cells with 1 nM ICRF-193 for 2 h, 24 h 72 h does not reduce levels of topo II $\beta$ , indeed ICRF-193 appears to up-regulate the expression of topo II $\beta$  at these times. It may be possible at 2 h of treatment the cell is up-regulating topo II $\beta$  expression to try alleviate the effects of ICRF-193 on the existing topo II $\beta$ . This may also be suggested for the increase in topo II $\beta$  protein expression seen after 24 h of ICRF-193 exposure; the cell may be over-expressing topo II $\beta$  to counteract the depletion in topo II $\beta$  seen after 6 h (Figure 5.1). Perez *et al.* (1997) report that upon 72 h of treatment with 0.3  $\mu$ M ICRF-193 an up-regulation of PKC is observed, furthermore McNamara *et al.*, (2010) demonstrate that an up-regulation of PKC is accompanied by an up-regulation of topo II $\beta$  due to an increase in protein stability caused by the PKC mediated phosphorylation of topo II $\beta$ . Indeed the slight up-regulation of topo II $\beta$  seen after 72 h of 1 nM ICRF-193 treatment seen in Figure 5.1 may be due to a similar mechanism.

A down-regulation of topo II $\beta$  protein expression is seen after 6 h and 48 h of 1 nM ICRF-193 treatment, thus suggesting that ICRF-193 is causing the degradation of topo II $\beta$  and thus successfully inhibiting its actions. In addition the down-regulation of topo II $\beta$  protein expression is maintained after cells have been treated with PMA and LPS following the 6 h of pre-treatment with 1 nM ICRF-193 (see Appendix Figure B.3), therefore it is suggested that the results obtained from the following experiments with regards to a 6 hour pre-treatment are due to a down-regulation of topo II $\beta$ . Further to this the protein expression of topo II $\beta$  after cells had been treated with PMA and LPS following 72 h of pre-treatment with 1 nM ICRF-193 does not appear any different to that of the control (see Appendix Figure B.4). This is in support of the measurement of topo II $\beta$  protein expression following treatment with 1 nM ICRF-193 for 72 h, in which levels of topo II $\beta$  appear to have recovered (Figure 5.1).

#### **5.4 Effect of the topoisomerase II inhibitor, ICRF-193 on levels of macrophage cell surface antigens.**

Flow cytometry was utilised to determine the effects of 1 nM ICRF-193 pre-treatment prior to differentiation with 5 ng/ml PMA and stimulation with 10 ng/ml LPS on expression of the cell surface proteins, CD11b, HLA-DR and TLR4, all of which are



shown to be up-regulated during differentiation of monocytes to macrophages (Gordon, 2005; Rey-Giraud, 2012; Traore *et al.*, 2012).

#### **5.4.1 Effect of bacterial lipopolysaccharide on CD11b expression on PMA treated cells**

As previous studies to determine optimal conditions for differentiation (Chapter 3) used PMA it was necessary to determine the effect of PMA and LPS on CD11b surface expression. Bacterial Lipopolysaccharide (LPS) is a major constituent of Gram-negative cell walls. (Triantafilou & Triantafilou, 2004; Leonardo *et al.*, 2004; Ngkelo *et al.*, 2012). Previous studies have shown that macrophages exposed to an acute stimulation by LPS display an increase in the cell surface marker, CD11b (Lichte *et al.*, 2013).

In order to determine if levels of the cell surface antigen, CD11b could be increased further, than when treated with PMA alone, LPS and PMA were simultaneously used to stimulate cells. Data presented in Figure 5.2 reveals that stimulation with LPS did not significantly increase cell surface expression of CD11b compared to PMA treatment alone. This suggests that maximal cell surface expression of CD11b is achieved using 5 ng/ml PMA for 72 h.

These results are in disagreement with Lichte *et al.*, (2013) who demonstrated that CD11b expression on macrophages was increased in response to LPS. However the latter study only looked at acute stimuli by LPS (>3hrs) whereas stimulus to LPS for 72 h as seen in Figure 3.4 can be considered a chronic stimulation. The difference in methodology between the studies makes it difficult to compare results. For the purposes of this study, as demonstrated by the results in both cell lines (Figure 5.2) simultaneous stimulation by LPS and PMA is not considered to have any further effect on CD11b expression.

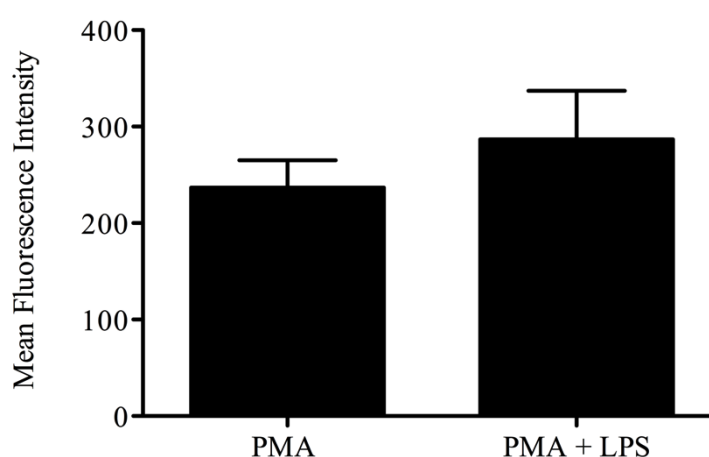


**Figure 5.2 Comparison of CD11b expression on LPS stimulated PMA treated cells and non LPS stimulated PMA treated cells.**

U937 cells were seeded at a density of  $3 \times 10^5$  cells/ml and incubated with 5 ng/ml PMA, with and without 10 ng/ml LPS for 72 h. Cells were then labelled with anti-human CD11b-APC conjugated antibody. Flow cytometry was performed using the Becton Dickinson flow cytometer (detailed in materials and methods). Results are presented as the mean fluorescence intensity of  $1 \times 10^5$  captured cells.

The means of three independent experiments are shown +/- standard error.

#### **5.4.2 Effect of ICRF-193 pre-treatment on CD11b expression**

The inhibition of topoisomerase II $\beta$  using a sub-lethal dose of the topo II $\beta$  specific inhibitor, ICRF-193 (as determined by a previous experiment, see Figure 4.16) prior to differentiation and stimulation was used to determine if topo II $\beta$  played a role in the transcription of genes required for surface antigen expression associated with differentiation.

CD11b cell surface expression is up-regulated during monocyte to macrophage differentiation and thus is often used as a macrophage differentiation marker (Garcia *et al.*, 1999; Deszo *et al.*, 2000; Murphy *et al.*, 2008) due to the up-regulation of mRNA expression and protein during normal differentiation (Dziennis *et al.*, 1995). CD11b is part of the  $\beta$  integrin MAC-1 complex. MAC-1 is a heterodimer consisting of CD11b,

the  $\alpha$  subunit and CD18, the  $\beta$  subunit (Benimetskaya *et al.*, 1997; Klugewitz *et al.*, 1997).

The role of this complex is involved in cellular adhesion (Gomes *et al.*, 2010), which facilitates the recruitment of neutrophils to sites of infection (Moreland *et al.*, 2002) and more recently has been shown to be a cell surface receptor recognising double stranded RNA (Zhou *et al.*, 2013).

Upon morphological examination of cells post ICRF-193, PMA and LPS treatment it appeared cells had indeed become adherent suggesting differentiation had occurred (data not shown).

Flow cytometry using an antibody to CD11b was then used to determine if ICRF-193 had any effect on the expression of this cell surface antigen on PMA and LPS treated U937 cells. The effect of different lengths of exposure to ICRF-193 before treatment with PMA and LPS was also investigated. The results of this experiment are shown in Figure 5.3.

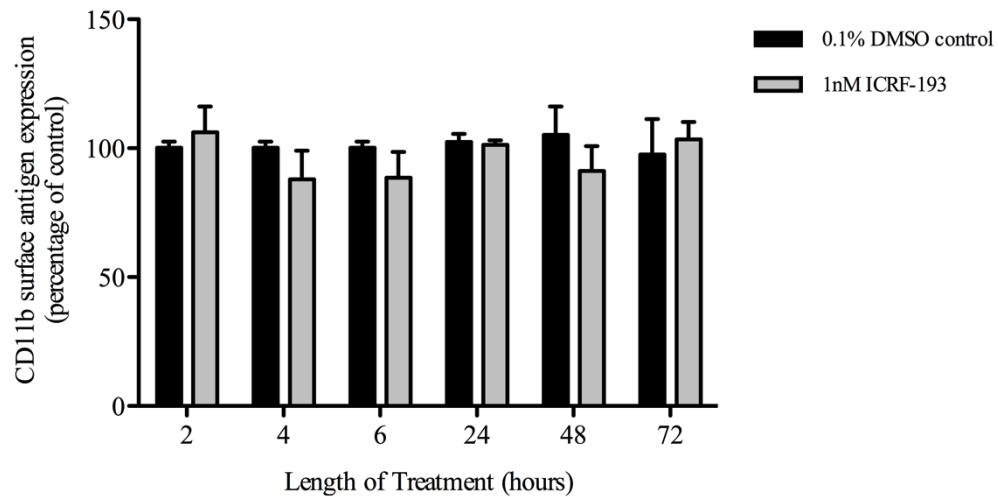


**Figure 5.3 Determining the effects of ICRF-193 on expression of surface antigen, CD11b**

U937 cells were seeded at a density of  $3 \times 10^5$ /ml in a 12 well tissue culture plate in complete media (detailed in materials and methods) with 1 nM ICRF-193 or the 0.1% DMSO (v/v). Cells were allowed to incubate for 2, 4, 6, 24, 48 or 72 h. Media was then changed and 5 ng/ml PMA and 10 ng/ml LPS was added. Cells were incubated for a further 72 h before harvesting. Cells were then labelled with anti-human CD11b - APC conjugated antibody. Flow cytometry was performed using the Becton Dickinson flow cytometer (detailed in materials and methods). Results are presented as the mean fluorescence intensity of  $1 \times 10^5$  captured cells as a percentage of the control sample. The means of three independent experiments are shown  $\pm$  standard errors.

Data revealed, that at 1 nM of ICRF-193, and at all time points of pre-treatment, 1 nM ICRF-193 had no effect on the expression level of CD11b on the cell surface (Figure 5.3) (Appendix B.1). Several transcription factors are involved in the transcription of CD11b, these include SP1 and PU.1 which have been shown to bind to the CD11b promoter region (Chen *et al.*, 1993; Pahl *et al.*, 1993). Studies have yet to show that topo II $\beta$  can interact with these transcription factors. Interestingly though, AP1, a transcription factor which is known to be involved in the regulation of transcription of other PMA responsive genes, has been shown to interact with topo II $\beta$  (Kroll *et al.*, 1993) but this transcription factor is not present in the CD11b promoter region (Pahl *et al.*, 1992).

It is most likely that topo II $\beta$  does not play a role in the up-regulation of genes associated with expression of the CD11b protein in response to PMA and LPS, however, the 72 h given for differentiation and stimulation following ICRF-193 treatment may be too long for any significant results to be observed, or that changes may be time dependent. Indeed a study by Lyu *et al.* (2006) revealed that topo II $\beta$  was required for the latter stages of neuronal development but dispensable in the earlier stages. Thus suggesting that the actions of topo II $\beta$  appear to be tightly restricted to specific stages of development, which may also be reflected in differentiation.

#### **5.4.3 Effect of ICRF-193 pre-treatment on HLA-DR expression.**

HLA-DR is a Major Histocompatibility Complex Class II (MHC Class II) molecule. It is a glycosylated cell surface transmembrane protein that is found on antigen presenting cells including monocytes and macrophages. It is essential in the presentation of foreign (microbe derived) peptides to cells of the adaptive immune system (Perry *et al.*, 2004). In order to examine the effects of topo II $\beta$  inhibition on the expression of the surface antigen, HLA-DR, flow cytometry using an antibody to HLA-DR was used to determine the effects of different exposure times to ICRF-193 prior to stimulation of PMA and LPS treatment on U937 cells. The results of this experiment are shown in Figure 5.4.

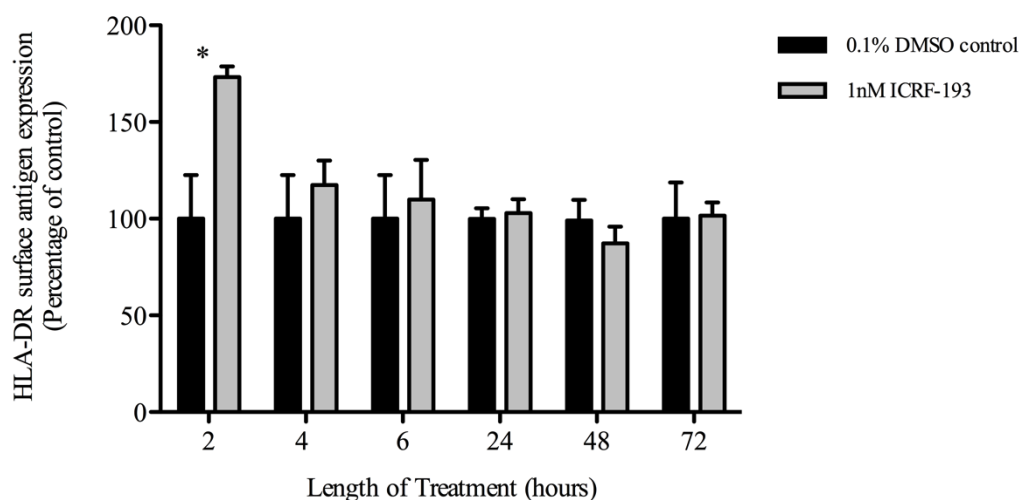


**Figure 5.4 Determining the effects of ICRF-193 on expression of surface antigen, HLA-DR**

U937 cells were seeded at a density of  $3 \times 10^5$ /ml in a 12 well tissue culture plate in complete media (detailed in materials and methods) with 1 nM ICRF-193 or the 0.1% DMSO (v/v). Cells were allowed to incubate for either 2, 4, 6, 24, 48 or 72 h. Media was then changed and 5 ng/ml PMA and 10 ng/ml LPS was added. Cells were incubated for a further 72 h before harvesting. Cells were then labelled with anti-human HLA-DR-FITC conjugated antibody. Flow cytometry was performed using the Becton Dickinson flow cytometer (detailed in materials and methods). Results are presented as the mean fluorescence intensity of  $1 \times 10^5$  captured cells as percentage of the control sample.

The means of three independent experiments are shown  $\pm$  standard errors.

An average 73% increase ( $p = 0.04$ , student t-test) in the expression of the cell surface antigen, HLA-DR was observed when cells were treated with ICRF-193 2 h prior to differentiation and stimulation compared to the control. No difference in HLA-DR protein expression was observed after 4, 6, 24, 48 and 72 h of exposure to ICRF-193 before differentiation (Appendix B.2). An increase in HLA-DR protein levels would suggest that if topo II $\beta$  is playing a role it is not in the up-regulation of HLA-DR gene expression, as inhibition would have resulted in a decrease in HLA-DR protein expression rather than an increase as shown in Figure 5.4. Instead topo II $\beta$  may possibly

be playing a time dependent inhibitory role, as its inhibition with ICRF-193 for 2 h prior to differentiation results in an increase in HLA-DR expression on the cell surface.

Regulation of HLA-DR expression is primarily controlled at a transcriptional level, by an atypical mechanism. An SXY module (from 5' end of region to 3' end contains an S box, an X box and a Y box) is situated upstream of the transcription start site. It is here that a multi-protein complex is formed. The transcription factors cAMP response binding protein (CREB) and nuclear transcription factor Y (NFY) bind to the X box of the SXY module along with an unknown factor that binds to the S box. This creates a platform that the class II trans-activator (CIITA) can be recruited to. Recruitment of CIITA is required for the transcription of all MHC Class II genes (Reith *et al.*, 2005). Interestingly topo II has been shown to associate with CREB, although the specific isoform was not determined (Kroll *et al.*, 1993). If topo II $\beta$  is indeed playing a role here then binding of topo II $\beta$  with CREB may inhibit HLA-DR gene transcription by inhibiting the ability of CIITA to be recruited to the SXY module. Inhibition of topo II $\beta$  may then decrease the association with CREB allowing a transient up-regulation of HLA-DR expression as seen in Figure 5.4. Additionally the actions of topo II $\beta$  have been implicated in gene silencing. Huang *et al.*, (2012) reported that treatment of murine neurons with topo II drugs resulted in the de-repression of the dominant allele of Ube3a. This de-repression effect was also mirrored in work by McNamara *et al.*, (2008) who showed that retinoic acid resistant cells treated with the topo II $\beta$  inhibitor, ICRF-193 became sensitive to the effects of retinoic acid. This was shown to be due to an up-regulation of transcription in retinoic acid target genes. Taken together these studies suggest that topo II $\beta$  plays a role in the regulation of transcription through gene silencing. Previous work in Figure 5.1 shows that there is still a substantial amount of topo II $\beta$  remaining in the cell after 2 h of ICRF-193 treatment and that degradation of the protein does not begin to occur until 4 h of ICRF-193 treatment. Indeed it is possible at this time that ICRF-193 is inhibiting the catalytic action of topo II $\beta$ , and detectable degradation has not yet taken place. However this does not explain why then an up-regulation of HLA-DR expression is not observed when cells are treated with PMA and LPS at a time when there is a substantial amount of topo II $\beta$  degradation such as 4 h and 6 h (Figure 5.1). It is possible that the up-regulation of HLA-DR expression after 2 h of ICRF-193 treatment prior to differentiation and stimulation may be the result of ICRF-193 inducing an acute immune response that then attenuates the response to stimulation

with LPS; resulting in the cell up-regulating HLA-DR expression in order to present more of the LPS peptide to neighbouring cells.

Thus in conclusion, cells treated with 1 nM ICRF-193 2 h prior to differentiation saw an increase in HLA-DR expression of 73%. This may be due to a silencing effect of topo II $\beta$  on the HLA-DR promoter region. Thus inhibition of topo II $\beta$  with ICRF-193 led to an up-regulation of HLA-DR surface antigen presentation. This effect however, was only seen when cells were treated 2 h prior to differentiation. Thus it is more likely an acute immune response to treatment with ICRF-193 rather than a topo II $\beta$  mediated effect.

#### **5.4.4 Effect of ICRF-193 pre-treatment on TLR4 expression**

Toll like receptor 4 (TLR4) is found on the surface of macrophages as part of a complex with cell surface antigens, CD14 and MD2 (O'Neill *et al.*, 2013). It recognises LPS via presentation by MD2. Recognition and binding of LPS results in homodimerisation of TLR4 at the plasma membrane; leading to activation of NF-kB and the MAPK signalling pathway (details of this pathway can be found in Figure 1.8). This then results in the expression of inflammatory associated genes (Yan *et al.*, 2006). TLR4 can also be endocytosed, activating an alternative pathway of transcription via the TRIF pathway (O'Neill *et al.*, 2013).

In order to examine the effects of topo II $\beta$  inhibition on the levels of the toll like receptor, TLR4, flow cytometry using an antibody to TLR4 was used to determine the effects of different exposure times to ICRF-193 prior to stimulation of PMA and LPS treatment on U937 cells. The results of this experiment are shown in Figure 5.5.



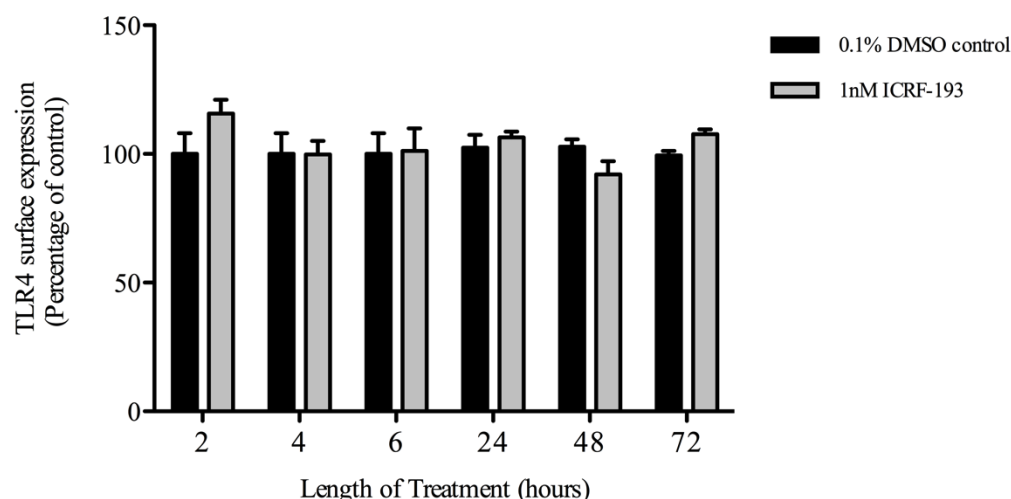


**Figure 5.5 Determining the effects of ICRF-193 on expression of surface antigen, TLR 4**

U937 cells were seeded at a density of  $3 \times 10^5$ /ml in a 12 well tissue culture plate in complete media (detailed in materials and methods) with 1 nM ICRF-193 or the 0.1% DMSO (v/v). Cells were allowed to incubate for 2, 4, 6, 24, 48 or 72 h. Media was then changed and 5 ng/ml PMA and 10 ng/ml LPS and was added. Cells were incubated for a further 72 h before harvesting. Cells were then labelled with anti-human TLR4-PE conjugated antibody. Flow cytometry was performed using the Becton Dickinson flow cytometer (detailed in materials and methods). Results are presented as the mean fluorescence intensity of  $1 \times 10^5$  captured cells as percentage of the control sample.

The means of three independent experiments are shown  $\pm$  standard errors.

No difference in TLR4 protein expression was observed after 2, 4, 6, 24, 48 and 72 h of exposure to ICRF-193 before differentiation compared to the 0.1% DMSO (v/v) (vehicle control) treated cells (Appendix B.3).

Transcription of the TLR4 gene has been shown to involve the actions of the transcription factor PU.1. Roger *et al.*, (2005) demonstrated that an overexpression of PU.1 in a murine cell line caused an increase in TLR4 promoter activity. However to date, there is no evidence to suggest that topo II $\beta$  interacts or associates with PU.1. It is most likely that topo II $\beta$  does not play a role in the regulation of the TLR4 gene. As discussed in Section 5.4.2, the results presented in Figure 5.5 may actually reflect the transient and time specific restriction of topo II $\beta$  action. Thus topo II $\beta$  may have little to

no effect on TLR4 expression after 72 h treatment with PMA but it may have an effect at a different time point in the differentiation process.

Concomitant with visual morphological observations that suggested that ICRF-193 did not inhibit differentiation, no reduction in specific markers of differentiation were seen when cells were treated with ICRF-193 prior to differentiation with PMA.

### **5.5 Effect of topoisomerase II inhibitor, ICRF-193 on expression of mRNA in a variety of transcription factors involved in macrophage activation.**

Hematopoiesis gives rise to multiple different cell types, for example macrophages, dendritic cells and neutrophils (Ceredig *et al.*, 2009). This cell fate is determined by the expression and repression of many specific genes (Lehtonen *et al.*, 2007).

The role of topo II $\beta$  has been implicated in both the activation of transcription, for example the activation of the AP-1 gene promoter in response to TPA (Ju *et al.*, 2006) and in the silencing of genes, as demonstrated by Huang *et al.* (2012) who showed that inhibition of topo II $\beta$  unsilenced the dominant allele of Ube3a. Additionally McNamara *et al.* (2010) also revealed that inhibition of topo II $\beta$  lead to an up-regulation of retinoic acid induced gene expression, and suggested that topo II $\beta$  may act with co-repressors such as HDAC to cause such gene silencing. Indeed topo II $\beta$  has previously been shown to physically interact with HDAC (Cowell *et al.*, 2011).

Therefore using qPCR, the effect of inhibition of topo II $\beta$  using 1 nM ICRF-193 pre-treatment on genes that are normally up-regulated upon treatment with PMA and LPS were investigated. In this experiment cells were exposed to 6 h and 72 h of ICRF-193 pre-treatment, thus representing an acute and chronic exposure respectively before being exposed to PMA and LPS.

### 5.5.1 POLR2A

POLR2A is the gene that encodes the largest subunit (alpha) of the 12 subunits that make up the ubiquitous transcription factor, RNA polymerase II. RNA polymerase II is responsible for synthesising mRNA in eukaryotes. RNA polymerase II associates with various other proteins, namely the suppressor of RNA polymerase B regulatory proteins (SRB proteins) to form the RNA polymerase II holoenzyme. Along with various different protein associations throughout transcription, RNA polymerase II requires the actions of proteins involved in chromatin remodelling in order for successful transcription to occur (Chao *et al.*, 1996). Samples were prepared as described in Section 5.5. RNA extraction was performed on samples that had been exposed to ICRF-193 for 6 and 72 h, both this method and the protocol for cDNA synthesis are described in Section 2.17. qPCR was performed with a hydrolysis probe to POLR2A. Details of the reaction conditions for the qPCR reaction can be found in Section 2.17.3. The results are shown in Figure 5.6.

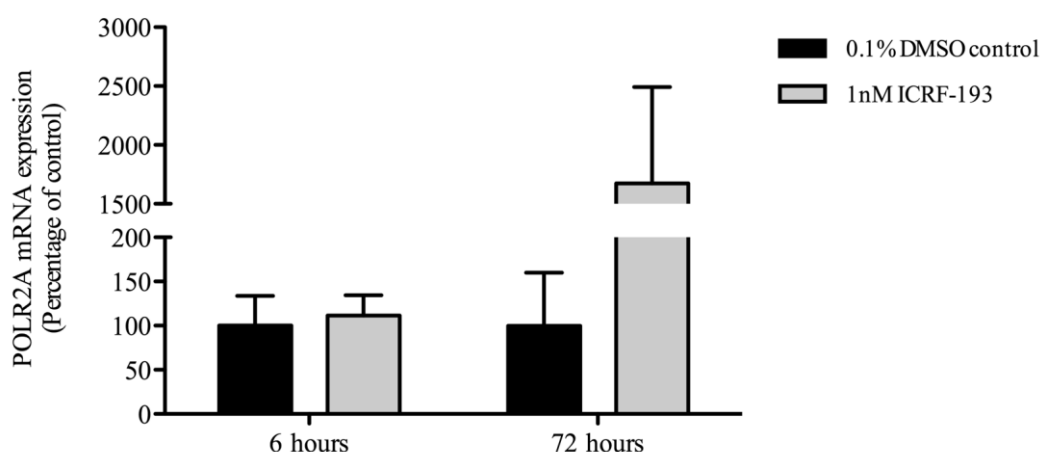


**Figure 5.6 Determining the effects of 1 nM ICRF-193 on mRNA expression of POLR2A**

U937 cells were seeded at a density of  $3 \times 10^5/\text{ml}$  in a 12 well tissue culture plate in complete media (detailed in materials and methods) with 1 nM ICRF-193 or the 0.1% DMSO (v/v). Cells were allowed to incubate for either 6 or 72 h. Media was then changed and 5 ng/ml PMA and 10 ng/ml LPS was added. Cells were incubated for a further 72 h before harvesting. RNA extraction and cDNA synthesis was performed as detailed in 2.16. qPCR was then performed with a hydrolysis probe to POLR2A (details of qPCR conditions in Section 2.17.3). Fold expression was calculated using the comparative  $\Delta/\Delta$  Ct method. Data is presented as percentage of the 0.1% DMSO (v/v) treated control. The means of three independent experiments are shown  $\pm$  standard error.

The results presented in Figure 5.6 show no difference in the level of POLR2A expression when U937 cells were treated with ICRF-193 6 h prior to differentiation and stimulation. When cells were treated with ICRF-193 for 72 h prior to differentiation, a large increase in POLR2A expression was exhibited, however the results displayed did not reach significance when compared to the 0.1% DMSO (v/v) (vehicle control) treated cells (Appendix B.5).

### **5.5.2 SP1**

Specificity Protein 1 (Sp1) is a zinc finger transcription factor encoded by the gene SP1. The activity of Sp1 has been associated with transcription of genes involved in murine development and macrophage differentiation. It acts by recruiting and forming a complex with other factors involved in transcription. Interestingly Sp1 is also suggested to play a role in the chromatin remodelling of the SV40 chromosome (Milavetz *et al.*, 2002). Samples were prepared as described in Section 5.5. RNA extraction was performed on samples that had been exposed to ICRF-193 for 6 and 72 h, both this method and the protocol for cDNA synthesis are described in 2.16. qPCR was performed with a hydrolysis probe to SP1. Details of the reaction conditions for the qPCR reaction can be found in Section 2.17.3. The results are shown in Figure 5.7.

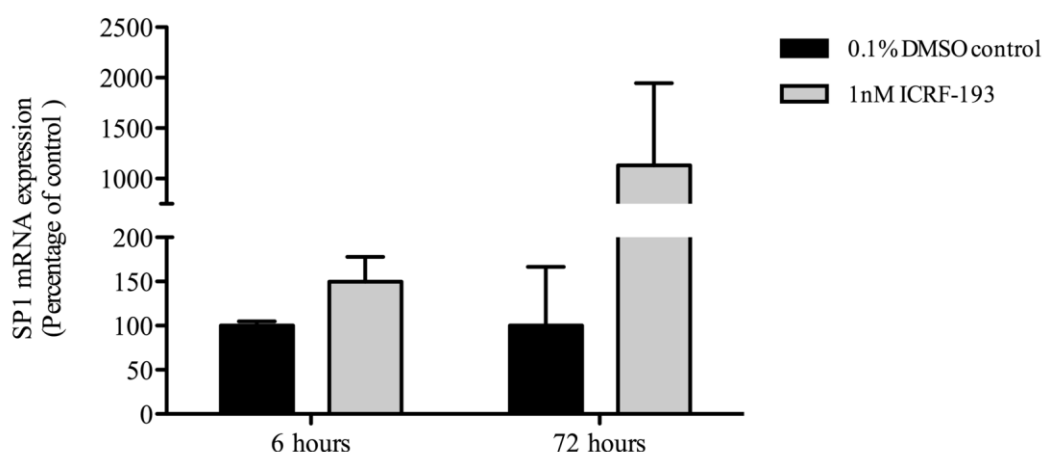


**Figure 5.7 Determining the effects of 1 nM ICRF-193 on mRNA expression of SP1**

U937 cells were seeded at a density of  $3 \times 10^5$ /ml in a 12 well tissue culture plate in complete media (detailed in materials and methods) with 1 nM ICRF-193 or the 0.1% DMSO (v/v). Cells were allowed to incubate for either 6 or 72 h. Media was then changed and 5 ng/ml PMA and 10 ng/ml LPS was added. Cells were incubated for a further 72 h before harvesting. RNA extraction and cDNA synthesis was performed as detailed in Section 2.17. qPCR was then performed with a hydrolysis probe to SP1 (details of qPCR conditions in Section 2.17.3). Fold expression was calculated using the comparative  $\Delta/\Delta$  Ct method. Data is presented as percentage of the 0.1% DMSO (v/v) treated control. The means of three independent experiments are shown  $\pm$  standard error.

The results presented in Figure 5.7 show no difference in the expression of SP1 when cells were treated with ICRF-193 6 h prior to differentiation and stimulation. Conversely, a large increase in SP1 expression was exhibited when cells were treated with ICRF-193 72 h prior to differentiation, however this was not significant when compared to the 0.1% DMSO (v/v) (vehicle control) treated cells (Appendix B.6).

Collectively the results in Figure 5.6 and 5.7 show a trend with regards to an apparent increase in the mRNA expression of POLR2A and SP1 when U937 cells are treated with 1 nM ICRF-193 for 72 hours followed by differentiation. The trend observed, although non-significant may be due to a DNA damage response mediated through Ataxia Telangiectasia Mutated (ATM) and Ataxia Telangiectasia and Rad3 related (ATR) (Park & Avraham, 2006). DNA damage response requires the up-regulation of

transcriptional activity in order to transcribe DNA repair proteins for example BRCA1, PARP1 and MDC1 and their respective transcriptional regulators, for example AP-1 (Li *et al.*, 2013; Kim *et al.*, 2005; Stewart *et al.*, 2003; Potapova *et al.*, 2001; Rodriguez *et al.*, 2010; Christmann & Kaina, 2013). It is then postulated that the trend seen in the increase in mRNA expression of POLR2A and SP1 after 72 h of treatment with ICRF-193 (Figure 5.6 and 5.7) may have been the result of a prolonged exposure to ICRF-193, leading to a DNA damage response. Indeed an increase in transcriptional activity as activated by a DNA damage response would require the activity of RNA polymerase; encoded for by POLR2A, as seen in Figure 5.6.

Sp1 in addition has been shown to facilitate the repair of double strand breaks (dsb), although the induction of double strand breaks directly induced by ICRF-193 is controversial (Huang *et al.*, 2001; Larsen *et al.*, 2003). However intolerable strain on the DNA caused by the ICRF-193 induced closed clamp or collision of replicational and/or transcriptional machinery with the closed clamp may lead to generation of double strand breaks (Oestergaard *et al.*, 2004). Therefore an extensive exposure to ICRF-193 may require the actions of Sp1 in dsb repair, ultimately leading to an up-regulation of SP1. The results in Figure 5.7 reflect this to some extent by displaying a trend in the increase of SP1 mRNA expression after 72 h treatment with ICRF-193, however these results did not reach significance. Furthermore the results shown in Figure 5.1 reveal that after 72 h of treatment with 1 nM ICRF-193 levels of topo II $\beta$  protein have returned back to normal levels, compared to a 0.1% DMSO (v/v) control. Therefore it is most likely that the trend demonstrated in Figures 5.6 and 5.7 with regards to an apparent increase in POLR2A and SP1 mRNA expression when cells were treated with 1 nM ICRF-193 prior to differentiation and stimulation is most likely not due to topo II $\beta$  mediated effect but is due to a DNA damage response induced by a prolonged exposure to ICRF-193.

This work supports a previous study by Perez *et al.* (1997) who reported an increase in protein kinase C (PKC) whole protein in response to 0.3  $\mu$ M ICRF-193 after 72 h of treatment, and suggested this late up-regulation may be in response to DNA damage. Interestingly this study alludes to ICRF-193 inducing differentiation. Indeed it may be possible that treatment of cells with ICRF-193 results in a drive towards differentiation, however this may be a mechanism of protection; as shown in Chapter 4, differentiated cells are resistant to the cytotoxic effects of ICRF-193 treatment (Figures 4.16 & 4.17).

### 5.5.3 Early Growth Response Protein 2

Early Growth Response Protein 2 (Egr2) is a zinc finger transcription factor encoded by the gene EGR2. It has been associated with the transcription of genes involved in differentiation, growth and neuronal development. Activity of EGR2 is modulated by the NAB family and is specifically associated with transcription of genes related to the response of extra-cellular signals (Kumbrink *et al.*, 2010). EGR2 has previously been shown to be up-regulated in response to PMA and LPS stimulation (Baek *et al.*, 2009; Zaman *et al.*, 2012).

Samples were prepared as described in Section 5.5. RNA extraction was performed on samples that had been exposed to ICRF-193 for 6 and 72h, both this method and the protocol for cDNA synthesis are described in Section 2.17. qPCR was performed with a hydrolysis probe to EGR2. Details of the reaction conditions for the qPCR reaction can be found in Section 2.17.3. The results for this experiment are presented in Figure 5.8.

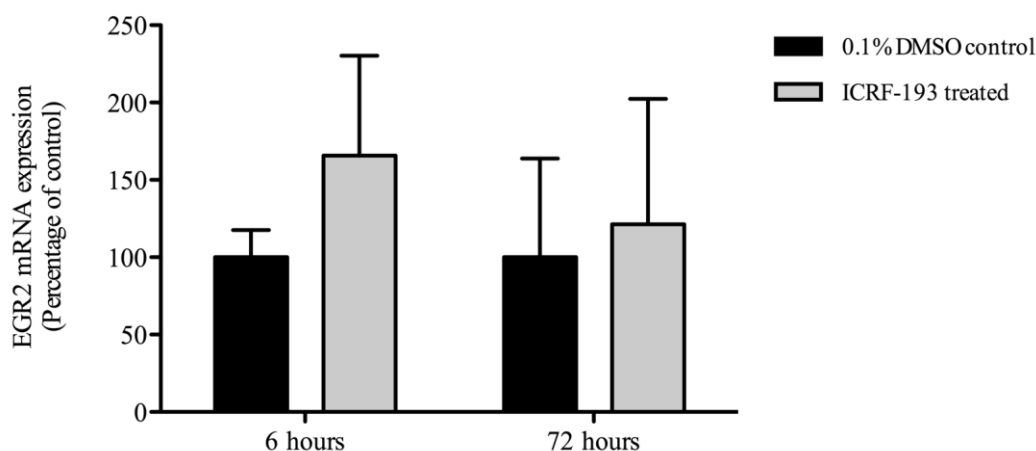


**Figure 5.8 Determining the effects of 1 nM ICRF-193 on mRNA expression of EGR2**

U937 cells were seeded at a density of  $3 \times 10^5$ /ml in a 12 well tissue culture plate in complete media (detailed in materials and methods) with 1 nM ICRF-193 or the 0.1% DMSO (v/v). Cells were allowed to incubate for either 6 or 72 h. Media was then changed and 5 ng/ml PMA and 10 ng/ml LPS was added. Cells were incubated for a further 72 h before harvesting. RNA extraction and cDNA synthesis was performed as detailed in Section 2.17. qPCR was then performed with a hydrolysis probe to EGR2 (details of qPCR conditions in Section 2.17.3). Fold expression was calculated using the

$\Delta/\Delta$  Ct method. Data is presented as percentage of the 0.1% DMSO (v/v) treated control. The means of three independent experiments are shown  $\pm$  standard error.

Statistical analysis of the data displayed in Figure 5.8 showed that there was no significant difference in EGR2 mRNA expression in cells treated with ICRF-193 for 6 h or 72 h prior to differentiation and stimulation by PMA and LPS when compared to the 0.1% DMSO (v/v) (vehicle control) treated cells (Appendix B.7).

#### **5.5.4 NF- $\kappa$ B**

Nuclear factor kappa light-chain enhancer of activated B cells (NF- $\kappa$ B) is a family of transcription factors that include various heterodimers of p50, p52 and p65/RelA (Hayden., 2008). NF- $\kappa$ B is a transcription factor primarily associated with the innate immune system. It is found in its inactive state bound to IK $\alpha$ B $\alpha$  in the cytosol. Activation via extracellular signalling leads to the phosphorylation and subsequent degradation of IK $\alpha$ B $\alpha$ , leaving NF- $\kappa$ B free to translocate to the nucleus and act as a transcription factor (Hayden, 2008).

NF- $\kappa$ B is involved in the transcription of genes encoding chemokines, cytokines and adhesion molecules. Genes regulated by NF- $\kappa$ B have been divided into two distinct subgroups; those that require chromatin re-modification and those that do not (Saccani *et al.*, 2001; Ramirez-Carrozzi *et al.*, 2006).

NF- $\kappa$ B gene expression and activity has previously been shown to be up-regulated in U937 and THP-1 cells when exposed to PMA and LPS stimulation (Baek *et al.*, 2009; Sharif *et al.*, 2007).

Samples were prepared as described in Section 5.5. RNA extraction was performed on samples that had been exposed to ICRF-193 for 6 and 72 h, both this method and the protocol for cDNA synthesis are described in Section 2.17. qPCR was performed with a hydrolysis probe to NF- $\kappa$ B. Details of the reaction conditions for the qPCR reaction can be found in Section 2.17.3. The results for this experiment are presented in Figure 5.9.



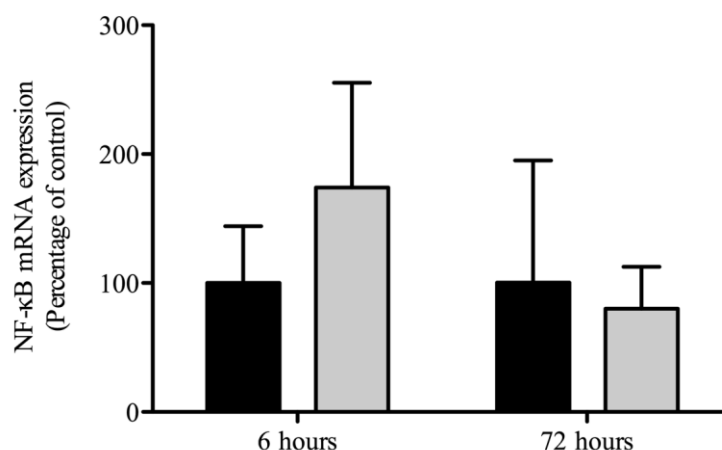


**Figure 5.9 Determining the effects of 1 nM ICRF-193 on mRNA expression of NF- $\kappa$ B**

U937 cells were seeded at a density of  $3 \times 10^5$ /ml in a 12 well tissue culture plate in complete media (detailed in materials and methods) with 1 nM ICRF-193 or the 0.1% DMSO (v/v). Cells were allowed to incubate for either 6 or 72 h. Media was then changed and 5 ng/ml PMA and 10 ng/ml LPS was added. Cells were incubated for a further 72 h before harvesting. RNA extraction and cDNA synthesis was performed as detailed in Section 2.17. qPCR was then performed with a hydrolysis probe to NF- $\kappa$ B (details of qPCR conditions in Section 2.17.3). Fold expression was calculated using the comparative  $\Delta/\Delta$  Ct method. Data is presented as percentage of the 0.1% DMSO (v/v) treated control. The means of three independent experiments are shown  $\pm$  standard error.

Statistical analysis of the data displayed in figure 5.9 showed that there was no significant difference in NF- $\kappa$ B mRNA expression in cells treated with ICRF-193 for 6 h or 72 h prior to differentiation and stimulation by PMA and LPS when compared to the 0.1% DMSO (v/v) (vehicle control) treated cells (Appendix B.8).

#### **5.5.5 Toll Like Receptors 2 and 4**

Toll receptors are type 1 transmembrane proteins, they are involved in the mediation of the innate immune response. Toll like receptors respond to ‘foreign’ stimuli, resulting in the release of NF- $\kappa$ B transcriptionally regulated pro-inflammatory cytokines. To date, 10 Toll like receptors have been identified. The most widely investigated are TLR2 and

TLR4. TLR2 responds to stimuli from lipoprotein, a commonly found in gram positive cell walls. TLR4 responds to stimuli from lipopolysaccharide, a component of the Gram negative cell membrane. Other TLRs such as TLR5 and TLR9 respond to stimuli from bacteria flagellin and foreign DNA respectively (Vasselon *et al.*, 2002). TLR2 and TLR4 mRNA expression have both previously been shown to be increased in response to PMA (Traore *et al.*, 2012; Zarembek *et al.*, 2002).

Samples were prepared as described in Section 5.5. RNA extraction was performed on samples that had been exposed to ICRF-193 for 6 and 72 h, both this method and the protocol for cDNA synthesis are described in Section 2.17. qPCR was performed with hydrolysis probes to TLR2 and TLR4. Details of the reaction conditions for the qPCR reaction can be found in Section 2.17.3. The results for this experiment are presented in Figure 5.10.

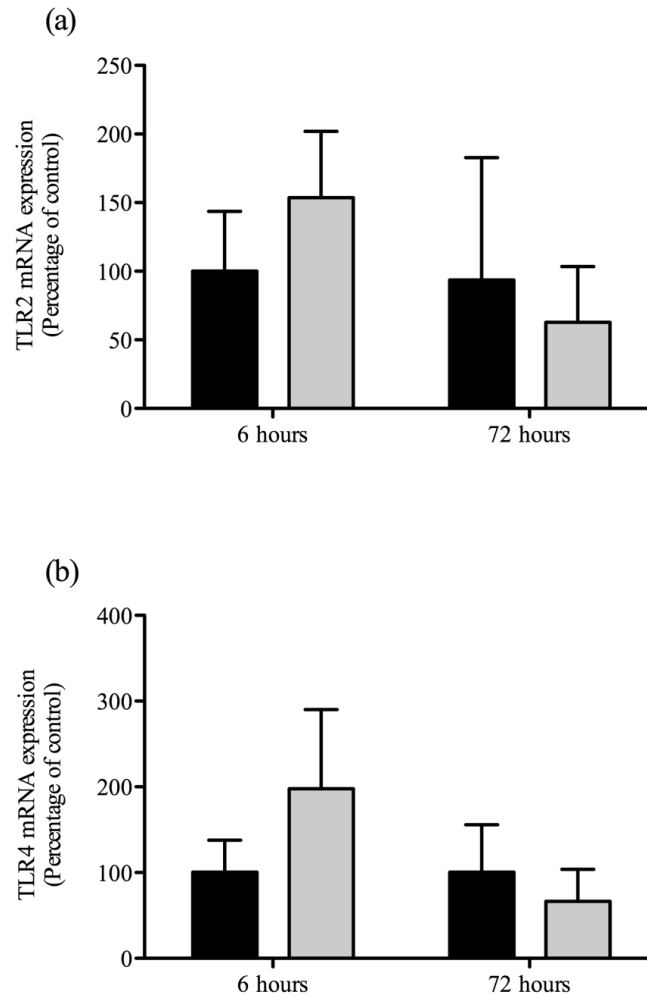


**Figure 5.10 Determining the effects of 1 nM ICRF -193 on mRNA expression of TLR2 and TLR4.**

U937 cells were seeded at a density of  $3 \times 10^5/\text{ml}$  in a 12 well tissue culture plate in complete media (detailed in materials and methods) with 1 nM ICRF-193 or the 0.1% DMSO (v/v). Cells were allowed to incubate for either 6 or 72 h. Media was then changed and 5 ng/ml PMA and 10 ng/ml LPS was added. Cells were incubated for a further 72 h before harvesting. RNA extraction and cDNA synthesis was performed as detailed in Section 2.17. qPCR was then performed using hydrolysis probes to TLR2 (a) and TLR4 (b) using 18S as the reference gene (details of qPCR conditions in Section 2.17.3) Fold expression was calculated using the  $\Delta/\Delta$  Ct method. Data is presented as percentage of the 0.1% DMSO (v/v) treated control. The means of three independent experiments are shown  $\pm$  standard error.

Statistical analysis of the data displayed in figure 5.10 revealed that there was no significant difference in either TLR2 or TLR4 mRNA expression in cells treated with ICRF-193 for 6 h or 72 h prior to differentiation and stimulation by PMA and LPS when compared to the 0.1% DMSO (v/v) (vehicle control) treated cells (Appendix B.9 & B10).

#### **5.5.6 TNF $\alpha$**

In order to determine if ICRF-193 affected the expression of mRNAs encoding cytokines; that are released in response to extracellular stimuli (in this experiment LPS is used as the extracellular stimuli), levels of TNF $\alpha$  mRNA were quantified. This particular cytokine was investigated as it is the most potent and clinically important cytokine in the inflammatory response.

Tumour Necrosis Factor  $\alpha$  is a pro-inflammatory cytokine (Oprea *et al.*, 2000; Brabers *et al.*, 2006; Malo *et al.*, 2006) released by activated macrophages in response to extracellular stimuli (Heming *et al.*, 2001). It is found as a transmembrane homotrimer in activated macrophages and is converted into a soluble homotrimer by the metalloproteinase, TACE (TNF $\alpha$  converting enzyme) (Horiuchi *et al.*, 2010). Transcriptional regulation of the TNF $\alpha$  gene has been shown to involve multiple different transcription factors, for example NF- $\kappa$ B, SP1 and C/EBP $\beta$  (Collart *et al.*, 1990; Pope *et al.*, 2000; Barthel *et al.*, 2003). TNF $\alpha$  mRNA expression has previously been shown to be up-regulated in response to PMA and LPS stimulation (Liu *et al.*, 2000; Sharif *et al.*, 2007).

Samples were prepared as described in Section 5.5. RNA extraction was performed on samples that had been exposed to ICRF-193 for 6 and 72 h, both this method and the protocol for cDNA synthesis are described in Section 2.17. qPCR was performed with a hydrolysis probe to TNF $\alpha$ . Details of the reaction conditions for the qPCR reaction can be found in Section 2.17.3. The results are shown in Figure 5.11.

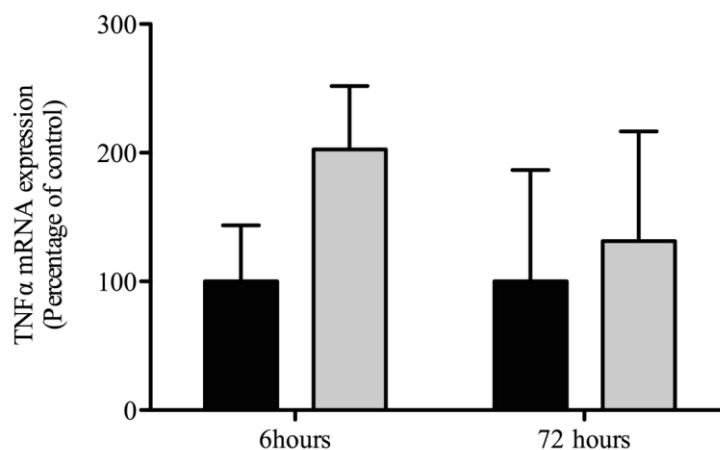


**Figure 5.11 Determining the effects of 1 nM ICRF-193 on mRNA expression of TNFα**

U937 cells were seeded at a density of  $3 \times 10^5/\text{ml}$  in a 12 well tissue culture plate in complete media (detailed in materials and methods) with 1 nM ICRF-193 or the 0.1% DMSO (v/v). Cells were allowed to incubate for either 6 or 72 h. Media was then changed and 5 ng/ml PMA and 10 ng/ml LPS was added. Cells were incubated for a further 72 h before harvesting. RNA extraction and cDNA synthesis was performed as detailed in Section 2.17. qPCR was then performed using a hydrolysis probes to TNFA, using 18S as the reference gene (details of qPCR conditions in Section 2.17.3) Fold expression was calculated using the comparative  $\Delta/\Delta C_t$  method. Data is presented as percentage of the 0.1% DMSO (v/v) treated control. The means of three independent experiments are shown  $\pm$  standard error.

Statistical analysis of the results shown in figure 5.11 showed that there was no significant difference in TNFα mRNA expression in cells treated with ICRF-193 for 6 h or 72 h prior to differentiation and stimulation by PMA and LPS when compared to the 0.1% DMSO (v/v) (vehicle control) treated cells (Appendix B.11).

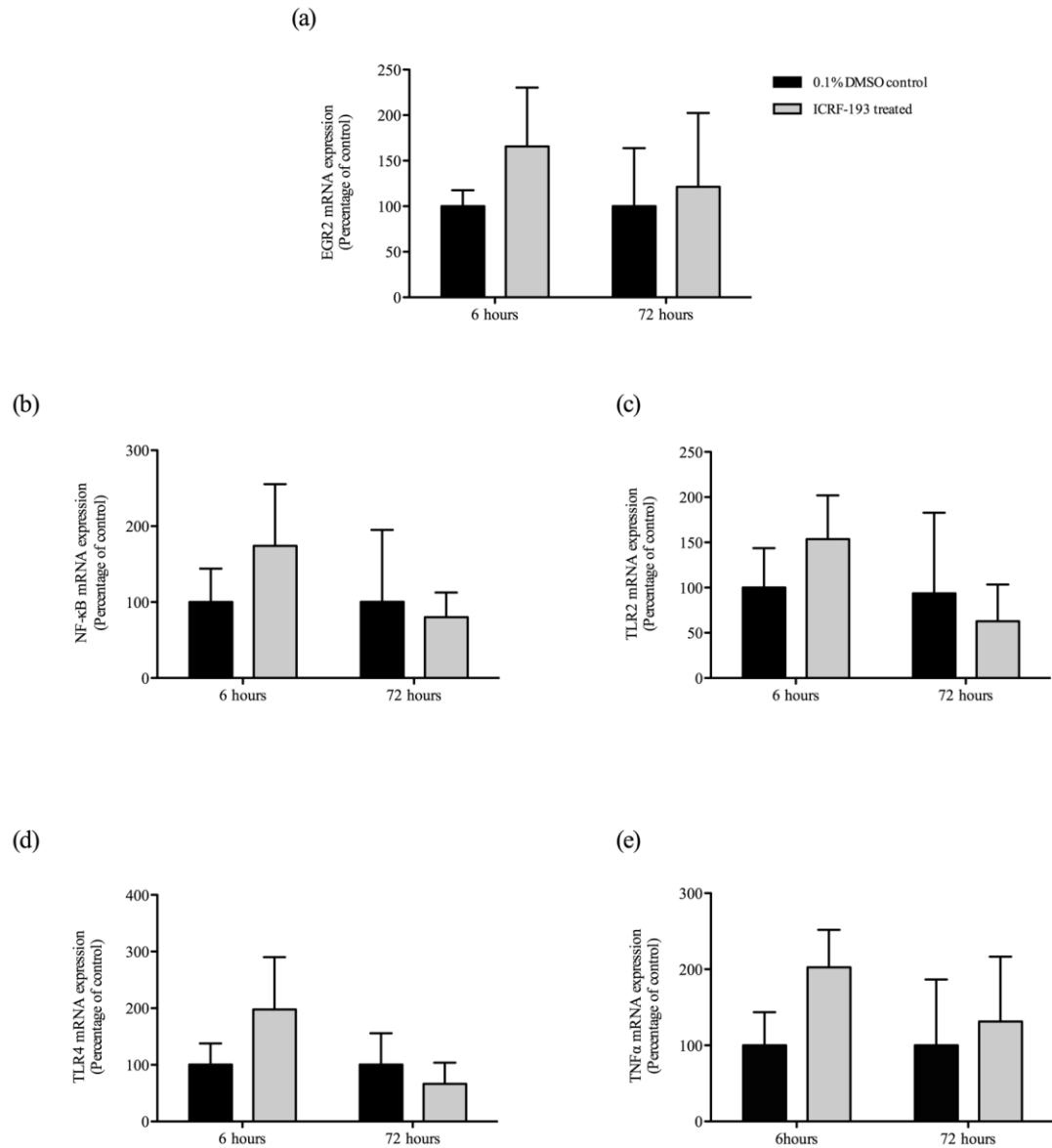


**Figure 5.12** An overview of some of the genes quantified following pre-treatment with 1 nM ICRF-193.

Collated data shows the quantification of EGR2 mRNA (a), NF-κB mRNA (b), TLR2 mRNA (c), TLR4 mRNA (d) and TNFα mRNA (e) following pre-treatment of cells with 1 nM ICRF-193 prior to differentiation and stimulation with PMA and LPS. Collated data is taken from Figures 5.8 – 5.11.

The results in Figure 5.12 show that although pre-treatment with 1 nM ICRF-193 prior to differentiation and stimulation does not significantly change the expression level of these key genes at either time point compared to controls, it does reveal an interesting trend whereby there is an increase in expression after 6 hours in all five genes examined.

Figure 5.1 reveals that 6 h of treatment with 1 nM ICRF-193 results in a substantial degradation of topo II $\beta$  protein, thus suggesting that the results seen in Figure 5.12 with regards to 6 h of 1 nM ICRF-193 pre-treatment may be due to inhibition of topo II $\beta$ . In contrast Figure 5.1 shows that 72 h of ICRF-193 treatment sees the recovery of topo II $\beta$  protein levels comparable to the levels shown in the 0.1% DMSO (v/v) control. The results in Figure 5.12 with regards to 72 h of ICRF-193 pre-treatment show little difference in mRNA expression of all genes compared to the control, thus reflective of the recovery of topo II $\beta$  protein.

Increasing evidence suggests a role for topo II $\beta$  in gene regulation. Interestingly the action of topo II $\beta$  has been shown to be required for the up and down regulation of genes involved in neuronal development. Other studies support these findings by revealing that topo II $\beta$  is involved in both the activation and repression of gene expression (Ju *et al.*, 2006; McNamara *et al.*, 2010; Huang *et al.*, 2012).

The trend in results shown in Figure 5.12 with regards to 6 h of 1 nM ICRF-193 pre-treatment may reflect the transient and global actions of topo II $\beta$  in gene expression during differentiation. Indeed the results show that inhibition of topo II $\beta$  drives the expression of these genes. The mechanism by which these changes occur are not clear but the actions of topo II $\beta$  in both the activation and repression of genes suggests that topo II $\beta$  does not act alone; that it may act via interactions with different proteins involved in gene expression or repression. Ju *et al.*, (2006) showed that activation of the ps2 promoter by 17 $\beta$ -estradiol resulted in the recruitment of multiple proteins including topo II $\beta$ , PARP-1, DNA-pK, Ku86 and Ku60 to the same DNA piece, and further suggested that these proteins may be forming a multi-protein complex. In addition, topo II $\beta$  has also been shown to associate with co-repressors such as HDACs (McNamara *et al.*, 2010; Huang *et al.*, 2012; Johnson *et al.*, 2001). McNamara *et al.*, (2010) suggest that silencing of retinoic acid induced gene expression by topo II $\beta$  may require the actions of co-repressors such as HDAC that act by reducing accessibility of the

chromatin, and that topo II $\beta$  may form a large co-repressor complex with these proteins similarly to the co-activator complex proposed by Ju *et al.*, (2006). It may be postulated that the trend in the results in Figure 5.12, although non-significant may reflect a normal mechanism by which these genes are regulated by a transcriptional repressor complex that includes the physical interaction of topo II $\beta$  with the complex. Inhibition of topo II $\beta$  may then lead dissociation of the complex leading to a possible increase in chromatin accessibility and an increase in transcription that is to some extent exhibited by the trend seen in Figure 5.12. This is supported by work that shows that methylation of CpG islands in the TLR2 promoter causes silencing of the gene. Topo II $\beta$  has previously been shown to be highly associated with sites of methylation, particularly H3k4 methylation (Tiwari *et al.*, 2012). Thus suggesting that topo II $\beta$  along with other factors such as methyltransferases may repress the expression of TLR2. However, as the results did not reach significance, further work will be required to confirm this theory.

The small increase in NF- $\kappa$ B expression seen after 6 h of 1 nM ICRF-193 pre-treatment, although non-significant, may be due to topo II $\beta$  being involved in the repression of NF- $\kappa$ B, thus when topo II $\beta$  is inhibited, a small up-regulation of gene expression can be observed. However this small increase may also be a result of a DNA damage response induced by ICRF-193. An increase in NF- $\kappa$ B activation has been shown in response to DNA damage, in particular to double strand breaks (see Section 1.12.4 for more detail). The role of NF- $\kappa$ B in the DNA damage response is to promote a cell survival pathway. As discussed previously in this chapter, the induction of double strand breaks (dsbs) directly by ICRF-193 is controversial; however indirect mechanisms may lead to the formation of dsbs. Therefore after 6 h of ICRF-193 pre-treatment, followed by PMA and LPS stimulation, the small increase in NF- $\kappa$ B mRNA expression may be the result of activation of NF- $\kappa$ B by DNA damage and LPS stimulation. This may then lead to depletion in intracellular stores the cell responding by up-regulating NF- $\kappa$ B transcription.

The trend in the results in Figure 5.12 are in agreement with Perez *et al.*, (1997) who showed that treatment of U937 cells with 300 nM ICRF-193 lead to differentiation as measured by an up-regulation of CD11b expression and Nitric oxide synthesis. The study did not report changes in morphology in U937 cells treated with ICRF-193. Indeed at concentrations similar to that used by Perez *et al.* (1997) shown in Figure 4.16 no morphological changes in cells were seen at this time (data not shown). The results



in Figure 5.12, although not significant do show that inhibition of topo II $\beta$  for 6 h prior to differentiation with 1 nM ICRF-193 leads to a trend in the up-regulation of genes associated with differentiation. Taken together these results suggest that inhibition of topo II $\beta$  drives differentiation, suggesting that normally topo II $\beta$  may act to repress the transcription of these genes.

As Figure 5.11 demonstrated an interesting increase in TNF $\alpha$  mRNA expression when cells were treated with ICRF-193 6 h prior to differentiation, it was then decided to investigate the TNF $\alpha$  protein secretion from cells that had been treated with 1 nM ICRF-193 for varying exposure times prior to differentiation and stimulation. The results of this are shown in Figure 5.13.

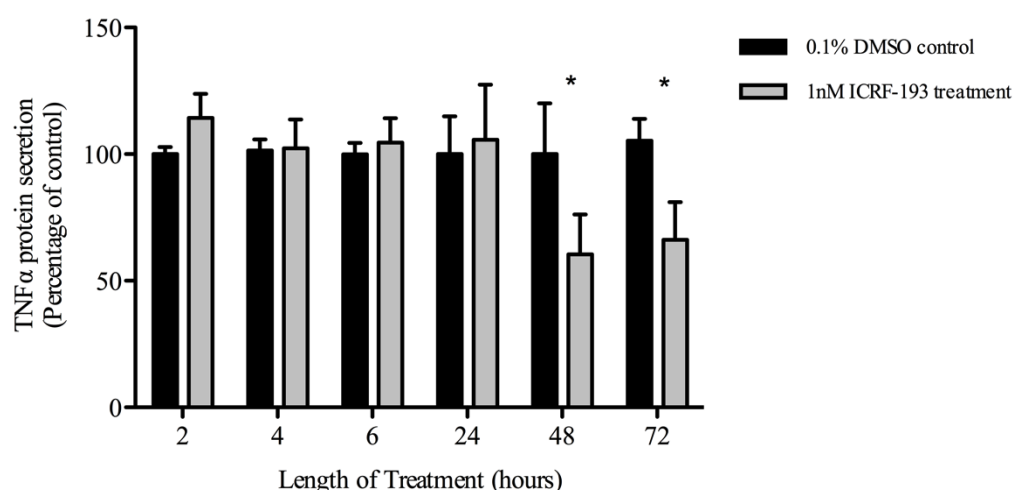


**Figure 5.13 Comparing the effects of different exposure times to 1 nM ICRF-193 prior to PMA and LPS treatment on TNF $\alpha$  protein secretion.**

U937 cells were seeded at a density of  $3 \times 10^5$ /ml in a 12 well tissue culture plate in complete media (detailed in materials and methods) with 1 nM ICRF-193 or 0.1% DMSO (v/v). Cells were allowed to incubate for 2, 4, 6, 24, 48 or 72 h. Media was then changed and 5 ng/ml PMA and 10 ng/ml LPS was added. Cells were incubated for a further 72 h before the supernatant was harvested. An ELISA to human TNF $\alpha$  was then performed (detailed in Section 2.18.1). Data is presented as percentage of the 0.1% DMSO (v/v) control. The means of three independent experiments are shown  $\pm$  standard error. \* =  $p < 0.05$ .

The results show a small increase in TNF $\alpha$  protein secretion when cells were treated with ICRF-193 for 2 h prior to differentiation and stimulation, however this result was not significantly different to the 0.1% DMSO (v/v) control (see Appendix Table B.4). Very little difference in TNF $\alpha$  protein secretion was observed when cells were treated with ICRF-193 4, 6 and 24 h prior to differentiation and stimulation compared to their respective controls (Appendix Table B.4). Interestingly significant decreases were seen in TNF $\alpha$  protein secretion when cells were treated with ICRF-193 for 48 h and 72 h prior to differentiation and stimulation. An average decrease of 29% was seen in TNF $\alpha$  protein secretion from cells treated with ICRF-193 for 48 h prior to differentiation and stimulation ( $p=0.028$ , student t-test). An average decrease of 34% in TNF $\alpha$  protein secretion was seen from cells treated with ICRF-193 for 72 h prior to differentiation and stimulation ( $p= 0.043$ , student t-test).

TNF $\alpha$  protein exists as a transmembrane homodimer; upon stimulation of cells (in this case by LPS) TNF $\alpha$  is cleaved by the metalloproteinase, TNF $\alpha$  converting enzyme (TACE) allowing its secretion into the extracellular environment (Horiuchi *et al.*, 2010). Storage of TNF $\alpha$  as a transmembrane protein allows a rapid release of the cytokine in response to potential pathogenic stimuli (Stanley & Lacy, 2010). However, despite TNF $\alpha$  being stored by the cell for such events, TNF $\alpha$  mRNA expression is seen to increase when cells are stimulated (Suzuki *et al.*, 2000), possibly to replenish secreted protein at the membrane, thus enabling a prolonged immune response.

In order for TNF $\alpha$  to be secreted there are multiple steps that are required beforehand; transcription of the TNF $\alpha$  gene, post transcriptional modifications and translation of mRNA and synthesis of the TNF $\alpha$  protein, transport and insertion into the cell membrane and cleavage of transmembrane TNF $\alpha$  by TACE.

Figure 5.13 shows very little difference in protein secretion of TNF $\alpha$  when cells were treated with 1 nM ICRF-193 for 6 h prior to differentiation and stimulation. This is in contrast to results shown in Figure 5.11 that show an increase in TNF $\alpha$  mRNA expression under the same conditions, however the results in Figure 5.11 did not reach significance. It is not known whether this increase in mRNA levels is mediated via increased transcriptional rate or due to an increase in mRNA stability i.e., some post-transcriptional modification. In addition it is not known whether an increase in mRNA level is accompanied by an increase in translation and production of TNF $\alpha$  protein.

Indeed levels of mRNA do not always correlate with protein levels; Krämer *et al.* (1995) reported that an un-translated region in the TNF $\alpha$  mRNA was implicated in the predisposition of mRNA degradation by RNAses. Thus it may be suggested that the increased amount of TNF $\alpha$  mRNA seen in Figure 5.11 may not have all been translated, however, the results in Figure 5.11 did not reach significance, making it difficult to speculate.

A decrease in TNF $\alpha$  protein secretion was observed when cells were treated with ICRF-193 for 48 and 72 h prior to differentiation and stimulation. In contrast an increase in TNF $\alpha$  mRNA was observed when cells were treated with ICRF-193 for 72 h prior to differentiation and stimulation (Figure 5.11), however this result was not significantly different from the control. Indeed this increase in mRNA expression of TNF $\alpha$  after 72 h of pre-treatment with ICRF-193 is most likely not due to topoisomerase II $\beta$  inhibition, as Figure 5.1 shows that after 72 h of exposure to 1 nM ICRF-193 levels of topoisomerase II $\beta$  have recovered back to levels comparable with the control. The decrease in protein secretion may be a result of previous inhibition of topoisomerase II $\beta$  (after 6 h) causing the down-regulation of transcription of another protein required for TNF $\alpha$  secretion, and thus due to translation of mRNA and protein synthesis, in addition to protein degradation of the residual protein the effects of this inhibition are not seen until this time (48 h and 72 h pre-treatment).

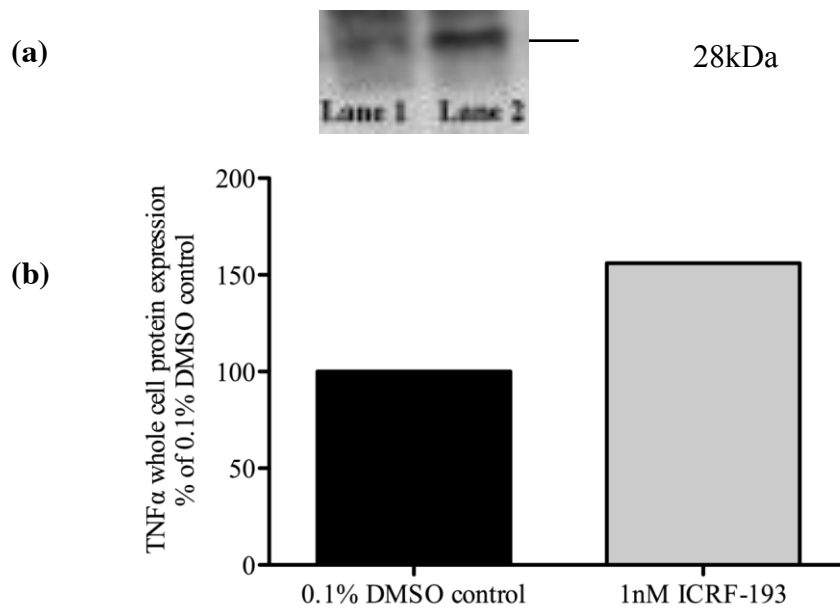


**Figure 5.14 Semi-quantification of TNF $\alpha$  protein expression from a whole cell lysate.**

Cells were treated with 0.1% DMSO (v/v) (Lane 1) or 1 nM ICRF-193 (Lane 2) for 6 h prior to differentiation and stimulation for 72 h with 5 ng/ml PMA and 10 ng/ml LPS respectively. Cells were harvested and whole cell extracts were performed as described in Section 2.16. 31.9  $\mu$ g of whole protein was loaded onto an SDS gel and SDS PAGE was then performed followed by wet western blotting. Nitrocellulose blots were then probed with antibodies to human TNF $\alpha$  (a). Quantification of protein was performed using the densitometry software, Syngene genetools See Appendix Figure B.5 for GAPDH loading control. Results are expressed as percentage of 0.1% DMSO (v/v) treated samples (b).

The results from Figure 5.14 show that 6 h of 1 nM ICRF-193 pre-treatment causes an increase in TNF $\alpha$  protein expression compared to the 0.1% DMSO (v/v) control. This is in support of the results shown in Figure 5.14 that shows an increase in TNF $\alpha$  mRNA expression after 6 h of pre-treatment with 1 nM ICRF-193. However the increase in secreted TNF $\alpha$  is small in comparison to the increase seen at the whole cell protein level, this is not unexpected as other mechanism are needed for its secretion for example the actions TACE, the enzyme responsible for the cleavage of TNF $\alpha$  to allow its secretion into the extracellular environment. As it appears that despite an up-regulation of TNF $\alpha$  protein expression there is not an up-regulation of cleavage events leading to TNF $\alpha$  secretion.

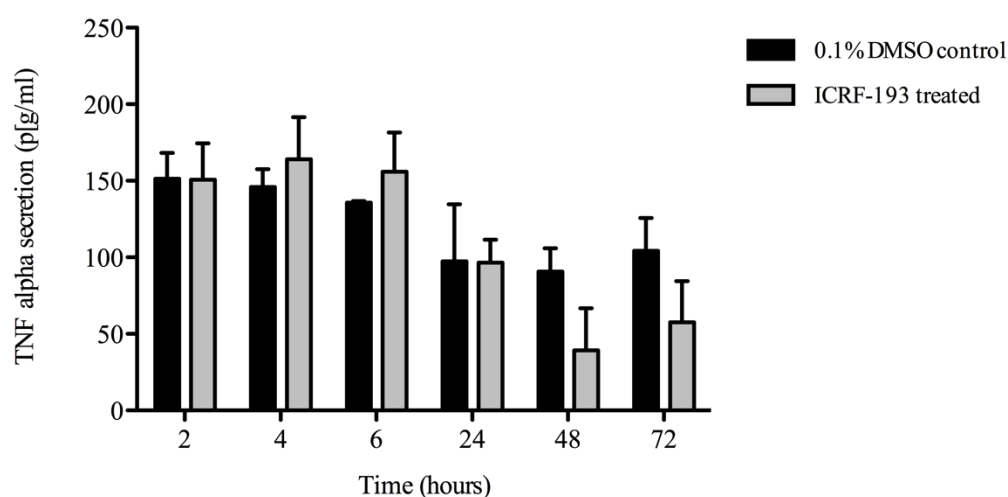


**Figure 5.15 Comparing the effects of different exposure times to 1 nM ICRF-193 prior to PMA and LPS treatment on TNF $\alpha$  protein secretion – raw data.**

Raw data used to generate Figure 5.13. Amount of TNF $\alpha$  protein secreted in pg/ml was determined by  $y = mx + c$  of standard curve. A standard curve was generated for each independent experiment. Results shown are the means of three independent experiments are shown  $\pm$  standard error.

Figure 5.15 Shows ELISA raw data used to generate Figure 5.13. It shows that cells that had been in culture for longer prior to differentiation and stimulation (0.1% DMSO (v/v) and ICRF-193 treated) appear to secrete less TNF $\alpha$  in response to LPS than those cells that were in culture for less than 24 h before differentiation and stimulation. Interestingly, as reflected in Figures 5.13 and 5.14 cells that had been treated with 1 nM

ICRF-193 for 48 and 72 h prior to differentiation and stimulation appear to secrete even less TNF $\alpha$  than their 0.1% DMSO (v/v) counterparts. Indeed cells that had been in culture for a total of 100, 124 and 148 h, despite being differentiated for the last 72 h of their time in culture may be undergoing a programmed cell death. This cell death may be attenuated by TNF $\alpha$  induced apoptosis. Secreted TNF $\alpha$  is known to bind to the tumour-necrosis factor receptor-1 (TNFR1) found on the cell surface, this results in the recruitment of TNF $\alpha$  associated death domain protein (TRADD), which in turn promotes the association of the TNFR1 complex with Fas associated death domain (FADD) inducing caspase-8 activation and cell death. The sum of this programmed cell death would ultimately lead to a down regulation of TNF $\alpha$  secretion as seen in 0.1% DMSO (v/v) treated cells in Figure 5.15. In addition, as described previously in this chapter, a prolonged exposure to ICRF-193 may lead to a DNA damage response, possibly resulting in apoptosis, and therefore attenuating any apoptosis that may already be occurring. It could also be that inhibition of topo II $\beta$  at 6 h caused a down-regulation of proteins involved in promoting cell survival when challenged with a pathogen, for example bacterial LPS. Indeed this down-regulation of protein expression may also still be occurring even when topo II $\beta$  has recovered (after 72 h of ICRF-193 treatment) and upon differentiation and stimulation the cell has been unable to promote a cell survival response and thus succumbed to apoptosis. Therefore the down-regulation in TNF $\alpha$  secretion seen after 48 h and 72 h of ICRF-193 pre-treatment followed by differentiation and stimulation with PMA and LPS is actually due to a reduction in viable cells able to secrete the cytokine.

It may also be postulated that topo II $\beta$  may be required for the repression of TNFR1 expression by association with a co-repressor complex. Treatment with ICRF-193 may then lead to disassociation of topo II $\beta$  from the complex, thus allowing transcription to occur and an up-regulation of TNFR1. An increase in TNFR1 at the cell surface would then increase the amount of target for TNF $\alpha$  to bind and thus increase the cascade of events leading to caspase activation and cell death. It should also be noted that prolonged treatment with ICRF-193 (48 and 72 h) could also generate post-translational modifications of key proteins involved in mediating apoptosis in this scenario such as TNFR1 which could account for the further decrease in TNF $\alpha$  secretion seen. As described previously Figure 5.13 was generated by measuring secreted TNF $\alpha$  and not TNF $\alpha$  whole protein. Therefore the protein measured required cleavage by TACE to facilitate its secretion. It would also be sensible to suggest a down regulation of TACE

may lead to a down regulation of secreted TNF $\alpha$ . Therefore it could be postulated that ICRF-193 may affect the expression of TACE.

All of these scenarios are not mutually exclusive and taken together would lead to the attenuated down-regulation of TNF $\alpha$  protein secretion when cells are treated with ICRF-193 for 48 and 72 h prior to differentiation.

### **5.6 Effect of a co-treatment of ICRF-193, PMA and LPS on mRNA expression and protein secretion of the pro-inflammatory cytokines TNF $\alpha$ and IL-1 $\beta$ .**

Results from Section 5.5 yielded some interesting results with regards to the effect of ICRF-193 treatment on TNF $\alpha$  mRNA expression and protein secretion. Therefore it was decided that the effect of this topo II inhibitor would be further investigated. In addition to TNF $\alpha$ , the effect of ICRF-193 on IL-1 $\beta$ , another important pro-inflammatory cytokine was investigated.

Research into the regulation of these cytokines is important as they play a crucial role in the inflammatory response. This response is the result of extracellular stimuli which in turn cause a cascade of intra and intercellular signals, leading to the secretion of pro-inflammatory cytokines including, TNF $\alpha$ , IL-1 $\beta$  and IL-6. It is highly regulated through negative feedback signals and anti-inflammatory cytokines and dysregulation of this process can lead to chronic inflammatory disease. Such diseases including autoimmune diseases are characterised by the hosts' inability to recognise 'self'. The cause of this is still to be fully elucidated. One mechanism, supported by the association of untreated *Streptococcus Pyogenes* throat infections and rheumatic heart disease suggests that microbes display molecular mimicry leading to the host's immune system targeting 'self' antigens and therefore causing a constant stimuli for pro-inflammatory producing cells. Another mechanism suggests the inactivity of endogenous anti-inflammatory cytokines (Karin *et al.*, 2006).

An example of a chronic inflammatory disease is Rheumatoid Arthritis (RA), affecting approximately 1% of the population in the developed world. It is a chronic inflammation of the synovial membrane in diarthrodial joints, causing pain, stiffness and deformity (NICE; Brennan & McInnes, 2008).

Previous work using a mouse model has shown the topo II poisons, etoposide and mitoxantrone can inhibit progression of collagen-induced arthritis (a model used to

study RA) in a dose dependent manner. Results were established by clinical observation and histological samples (Verdrengh *et al.*, 2005) This is of particular importance as it suggests that Topoisomerase II  $\alpha$  and/or  $\beta$  are necessary for macrophage and lymphocyte-associated joint inflammatory processes and that their inhibition can prevent this process.

#### **5.6.1 TNF $\alpha$**

As described previously TNF $\alpha$  is a pro-inflammatory cytokine that is released by activated macrophages in response to extracellular stimuli (Oprea *et al.*, 2000; Brabers *et al.*, 2006; Malo *et al.*, 2006).

Cells were exposed to a co-treatment of ICRF-193, 5 ng/ml PMA and 10 ng/ml LPS for 72 h. In this experiment two concentrations of ICRF-193 were used: 1 nM, which has been shown to cause degradation of topo II $\beta$  (see Figure 5.1) and 150 nM that has previously been shown to inhibit and lead to the degradation of topo II $\beta$  (McNamara *et al.*, 2010). qPCR and ELISA were performed to measure TNF $\alpha$  mRNA expression and protein secretion. The results are shown in Figures 5.16 and 5. 17 respectively.



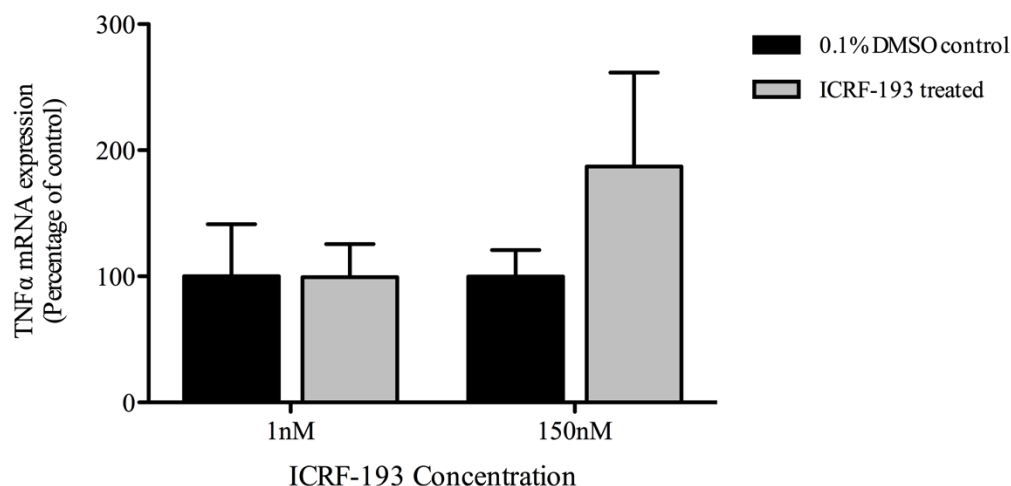


**Figure 5.16 Determining the effect of 1 nM and 150 nM ICRF-193, PMA, and LPS co-treatment on the expression of TNF $\alpha$  mRNA.**

U937 cells were seeded at a density of  $3 \times 10^5$ /ml in a 12 well tissue culture plate in complete media (detailed in materials and methods) with either 1 nM ICRF-193, 150 nM ICRF-193 or 0.1% DMSO (v/v). 5 ng/ml PMA and 10 ng/ml LPS was also added. Cells were then allowed to incubate for 72 h before harvesting. RNA extraction and cDNA synthesis was performed as detailed in Section 2.17. qPCR was then performed using a hydrolysis probe to TNFA, using 18S as the reference gene (details of qPCR conditions in Section 2.17.3) Fold expression was calculated using the  $\Delta/\Delta$  Ct method. Data is presented as percentage of the 0.1% DMSO (v/v) treated control. The means of three independent experiments are shown  $\pm$  standard error.

The results presented in Figure 5.16 show very little difference in TNF $\alpha$  mRNA expression when cells were co treated with 1 nM ICRF-193, PMA and LPS for 72 h compared to the DMSO control (Appendix Table B.12). A slight, but non-significant increase in TNF $\alpha$  mRNA expression was exhibited when cells were co-treated with 150 nM ICRF-193, PMA and LPS for 72 h (Appendix Table B.12).

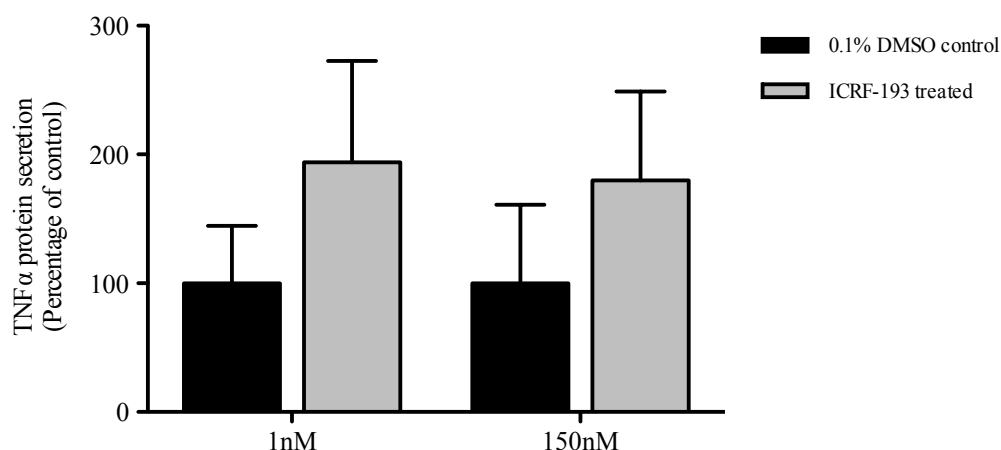


**Figure 5.17 Comparing the effects of different concentrations of 1 nM and 150 nM ICRF-193 when cells are co-treated with ICRF-193, PMA and LPS on TNF $\alpha$  protein secretion**

U937 cells were seeded at a density of  $3 \times 10^5$ /ml in a 12 well tissue culture plate in complete media (detailed in materials and methods) with either 1 nM ICRF-193, 150 nM ICRF-193 or 0.1% DMSO (v/v). 5 ng/ml PMA and 10 ng/ml LPS were also added. Cells were then allowed to incubate for 72 h before the supernatant was harvested. An ELISA to human TNF $\alpha$  was then performed (detailed in Section 2.18.1). Data is presented as percentage of the 0.1% DMSO (v/v) control. The means of three independent experiments are shown  $\pm$  standard error.

Figure 5.17 shows the cellular response to a 72 h ICRF-193 (1 nM & 150 nM), PMA and LPS co-treatment in terms of TNF $\alpha$  secretion. Statistical analysis of the results showed that there was no significant difference in TNF $\alpha$  secretion with either concentration of ICRF-193 when compared to each other or the 0.1% DMSO (v/v) (vehicle control) treated cells (Appendix B.13).

Figures 5.16 and 5.17 reveal that when cells were exposed to a co-treatment of 150 nM ICRF-193, PMA and LPS for 72 h there appeared an upward trend in the level of TNF $\alpha$  mRNA expression and protein secretion, however neither results reached significance. As described previously in this chapter, topo II $\beta$  has been implicated in the activation

and repression of gene expression (Ju *et al.*, 2006; McNamara *et al.*, 2010; Huang *et al.*, 2012) and it has been postulated that it may act as part of a co-activator or co-repressor complex with regards to regulation of different genes (Ju *et al.*, 2006; McNamara *et al.*, 2008). It may be postulated that the small increase in TNF $\alpha$  mRNA expression as shown in Figure 5.16 may reflect a normal mechanism by which this gene is regulated by a transcriptional repressor complex that includes the physical interaction of topo II $\beta$ , however as this result did not reach significance it is difficult to speculate.

Levels of topo II $\beta$  protein have previously been shown to be decreased following 48 h of 150 nM ICRF-193 treatment. This is due to ICRF-193 mediated inhibition of the topo II $\beta$  leading to the proteosomal degradation of the enzyme (McNamara *et al.*, 2008). Furthermore levels of topo II $\beta$  also maintain decreased following 72 h of treatment with 150 nM ICRF-193, PMA and LPS (see Appendix Figure B.3). Thus inhibition of topo II $\beta$  may lead to disassociation of the inhibitory complex, leading to changes in local chromatin architecture thus facilitating an increase in TNF $\alpha$  mRNA expression.

When cells were co-treated with 1 nM ICRF-193, PMA and LPS for 72 h, no effect in expression of TNF $\alpha$  mRNA was exhibited (Figure 5.16). This reflects the result in Figure 5.1 that shows treatment of cells with 1 nM ICRF-193 resulted in the recovery of topo II $\beta$  protein levels to levels comparable in the 0.1% DMSO (v/v) control. However, in contrast, an increase in protein secretion was measured (Figure 5.17), although this result did not reach significance (Appendix B.13). This increase in protein secretion, may be the result of a previous up-regulation in TNF $\alpha$  mRNA caused by inhibition of topo II $\beta$  after the first 6 h of ICRF-193 treatment, however the resultant up-regulation in protein secretion is not seen for a further 66 h. Indeed it is possible that if a sample had been taken at an earlier time point a greater increase in TNF $\alpha$  secretion may have been seen, thus suggesting that the effects of topo II $\beta$  inhibition are very much transient. However, further work will be required to confirm this theory.

Furthermore it may be postulated that differences seen between mRNA and protein levels may be due to the involvement of topo II $\beta$  in the regulation of other genes involved in the secretory pathway of TNF $\alpha$ . TNF $\alpha$  protein exists as a transmembrane homodimer; upon stimulation of the cell (in this case by LPS) TNF $\alpha$  is cleaved by the metalloproteinase, TNF $\alpha$  converting enzyme (TACE) allowing its secretion into the extracellular environment (Horiuchi *et al.*, 2010). Storage of TNF $\alpha$  as a transmembrane protein allows a rapid release of the cytokine in response to potential pathogenic

stimuli. However, despite TNF $\alpha$  being stored by the cell for such events, TNF $\alpha$  mRNA expression is seen to increase when cells are stimulated (Suzuki *et al.*, 2000), possibly to replenish secreted protein at the membrane, thus enabling a prolonged immune response.

Additionally, as stated previously, in order for TNF $\alpha$  to be secreted there are multiple steps that are required beforehand; transcription of the TNF $\alpha$  gene, translation of mRNA and synthesis of the TNF $\alpha$  protein, transport and insertion into the cell membrane and cleavage of transmembrane TNF $\alpha$  by TACE.

Thus the small increase in TNF $\alpha$  protein secretion seen in Figure 5.17, although not significant (Appendix B.13) could be due to an up-regulation of TACE. Indeed an up-regulation of TACE has been shown to increase the amount of TNF $\alpha$  transmembrane protein that is cleaved (Guinea-Viniegra *et al.*, 2009). In support of previous discussions it may be postulated that topo II $\beta$  may be part of a co-repressor complex that regulates the gene that encodes TACE. Therefore treatment of cells with ICRF-193 may lead to disassociation of topo II $\beta$  from the co-repressor complex, thus leading to the up-regulation of TACE expression and therefore leading to an up-regulation of TNF $\alpha$  cleavage resulting in an increase in secretion. It may also be due to post-translational modification of TACE in response to exposure to ICRF-193 such that its activity increases thus resulting in increased TNF $\alpha$  secretion. Interestingly, in contrast, topo II $\beta$  could be driving the expression of genes involved in TNF $\alpha$  secretion. Interestingly, in contrast, topo II $\beta$  could be driving the expression of genes involved in TNF $\alpha$  secretion. Perez *et al.* (1997) showed that treatment of U937 cells with 0.3  $\mu$ M ICRF-193 for 72 h elicited an increase in PKC protein expression. Further to this McNamara *et al.* (2010) showed that an increase in PKC $\delta$  protein expression correlated with an increase in topo II $\beta$  protein expression, possibly by stabilisation of the protein by phosphorylation. However an up-regulation of topo II $\beta$  protein expression is not seen following a co-treatment with 150 nM ICRF-193, PMA and LPS (Appendix Figure B.3) it may be postulated that topo II $\beta$  is hyperphosphorylated due to an increase in PKC, and this in turn increases its enzymatic activity (DeVore *et al.*, 1992; Matsumoto *et al.*, 1999), thus leading to an increase in gene expression. Again further work will be required in order to support this hypothesis.

It is interesting to note that mRNA data from Figures 5.11 and 5.16 do not correlate. Figure 5.11 shows that 6 h of ICRF-193 treatment prior to differentiation and stimulation results in a significant increase in TNF $\alpha$  mRNA expression, in contrast a co-treatment of cells with 1 nM ICRF-193, PMA and LPS for 72 h has little effect on TNF $\alpha$  mRNA expression. It may be that pre-treatment of cells with ICRF-193 is 'priming' the TNF $\alpha$  gene ready for transcription; for example by causing disassociation of a co-repressor complex. Indeed it has been shown the ICRF-193 may actually induce differentiation (Perez *et al.*, 1997). Therefore pre-treatment of cells with ICRF-193 may drive the up-regulation of genes associated with macrophage like cells. It is likely that the co-treatment of 1 nM ICRF-193 with PMA and LPS does not affect mRNA expression of TNF $\alpha$  as topo II $\beta$  is not being down-regulated at this time; as previously treatment of cells with 1 nM ICRF-193 for 72 h actually sees the recovery of topo II $\beta$  back to levels comparable with the 0.1% DMSO (v/v) control.

In addition to this, protein data from Figure 5.13 and 5.17 do not correlate. A 72 h co-treatment of 1 nM ICRF-193, PMA and LPS shows an up-regulation of protein secretion, in comparison a 72 h pre-treatment with 1 nM ICRF-193 causes a significant down-regulation in protein secretion. However a direct comparison between this data cannot be made. Cells used for the two sets of experiments were in culture for very different times; pre-treated cells were in culture for up to 148 h (72 h pre-treatment + 72 h PMA and LPS treatment) whilst co-treated cells were only in culture for 72 h. Additionally for both experiments levels of topo II $\beta$  protein were shown to be comparable to levels in the 0.1% DMSO (v/v) control samples. However the down-regulation of TNF $\alpha$  following 72 h of 1 nM ICRF-193 pre-treatment may be, as described previously, due to the effects of earlier inhibition of topo II $\beta$  at 6 h effecting the gene expression of other proteins involved in TNF $\alpha$  secretion. It may also be due to pre-treatment with ICRF-193 driving apoptosis of the cells, thus seemingly causing a down-regulation of TNF $\alpha$  secretion. The up-regulation of TNF $\alpha$  secretion observed when cells are co-treated with 1 nM ICRF-193 for 72 h may possibly be due the antagonism of the immune response by ICRF-193 itself.

It could be suggested that possible LPS contamination of ICRF-193 and PMA could lead to an up-regulation of TNF $\alpha$  mRNA or protein secretion. Following these experiments, the stocks of ICRF-193 and PMA used were tested for LPS contamination, of which none was found (data not shown).

### 5.6.2 IL-1 $\beta$

Interleukin -1 $\beta$  is a pro-inflammatory cytokine produced by cells of the innate immune system (Oprea *et al.*, 2000; Brabers *et al.*, 2006; Malo *et al.*, 2006). It is produced as a 35kDa inactive precursor, pro-IL-1 $\beta$  in response to cell signalling induced by binding of Pattern associated molecular patterns (PAMPs). Processing of pro-IL-1 $\beta$  is via cleavage by the pro-inflammatory protease, caspase-1. Caspase-1 is activated via recruitment to the inflammasome; a multi-protein complex consisting of ASC, NLPR3, PRR and pro-caspase-1. The resulting cleavage of pro-IL-1 $\beta$  leads to the secretion of active IL-1 $\beta$ . (Lopez-Castejon *et al.*, 2011).

Cells were prepared as described in Section 5.7.1. qPCR and ELISA were performed to measure IL-1 $\beta$  mRNA expression and protein secretion. The results are shown in Figures 5.18 and 5.19, respectively.

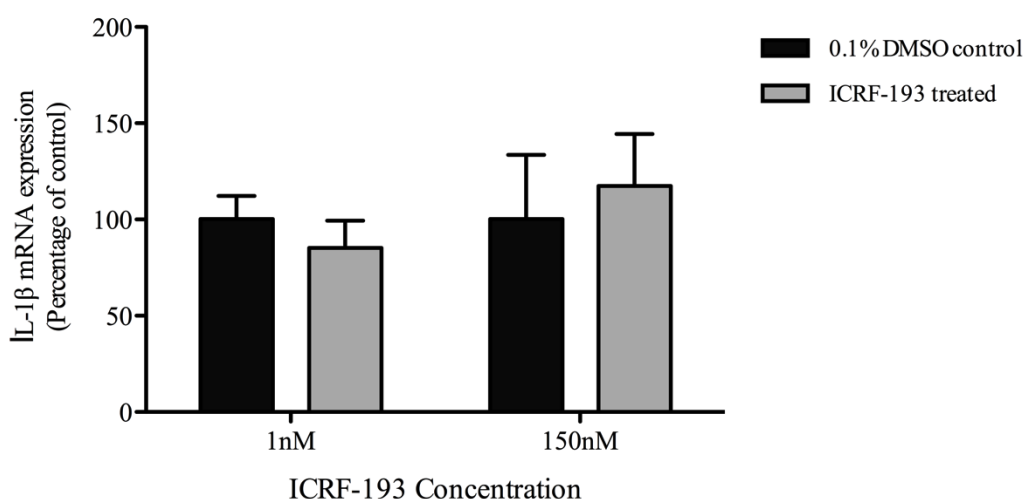


**Figure 5.18 Determining the effect 1 nM and 150 nM ICRF-193, PMA, and LPS co-treatment on the expression of IL-1 $\beta$  mRNA.**

U937 cells were seeded at a density of  $3 \times 10^5$ /ml in a 12 well tissue culture plate in complete media (detailed in materials and methods) with either 1 nM ICRF-193, 150 nM ICRF-193 or the 0.1% DMSO (v/v). 5 ng/ml PMA and 10 ng/ml LPS was also added. Cells were then allowed to incubate for 72 h before harvesting. RNA extraction and cDNA synthesis was performed as detailed in Section 2.17. qPCR was then performed using a hydrolysis probe to IL1B, using 18S as the reference gene (details of qPCR conditions in Section 2.17.3) Fold expression was calculated using the comparative  $\Delta/\Delta$  Ct method. Data is presented as percentage of the 0.1% DMSO (v/v)

treated control. The means of three independent experiments are shown  $\pm$  standard error.

The results presented in Figure 5.18 reveal that there is no significant difference in IL-1 $\beta$  mRNA expression in cells that had been co-treated with either 1 nM or 150 nM ICRF-193, along with PMA and LPS for 72 h or compared to the DMSO controls (Appendix Table B.14).

Under the same conditions, using an ELISA to human IL-1 $\beta$ , protein secretion was quantified. The results are shown in Figure 5.19.

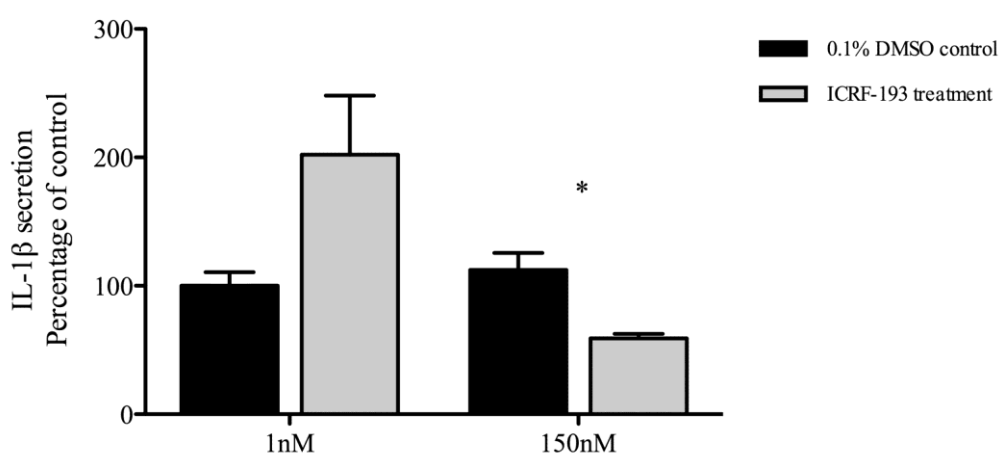


**Figure 5.19 Comparing the effects of different concentrations of ICRF-193 when cells are co-treated with ICRF-193, PMA and LPS on IL-1 $\beta$  protein expression.**

U937 cells were seeded at a density of  $3 \times 10^5$ /ml in a 12 well tissue culture plate in complete media (detailed in materials and methods) with either 1 nM ICRF-193, 150 nM ICRF-193 or 0.1% DMSO (v/v). 5 ng/ml PMA and 1ng/ml LPS were also added. Cells were then allowed to incubate for 72 h before the supernatant was harvested. An ELISA to human IL-1 $\beta$  was then performed (detailed in Section 2.18.2). Data is presented as percentage of the 0.1% DMSO (v/v) treated control. The means of three independent experiments are shown  $\pm$  standard error. \* =  $p < 0.05$ .

The results presented in Figure 5.19 reveal an increase in IL- $\beta$  protein secretion in cells that had been co-treated with 1 nM ICRF-193, PMA and LPS for 72 h, however this

result was not significantly different from the 0.1% DMSO (v/v) control (Appendix Table B.15). In comparison cells that had been co-treated with 150 nM ICRF-193, PMA and LPS for 72 h displayed a significant average decrease of 41% ( $p=0.03$ , student t-test) in IL-1 $\beta$  protein secretion.

The results from Figure 5.18 suggest that co-treatment of cells with PMA, LPS and 1 nM or 150 nM ICRF-193 has little effect on IL-1 $\beta$  mRNA expression. However, it does appear to affect IL-1 $\beta$  protein secretion, and the effect appears to be dose dependent with low doses eliciting a higher secretory response.

A co-treatment of cells with 1 nM ICRF-193, PMA and LPS appears to increase protein expression. Previous work has shown an increase in serum levels of IL-1 $\beta$  when mice were exposed to the topo II inhibitor, doxorubicin (Zhu *et al.*, 2010). Sauter *et al.* (2011) later proposed that this response to doxorubicin could be due to activation of the inflammasome. Indeed it may be postulated that cells treated with 1 nM ICRF-193 may be eliciting an attenuated immune response mediated by the inflammasome, thus secreting more IL-1 $\beta$ . This scenario is more likely than an effect caused by a down-regulation of topo II $\beta$  protein, which as shown previously actually has recovered back to levels comparable with the 0.1% DMSO (v/v) control after treatment with 1 nM ICRF-193 for 72 h.

Conversely cells that were co-treated with 150 nM ICRF-193, PMA and LPS demonstrated a significant ( $p=0.03$ , student t-test) decrease in IL-1 $\beta$  protein secretion. The results in Figures 5.18 and 5.19 suggest that inhibition of topo II $\beta$  with 150 nM ICRF-193 (McNamara *et al.*, 2010) has little effect on mRNA expression of IL-1 $\beta$ , thus suggesting it is not inhibiting IL-1 $\beta$  gene expression, however it does appear to inhibit IL-1 $\beta$  secretion. As described earlier IL-1 $\beta$  exists in the cell in its inactive form, pro-IL-1 $\beta$ , once processed by the protease, caspase-1 it is secreted from the cell. Indeed it is possible that topo II $\beta$  may regulate the expression of caspase-1. Therefore inhibition of topo II $\beta$  may lead to the down-regulation of caspase-1, resulting in a decrease in IL-1 $\beta$  secretion. As discussed previously topo II $\beta$  has been reported to play a role in the activation and repression of many genes (Lyu *et al.*, 2006; Ju *et al.*, 2006; Tiwari *et al.*, 2012). Tiwari *et al.* (2012) reported that topo II $\beta$  is associated with transcriptionally active sites of DNA, and that it actually exhibited a preference for binding to promoter regions of genes involved in neuronal development; interestingly an absence of topo II $\beta$



in mice is associated with abnormalities in the cerebral cortex of the brain (Lyu *et al.*, 2003). Additionally knockdown of topo II $\beta$  in mouse embryos was shown to change the expression of 30% of developmentally regulated genes (Lyu *et al.*, 2006). However as described in Section 1.13.2.1 the events leading to IL-1 $\beta$  secretion are not quite as simple as this hypothesis would suggest. Indeed due to the transient and global actions of topo II $\beta$ , it may be involved in the regulation of gene expression of one or more components involved in IL-1 $\beta$  secretion.

In addition an ICRF-193 dose of 150 nM may be leading to apoptosis of the cells, this would in turn lead to a decrease in IL-1 $\beta$  protein secretion as seen in Figure 5.19.

## **5.7 Comparing cytokine expression of wild type mouse embryonic fibroblasts with topo II $\beta$ deficient mouse embryonic fibroblasts (#5).**

In order to support data collected on topo II $\beta$  down-regulation using ICRF-193, mouse embryonic fibroblasts (MEFs) that were topo II $\beta$  deficient due to a stable knockdown were utilised to investigate the absence of topo II $\beta$  in production of the cytokines, IL-6 and IL-1 $\alpha$  compared to their secretion by wild type MEFs.

MEFs have previously been shown to secrete IL-6 and IL-1 $\alpha$  in response to LPS and thus provided suitable targets for investigation (Tominaga *et al.*, 1997).

### **5.7.1 Comparing differences in IL-6 protein expression**

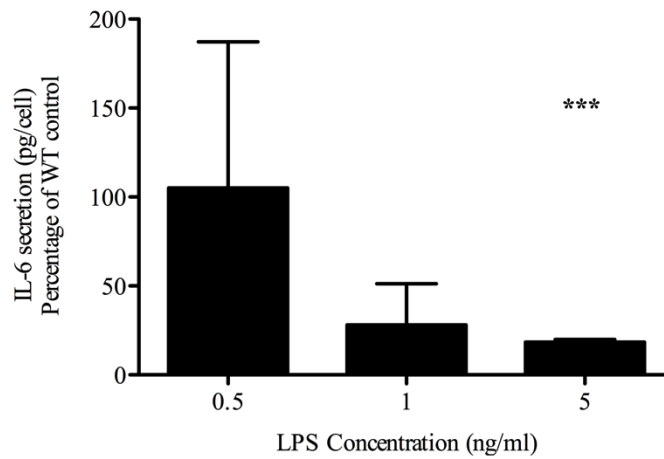
IL-6 is often described as a cytokine and a myokine (a cytokine related to muscle) (Muñoz-Cánores *et al.*, 2013). It can act both in a pro-inflammatory and anti-inflammatory capacity and is secreted by immune cells and non-immune cells, such as osteoblasts and keratinocytes (Ishimi *et al.*, 1990; Neuner *et al.*, 1991; Scheller *et al.*, 2011). Exercise induced IL-6 secretion has been shown to elicit anti-inflammatory effects particular in chronic low grade systemic inflammatory diseases such as cardiovascular disease and Type II Diabetes (Peterson & Pederson, 2006; Pederson, 2006). It is therefore an attractive target to investigate.

In order to investigate the effect of topo II $\beta$  inhibition on IL-6, two different exposure times were used in addition to three different concentrations of LPS.

As the proliferation rate of wild type MEFs and #5 MEFs was slightly different (data not shown) a cell count was performed when the supernatant was removed. Following

the ELISA, the amount of IL-6 secreted by the samples was divided by the cell number to give a final value in pg/ml/cell. The amount of IL-6 secreted in #5 MEFS as pg/ml/cell was then expressed as percentage of IL-6 secreted in pg/ml/cell of wild type MEFs. The results are shown in Figure 5.20

(a)



(b)

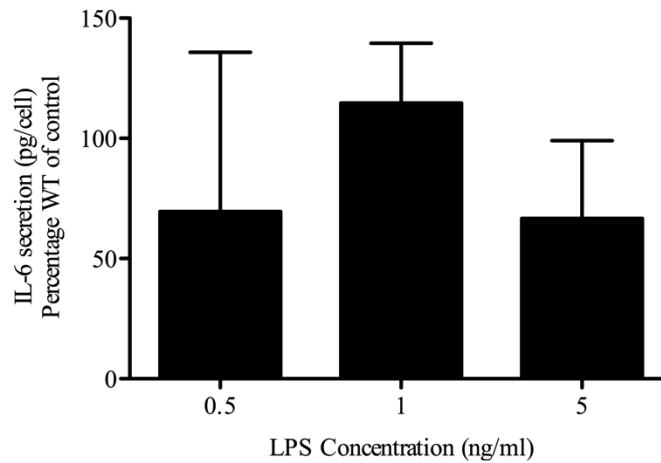


**Figure 5.20 Determining the difference in levels of IL-6 protein in wild type mouse embryonic fibroblasts and topo II $\beta$  deficiency MEFs (#5).**

WT MEFs and #5 MEFs were seeded at a cell density of  $3 \times 10^5$  cells/ml and allowed to incubate for 24 h, this was followed by the addition of 0.5, 1 and 5 ng/ml LPS was then added to both cell lines and cells were incubated for either 48 h (a) and 72 h (b) before the supernatant was harvested. A cell count was also performed at this time. An ELISA to mouse IL-6 was then performed (see Section 2.18.3 for details). Using the cell count pg/ml per cell was calculated. Data is represented as percentage of WT MEF result. The means of two independent experiments are shown  $\pm$  standard error for 0.5 and 1 ng/ml (levels of IL-6 secretion in experiment were below levels of detection). The means of three independent experiments are shown  $\pm$  standard error for 5 ng/ml. \*\*\* =  $p < 0.001$

A significant average 82% decrease ( $p < 0.001$ , student t-test). in IL-6 secretion was seen in topo II $\beta$  knockout MEFs compared to wildtype MEFs after 48 h of 5 ng/ml LPS stimulation (Figure 5.20a). A decrease was also observed when using 1ng/ml LPS for 48 h, however this result was not significant (see Appendix Table B.16) this is most likely due to a low sample set (see Figure 5.20). There was very little difference observed in IL-6 secretion when cells were treated with 0.5 ng/ml LPS for 48 h. In contrast, no significant differences were seen when cells were exposed to all concentrations of LPS for 72 h. Indeed a small decrease was seen in cells treated with 5 ng/ml for 72 h (Figure 5.20b), following the same trend demonstrated using the same LPS concentration in Figure 5.20a.

The data in Figure 5.20a suggests that topo II $\beta$  is required for the secretion of IL-6, as topo II $\beta$  deficient cells are secreting significantly less IL-6 in response to 5 ng/ml LPS than the wild type cells. This is in agreement with previous work that has demonstrated that topo II $\beta$  is required for the transcription of certain genes to occur (Ju *et al.*, 2006, Tiwari *et al.*, 2012). The transcription of the IL-6 gene requires the cooperative effects of various transcription factors including AP-1, C/EBP and NF- $\kappa$ B (Grassl *et al.*, 1999). Previous work by Ju *et al.* (2006) supports this result, as this study revealed that treatment with TPA (PMA) resulted in recruitment of topo II $\beta$  to the AP-1 regulated, MMP12 promoter, along with induction of a strand break. Thus suggesting topo II $\beta$  is involved in the regulation of transcription of AP-1 regulated genes. Additionally topo II $\beta$  has previously been found to associate with the c-Jun subunit of the AP-1 transcription factor (Kroll *et al.*, 1993). Taken together, it may be suggested that topo II $\beta$  cooperatively acts with other transcription factors, in particular AP-1 at the IL-6 gene in order to facilitate its transcription.

The difference in results between 48 and 72 h may be due to the extended exposure of cells to LPS allowing the cells to subvert the inhibition of gene expression, possibly by recruitment of other transcription factors. Indeed multiple other transcription factors, for example, CREB, Notch1 and IRF-1 are involved in IL-6 gene expression (Sanceau *et al.*, 1995; Grassl *et al.*, 1999; Spooren *et al.*, 2010; Wongchana & Palaga, 2012) however their recruitment appears to be cell specific, thus suggesting multiple modes of gene activation. The difference in IL-6 secretion between time points may also reflect the time specific action of topo II $\beta$ . Lyu *et al.* (2006) showed that topo II $\beta$  was required

in the later stages of neuronal development and dispensable at the earlier stages. Indeed it is possible that topo II $\beta$  is required at the promoter region of IL-6 early in response to LPS, and therefore a down-regulation is not seen after 72 h. This also suggests that an even greater repression of IL-6 secretion may be seen after a shorter exposure to LPS. However as the data presented focuses on the secretion of IL-6 and not the mRNA expression of IL-6 then it is difficult to conclude that topo II $\beta$  is actually affecting IL-6 gene expression, indeed its absence may cause the down-regulation of other genes associated with the expression and secretion of IL-6, conversely its absence could prevent the repression of genes involved in suppressing IL-6 secretion.

### **5.7.2 Comparing differences in IL-1 $\alpha$ protein expression**

IL-1 $\alpha$  is a pro-inflammatory cytokine produced mainly by macrophages and neutrophils but can also be expressed by epithelial cells and fibroblasts. IL-1 $\alpha$  is produced as a 31kDA precursor protein that requires the removal of the N terminal amino acids in order to become active. This occurs via cleavage by the protease calpain. IL-1 $\alpha$  exists as is active in a membrane bound and soluble form.

Cells were prepared as previously described in Figure 5.20 and an ELISA to mouse IL-1 $\alpha$  was performed. The results obtained for all three experiments from both the wild type and #5 MEFs were below the limits of detection (data not shown), suggesting that either the doses of LPS used were too low to stimulate cells or indeed 48 h and 72 h was too long, and the IL-1 $\alpha$  response was missed.

## **5.8 Knockdown of topoisomerase II $\beta$ in U937 cells using siRNA**

In order to further establish the effects of an absence of topo II $\beta$  protein on TNF $\alpha$  and IL-1 $\beta$  secretion in PMA and LPS treated U937 cells, small interfering RNA oligonucleotides (siRNA) were used to target topo II $\beta$  mRNA. This should result in a lack of topo II $\beta$  mRNA translation and therefore protein synthesis. This accompanied with the normal degradation of the existing topo II $\beta$  protein due to its finite half-life results in a depletion of the protein.

### **5.8.1 Determination of appropriate oligonucleotide to use**

Four siRNA oligonucleotides were obtained from Qiagen that targeted topo II $\beta$ . In order to determine which siRNA oligonucleotide would provide the optimal knockdown of topo II $\beta$ , protein quantification of topo II $\beta$  using SDS-PAGE and western blotting was performed following treatment with non-PMA treated U937 cells with each siRNA nucleotide. The results of this are shown in Figure 5.21.

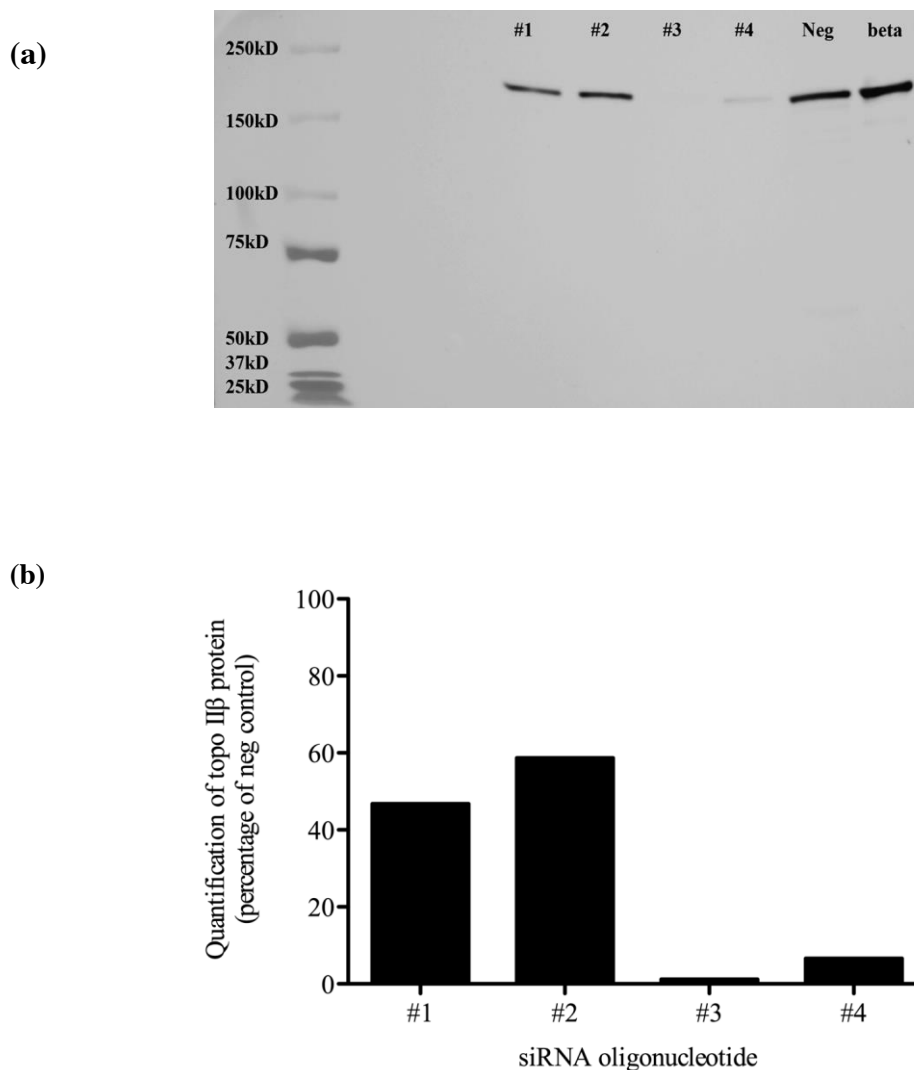


**Figure 5.21 Quantification of topo II $\beta$  protein following transfection with siRNA oligonucleotides in non-PMA treated U937 cells.**

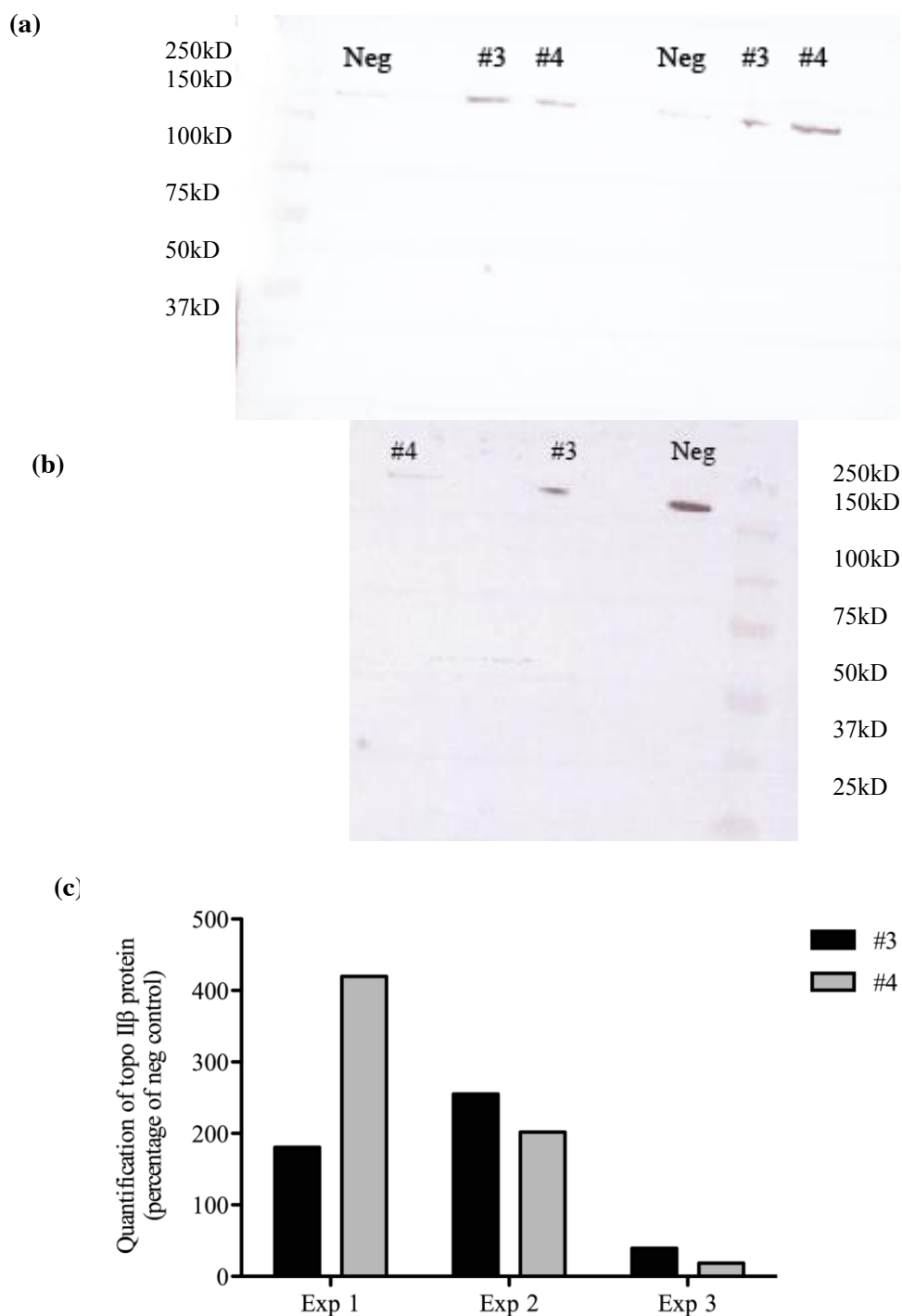
U937 cells were seeded at  $1 \times 10^5$  cells/ml in a 12 well plate and allowed to incubate for 24 h. siRNA oligonucleotides were then added (see materials and method) and cells were left to incubate for 4 h before media was changed. Cells were then left for a further 48 h before harvesting. Whole cell extractions, SDS-PAGE, and western blots were performed as described in materials and methods Section 2.16. Blots were then probed with an anti-human topo II $\beta$  antibody (Section 2.16.7) Lanes are labelled with siRNA treatment (a) Quantification of protein was performed using the densitometry software, Syngene genetools, data is presented as amount of protein in the topo II $\beta$  targeting siRNA treated cells as a percentage of that in the negative siRNA treated cells (b). Results shown are representative of one sample set. See Appendix Figure B.6 for GAPDH loading control.

Figure 5.21 shows that siRNA oligonucleotides #3 and #4 appear to be the optimal siRNA oligonucleotides to use for topo II $\beta$  knockdown. Treatment of U937 cells with siRNA #3 and #4 appear to cause a 99% and 93% reduction in topo II $\beta$  protein expression compared to the negative control, respectively (Figure 5.21). The #1 and #2 siRNA oligonucleotides also appear to induce a decrease in topo II $\beta$  protein expression, although not as effective as #3 and #4; causing a 53% and 42% decrease in topo II $\beta$  protein expression compared to the negative control (Figure 5.21).

### **5.8.2 Quantification of topoisomerase II $\beta$ protein post siRNA experiment**

Following siRNA, PMA and LPS treatment, supernatant was removed from cells in order to quantify TNF $\alpha$  and IL-1 $\beta$  protein secretion. In addition, cells were harvested and protein extracted in order to quantify the levels of topo II $\beta$  post siRNA, PMA and LPS treatment. This was necessary as knockdown of topo II $\beta$  was only previously established after 48 h of incubation, in contrast this experiment requires a further 72 h of incubation. Quantification of topo II $\beta$  protein at this time would then ensure that any significant result that may be observed during quantification of TNF $\alpha$  and IL-1 $\beta$  secretion is due to a decrease in topo II $\beta$  protein. The results of this are shown in Figure 5.22.





**Figure 5.22 Quantification of topo II $\beta$  protein following transfection with siRNA oligonucleotides and subsequent addition of PMA and LPS in U937 cells.**

U937 cells were seeded at  $1 \times 10^5$  cells/ml in a 12 well plate and allowed to incubate for 24 h. siRNA oligonucleotides were then added (see materials and method) and cells were left to incubate for 4 h before media was changed. Cells were then left for a further 48 h before media was again changed with the addition of 5 ng/ml PMA and 10 ng/ml LPS. Cells were left for a further 72 h to incubate. Whole cell extractions, SDS-PAGE,

and western blots were performed as described in materials and methods Section 2.16. Blots were then probed with an anti-human topo II $\beta$  antibody (Section 2.16.7) Lanes are labelled with siRNA treatment, (a) western blot using protein from experiments 1 & 2. (b) Western blot using protein from experiment 3 Quantification of protein was performed using the densitometry software, Syngene genetools, data is presented as amount of protein in the topo II $\beta$  targeting siRNA (siRNA #3 in black, siRNA #4 in grey) treated cells as a percentage of that in the negative siRNA treated cells (c).

Figure 5.22 shows that protein extracted from cells during experiment 1 revealed that topo II $\beta$  protein expression had recovered, additionally the level of topo II $\beta$  protein quantified was higher than the level found in the negative control. An 80% increase in topo II $\beta$  protein expression was observed when cells were transfected with the #3 siRNA oligonucleotide compared to the negative control. An even higher, 319% increase in topo II $\beta$  protein expression was seen in cells transfected with the #4 siRNA oligonucleotide.

Protein extracted from cells during experiment 2, again showed an increase in topo II $\beta$  levels compared to the negative control. A 155% increase was observed in cells transfected with the #3 siRNA oligonucleotide compared to the negative control, whilst a 101% increase in topo II $\beta$  protein expression was seen in cells transfected with the #4 siRNA oligonucleotide.

In comparison, protein extracted from experiment 3 showed that levels of topo II $\beta$  were still decreased compared to the negative control, but not as much as that seen in Figure 5.22b. A 60% decrease in topo II $\beta$  protein expression was observed in cells transfected with the #3 siRNA oligonucleotide, whereas a 82% decrease was seen in cells transfected with the #4 siRNA oligonucleotide.

### 5.8.3 Effect of topoisomerase II $\beta$ knockdown on TNF $\alpha$ protein expression

Following siRNA, PMA and LPS treatment, supernatant was removed from cells and TNF $\alpha$  protein secretion was quantified using an ELISA to human TNF $\alpha$ . The results are shown in Figure 5.23.

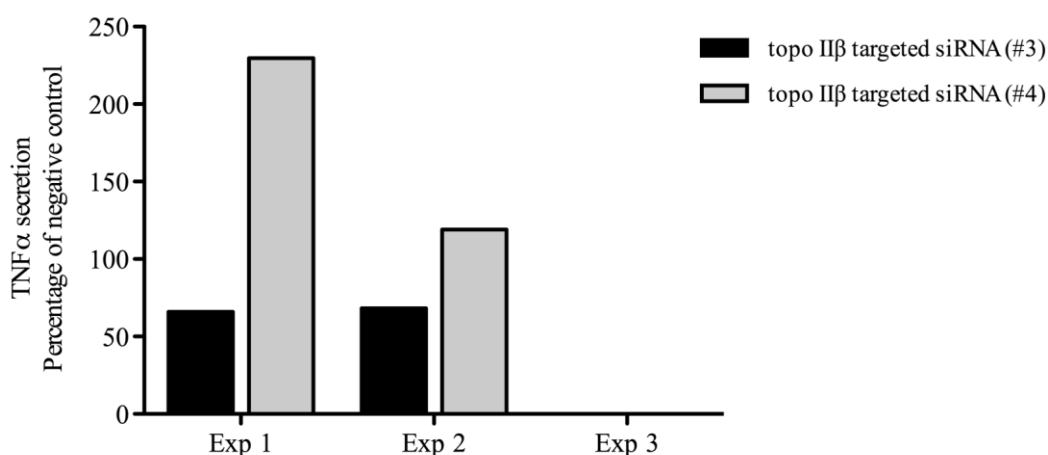


**Figure 5.23 Determining the effect of topoisomerase II $\beta$  targeted siRNA transfection on expression of TNF $\alpha$  protein secretion.**

U937 cells were seeded at  $1 \times 10^5$  cells/ml in a 12 well plate and allowed to incubate for 24 h. siRNA oligonucleotides were then added (see materials and method) and cells were left to incubate for 4 h before media was changed. Cells were then left for a further 48 h before media was again changed with the addition of 5 ng/ml PMA and 10 ng/ml LPS. Cells were left for a further 72 h to incubate before supernatant was removed and an ELISA to human-TNF $\alpha$  was performed. Results are expressed as percentage of negative control. Experiment 3 yielded results lower than the limits of detection and therefore results are shown as 0.

Figure 5.23 reveals that in experiment 1, when cells are transfected with the #3 siRNA oligonucleotide, TNF $\alpha$  protein secretion is decrease by 34% compared to the control. Conversely cells transfected with the #4 siRNA oligonucleotide demonstrated a 124% increase in TNF $\alpha$  secretion compared to the control.

In experiment 2, cells transfected with the #3 siRNA oligonucleotide displayed a 32% decrease in TNF $\alpha$  secretion compared to the control. In comparison, cells treated with the #4 siRNA oligonucleotide exhibited a 20% increase in TNF $\alpha$  secretion.

Interestingly, in experiment 3, TNF $\alpha$  secretion from cells treated with the #3 siRNA oligonucleotide and cells treated with the #4 siRNA oligonucleotide was below the detectable limits of the assay.

#### 5.8.4 Effect of topoisomerase II $\beta$ knockdown on IL-1 $\beta$ protein expression.

Following siRNA, PMA and LPS treatment, supernatant was removed from cells and IL-1 $\beta$  protein secretion was quantified using an ELISA to human IL-1 $\beta$ . The results are shown in Figure 5.24.

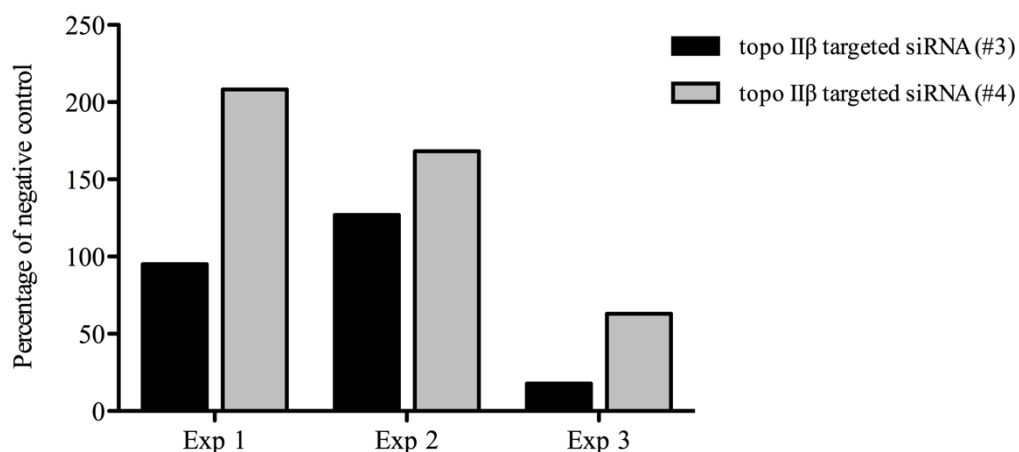


**Figure 5.24 Determining the effect of topoisomerase II $\beta$  targeted siRNA transfection on expression of IL-1 $\beta$  protein secretion**

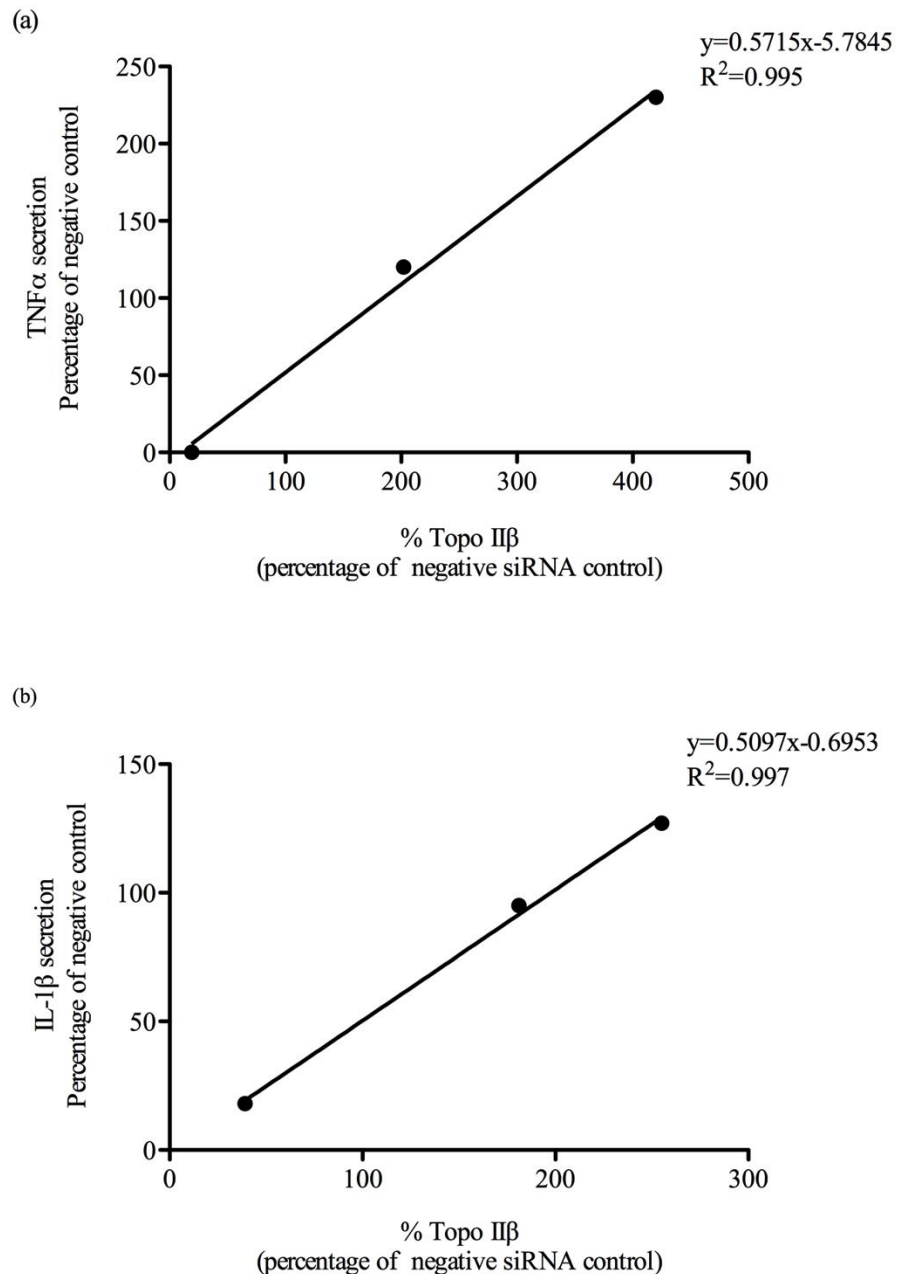
U937 cells were seeded at  $1 \times 10^5$  cells/ml in a 12 well plate and allowed to incubate for 24 h. siRNA oligonucleotides were then added (see materials and method) and cells were left to incubate for 4 h before media was changed. Cells were then left for a further 48 h before media was again changed with the addition of 5 ng/ml PMA and 10 ng/ml LPS. Cells were left for a further 72 h to incubate before supernatant was removed and an ELISA to human-IL-1 $\beta$  was performed. Results are expressed as percentage of negative control.

Figure 5.24 Shows that IL-1 $\beta$  secretion in experiment 1 in cells transfected with the #3 siRNA oligonucleotide is not largely different from the control, however cells transfected with the #4 siRNA oligonucleotide display a 108% increase in IL-1 $\beta$  secretion.

IL-1 $\beta$  secretion in experiment 2 in cells transfected with the #3 siRNA oligonucleotide display an increase of 26%, whereas cells transfected with the #4 siRNA oligonucleotide exhibit a 68% increase compared to the control.

Conversely, IL-1 $\beta$  secretion in experiment 3 is decreased compared to the control. A decrease of 83% in IL-1 $\beta$  secretion was observed from cells transfected with the #3 siRNA oligonucleotide, whilst cells transfected with the #4 siRNA oligonucleotide exhibited a 38% decrease in IL-1 $\beta$  secretion compared to the control.

Interestingly when investigating the correlation between topo II $\beta$  protein expression and TNF $\alpha$  and IL-1 $\beta$  secretion in this set of experiments, there did in fact appear to be a significant positive correlation between topo II $\beta$  protein expression and TNF $\alpha$  secretion in #4 siRNA treated cells ( $p=0.048$ , linear correlation) (Figure. 5.25a). In addition a significant correlation between topo II $\beta$  protein expression and IL-1 $\beta$  secretion in #3 siRNA treated cells was also determined ( $p= 0.0345$ , linear correlation) (Figure. 5.25b). These results strengthen the other data in this chapter that suggest that topo II $\beta$  may be involved in the transcription of genes involved in both the TNF $\alpha$  and IL-1 $\beta$  pathways of secretion.



**Figure 5.25 Correlation of topo II $\beta$  expression with TNF $\alpha$  secretion (a) and IL-1 $\beta$  secretion (b).**

Percentage of topo II $\beta$  protein expression (compared to negative control) following treatment with the #4 siRNA oligonucleotide, PMA and LPS was plotted against percentage of TNF $\alpha$  secreted (compared to negative control) from the corresponding experiment (a). Percentage of topo II $\beta$  protein expression (compared to negative control) following treatment with the #3 siRNA oligonucleotide, PMA and LPS was plotted against percentage of IL-1 $\beta$  secreted (compared to negative control) from the corresponding experiment (b). Linear regression analysis was performed using GraphPad (Prism).

## 5.9 Summary

The work in this Chapter reveals that inhibition of topo II $\beta$  using ICRF-193 has only small and mainly non-significant effects on factors associated with differentiation and stimulation. However some interesting trends have been identified such as the transient increases in the levels of NF- $\kappa$ B, EGR2, TLR4, TLR2 and TNF $\alpha$  mRNA after 6 h 1 nM ICRF-193 exposure. In addition a small transient increase in TNF $\alpha$  whole protein expression was seen. However it also highlights the possible caveats of using a topo II drug to inhibit topo II $\beta$ . Use of the topo II $\beta$  inhibitor, ICRF-193, due to the possible DNA damaging effects and ultimately due to it being a foreign material to the cell leaves it difficult to determine if the effects seen when using ICRF-193 are due to topo II $\beta$  inhibition or dose and time dependent effects of treatment with ICRF-193 itself.

The work using the mouse embryonic topo II $\beta$  knockout cells line does not have this disadvantage. Therefore the down-regulation of IL-6 secretion after 48 h of 5 ng/ml LPS treatment can be assumed to be due to an absence of topo II $\beta$ .

In addition, the positive correlation seen between siRNA induced topo II $\beta$  depletion and TNF $\alpha$  and IL-1 $\beta$  secretion, where when topo II $\beta$  is decreased, TNF $\alpha$  and IL-1 $\beta$  secretion is also decreased is very interesting. Therefore further work will utilise Chromatin Immuno-precipitation (ChIP) to investigate the association of topo II $\beta$  with regions proximal to the TNF $\alpha$  and IL-1 $\beta$  gene promoters.

## Chapter 6

### The association of Topoisomerase II $\beta$ at discrete regions of interest within the TNF $\alpha$ and IL-1 $\beta$ genes in non-LPS and LPS treated cells.

---

#### 6.1 Introduction

There is increasing evidence to suggest that topo II $\beta$  is involved in the regulation of transcription and that this involvement includes its physical association at areas of transcriptional activity. For example, Pommier *et al.* (1992) reported that topo II induced double strand breaks in the p2 promoter of the *c-myc* gene in the plasmid, JB327. More recently, Ju *et al.* (2006) proposed a mechanism by which a topo II $\beta$  generated double strand break was required at the ps2 promoter in response to 17 $\beta$ -estradiol in order for transcription to occur. Interestingly, Tiwari *et al.* (2012) reported that topo II $\beta$  is more highly associated with promoter regions than exon or introns, and association was up-regulated during differentiation from neuronal progenitor to terminal neuronal state. In addition to association at promoter regions, topo II $\beta$  binding sites were identified in DNase hypersensitivity regions within the  $\beta$ -globulin loci in chickens (Reitman & Felsenfeld, 1990).

DNase I hypersensitivity regions are regions of chromatin which are sensitive to the cleavage activities of DNase I. DNase hypersensitivity sites are often found on chromatin that is 'open', and often associated with transcriptional activity. Identification of DNase hypersensitivity I aids in the understanding of DNA regulatory elements such as enhancer and promoter regions (Song *et al.*, 2011; Thurman *et al.*, 2012).

In Chapter 5 it was shown that treatment of U937 cells with ICRF-193 led to significant perturbations in secreted levels of TNF $\alpha$  and IL-1 $\beta$  (Figures 5.13 and 5.19). TNF $\alpha$  and IL-1 $\beta$  are the most potent cytokines released during the inflammatory response and are thus a great source of interest. The inflammatory response is triggered by binding of a pathogen associated molecular pattern (PAMP) to a pattern recognition receptor (PRR) on the cell surface, most notably a toll like receptor. One such PAMP is LPS, which is found in the cell wall of Gram-negative bacteria. Binding of LPS to TLR4 leads to a cascade of signalling events ultimately leading to the secretion of pro-inflammatory cytokines, including TNF $\alpha$  and IL-1 $\beta$ . Stimulation of cells with LPS has also been



shown to cause an increase in TNF $\alpha$  and IL-1 $\beta$  mRNA expression (Cassatellas *et al.*, 1993; Reimann *et al.*, 1994).

In order to determine if topo II $\beta$  is associated with areas at, or within close proximity to the TNF $\alpha$  and IL-1 $\beta$  promoter regions, ChIP-qPCR was used to compare relative levels of topo II $\beta$  association in non-LPS and LPS treated cells.

## **6.2 Aim**

To identify regions in the IL-1 $\beta$  and TNF $\alpha$  genes which contain putative topoisomerase II cleavage sites.

To determine if topoisomerase II $\beta$  physically associates with the regions identified.

To determine if there is a change in topo II $\beta$  association at these regions when PMA treated cells are stimulated with LPS compared to non-LPS stimulated cells.

## **6.3 Designing primers to be used in qPCR following ChIP**

The aim of this section was to determine if topo II $\beta$  is physically associated with areas in or in close proximity to the TNF $\alpha$  and IL-1 $\beta$  promoter which could indicate a role in the regulation of gene expression. In order to do this, ChIP-qPCR was utilised to analyse topo II $\beta$  interactions with DNA. This method combines ChIP with qPCR to determine if the protein of interest binds to the DNA site of interest. In order to identify whether topo II $\beta$  DNA binding sites are enriched in areas at or near to the TNF $\alpha$  and IL-1 $\beta$  promoter regions, primer pairs were used to amplify these regions of interest following protein unlinking and purification. These primer pairs were designed based on known DNase hypersensitivity sites and putative topo II $\beta$  cleavage sites within the TNF $\alpha$  and IL-1 $\beta$  genes, an outline of which is shown in Figure 6.1.

Use UCSC genome browser to determine DNase hypersensitivity sites within the gene



Determine putative topo II cleavage sites using literature search (Figure 6.2)



Use BLAST software to determine if putative topo II cleavage sites are found within the DNase hypersensitivity sites (Tables 6.1 and 6.2)



Use DNase I hypersensitivity sequences that contain putative topo II cleavage sites to generate primers (using BLAST primer design software)

**Figure 6.1 Designing primers towards areas of interest within the IL-1 $\beta$  and TNF $\alpha$  genes.**

Using the NCBI database, the specific loci of the TNF $\alpha$  and IL-1 $\beta$  genes were determined. Encode data (Rosenbloom *et al.*, 2013) was then used to determine if any DNase hypersensitivity sites were located within the genes. A literature search was used to determine the sequence of any possible topo II $\beta$  binding sites. Using BLAST software an alignment using the DNase hypersensitivity site sequences and putative topo II $\beta$  cleavage site sequences was performed. BLAST primer design software was then used to generate primer sequences that included the DNase hypersensitivity sequence and putative topo II $\beta$  cleavage site sequence within their product.

The UCSC genome browser, a database that collates genomic sequence data from vertebrate and invertebrate species including cell lines was used to examine the TNF $\alpha$  and IL-1 $\beta$  genes (Step 1, Figure 6.1). A feature of the UCSC genome browser is the extensive range of tools to examine functional elements of the genome; including

regions of methylation, CpG islands and DNase hypersensitivity sites, as determined by the public research project, ENCODE (Encyclopedia of DNA Elements). This then enabled the identification of DNase hypersensitivity sites within the vicinity of the TNF $\alpha$  and IL-1 $\beta$  promoter regions (Table 6.1 and Table 6.2 respectively).

Once DNase hypersensitivity sites had been identified, a literature search was performed to identify any published topo II $\beta$  cleavage sites within these hypersensitivity regions. Previously studies using topo II poisons have shown that topo II preferably cleaves certain short sequences of DNA, however the sequences appear to differ depending on the poison used (Pommier *et al.*, 1991; Marsh *et al.*, 1996; Gao *et al.*, 2003). Data on putative topo II cleavage sites was collated (Figure 6.2) and revealed that there was a short sequence that was recurrent in multiple studies using different poisons; AGCT (Pommier *et al.*, 1992; Cornarotti *et al.*, 1996; Marsh *et al.*, 1996). Using the nucleotide alignment tool in the NCBI blast software (blastn) the sequences of the DNase hypersensitivity sites previously identified were then aligned against this putative topo II $\beta$  cleavage site. The sites identified are highlighted in red in Table 6.1 and 6.2. Only hypersensitivity sites that contained a putative topo II $\beta$  cleavage site were considered suitable targets to be used in the design of primers for qPCR.

NCBI blast primer design software (Primer-blast) was used to generate primers. Primers were designed to either contain the putative topo II $\beta$  cleavage site within the primer sequence or within the product. Primers were chosen that would generate products between 100-200bp in length, to ensure specificity.

In addition to primers that were generated to include sequences that topo II $\beta$  may associate to, primers were also designed that did not contain areas of DNase hypersensitivity and putative topo II $\beta$  cleavage sites, and were actually very close to the end of the TNF $\alpha$  and IL-1 $\beta$  genes. These primers were designed as a control (Table 6.3).

Primer sequences generated for qPCR with TNF $\alpha$  and IL-1 $\beta$  as the target are shown in Tables 6.1 and 6.2 respectively.

**Table 6.1 Location and sequences of DNase hypersensitivity regions within the IL-1 $\beta$  gene.**

Locations of DNase hypersensitivity regions in the IL-1 $\beta$  gene used to generate primers are reported in this table. DNase hypersensitivity sequences along with putative topo II $\beta$  cleavage sites (shown in red) are also reported. Additionally primer sequences generated as described in Figure 6.1 are also documented. Sequence identity will be used to describe the primers used when discussed in the text.

Sequence ID	DNase hypersensitivity site location	DNase hypersensitivity sequence including putative topo II $\beta$ cleavage site	Forward primer sequence	Reverse primer sequence
<b>IL-1<math>\beta</math> -1</b>	Chromosome 2 113,587,541 - 113,587,935bp	TTGAATAAATTAGACCAATGAATAAAACAAACAAACAAATAAATAAATAAATAGGGAAGCG GTTGCTCATCAGAATGTGGGAGCGAATGACAGAGGGTTTCTTAGAACCAAATGTGGCCGGTT TCTGTCAGGCGGGCTTTAAGTGAGTAGGAGAGGTGAGAGAGGCCTGGCTCAACAAAAGGGC TGGGGATTGGCCCTGAAAGGAGAGAGCTGACTGTCCTGGCTGATGGACAGGAGATCCTCTTA GCACTACCCTAAGGCAGGCAGTTGGGCATTGGTGTAGACAACAGGAAAGTCCAGGCTATAGC CGTACTCAAAAACCTTCTGTTCCCTTCTGCCAGCCCTAGGGATTGAGTCCACATTCAGCACAG GACTCTCTGGGTACAGCTCTCTTTAGGAAGACACAAATTGCATGGTGAAGATCAGTTATATCC TGGCCGCCTTTGGTCCCTCCCAGGAAGACGGGCATGTTTTCTGCTTGAGAGGTGCTGATGTAC CAGTTGGGGA	TTACTT GGCACC CTGTTT GC	ATTAC AGGTC AGTGG AGACG C
<b>IL-1<math>\beta</math> -2</b>	Chromosome 2 113,589,441 - 113,590,175bp	AACTGGGAGAGGAGAGGCTGAGCTGGGAAAGTGGCTCCAAAGAGAGACACTCATTTTGATC TTCCTCAGTCACAGCAGTGTCAATTGGAGGCCCTGGGATCACTCTTACTACCCGATTCCAAAG AAACAGGATTTTCTTGGCCTGGCTGAGAGCAAATAGCTTCCCCCTGAGTGAGGCTGTCCTTCA AAGTCAGCAGCCTTAGTTGCCACACTCCTGTGCAGAGGCTTTGGCTACTGTGGCACGATGCC AGGCAGATCACCACAGCTATGATGGGTACCCGCACTTGAACTTTTGCCCGTTACAGCGGAG AGATATAAGTTCCTGCTGGGCGGTAAAATTTCCCTACAAGGAACCACCTGGCATTGGGTGGG ACGGATGTTGGGGCAAGGGGGGAAGACTGGGGAGGGGGATGGACACATTATCGCTCCAGCA CTCTTGTTTCAGCCTCAACAACAGGAAGAGAGAACCCACAGGCAGTTAGGCCATGTCCATCA AATGACCCCATATTGTGGAAGAATTGACATTGCACTATGCCCAAGAGACTTGGGTGGACATG GTCCTGGGAGTGCTTGAGCCGTCTAATTTCTCAGGGTCAC	AGCTAT GATGG GTTAC CGC	AAACA AGAGT GCTGG AGCGA
<b>IL-1<math>\beta</math> -3</b>	Chromosome 2 113,590,981 - 113,591,370bp	TCAGGTCATTCTCCTGGAAGGTCTGTGGGCAGGGAACCAGCATCTTCCTCAGCTTGTCATGG CCACAACAACACTGACGCGGCCTGCCTGAAGCCCTTGCTGTAGTGGTGGTCGGAGATTTCGTAGC TGGATGCCGCCATCCAGAGGGCAGAGGTCCAGGTCCTGGAAGGAGCACTGCGGAGAGAGCG AGGGAGGGAGCCTGGTGAGGTGGTCCTGCCAGGAACCATGCTTTGACATCAGAGAGTAGAA AGCTCAGAGAGGAGGAAAGGGCTTGAAAGAATCCCAGACTTCTAAAGATCATCC	TCTGTT CCCTTT CTGCCA GC	AGCAG AAACA TGCCC GTCT

**Table 6.2 Location and sequences of DNase hypersensitivity regions within the TNF $\alpha$  gene.**

Locations of DNase hypersensitivity regions in the TNF $\alpha$  gene used to generate primers are reported in this table. DNase hypersensitivity sequences along with putative topo II $\beta$  cleavage sites (shown in red) are also reported. Additionally primer sequences generated as described in Figure 6.1 are also documented. Sequence identity will be used to describe the primers used when discussed in the text.

Sequence ID	DNase hypersensitivity site location	DNase hypersensitivity sequence including putative topo II $\beta$ cleavage site	Forward primer sequence	Reverse primer sequence
<b>TNF<math>\alpha</math> -1</b>	Chromosome 6 31,543,241- 31,543,390bp	AAGGTGCAGGGCCCACTACCGCTTCCTCCAGATGAGCTCATGGGTTTCTCCACCAAGGAA GTTTTCCGCTGGTTGAATGATTCTTTCCCCGCCCTCCTCTCGCCCCAGGGACATATAAAGG CAGTTGTTGGCACACCCAGCCAGCAGACGTCCCTCAGCAAGGACAGCAGAGGAC <b>CAGCT</b> <b>A</b> AGAGGGAGAGAAGCAACTACAGACCCCCCTGAAAACAACCCTCAGACGCCACATCCC C	TGGGTT TCTCCA CCAAG GAAG	ATGTGG CGTCTG AGGGTT G
<b>TNF<math>\alpha</math> -2</b>	Chromosome 6 31,544,221 – 31,544,370bp	CAGGGAAAGAGCTGTTGAATGCCTGGAAGGTGAATACACAGATGAATGGAGAGAGAAAA CCAGACACCTCAGGGCTAAGAGCGCAGGCCAGACAGGCAGCCAGC <b>CAGCTG</b> TTCTCCTT TAAGGGTGACTCCCCGATGTTAACCATTCTCCTTCTCCCCAACAGTTCCCCAGGGACCTCT CTCTAATCAGCCCTCTGGCCCAGGCAGTCAGTAAGTGTCTCCAAACCTCTTTCTAATTCT GGGTTTGGGTTTG	AGCTGT TGAATG CCTGGA AGG	GCCAGA GGGCTG ATTAGA GAG
<b>TNF<math>\alpha</math> -3</b>	Chromosome 6 31,543,068 – 31,543,302bp	CAGTCAGTGGCCCAGAAGACCCCCCTCGGAATCGGAGCAGGGAGGATGGGGAGTGTGAG GGGTATCCTTGATGCTTGTGTGTCCCCAACTTTCCAAATCCCCGCCCCCGCGATGGAGAAG AAACCGAGACAGAAGGTGCAGGGCCCACTACCGCTTCCTCCAGATG <b>AGCT</b> CATGGGTTTC TCCACCAAGGAAGGTTTTCCGCTGGTTGAATGATTCTTTCCCCGCCCTCCTCTC	TTGATG CTTGTG TGTCCC CA	AACCAG CGGAAA ACCTTC CT

**Table 6.3 Primer sequences for controls when investigating the IL-1 $\beta$  and TNF $\alpha$  genes.**

Primers were generated using BLAST primer design software. They were designed against areas of the IL-1 $\beta$  and TNF $\alpha$  genes that contain no DNase hypersensitivity sites, are non-coding (as determined by ENCODE data) and contain no topo II $\beta$  putative cleavage sites. Sequence identity will be used to describe the primers used when discussed in the text.

Sequence Identification	Forward Primer	Reverse Primer
IL-1 $\beta$ control	TTACTTGGCACCCCTGTTTGC	ATTACAGGTCAGTGGAGACGC
TNF $\alpha$ control	TGGGATCATTGCCCTGTGAG	GGTGTCTGAAGGAGGGGGTA

(a)

	-5	-4	-3	-2	-1	+1	+2	+3	+4	+5
VM-26	A	Not T	A	A	C	A	G/T	C	A/T	G
m-AMSA	T	G	A	A	T	A	G	C	T	A
native	C	G	A	A	C/T	A	A/G	A/C	T	A

(b)

	-5	-4	-3	-2	-1	+1	+2	+3	+4	+5
VM-26	-	-	A/T	-	C	T	-	-	-	-
dn-EPI	-	-	-	-	A	A	-	-	T	T
native	C	G	A	-	C	-	-	-	-	-

(c)

	-5	-4	-3	-2	-1	+1	+2	+3	+4	+5
pBR322	C	-	G	-	C	A	G	C	T	G
SV40	-	G	A	-	-	A	G	C	-	-

(d)

	-5	-4	-3	-2	-1	+1	+2	+3	+4	+5
Common sequence	C	G	A	A	C	A	G	C	T	A/G

**Figure 6.2 Tables containing published data on putative topoisomerase II cleavage sites.**

(a) Pommier *et al.* (1991) used topoisomerase II extracted from the cell nuclei of the mouse leukemic cell line, L1210, they utilised SV40 DNA to identify putative topo II cleavage sites in the presence of tenoposide (VM-26), m-AMSA and no drug. (b) Cornarotti *et al.* (1996) used recombinant human topo II $\beta$  along with SV40 DNA in the presence of VM-26, doxorubicin derivative, dh-EPI and no drug to identify putative topo II $\beta$  cleavage sites. (c) Marsh *et al.* (1996) used recombinant topo II $\beta$  along with HindIII-ECO-RI fragment, pBR322 and SV40 DNA to identify putative topo II $\beta$  cleavage sites in the presence of m-AMSA. (d) data from (a-c) was collated to determine the most common base pairs found at topo II $\beta$  cleavage sites. (+) and (-) represent the position of the base pair in respect of the topo II cleavage site, (+) being down stream and (-) being up stream of the cleavage site.

## 6.4 Optimisation of sonication step for ChIP

Sonication is the process in which ultrasound causes the production of small gaseous cavities (bubbles) within a sample. Continuous irradiation with ultrasound causes oscillation of the bubble causing their collapse which releases energy that is strong enough to induce shearing of DNA within a biological sample. Continuous sonication would eventually lead to shearing of the DNA into fragments less than 100 bp. However, the size of the fragments required for ChIP need to be between 100-500 bp. Therefore it was necessary to optimise the sonication conditions to ensure that the DNA fragments were within this size range (Figure 6.3). As sonication causes foaming and heating of samples it was performed in cycles of 15 second bursts, with the point of the sonicator held above the bottom of the microfuge tube containing the sample. The sample was also submerged in ice when sonication took place, and between cycles. These steps were employed to reduce protein and DNA degradation caused by excessive heat production.

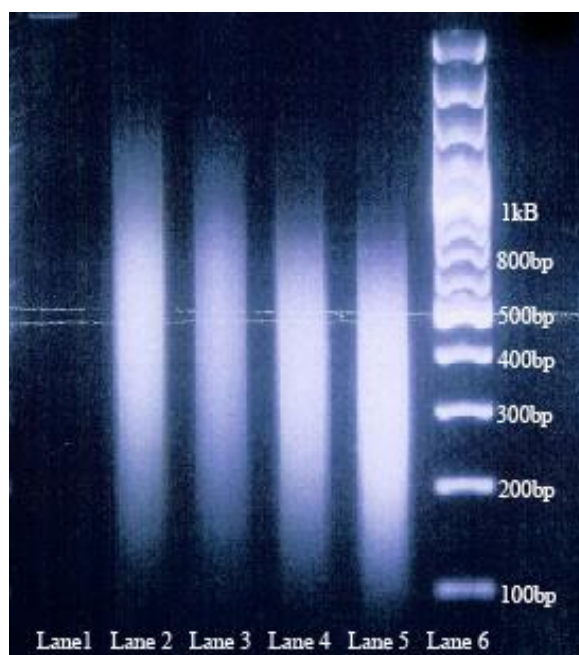


**Figure 6.3 Determining the amount of sonication cycles to generate the correct size of DNA fragments.**

Samples were prepared as described in materials and methods (Section 2.19). After addition of nuclear lysis buffer and protease inhibitors, sonication of the sample was performed. The samples were split into 5 tubes each in order to perform a different amount of sonication samples on each (0, 5, 7, 9 and 11 cycles). Each sonication step was performed at 25% for 15 s on ice. Samples were then loaded on a 2% agarose gel and ran for 2 h at 75 V. Lane 1 contains a sample that has undergone 0 cycles of sonication; Lane 2, 5 cycles of sonication; Lane 3, 7 cycles of sonication; Lane 4, 9 cycles of sonication; Lane 5, 11 cycles of sonication; Lane 6 contains the 1kb ladder.



The smearing in lanes Figure 6.3 show the spread of different sizes of DNA fragments obtained using different numbers of cycles of sonication. The middle and most intense part of the smear shows at what size the majority of the DNA fragment are in the sample is at. In lane 1, there is a clear band at the top of the gel. This sample had not undergone any cycles of sonication, therefore the DNA remained intact as demonstrated by its size and lack of motility down the lane. The sample in lane 2 has undergone 5 cycles of sonication and it appears the majority of the DNA is approximately 300-700bp. Lane 2 and 4 contain samples that have undergone 7 and 9 cycles of sonication respectively. The majority of DNA is between 200-600bp. The sample in lane 5 has undergone 11 cycles of sonication, it appears the majority of DNA is under 500bp, with some being below 100bp in size. It was decided that 7 cycles of sonication would be sufficient in order to generate DNA between 150 and 500bps.

## 6.5 Analysis of ChIP-qPCR data.

The complete ChIP procedure can be found in materials and methods (Section 2.19) Immuno-precipitations from non-LPS/PMA and LPS/PMA treated U937 cells were performed using antibodies to topo II $\beta$  (target), green fluorescent protein (negative control) and Acetylated histone 3 (positive control). Green Fluorescent protein (GFP) was used as the negative control as the mammalian genome does not contain the GFP gene and so therefore cannot synthesise the protein. GFP was originally isolated from the jellyfish *Aequarae victoria* and is often used in molecular biology as a reporter protein. Therefore when using the GFP antibody no protein should be immune-precipitated and thus no DNA should be in these samples. Acetylated histone 3 was used as the positive control as it is widely published commercially advertised to associate with the GAPDH gene (Calcagno *et al.*, 2008; To *et al.*, 2008).

Data from the ChIP-qPCR has to be normalised for sources of variability between samples, including the amount of chromatin. This was carried out using the percent input method. With this method the signals obtained from the ChIP experiment are divided by signals obtained from an input sample. The input sample did not undergo any immune-precipitation and was diluted so that it represented 5% of the chromatin in samples that did undergo immune-precipitation. Analysis of the qPCR data is

represented as percentage of input, the calculation used to determine this is outlined in Figure 6.4.

$$\% \text{ INPUT} = \frac{100}{2^{[\text{SAMPLE Ct} - (\text{INPUT Ct} - \text{Log}_2 \text{ INPUT dilution fold})]}}$$

**Figure 6.4 Calculating percentage of input using qPCR data.**

In log phase qPCR, the amount of DNA doubles with each cycle. This can be represented as  $2^{\text{Ct value}}$ , for example 3 cycles of PCR =  $2 \times 2 \times 2 = 2^3$ . To calculate the ratio of input to sample, the input Ct value can be subtracted from the sample Ct value as  $2^{(\text{Sample Ct} - \text{Input Ct})}$  is the same as  $2^{(\text{Sample Ct})}/2^{(\text{Input Ct})}$ . However before this step, the input ct value needs to be adjusted for dilution. The chromatin contained in the input sample is equal to 5% of the chromatin in the samples that have undergone IP. Therefore the dilution factor is 20 ( $20 \times 5\% = 100\%$ ). As the calculations are based on Ct values, the dilution fold requires to be converted into Ct cycles. This is achieved by using Log2 (as 1 ct = 2 fold difference) of the dilution fold. Dividing the resulting number into 100 gives the quantity of DNA fragments amplified in non-INPUT samples as a percentage of DNA fragments amplified in INPUT samples.

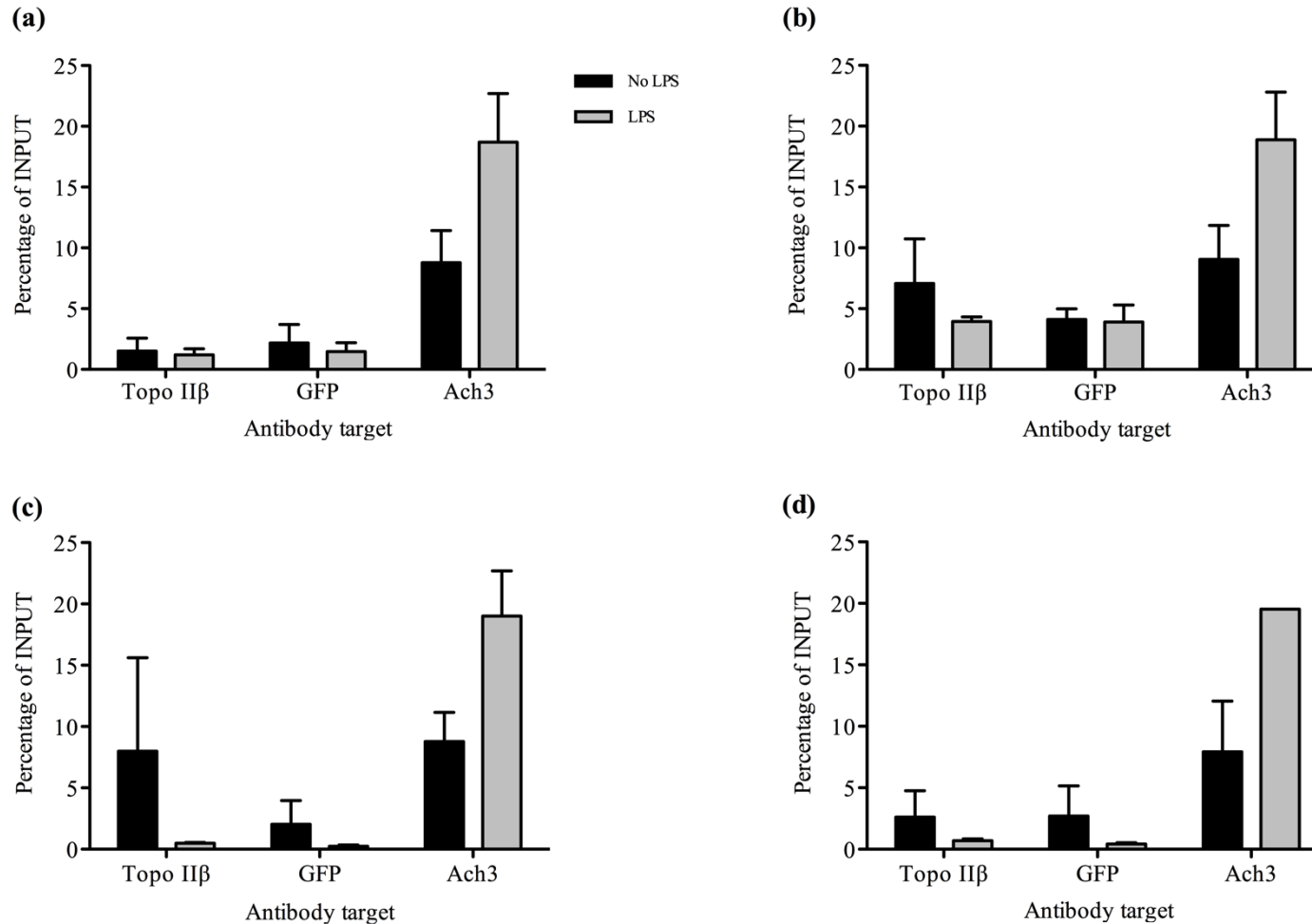


**Figure 6.5 Determining if topo II $\beta$  association increases at sites proximal to the promoter region of the IL-1 $\beta$  gene when cells are PMA treated cells are stimulated with LPS.**

Cells were seeded at a cell density of  $3 \times 10^5$  cells/ml with 5 ng/ml PMA with and without 1 ng/ml LPS and allowed to incubate for 72 h before being harvested. Cells were fixed and ChIP was performed as described in material and methods (Section 2.19). Immuno-precipitations used in the ChIP utilised antibodies to topo II $\beta$  (target), Green fluorescent protein (negative control) and Acetylated histone 3 (positive control). qPCR was then performed using primers documented in Table 6.1, IL-1 $\beta$ -1 (a), IL-1 $\beta$ -2 (b), IL-1 $\beta$  3 (c) and 6.3, IL-1 $\beta$  control (d). A primer generated to GAPDH was used in the qPCR of the positive AcH<sub>3</sub> control. Results are reported as percentage of input (no IP performed on this sample). The means of three independent experiments are shown  $\pm$  standard errors.

## 6.6. Association of topo II $\beta$ at regions of the IL-1 $\beta$ gene

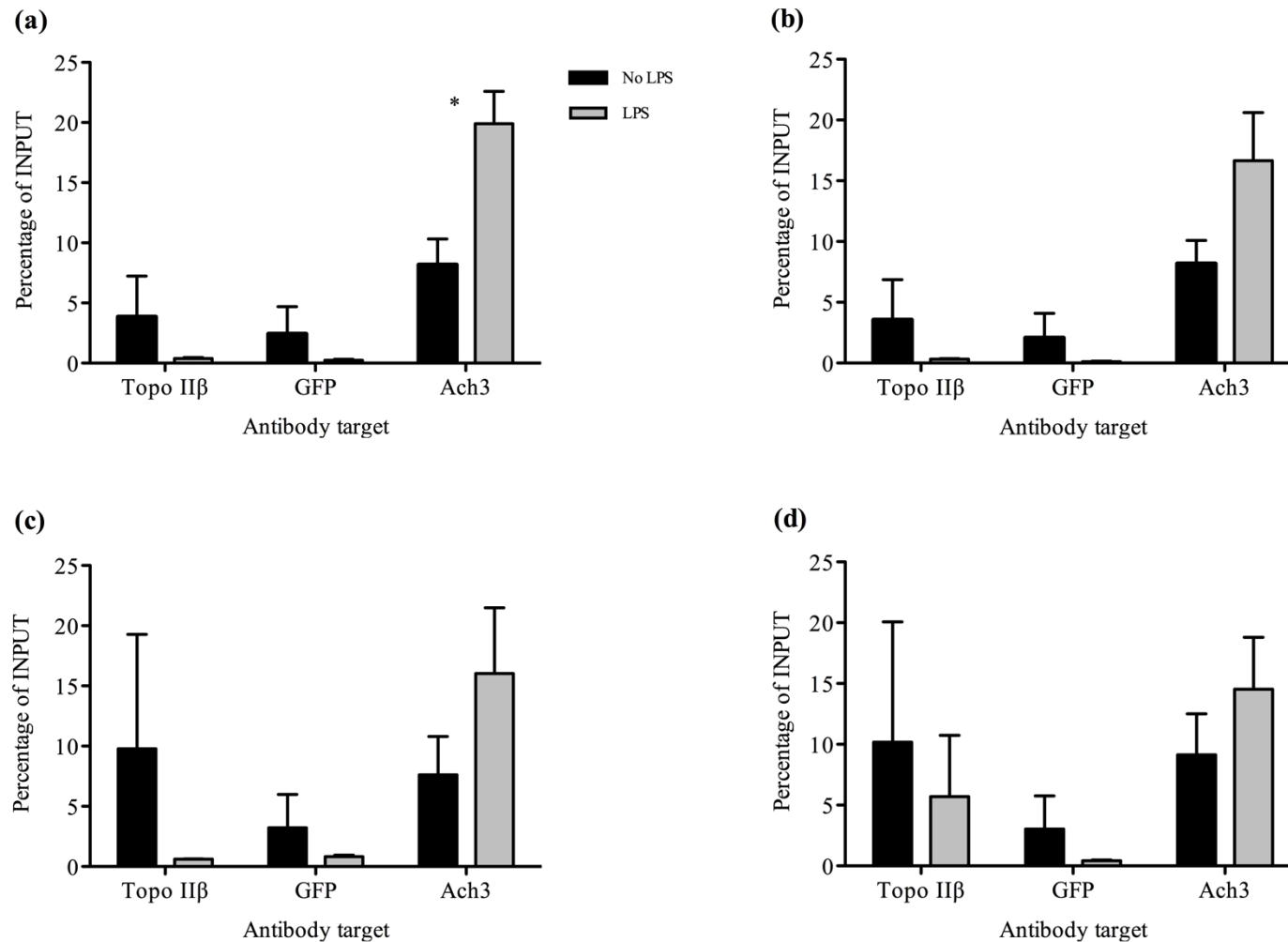
Four primer pairs (Table 6.1 and 6.3) designed to amplify different regions of the IL-1 $\beta$  gene were used in the qPCR reaction following ChIP with non-LPS and LPS treated samples. These primer pairs were used in the qPCR for the GFP sample (that should have no DNA). In addition, primers used to amplify GAPDH were used as a positive control, as AcH<sub>3</sub> is known to associate highly with this gene (Calcagno *et al.*, 2008; To *et al.*, 2008). The results of the qPCR reaction are shown in Figure 6.5.

Figure 6.5a shows the results from the qPCR experiment using the IL-1 $\beta$  -1 primer pair (Table 6.1). There is no significant difference in topo II $\beta$  association between the non-LPS treated samples and the LPS treated samples when using this primer pair. Additionally there is no significant difference between levels of topo II $\beta$  association and levels of GFP association (negative control), thus suggesting there is little or no detectable topo II $\beta$  associating at the region of the IL-1 $\beta$  gene, the IL-1 $\beta$  -1 primers are designed to amplify.

Figure 6.5b shows the results collated from the qPCR experiment using the IL-1 $\beta$  -2 primers (Table 6.1). The non – LPS treated samples appear to have a slightly higher topo II $\beta$  occupancy than the LPS treated samples. Similarly, Figure 6.5c shows the results collated from the qPCR experiment using the IL-1 $\beta$  -3 primers (Table 6.1) again revealing that non – LPS treated cells appear to have a slightly higher topo II $\beta$  occupancy than their LPS treated counterparts. However the results are not significantly different from the respective GFP negative controls or the AcH<sub>3</sub> positive controls (see Appendix C). Thus suggesting there is little topo II $\beta$  associated at the region of the IL-1 $\beta$  gene that the IL-1 $\beta$  -2 and IL-1 $\beta$  -3 primers are designed to amplify.

Results collated in Figure 6.5d show the data collated from the qPCR experiment using the IL-1 $\beta$  – control primers (Table 6.3) There is a small increase in topo II $\beta$  association in non-LPS treated samples compared to LPS treated samples. However the results are not significantly different to the negative control (see Appendix C). This would suggest that topo II $\beta$  does not associate at the region of the IL-1 $\beta$  gene that the IL-1 $\beta$  -control primers are designed to amplify. This result is as expected as these control primers were designed to amplify regions which did not contain a DNase hypersensitivity or a putative topo II $\beta$  binding site and was located downstream of the promoter region

within the gene. This result is in agreement with Tiwari *et al.* (2012) showed that topo II $\beta$  preferentially targets promoter regions of genes rather than exons or introns.



**Figure 6.6 Determining if topo IIβ association increases at sites proximal and within the promoter region of the TNFα gene when PMA treated cells are stimulated with LPS.**

Cells were seeded at a cell density of  $3 \times 10^5$  cells/ml with 5 ng/ml PMA with and without 1ng/ml LPS and allowed to incubate for 72 h before being harvested. Cells were fixed and ChIP was performed as described in material and methods (Section 2.19) Immunoprecipitations used in the ChIP utilised antibodies to topo IIβ (target), Green fluorescent protein (negative control) and Acetylated histone 3 (positive control). qPCR was then performed using primers documented in table 6.1, TNFα-1 (a), TNFα-2 (b), TNFα -3 (c) and 6.3, TNFα control (d). A primer generated to GAPDH was used in the qPCR of the positive Ach3 control. Results are reported as percentage of input (no IP performed on this sample). The means of three independent experiments are shown +/- standard errors.

## 6.7 Association of topo II $\beta$ at regions of the TNF $\alpha$ gene

Four primer pairs (Table 6.2 and 6.3) designed to amplify different regions of the TNF $\alpha$  gene were used in the qPCR reaction following ChIP with non-LPS and LPS treated samples. Again as previously described these primer pairs will also be used in the qPCR for the GFP sample (that should have no DNA). In addition, primers used to amplify GAPDH were used as a positive control, as AcH<sub>3</sub> is known to associate highly with this gene (Calcagno *et al*, 2008; To *et al*, 2008). The results of the qPCR reaction are shown in Figure 6.6.

Figure 6.5a shows the results collated from the qPCR experiment using the TNF $\alpha$ -1 primers (Table 6.2). The non – LPS samples treated appear to have a slightly higher topo II $\beta$  occupancy than the LPS treated samples. Similarly, Figures 6.6b and Figure 6.6c using TNF $\alpha$ -2 and TNF $\alpha$ -3 primers, (Table 6.2) shows that non – LPS samples treated appear to have slightly higher topo II $\beta$  occupancies than the respective LPS treated samples. The results in Figure 6.6 show a slight up-regulation of topo II $\beta$  association at various sites of the TNF $\alpha$  gene in non-LPS stimulated cells compared to LPS stimulated cells. However these results are not significantly different from their respective GFP negative controls and AcH<sub>3</sub> positive controls (see Appendix C). Thus suggesting there is little topo II $\beta$  associated at the region of the TNF $\alpha$  gene that the TNF $\alpha$ -1, TNF $\alpha$ -2 and TNF $\alpha$ -3 primers are designed to amplify.

Interestingly the primer pair that showed the most amount of topo II $\beta$  association was TNF $\alpha$ -control. Using this primer pair, although again not significantly different there was an increase in topo II $\beta$  association in non-LPS and LPS treated samples when compared to their respective negative controls. The primers used to amplify product in this data set (Figure 6.6d) were designed so that their product did not contain any DNase hypersensitivity sites or putative topo II $\beta$  binding sites. They were also designed to amplify a sequence downstream of the promoter region of the TNF $\alpha$  gene. These results are in disagreement with Tiwari *et al.*, (2012) who showed that topo II $\beta$  preferentially binds to promoter regions rather than exon or intronic regions. The increase in topo II $\beta$  association in LPS treated cells at this region compared to the other sites within the TNF $\alpha$  gene may be reflective of a re-localisation of topo II $\beta$  upon LPS stimulation, from a region of high transcriptional activity to that of relatively low transcriptional activity. Zwelling *et al.* (1988) suggest that PMA treatment may cause a re-localisation of topo II $\beta$ , whilst Cowell *et al.* (2011) show that treatment of cells with

the HDAC inhibitor, TSA causes re-localisation of topo II $\beta$  from heterochromatin to euchromatin.

## 6.8 Discussion of results generated by ChIP-qPCR

The innate immune response is the first line of defence against infection; therefore its actions must occur quickly. Both IL-1 $\beta$  and TNF $\alpha$  are synthesised in inactive forms and must be cleaved by the proteases caspase 1 and TNF $\alpha$  converting enzyme (TACE) in order to be secreted. Therefore basal transcription of the IL-1 $\beta$  gene and TNF $\alpha$  must occur in un-stimulated cells (Mauviel *et al.*, 1988; Collart *et al.*, 1990). Topo II has also been shown to associate with promoter regions (Tiwari *et al.*, 2012), thus suggesting that as well as playing an active role in recruitment of transcription factors (Ju *et al.*, 2006) it may also play a role in the maintenance of an open chromatin state. It may be suggested again, that if topo II $\beta$  is acting on the IL-1 $\beta$  and TNF $\alpha$  genes in non-stimulated cells, it may be doing so to maintain an 'open' chromatin structure possibly through interaction with other chromatin modifying proteins, and thus facilitating a rapid transcriptional response. Topo II $\beta$  has previously been shown to play a role in the modification of chromatin architecture; it has been shown to associate with HDAC, a protein involved in chromatin condensation; this association is suggested as mechanism by which topo II $\beta$  represses gene expression (McNamara *et al.*, 2008). In addition topo II $\alpha$  has been shown to prime developmental genes for activation upon differentiation (Thakurela *et al.*, 2013), it is possible that both isoforms are involved in changes in chromatin architecture.

Results from Figure 5.18 and 5.19 suggest that a down-regulation of topo II $\beta$  with 150 nM ICRF-193 has little effect on mRNA expression of IL-1 $\beta$  in response to LPS, however it did significantly decrease the amount of IL-1 $\beta$  protein secreted in response to LPS stimulation. However, it is suggested that treatment with 150 nM ICRF-193 may have caused a transient down-regulation of IL-1 $\beta$  mRNA expression at an earlier unobserved time-point and that the down regulation in protein secretion seen remained as a consequence of this (RNA extractions and removal of supernatant containing IL-1 $\beta$  occurred at the same time). IL-1 $\beta$  transcription occurs rapidly in response to LPS (Suzuki *et al.*, 2000), however a prolonged exposure to LPS has been shown to result in the down-regulation of IL-1 $\beta$  mRNA expression (Schilling *et al.*, 2001). Indeed a 72



hour exposure to LPS may be considered a chronic exposure, therefore a normal down-regulation of IL-1 $\beta$  gene expression may be occurring. If topo II $\beta$  is involved in the activation of IL-1 $\beta$  transcription in response to LPS, then association of topo II $\beta$  with the IL-1 $\beta$  gene would decrease along with a decline in requirement for transcription. In addition the results from Figure 6.5b and Figure 6.5c together suggest that topo II $\beta$  associates with multiple parts of the IL-1 $\beta$  gene, possibly playing different roles at different regions.

Fig 6.6 a-c shows a general trend of reduced topo II $\beta$  occupancy in response to LPS. This is interesting as it may indicate that topo II $\beta$  is acting to repress TNF $\alpha$  transcription in the absence of TNF $\alpha$  and upon addition of LPS this repression is relieved. Previously, an increase in TNF $\alpha$  mRNA expression has been shown to occur in response to LPS previously (Suzuki *et al.*, 2000). Although not significant, results in Figure 5.16 and 5.17 showed an upward trend in TNF $\alpha$  mRNA expression in response to 150 nM ICRF-193 more than that seen in response to PMA and LPS alone. This trend was also seen when cells were exposed to 1 nM ICRF-193 for 6 h prior to differentiation (Figure 5.11). Again, it was suggested that this may be due to release of negative regulation of transcription by topo II $\beta$  inhibition by ICRF-193. However further analysis would be required to verify this.

One caveat to the data presented in this Chapter was the high signal obtained for the GFP control. Although the human genome does contain the GFP gene, and thus no GFP protein, a low signal output is seen in these experiments. This is not unusual and represents background noise from the experiments (Cowell *et al.*, 2012). However, average background signal in some of these experiments represents ~5% of input. This was thought to be as a result of prolonged exposure to primary antibody (see Material and Methods 2.19).

In addition, an up-regulation of AcH<sub>3</sub> association with GAPDH when cells are treated with LPS is also seen all experiments, thus suggesting an up-regulation of GAPDH gene expression. Xie *et al.* (2006) report that LPS induces an up-regulation of GAPDH mRNA expression in rat liver and lungs, and that this up-regulation may be important in the signalling pathway of LPS induced apoptosis. It is also suggested that GAPDH is not a suitable internal control for gene expression assays. Indeed it may be sensible to suggest that the down-regulation in topo II $\beta$  association with regions of the IL-1 $\beta$  and

TNF $\alpha$  genes seen when cells are treated with LPS may be a result of apoptosis induced by chronic LPS exposure.

The results in this chapter most likely reflect the fleeting and transient nature of topo II activity; Ding *et al.* (2013) reported that the catalytic cycle of topo II took 0.84 s to complete. Previous ChIP work investigating topo II $\beta$  associations has utilised the topo II poison, etoposide to form a topo II –DNA complex in place of traditional cross-linking by formaldehyde (Sano *et al.*, 2008; Cowell *et al.*, 2012). Traditional cross-linking with formaldehyde acts by cross-linking all proteins with DNA at that particular moment of when it is added; in contrast etoposide is added to the cell culture for up to an hour, thus increasing the chances of forming topo II-DNA complexes, inevitably yielding better results. Furthermore, this experiment investigated only one time point of LPS stimulation. Previous work has demonstrated that prolonged exposure to LPS results in a down-regulation of TNF $\alpha$  and IL-1 $\beta$  gene expression (Schilling *et al.*, 2001), taken together with previous work that suggests topo II $\beta$  is required at different stages of development (Lyu *et al.*, 2006) future work using ChIP would investigate various time points of LPS stimulation, along with utilisation of topo II poisons.

## Chapter 7

### Conclusions and Future Work

---

#### 7.1 Comparative Quantification of topo II $\alpha$ and topoII $\beta$ in non-PMA and PMA treated cells

The initial aim of this project was to determine if topo II $\beta$  was required for the differentiation of monocytes into macrophages. Indeed previous work has shown that topo II $\beta$  is required for neuronal differentiation (Lyu *et al.*, 2006), it is so important in fact, that topo II $\beta$  knockout embryos are non-viable due to defects in neuronal development (Yang *et al.*, 2000). Studies have also shown that requirement of topo II $\beta$  for neuronal differentiation correlates with an increase in its expression (Tiwari *et al.*, 2012).

Comparative quantification of topo II $\beta$  in non-PMA (monocytes) and PMA treated (macrophage) HL-60 and U937 cells by Western Blot and q-RT-PCR revealed a decrease in topo II $\beta$  mRNA and protein expression when cells were differentiated with PMA (Figure 4.3 & 4.4). In addition this result was also reflected in primary monocytes differentiated with M-CSF compared to non-MCSF treated cells that also displayed a decrease in topo II $\beta$  mRNA expression (Figure 4.10). This result is in disagreement with McNamara *et al.* (2010) who showed an increase in topo II $\beta$  protein expression in PMA treated NIH-3TC cells. However not only was a different cell line used but exposure of cells to PMA was for 2 h in comparison to the 72 h used in the experiments in this project. It may also suggest that levels of topo II $\beta$  change can either increase or decrease in a time-dependent manner during differentiation with PMA.

Additionally comparative quantification of topo II $\alpha$  in non-PMA and PMA treated HL-60 and U937 cells revealed a down regulation of protein and mRNA expression of topo II $\alpha$  when cells were treated with PMA (Figures 4.3, 4.4, 4.12 & 4.13). Indeed this down regulation has been attributed to the effects of cell cycle arrest induced by PMA that has previously been shown to result in a down-regulation topo II $\alpha$  (Woessner *et al.*, 1991). Furthermore a comparison of topo II $\alpha$  and topo II $\beta$  mRNA levels revealed that relative levels of mRNA were similar in non-PMA treated cells, however in PMA treated cells topo II $\beta$  mRNA levels were significantly higher (Figure 4.7). This suggests that topo II $\beta$

is the preferential isoform in PMA treated cells, and may reflect its importance in differentiated cells.

It would be interesting to quantify topo II $\beta$  protein and message expression after varying lengths of exposure to PMA, not only in the aforementioned cell lines but in other PMA responsive cells such as the monocytic cell line THP-1. It may also be sensible to suggest that absolute quantification of topo II $\alpha$  and topo II $\beta$  protein levels by the method described by Padget *et al.* (2000) be employed to determine the most abundant isoform after different exposure times of PMA. Furthermore it would also be useful to determine the phosphorylation state of topo II $\beta$  upon different exposure times of PMA; McNamara *et al.* (2010) postulate that an increase in topo II $\beta$  protein levels upon 2 h of PMA treatment is mediated by an increase in PKC $\delta$  phosphorylation of topo II $\beta$ . Phosphorylation of topo II $\beta$  may be analysed by western blotting using phospho-specific antibodies or by ELISA. It would also be interesting to use a kinase activity assay to determine the kinase responsible for the (possible) phosphorylation of topo II $\beta$  at different times of PMA exposure. Aoyama *et al.* (1998) report that there was no change in the catalytic activity of topo II $\beta$  when HL-60 cells were treated with ATRA, however Plo *et al.* (2002) demonstrate that an overexpression of PKC $\zeta$  results in the phosphorylation of topo II $\beta$  and subsequent decrease in its catalytic activity. Therefore it may be useful to investigate the catalytic activity of topo II $\beta$  at varying exposure times of PMA by use of a de-catenation assay. Additionally research using primary monocytes would be advantageous; however successfully isolating enough CD14<sup>+</sup> cells from PBMC samples, together with the invasive nature of obtaining whole blood samples makes it difficult to complete extensive studies. Such studies would lead to a clearer understanding of the fluctuation of topo II $\beta$  message and protein levels over time in the process of differentiation, as well as its phosphorylation status and catalytic activity.

As the results appear to refute the hypothesis that topo II $\beta$  is required for differentiation with regards to a reduction in the expression of topo II $\beta$  in PMA treated cells compared to non-PMA treated cells; and as subsequent experiments in this thesis use PMA and LPS together to differentiate and stimulate cells, it would also be useful to examine the effect of treatment with PMA and LPS on topo II $\beta$  mRNA, protein and phosphorylation levels in addition to its catalytic activity. Stimulation of cells with LPS also leads to the up-regulation of expression of many genes encoding for proteins involved in the inflammatory response, for example cytokines such as TNF $\alpha$  and IL-1 $\beta$  (Suzuki *et al.*,

2000). Therefore it would be interesting to determine whether topo II $\beta$  is involved in the up-regulation of transcription of such genes in response to LPS stimuli alone. It may also be interesting to use other biologically relevant molecules to stimulate cytokine expression, for example TNF $\alpha$  or a combination of IFN $\gamma$  and LPS. This would then establish if topo II $\beta$  acts to mediate the transcription of factors involved in various pathways of signalling in response to different stimuli (Lin *et al.*, 1995; Paulnock *et al.*, 2000).

## **7.2 The effect of PMA treatment on the cytotoxicity of the topo II poison, VP-16 and the inhibitor, ICRF-193.**

The decrease in topo II $\alpha$  and  $\beta$  protein expression in PMA treated cells compared to non-PMA treated cells lead to the investigation of the effect this had on the cytotoxicity of the topo II poison, VP-16 and the topo II inhibitor, ICRF-193. The XTT assay, an assay that measures cell viability was used to measure the proportion of cells that remained viable after treatment with the drugs, thus measuring the cytotoxic effects of these drugs. The results showed that cells treated with PMA prior to drug exposure were protected from the cytotoxic actions of VP-16 and ICRF-193 (Figure 4.14, 4.15, 4.17 & 4.18). The mechanism by which they are protected from the cytotoxic effects of these drugs is thought to be multi-variable. But the first main factor is the decrease in the amount of topo II $\alpha$  and  $\beta$  protein in the cells. Down-regulation of the expression of topo II has been shown to render cells less sensitive to drugs which stabilise the topo II cleavable complexes. In some cell lines selected for resistance to anti topo II drugs, the levels of topo II $\alpha$  have been shown to be reduced (Webb *et al.*, 1991 & Eijdens *et al.*, 1992). In addition, levels of topo II $\beta$  rather than topo II $\alpha$  have been found to serve as a marker for drug resistance in some cell lines (Brown *et al.*, 1995 & Dereuddre *et al.*, 1997). Consequently, alterations in the relative amounts of the two isoforms could result in or contribute to resistance. The result corroborates the previous finding that both topo II $\alpha$  and  $\beta$  protein are decreased following 72 h exposure to PMA (Figure 4.12 & 4.13), thus decreasing the amount of target for the drugs to exert their effects. VP-16 and ICRF-193 preferentially target topoII $\alpha$  and  $\beta$ , respectively and as both isoform are reduced in PMA treated cells then protection against both of these drugs would be expected and was indeed shown to be the case.

In addition it is proposed that the cell cycle block induced by PMA may decrease the amount of DNA damage caused by the drugs, via the collateral damage model. Previous studies have shown that VP-16 requires processing of cleavable complexes by the replication or transcription machinery to expose the induced double strand breaks (Li & Lui., 2001; Guo *et al.*, 2007). ICRF-193 in comparison requires progression through mitosis to induce DNA damage via accumulation of multiploid cells due to inhibition of chromosome segregation. It is also proposed by Zwelling *et al.* (1988) that PMA induced VP-16 resistance may be due to PMA induced re-localisation of topo II in the nucleus to areas less susceptible to topo II interaction or to areas not associated with DNA. They could also not rule out the possibility of chromatin compaction preventing the formation of drug-stabilised cleavable complexes in the cells.

It would be interesting to investigate whether treatment with PMA causes a sub-cellular redistribution of topo II $\beta$  by employing immunofluorescence microscopy to compare the sub-cellular localisation of topo II $\beta$  in non-PMA and PMA treated cells. Future work may also involve the measurement of cleavable complexes using the TARDIS (trapped in agarose DNA immune-staining) assay, as described by Willmore *et al.* (1998). Indeed if PMA is protecting the cell by causing a cell block and thus reducing cleavable complex processing then the amount of cleavable complexes observed should remain the same. It would also be interesting to compare the amount of double strand breaks generated in the presence of VP-16 in non-PMA and PMA treated cells. This could involve measuring a marker for dsbs,  $\gamma$ H2AX using flow cytometry (Muslimovi *et al.*, 2008).

As topo II $\beta$  message is present in a higher amount in macrophage-like cells, then topo II $\beta$  may represent a better target for inhibiting activated synovial macrophages in Rheumatoid arthritis for example, whose secreted soluble products lead to joint destruction. At present mitoxantrone is used to ameliorate the inflammatory response in RA patients, this topo poison targets  $\alpha$  and  $\beta$  equally. Thus it is important to quantify relative levels of  $\alpha$  and  $\beta$  in macrophages and to test whether they are more sensitive to beta inhibitors both in respect to their survival and to their secretion of pro-inflammatory products such as iNOS and TNF $\alpha$ . This type of study is an important step in understanding the molecular pharmacology of topo II poisons and inhibitors in macrophages.

### **7.3 The effects of 1 nM ICRF-193 pre-treatment on mRNA expression of proteins involved in differentiation and stimulation.**

As stated previously, the aim of this project was to determine if topo II $\beta$  was required for differentiation of monocytes into macrophages. As treatment of cells with 1 nM ICRF-193 for 6 h resulted in degradation of topo II $\beta$ , cells were exposed to ICRF for 6 h prior to the addition of PMA and LPS. The effect of down-regulation of topo II $\beta$  on the expression of genes involved in differentiation and stimulation was then investigated. Results revealed no significant change in the levels of mRNA for all genes studied including POR2A (5.6), SP1 (5.7), EGR2 (5.8), NF- $\kappa$ B (5.9), TLR2 (5.10), TLR4 (5.10) and TNF $\alpha$  (5.11). However a general trend emerged whereby levels of SP1, EGF2, NF- $\kappa$ B, TLR2, TLR4 and TNF $\alpha$  mRNA were increased. The upwards trend in TNF $\alpha$  mRNA level was also mirrored by a slight up-regulation of whole cell TNF $\alpha$  protein. It could be hypothesised that in the monocyte-like state, topo II $\beta$  may regulate the transcription of these genes in a negative manner. It could be postulated that topo II $\beta$  may form a complex with other proteins associated with gene repression, for example HDACs to compact the area of chromatin containing these genes and thus preventing transcription. Inhibition of topo II $\beta$  may then lead to disassociation of the complex, resulting in the relaxation of the chromatin and increased access to these genes by transcription machinery and thus an increase in the levels of mRNA & protein. However, other studies on certain other genes (SP1 and NF- $\kappa$ B) suggest that their upregulation may be due to a DNA damage response induced by ICRF-193 treatment. For example Huang *et al.* (2001) have detected dsbs induced by treatment of cells with ICRF-193. In turn activation of NF- $\kappa$ B has been shown to occur in response to induction of dsbs as part of a pro-survival response. In addition to repeating these experiments again in order to determine if significance can indeed be reached, the  $\gamma$ H2AX assay could be used to quantify DNA damage at the time points and doses of ICRF-193 used.

As expected when ICRF-193 exposure was extended to 72 hours when levels of topo II $\beta$  had recovered (Figure 5.1), no upward trend in the levels of EGR2 (5.8), NF- $\kappa$ B (5.9), TLR2 (5.10), TLR4 (5.10) and TNF $\alpha$  (5.11) mRNA was noted. However, levels of POLR2A and SP1 were increased although not significantly, Figure 5.6 and 5.7, respectively. It is proposed that this is a result of the DNA damage response as both genes may be required to facilitate the repair of DNA double strand breaks.

Interestingly though, unlike the increase in the levels of TNF $\alpha$  protein seen after a 6 hour exposure, after a 48 and 72 hour exposure of ICRF-193, TNF $\alpha$  secretion was significantly decreased compared to controls (5.13). It is postulated that this may be due to an accumulation of DNA damage leading to apoptosis of cells, thus decreasing the amount of cells able to secrete TNF $\alpha$ .

As these results did not support the original hypothesis that topo II $\beta$  is required for macrophage differentiation, it may be interesting to use DNA microarray technology and exome sequencing to determine if ICRF-193 induced down-regulation of topo II $\beta$  changes the gene expression, particularly the expression of protein encoding genes in cells that are undergoing differentiation with PMA, compared with non ICRF-193 treated cells under the same conditions.

#### **7.4 The effects of co-treatment with ICRF-193, PMA and LPS on mRNA expression and protein secretion of the pro-inflammatory cytokines TNF $\alpha$ and IL-1 $\beta$ .**

An investigation into the effects of co-treatment with ICRF-193, PMA and LPS for 72 h on TNF $\alpha$  and IL-1 $\beta$  gene expression and protein secretion utilised two different concentrations of ICRF-193, 1 nM and 150 nM.

No significant change in the levels of TNF $\alpha$  or IL-1 $\beta$  mRNA was seen in samples co-treated with either 1 nM or 150 nM ICRF-193, PMA and LPS for 72 hours. At 1nM ICRF-193 a slight increase in the levels of TNF $\alpha$  and IL-1 $\beta$  was observed although this did not reach significance. This slight increase was also noted for TNF $\beta$  at a dose of 150 nM ICRF-193.

It is postulated that co-treatment has little effect of the transcription of these genes as the response to PMA and LPS is mediated more quickly than inhibition of topo II $\beta$  by the drug. Indeed the slight increase in TNF $\alpha$  at both 6 and 72 hour exposure and IL-1 $\beta$  at 6 hr may be as a result of activation of an immune response and the subsequent secretion of these cytokines in response (Sauter *et al.*, 2011).

Unexpectedly though a significant decrease in the levels of secreted IL-1 $\beta$  was seen after 72 hours ( $p = 0.03$ ) (Figure 5.19). As levels of IL-1 $\beta$  are not altered after a 72 hours exposure, this suggests that topo II $\beta$  is not involved in the regulation of IL-1 $\beta$



gene expression but may be involved in the regulation of gene expression of proteins involved in the IL-1 $\beta$  pathway of secretion.

Taken together the co-treatment results do not support the hypothesis that topo II $\beta$  plays a role in the transcription of TNF $\alpha$  or IL-1 $\beta$ . However the results point to a complex control of secretion of these cytokines and this does not rule out the possibility that topo II $\beta$  may be involved in the regulation of gene expression of other proteins involved in the TNF $\alpha$  and IL-1 $\beta$  pathways of secretion, for example in the regulation of TNF $\alpha$  converting enzyme expression.

As many of the results in Chapter 5 follow a trend in which mRNA and protein secretion is up-regulated, although often not significantly following ICRF-193 treatment, it is suggested that ICRF-193 possibly activates the inflammasome and thus stimulates an immune response, additionally, as described previously the DNA damaging effects induced by ICRF-193 may lead to an up-regulation of NF- $\kappa$ B activation and therefore may also effect the production of pro-inflammatory cytokines. Furthermore, it is possible that ICRF-193 may bind to cell surface receptors for example, TNF-R1, thus preventing activation of neighbouring cells or modulation of positive feedback loops. Taken together these possibilities suggest that the effects of ICRF-193 are far more extensive than previously reported, and that using ICRF-193 to measure the effects of topo II $\beta$  down-regulation on cytokine production may not be the most reliable method. Indeed a previous study has suggested that ICRF-193 itself can induce differentiation, however this study used different characteristics to measure differentiation, for example the NBT assay. They did however report that ICRF-193 led to an increase in the binding activity of the differentiation associated transcription factor, AP-1, however they did fail to report on the morphology of the cells following treatment with ICRF-193 (Perez *et al.*, 1997), nevertheless this study supports the data shown in this thesis, suggesting inhibition of topo II $\beta$  not only affects the expression of transcription factors involved in differentiation but also increases their binding activity.

These results partially support the original hypothesis that topo II $\beta$  is required for differentiation of monocytes to macrophages. The results suggest that topo II $\beta$  is required for the actual function of macrophages in the immune response, in particular in the regulation of genes that encode pro-inflammatory cytokines,.

In order to strengthen this data it may also be useful to use DNA microarray technology and exome sequencing as described previously (Chapter 7.3) to determine if ICRF-193 induced down-regulation of topo II $\beta$  changes the gene expression of LPS induced genes, compared with non ICRF-193 treated cells under the same conditions.

### **7.5 The effect of topo II $\beta$ directed siRNA knockdown on the protein secretion of the pro-inflammatory cytokines, TNF $\alpha$ and IL-1 $\beta$**

In light of previous results and the disadvantages of utilising a topo II $\beta$  inhibitor, an investigation into the effect on TNF $\alpha$  and IL-1 $\beta$  secretion was performed when topo II $\beta$  protein expression was knocked down by transfection of cells with topo II $\beta$  directed siRNA oligonucleotides. The results from this showed in two out of three experiments performed, topo II $\beta$  protein expression had returned after treatment with PMA and LPS (Figure 5.22). However one experiment showed that topo II $\beta$  protein expression remained decreased after PMA and LPS treatment. Correlation of topo II $\beta$  protein expression with TNF $\alpha$  and IL-1 $\beta$  secretion revealed a positive correlation; when topo II $\beta$  protein was decreased, TNF $\alpha$  and IL-1 $\beta$  secretion was reduced (Figure 5.25). The TNF $\alpha$  results are in contrast to previous work utilising ICRF-193 as a topo II $\beta$  inhibitor that showed that inhibition of topo II $\beta$  lead to an increase in TNF $\alpha$  secretion (Figure 5.17), although this result did not reach significance. The IL-1 $\beta$  results however, are in agreement with previous work using ICRF-193 that also showed a decrease in IL-1 $\beta$  secretion (Figure 5.19). The results do suggest that topo II $\beta$  is involved in the gene expression of proteins involved in both the TNF $\alpha$  and IL-1 $\beta$  pathways of secretion. Further work would utilise qRT-PCR to determine the effect of siRNA-mediated topo II $\beta$  knockdown on the expression of TNF $\alpha$  and IL-1 $\beta$ . In addition the effect of siRNA treatment on PMA pre-treated cells would be investigated to determine if topo II $\beta$  knockdown is possible at this time, from this further work measuring cytokine mRNA and protein expression would be investigated.

One caveat in measuring the cytokine response to LPS and topo II $\beta$  inhibition in chapter 5 was that only secreted protein was measured from IL-1 $\beta$ . This requires the cleavage action of proteases in order to be secreted into the extracellular environment. It is suggested that further work would utilise western blotting to quantify IL-1 $\beta$  cellular protein levels and these results be combined with secreted protein levels to give a more

robust overview of IL-1 $\beta$  whole protein levels. Levels of TNF $\alpha$  in co-treatment experiments would also be investigated further.

For future work it may be useful to dissect the pathways involved in the secretion of TNF $\alpha$  and IL-1 $\beta$ , and thus thoroughly investigate the role of topo II $\beta$  in the gene expression of the proteins involved in the pathways of secretion. Investigations would include measurement of mRNA levels and protein levels in the presence and absence of topo II $\beta$ . Also thorough investigations of topo II $\beta$  upon stimulation of cells with LPS with regards to cellular localisation, activity and post-translational modifications may also be insightful. Additionally cleavage assays could be utilised to investigate whether topo II $\beta$  can bind and cleave at specific sequences of these genes.

This result again partially supports the original hypothesis that topo II $\beta$  is required for differentiation of monocytes to macrophages. The results support the work performed using ICRF-193 that shows that topo II $\beta$  may be required for regulation of functional aspects of macrophages during the immune response, for example, in the regulation of gene expression of pro-inflammatory cytokines or other proteins involved in the secretion of pro-inflammatory cytokines.

#### **7.6 Topo II $\beta$ association at discrete locations proximal to the TNF $\alpha$ and IL-1 $\beta$ promoters in non-LPS and LPS stimulated PMA treated U937 cells.**

The suggestion that topo II $\beta$  positively regulated the secretion of both TNF $\alpha$  and IL-1 $\beta$  lead to the utilisation of ChIP - qPCR to investigate the association of topo II $\beta$  at regions of interest proximal to the TNF $\alpha$  and IL-1 $\beta$  promoters in non-LPS and LPS treated cells. Results showed that there was little association of topo II $\beta$  at all regions examined on the TNF $\alpha$  and IL-1 $\beta$  gene both in non-LPS and LPS treated cells. There was a slight increase in association in non-LPS treated cells compared to LPS treated cells on the TNF $\alpha$  and IL-1 $\beta$  gene (Figure 6.5 & 6.6), however these results did not reach significance (Appendix C). This result neither supports nor refutes the original hypothesis. The trend seen is however worthy of further investigation as it suggests that topo II $\beta$  may be involved in either the priming of the gene, ready for response to a stimuli or in the normal repression of gene transcription when there is no stimuli.

One of the caveats with regards to sample preparation for the ChIP-qPCR is that cross-linking of DNA with proteins is performed at one moment in time. The catalytic cycle of topo II $\beta$  has been shown to be only 0.84 s (Ding *et al.*, 2013), therefore the chances

of crosslinking multiple topo II $\beta$  homodimers at their sites of action at one given time is poor. Future work would utilise the topo II poison VP-16 (Cowell *et al.*, 2011) in order to generate cleavable complexes thus capturing topo II $\beta$  at its site of action for longer than the length of its catalytic cycle. This would then increase the chances of seeing any association of topo II $\beta$  at the regions of interest. Another problem encountered during this experiment was the level of negative control (GFP – DNA association) being too high, possibly due to non-specific binding of the GFP antibody to proteins in the sample. Therefore no firm conclusions can be made from the data, as results obtained for topo II $\beta$  association may also be due to non-specific binding of that antibody also. If this experiment were to be repeated then an optimisation of antibody treatment would be carried out prior to processing of samples.

Another limitation of this experiment is that only 4 discrete regions of the TNF $\alpha$  and IL-1 $\beta$  were investigated, thus this does not provide a full picture of topo II $\beta$  association at these genes. It may therefore be interesting to use ChIP-seq, a method by which all regions of DNA that the protein of interest is associated with is sequenced, to look at the global differences in topo II $\beta$  association when PMA treated cells are stimulated with LPS compared to no-LPS.

Future work may also consider investigating the association of topo II $\alpha$  at regions of interest within the TNF $\alpha$  and IL-1 $\beta$  genes. A previous study has shown that topo II $\alpha$  is required for the priming of developmental genes in anticipation of response to stimuli. It is possible that topo II $\alpha$  and topo II $\beta$  may work in concert to facilitate the transcription of genes that are transcribed in response to stimuli.

### **7.7 The effect of an absence of topo II $\beta$ on LPS induced IL-6 expression in mouse embryonic fibroblasts**

It may be argued that when investigating the role of topo II $\beta$  in the expression of genes related to differentiation or stimulation, it is not ideal to treat cells with foreign material, for example, with ICRF-193 or siRNA, as this may cause the cell to elicit an immune response. Indeed the work in Chapter 5 with regards to NF- $\kappa$ B expression and IL-1 $\beta$  secretion, ICRF-193 may induce both a DNA damage response and an immune response. Further work in Chapter 5 utilises a mouse embryonic fibroblasts cell line that has a stable topo II $\beta$  knockout (Errington *et al.*, 1999) to investigate the secretion of IL-

6 in response to varying concentrations of LPS. The results demonstrated that compared to the wild-type cells, the topo II $\beta$  knockout cells secreted significantly less IL-6 ( $p < 0.001$ ) (Figure 5.20). Thus suggesting that topo II $\beta$  is involved in the secretion of IL-6. However the results also show that this decrease is time dependent, with the significant decrease only being seen after 48 h of LPS stimulation, and not after 72 h. These results are in support of previous work that shows that topo II $\beta$  is required in the earlier stages of response to stimuli such as PMA (McNamara *et al.*, 2010). Further work would utilise qRT-PCR to measure the mRNA levels of IL-6 after different exposure times to LPS to determine if topo II $\beta$  depletion actually effected the transcription of IL-6.

This result partially supports the original hypothesis that topo II $\beta$  is required for differentiation of monocyte to macrophage. The result actually is heavily in support of previous work in this thesis that suggests that topo II $\beta$  is required for the regulation of pro-inflammatory cytokine secretion, thus it appears that topo II $\beta$  is required for functional regulation of cells that secrete pro-inflammatory cytokines in the immune response.

One limitation with regards to the experiments in Chapters 5 and 6 is that measurements were taken after 72 h of LPS treatment. Indeed this is considered a chronic exposure to LPS. It may be sensible to suggest that future work also considers investigating multiple different exposure times to LPS, for example taking samples after 30 s, 1 min, 5 min and 30 min of exposure, all of which are considered acute exposures.

In addition, reintroducing topo II $\beta$  to the knockout cells and investigating whether this re-instates the secreted levels of IL-6 to those seen in the the wild-type cells is necessary to confirm the involvement of topo II $\beta$ . Further *in vitro* studies could then be carried out to identify whether topo II $\beta$  binds to this gene (ChIP and cleavage assays) and whether its presence can modulate the levels of transcription in an *in vitro* system.

It may be sensible to suggest that due to the possibility of ICRF-193 or siRNA eliciting an immune or DNA damage response in cells, that utilisation of the MEF topo II $\beta$  knockdown cell line may be a more reliable source to continue the investigation into the role of topo II $\beta$  in cytokine expression. In particular the future investigation of proteins and the genes that encode them that are involved in the immune or DNA damage response, for example SP1 and NF- $\kappa$ B. However this model has its limitations, preferably a stable topo II $\beta$  knockdown monocyte or macrophage cell line would be

used. This could be achieved using stable short hairpin RNA (shRNA) that, due to its longevity with regards to stability would possibly mean that an acute immune response to transfection could be ruled out. A relatively new system, termed CRISPRi may also be used to silence the topo II $\beta$  gene, a highlight of this system is that it has minimal off target effects (Gilbert *et al.*, 2013), ideal when examining factors related to the immune response. If possible, however, generation of a stable topo II $\beta$  knockout monocyte cell line would enable a more reliable source of investigation into the role of topo II $\beta$  in macrophage differentiation. It would also be interesting to investigate the role of topo II $\beta$  in the differentiation of cells into granulocytes and dendritic cells.

Taken together the results in this thesis suggest that the catalytic activity of Topo II $\beta$  is necessary for secretion of normal levels of the cytokines, TNF $\alpha$ , IL-1 $\beta$  and IL-6 in response to LPS at certain time points.

## **7.8 Conclusion.**

In conclusion, the work presented in this thesis demonstrates that topoisomerase II $\beta$  may be involved in the regulation of gene expression of proteins involved in the TNF $\alpha$  and IL-1 $\beta$  pathways of secretion. The results appear to vary depending on the technique used to down-regulate topo II $\beta$ . Additionally, results obtained when using the topo II $\beta$  inhibitor, ICRF-193, vary depending on when the cells were treated with the drug. For example when cells were treated with ICRF-193 prior to differentiation and stimulation, levels of TNF $\alpha$  mRNA and cellular protein are increased, however levels of secreted TNF $\alpha$  are decreased. In contrast when cells are co-treated with ICRF-193, PMA and LPS, TNF $\alpha$  is increased at both the mRNA and secretory protein levels. However when using siRNA to down-regulate topo II $\beta$  expression prior to differentiation and stimulation, TNF $\alpha$  secretion is seen to be decreased. Due to the caveats involved when using ICRF-193, in particular the DNA damaging effects, it would be sensible to suggest that the results when using the siRNA are more reliable and therefore suggest that topo II $\beta$  is involved in the activation of TNF $\alpha$  gene transcription. Furthermore levels of IL-1 $\beta$  secretion are decreased when cells are co-treated with ICRF-193, PMA and LPS, and when topo II $\beta$  is down-regulated by siRNAs, however unlike TNF $\alpha$ , no difference in IL-1 $\beta$  mRNA expression is seen in co-treated cells, suggesting that topo II $\beta$  is possibly involved in the transcription of another protein involved in the IL-1 $\beta$  secretory pathway.

Chronic Inflammatory diseases such as Rheumatoid Arthritis are the result of a dysregulation of the immune response, resulting in a chronic up-regulation of pro-inflammatory cytokines, for example  $\text{TNF}\alpha$  (Moelants *et al.*, 2013). Therefore elucidating the exact mechanism, by which these cytokines are expressed including factors that regulate their transcription will aid in the generation of new therapies to treat chronic inflammatory disorders. Previous studies have shown that treatment of cells with sub-lethal doses of etoposide, targeting topo II leads to the down-regulation of  $\text{TNF}\alpha$  and IL-6 secretion (Verdrengh *et al.*, 2003). However the mechanism by which this is occurring has not been fully investigated. Further to this long term treatment with etoposide may result in the patient experiencing a whole host of unwanted side effects. Therefore it is equally as important to determine if down-regulation or inhibition of topo II $\beta$  with ICRF-193 leads to an increase in pro-inflammatory cytokine production and thus increased inflammation.

Elucidating the exact involvement of topo II $\beta$  in the pathways of secretion may aid in the development of new treatments for chronic inflammatory diseases, possibly with the intention of directly targeting topo II $\beta$  in activated macrophages to inhibit the transcription of genes involved in  $\text{TNF}\alpha$  and IL-1 $\beta$  secretion. For instance, low levels or pulses of non-toxic quantities of topo II $\beta$  targeting agents could be delivered to infiltrating macrophages in the joints of individual sufferers via nanocarriers, for example sterically stabilised micelles (Koo *et al.*, 2011). Subsequent phagocytosis of the drug loaded particles by the macrophages would ensure this specific cell population was targeted. Once within the macrophage it is hypothesised that inhibition of the action of topo II $\beta$  would reduce transcriptional activity and thus reduce pro-inflammatory activity, thereby ameliorating the inflammatory response.

Future studies will be necessary to examine this possibility but are important as they lay the foundation for the development of novel treatments based on modulating macrophage function that could in the future be translated into a clinical scenario.

## References

---

- Adachi, Y., Luke, M. and Laemmli, U.K. (1991). Chromosome assembly *in vitro*: topoisomerase II is required for condensation. *Cell*. **64**, 137-148
- Adachi, N., Miyaike, M., Kato, S., Kanamaru, R., Koyama, H. and Kikuchi, A. (1997). Cellular distribution of mammalian DNA topoisomerase II is determined by its catalytically dispensable C-terminal domain. *Nucleic Acids Research*. **25**, 3135-3142
- Agostini, L., Martinon, F., Burns, K., McDermott, M.F., Hawkins, P.N. and Tschopp, J. (2004). NALP3 forms an IL-1 $\beta$ -processing inflammasome with increased activity in Muckle-Wells autoinflammatory disorder. *Immunity*. **20**, 319-325
- Ahn, G., Tseng, D., Liao, C., Dorie, M.J., Czechowicz, A. and Brown, J.M. (2010). Inhibition of Mac-1 (CD11b/CD18) enhances tumor response to radiation by reducing myeloid cell recruitment. *PNAS*. **107**, 8363-8368
- Akimitsu, N., Adachi, N., Hirai, H., Hossain, M.S., Hamamoto, H., Kobayashi, M., Aratani, Y., Koyama, H. and Sekimizu, K. (2003). Enforced cytokinesis without complete nuclear division in embryonic cells depleting the activity of DNA topoisomerase II $\alpha$ . *Genes Cells*. **8**, 393-402
- Allenbach, C., Launois, P., Mueller, C. and Tacchini-Cottier, F. (2008). An essential role for transmembrane TNF in the resolution of the inflammatory lesion induced by *Leishmania major* infection. *Eur J Immunol*. **38**, 720-731
- Alper, S., McBride, S.J., Lackford, B., Freedman, J.H. and Schwartz, D.A. (2007). Specificity and Complexity of the *Caenorhabditis elegans* Innate Immune Response. *Molecular and Cellular Biology*. **27**, 5544-5553
- Andreassen, P.R., Ho, G.P., D'Andrea, A.D. (2006). DNA damage responses and their many interactions with the replication fork. *Carcinogenesis*. **27**, 883-892
- Anrather, J., Csizmadia, V., Soares, M.P. and Winkler, H. (1999). Regulation of NF- $\kappa$ B RelA Phosphorylation and Transcriptional Activity by p21ras and Protein Kinase C $\zeta$  in Primary Endothelial Cells. *J Biol Chem*. **274**, 13594-13603
- Aoyama, M., Grabowski, D.R., Isaacs, R.J., Krivacic, K.A. and Rybicki, L.A. (1998). Altered expression and activity of topoisomerases during all-trans retinoic acid-induced differentiation of HL-60 cells. *Blood*. **92**, 2863-2870



- Aravind, L., Leipe, D.D. and Koonin, E.V. (1998) Toprim—a conserved catalytic domain in type IA and II topoisomerases, DnaG-type primases, OLD family nucleases RecR proteins. *Nucleic Acids Res.* **26**, 4205-13
- Austin, C.A., Sng, J.H., Patel, S. and Fisher, L.M. (1993). Novel HeLa topoisomerase II is the II $\beta$  isoform: complete coding sequence and homology with other type II topoisomerases. *Biochim Biophys Acta.* **1172**, 282-291
- Austin, C.A. and Marsh, K.L. (1998). Eukaryotic DNA Topoisomerase II $\beta$ . *Bioessays.* **20**, 215-226
- Auffray, C., Sieweke, M.H. and Geissmann, F. (2009). Blood Monocytes: Development, Heterogeneity, and Relationship with Dendritic Cells. *Annu Rev Immunol.* **27**, 669-692
- Baek, Y.S., Haas, S., Hackstein, H., Bein, G., Hernandez-Santana, M., Lehrach, H., Sauer, S. and Seitz, H. (2009). Identification of novel transcriptional regulators involved in macrophage differentiation and activation of U937 cells. *BMC Immunol.* **10**, 18
- Bailly, S., Fay, M., Israel, N. and Gougerot-Pocidalo, M.A. (1996). The transcription factor AP-1 binds to the human interleukin-1 $\alpha$  promoter. *Eur Cytokine Netw.* **7**, 125-128
- Bandelet, O.J. and Osheroff, N. (2008). The efficacy of topoisomerase II-targeted anticancer agents reflects the persistence of drug-induced cleavage complexes in cells. *Biochemistry.* **47**, 11900-11908
- Barboule, N., Lafon, C., Chadebecq, P., Vidal, S. and Valette, A. (1999). Involvement of p21 in the PKC-induced regulation of the G2/M cell cycle transition. *FEBS Lett.* **444**, 32-37
- Barbour, L., Xiao, W. (2003). Regulation of alternative replication bypass pathways at stalled replication forks and its effects on genome stability: a yeast model. *Mutat Res.* **27**, 137-155
- Barde, Y. and Schubeler, D. (2012). Target genes of topoisomerase II $\beta$  regulate neuronal survival and are defined by their chromatin state. *PNAS.* **109**, E934-E943.
- Barry, M.A., Reynolds, J.E. and Eastman, A. (1993). Etoposide-induced Apoptosis in Human HL-60 Cells Is Associated with Intracellular Acidification. *Cancer Research.* **53**, 2349-2357
- Barthel, R., Tsytsykova, A.V., Barczak, A.K., Tsai, E.Y., Dascher, C. C., Brenner, M.B. and Goldfeld, A.E. (2003) Regulation of tumor necrosis factor  $\alpha$  gene expression by mycobacteria

involves the assembly of a unique enhanceosome dependent on the coactivator proteins CBP/p300. *Mol Cell Biol.* **23**, 526-533

Basoni, C., Nobles, M., Grimshaw, A., Desgranges, C., Davies, D., Perretti, M., Kramer, I.M. and Genot E. (2005). Inhibitory control of TGF-  $\beta$ 1 on the activation of Rap1, CD11b, and transendothelial migration of leukocytes. *FASEB J.* **19**, 822-824

Baus, F., Gire, V., Fisher, D., Piette, J. and Dulic, V. (2003). Permanent cell cycle exit in G2 phase after DNA damage in normal human fibroblasts. *EMBO J.* **22**, 3992-4002

Baxter, J. and Diffley, J.F. (2008). Topoisomerase II inactivation prevents the completion of DNA replication in budding yeast. *Mol Cell.* **30**, 790-802

Benimetskaya, L., Loike, J.D., Khlaed, Z., Loike, G., Silverstein, S.C., Cao, L., el Khoury, J., Cai, T.Q. and Stein, C.A. (1997). Mac-1 (CD11b/CD18) is an oligodeoxynucleotide-binding protein. *Nat Med.* **3**, 414-420

Bennouana, S., Bliss, S.K., Curiel, T.J. and Denkers, E.Y. (2003). Cross-talk in the innate immune system: neutrophils instruct recruitment and activation of dendritic cells during microbial infection. *J Immunol.* **171**, 6052-6058

Berger, J.M., Gamblin, S.J., Harrison, S.C. and Wang, J.C. (1996). Structure and mechanism of DNA topoisomerase II. *Nature.* **18**, 225-232

Berridge, M.V., Herst, P.M. and Tan, A.S. (2005). Tetrazolium dyes as tools in cell biology: New insights into their cellular reduction. *Biotechnology Annual Review.* **11**, 1387-2656

Beuscher, H.U., Nickells, M.W. and Colten, H.R. (1988). The precursor of interleukin-1  $\alpha$  is phosphorylated at residue serine 90. *J Biol Chem.* **263**, 4023-4028

Beyaert, R., Beaugerie, L., Van Assche, G., Brochez, L., Renauld, J., Viguier, M., Cocquyt, V., Jerusalem, G., Machiels, J., Prenen, H., Masson, P., Louis, E. and De Keyser, F. (2013). Cancer risk in immune-mediated inflammatory diseases (IMID). *Molecular Cancer.* **12**, doi:10.1186/1476-4598-12-98

Birkland, T.P., Sypek, J.P. and Wyler, D.J. (1992). Soluble TNF and membrane TNF expressed on CD4+ T lymphocytes differ in their ability to activate macrophage antileishmanial defense. *J Leukoc Biol.* **51**, 296-299

- Bodely, A.L., Wu, H.Y. and Liu, L.F. (1987). Regulation of DNA topoisomerases during cellular differentiation. *NCI Monogr.* **4**, 31-35
- BoseDasgupta, S. and Pieters, J. (2014). Inflammatory Stimuli Reprogram Macrophage Phagocytosis to Macropinocytosis for the Rapid Elimination of Pathogens, *PLOS Pathogens*. **10**, e1003879
- Bower, J.J., Karaca, G.F., Zhou, Y., Simpson, D.A., Cordeiro-Stone, M. and Kaufmann, W.K. (2010). Topoisomerase II $\alpha$  maintains genomic stability through decatenation G(2) checkpoint signalling . *Oncogene*. **29**, 4787-4799
- Brabers, N. A. and Nottet, H.S. (2006). Role of the pro-inflammatory cytokines TNF- $\alpha$  and IL-1 $\beta$  in HIV-associated dementia. *Eur J Clin Invest*. **36**, 447-458
- Branzai, D. and Foiani, M. (2008). Regulation of DNA repair throughout the cell cycle. *Nature Reviews Molecular Cell Biology*. **9**, 297-308
- Brennan, F.M. and McInnes, I.B. (2008). Evidence that cytokines play a role in rheumatoid arthritis. *The Journal of Clinical Investigation*. **118(11)**, 3537-3545
- Brody, D.T. and Durum, S.K. (1989). Membrane IL-1: IL-1 $\alpha$  precursor binds to the plasma membrane via a lectin-like interaction. *J Immunol*. **143**, 1183-1187
- Bromberg, K.D., Burgin, A.B. and Osheroff, N. (2003). A Two-drug Model for Etoposide Action against Human Topoisomerase II $\alpha$ . *The Journal of Biological Chemistry*. **278**, 7406-7412
- Bullard, D.C., Hu, X., Schoeb, T.R., Axtell, R.C., Raman, C. and Barnum, S.R. (2005). Critical requirement of CD11b (Mac-1) on T cells and accessory cells for development of experimental autoimmune encephalomyelitis. *J Immunol*. **15**, 6327-6333
- Burden, D.A. and Sullivan, D.M. (1994). Phosphorylation of the  $\alpha$  - and  $\beta$ -isoforms of DNA topoisomerase II is qualitatively different in interphase and mitosis in Chinese hamster ovary cells. *Biochemistry*. **33**, 14651-14655
- Burden, D.A. and Osheroff, N. (1998). Mechanism of action of eukaryotic topoisomerase II and drugs targeted to the enzyme. *Biochim Biophys Acta*. **1400**, 139-154

Bustin, S.A., Benes, V., Garson, J.A., Hellemans, J., Huggett, J., Kubista, M., Mueller, R., Nolan, T., Pfaffl, M.W., Shipley, G.L., Vandesompele, J. and Wittwer, C.T. (2009). The MIQE guidelines: minimum information for publication of quantitative real-time PCR experiments. *Clin Chem.* **55**, 611-622

Calcagno, A.M., Fostel, J.M., To, K.K.W., Salcido, C.D., Martin, S.E., Chewning, K.J., Wu, C.P., Varticovski, L., Bates, S.E., Caplen, N.J. and Ambudkar, S.V. (2008). Single-step doxorubicin-selected cancer cells overexpress the ABCG2 drug transporter through epigenetic changes. *British Journal of Cancer.* **98**, 1515-1524zw

Caldecott, K., Banks, G., Jeggo, P. (1990). Double-Strand Break Repair Pathways and Cellular Tolerance to Inhibitors of Topoisomerase II. *Cancer Res.* **50**, 5778

Cao, Y., Jia, S.F., Chakravarty, G., de Crombrughe, B. and Kleinerman, E.S. (2008). The osterix transcription factor down-regulates interleukin-1 $\alpha$  expression in mouse osteosarcoma cells. *Mol Cancer Res.* **6**, 119-126

Capranico, G. and Binaschi, M. (1998). DNA sequence selectivity of topoisomerases and topoisomerase poisons. *Biochim Biophys Acta.* **1400**, 185–194

Carpenter, A.J. and Porter, A.C. (2004). Construction, characterization, and complementation of a conditional-lethal DNA topoisomerase II $\alpha$  mutant human cell line. *Mol Biol Cell.* **15**, 5700-11.

Carruba, G., D'Agostino, P., Miele, M., Calabro, M., Barbera, C., Bella, G.D., Milano, S., Ferlazzo, V., Carusa, R., Rosa, M.L., Cocciadiferro, L., Campisi, I., Castagnetta, L. and Cillari, E. (2003). Estrogen regulates cytokine production and apoptosis in PMA-differentiated, macrophage-like U937 cells. *J Cell Biochem.* **90**, 187-196

Cassatella, M.A., Meda, L., Bonora, S., Ceska, M. and Constantin, G. (1993). Interleukin 10 (IL-10) inhibits the release of proinflammatory cytokines from human polymorphonuclear leukocytes. Evidence for an autocrine role of tumor necrosis factor and IL-1 $\beta$  in mediating the production of IL-8 triggered by lipopolysaccharide. *J Exp Med.* **178**, 2207-2211

Catapano, C.V., Carbone, G.M., Pisani, F., Qiu, J. and Fernandes, D.J. (1997). Arrest of replication fork progression at sites of topoisomerase II-mediated DNA cleavage in human leukemia CEM cells incubated with VM-26. *Biochemistry.* **36**, 5739-5748

Cavaillon, J.M. (1993) Contribution of cytokines to inflammatory mechanisms. *Pathol Biol (Paris).* **41**,799-811

- Ceredig, R., Rolink, A.G. and Brown, G. (2009). Models of haematopoiesis: seeing the wood for the trees, *Nat Rev Immunol.* **9**, 293-300
- Chalaris, A., Gewiese, J., Paliga, K., Fleig, L., Schneede, A., Krieger, K., Rose-John, S. and Scheller, J. (2010). ADAM17-mediated shedding of the IL6R induces cleavage of the membrane stub by  $\gamma$ -secretase. *Biochim Biophys Acta.* **1803**, 234-245
- Chaly, N. & Brown. (1996) Is DNA topoisomerase IIbeta a nucleolar protein? *Journal of Cellular Biochemistry.* **63**, 162-173
- Champoux, J.J. (2001). DNA Topoisomerases: Structure, Function, and Mechanism. *Annual Review of Biochemistry.* **70**, 369-433
- Chandra, R.K. (1997). Nutrition and the immune system: an introduction. *Am J Clin Nutr.* **66**, 460S-403S
- Chang, Y., Hwang, J., Shang, H. and Tsai, S. (1996). Characterization of Human DNA Topoisomerase II as an Autoantigen Recognized by Patients With IDDM. *Diabetes.* **46**, 408-414
- Chang, M.S., Chen, B.C., Yu, M.T., Sheu, J.R., Chen, T.F. and Lin, C.H. (2005). Phorbol 12-myristate 13-acetate upregulates cyclooxygenase-2 expression in human pulmonary epithelial cells via Ras, Raf-1, ERK, and NF- $\kappa$ B, but not p38 MAPK, pathways. *Cell Signal.* **17**, 299-310
- Changela, A., DiGate, R.J. and Mondragon, A. (2001). Crysal structure of a complex of a type IA DNA topoisomerase with a single-stranded DNA molecule. *Nature.* **411**, 1077-1081
- Chao, D.M., Gadbois, E.L., Murray, P.J., Anderson, S.F., Sonu, M.S., Parvin, J. D. and Young, R.A. (1996). A mammalian SRB protein associated with an RNA polymerase II holoenzyme. *Nature.* **380**, 82-85
- Chen, H.M., Pahl, H.L., Scheibe, R.J., Zhang, D.E. and Tenen, D.G. (1993). The Sp1 transcription factor binds the CD11b promoter specifically in myeloid cells in vivo and is essential for myeloid-specific promoter activity. *J Biol Chem.* **268**, 8230 – 8239
- Chen, Z.J. (2005). Ubiquitin Signaling in the NF- $\kappa$ B pathway. *Nat Cell Biol.* **7**, 758-765

- Chen, C., Cheng, C., Chen, C., Sue, Y., Liu, C., Cheng, T., Hsu, Y. and Chen, T. (2014). MicroRNA-328 Inhibits Renal Tubular Cell Epithelial-to-Mesenchymal Transition by Targeting the CD44 in Pressure-Induced Renal Fibrosis. *PLoS ONE*. **9**, e99802
- Chene, P., Rudloff, J., Schoepfer, J., Furet, P., Meier, P., Qian, Z., Schlaeppli, J.M., Schmitz, R. and Radimerski, T. (2009). Catalytic inhibition of topoisomerase II by a novel rationally designed ATP-competitive purine analogue. *BMC Chem Biol*. doi: 10.1186/1472-6769-9-1
- Chikamori, K., Hill, J.E., Grabowski, D.R., Zarkhin, E., Grozav, A.G., Vaziri, S.A., Gudkov, A.V., Rybicki, L.R., Bukowski, R.M., Yen, A., Tanimoto, M., Ganapathi, M.K. and Ganapathi, R. (2006). Downregulation of topoisomerase II $\beta$  in myeloid leukemia cell lines leads to activation of apoptosis following all-trans retinoic acid-induced differentiation/growth arrest. *Leukemia*. **20**, 1809-181
- Chow, K.C. and Ross, W.E. (1987). Topoisomerase-specific drug sensitivity in relation to cell cycle progression. *Mol Cell Biol*. **7**, 3119-3123
- Chow, K.C., King, C.K., Ross, W.E. (1988). Abrogation of etoposide-mediated cytotoxicity by cycloheximide. *Biochem Pharmacol*. **37**, 1117-1122
- Christmann, M. and Kaina, B. (2013). Transcriptional regulation of human DNA repair genes following genotoxic stress: trigger mechanisms, inducible responses and genotoxic adaptation. *Nucleic Acids Res*. **41**, 8403-8420
- Ciubotaru, I., Potempa, L.A. and Wander, R.C. (2005). Production of modified C-reactive protein in U937-derived macrophages. *Exp Biol Med*. **230**, 762-770
- Clanchy, F.I.L., Holloway, A.C., Lari, R., Cameron, P.U. and Hamilton, J.A. (2006). Detection and properties of the human proliferative monocyte subpopulation. *J Leukoc Biol*. **79**, 757-766
- Classen, S., Olland, S. and Berger, J.M. (2003). Structure of the topoisomerase II ATPase region and its mechanism of inhibition by the chemotherapeutic agent ICRF-187. *PNAS*. **100**, 10629-10634
- Coelho, P.A., Queiroz-Machado, J. and Sunkel, C.E. (2003). Condensin-dependent localisation of topoisomerase II to an axial chromosomal structure is required for sister chromatid esultuion during mitosis. *J Cell Sci*. **116**, 4763-4776

- Collart, M.A., Baeuerle, P. and Vassalli, P. (1990). Regulation of tumor necrosis factor  $\alpha$  transcription in macrophages: involvement of four  $\kappa$ -B motifs and of constitutive and inducible forms of NF- $\kappa$ B. *Mol Cell Biol.* **10**, 1498-1506
- Constantinou, A.I., Vaughan, A.T.M., Yamaskai, H. and Kamath, N. (1996). Commitment to Erythroid Differentiation in Mouse Erythroleukemia Cells Is Controlled by Alterations in Topoisomerase II $\alpha$  Phosphorylation. *Cancer Research.* **56**, 4192-4199
- Cook, D.N., Pisetsky, D.S. and Schwartz, D.A. (2004). Toll-like receptors in the pathogenesis of human disease. *Nat Immunol.* **5**, 975-979
- Corbett, K.D. and Berger, J.M. (2004). Structure, Molecular Mechanisms, and Evolutionary Relationships in DNA Topoisomerases. *Annu.Rev.BIophys.Biomol.Struct.* **33**, 95-118
- Cornarotti, M., Tinelli, S., Willmore, E., Zunino, F., Fisher, L. M., Austin, C. A. and Capranico, G. (1996). Drug Sensitivity and Sequence Specificity of Human Recombinant DNA Topoisomerases II $\alpha$  (p170) and II $\beta$  (p180). *Molecular Pharmacology.* **50**, 1463-1471
- Cortes Ledesma, F., El Khamisy, S.F., Zuma, M.C., Osborn, K., Caldecott, K.W. (2009). A human 5'-tyrosyl DNA phosphodiesterase that repairs topoisomerase-mediated DNA damage. *Nature.* **461**, 674-678
- Costa, V.S., Mattana, T.C. and da Silva, M.E. (2010). Unregulated IL-23/IL-17 immune response in autoimmune disease. *Diabetes Res Clin Pract.* **88**, 222-226
- Coussens, L.M. and Werb, Z. (2002). Inflammation and cancer. *Nature.* **420**, 860-867
- Cowell, I.G., Willmore, E., Chalton, D., Marsh, K.L., Jazrawi, E., Fisher, L.M. & Austin, C.A. (1998). Nuclear distribution of human DNA topoisomerase II $\beta$ : a nuclear targeting signal resides in the 116-residue C-terminal tail. *Exp. Cell Res.* **243**, 232-40.
- Cowell, I.G., Okorokov, A.L., Cutts, S.A., Padget, K., Bell, M., Milner, J. and Austin, C.A. (2000). Human topoisomerase II $\alpha$  and II $\beta$  interact with the C-terminal region of p53. *Exp Cell Res.* **255**, 86-94

Cowell, I.G., Papageorgiou, N., Padget, K., Watter, G.P. and Austin, C.A. (2011). Histone deacetylase inhibition redistributes topoisomerase II $\beta$  from heterochromatin to euchromatin. *Nucleus*. **2**, 61-71

Cowell, I.G. and Austin, C.A. (2012). Mechanism of generation of therapy related leukemia in response to anti-topoisomerase II agents. *Int. J. Environ. Res. Public. Health*. **9**, 2075-2091

Cowell, I.G., Sondka, Z., Smith, K., Lee, K.C., Manville, C.M., Sidorczuk-Lesthuruge, M., Rance, H.A., Padget, K., Jackson, G.H., Adachi, N. and Austin, C.A. (2012). Model for MLL translocations in therapy-related leukemia involving topoisomerase II $\beta$ -mediated DNA strand breaks and gene proximity. *PNAS*. **109**, 8989-8994

Crisona, N.J., Strick, T.R., Bensimon, D., Corquette, V. and Cozzarelli, N.R. (2000). Preferential relaxation of positively supercoiled DNA by E.coli topoisomerase IV in single-molecule and ensemble measurements. *Genes Dev*. **14**, 2881-1892

Daigneault, M., Preston, J.A., Marriott, H.M., Whyte, M.K.B. and Dockrell, D.H. (2010). The Identification of Markers of Macrophage Differentiation in PMA-Stimulated THP-1 Cells and Monocyte-Derived Macrophages. *PLoS One*. **5**(1) e8668

D'Arpa, P., Beardmore, C. and Liu, L.F. (1990). Involvement of Nucleic Acid Synthesis in Cell Killing Mechanisms of Topoisomerase Poisons. *Cancer Research*. **50**, 6919

Das, A., Mandal, C., Dasgupta, A., Sengupta, T. and Majumder, H.K. (2002). An insight into the active site of a type I DNA topoisomerase from the kinetoplastid protozoan *Leishmania donovani*. *Nucleic Acids Res*. **1**, 794-802

De Boo, S., Kopecka, J., Brusa, D., Gazzano, E., Matera, L., Ghigo, D., Bosia, A. and Riganti, C. (2009). iNOS activity is necessary for the cytotoxic and immunogenic effects of doxorubicin in human colon cancer cells, *Mol Cancer*. **8**, 108

de Campos-Nebel, M., Larripa, I. and Gonzalez-Cid, M. (2010). Topoisomerase II-mediated DNA damage is differently repaired during the cell cycle by non-homologous end joining and homologous recombination. *PLoS One*. **5**, e12541

De Haro, L.P., Wray, J., Williamson, E.A., Durant, S.T., Corwin, L., Gentry, A.C., Osheroff, N., Lee, S.H., Hromas, R. and Nickoloff, J.A. (2010). Metnase promotes restart and repair of stalled and collapsed replication forks. *Nucleic Acids Res*. **38**, 5681-5691



Deming, P.B., Cistulli, C.A., Zhao, H., Graves, P.R., Piwnica-Worms, H., Paules, R.S., Downes, C.S. and Kaufmann, W.K. (2001). The human decatenation checkpoint. *Proc Natl Acad Sci.* **98**, 12044-12049

Depowski, P.L., Rosenthal, S.I., Brien, T.P., Stylos, S., Johnson, R.L. and Ross, J.S. (2000). Topoisomerase II $\alpha$  Expression in Breast Cancer: Correlation with Outcome Variables. *Mod Path*, **13**, 542-547

Deszo, E.L., Brake, D.K., Cengel, K.A., Kelley, K.W. and Freund, G.G. (2000). CD45 Negatively Regulates Monocytic Cell Differentiation by Inhibiting PMA-Dependent Activation and Tyrosine Phosphorylation of PKC $\delta$ . *The Journal of Biological Chemistry.* **276**, 10212-10217

Deweese, J.E., Osheroff, M.A. and Osheroff, N. (2008). DNA Topology and Topoisomerase: Teaching a 'Knotty' Subject. *Biochem Mol Biol Educ.* **37**, 2-10

Diamant, M., Rieneck, K., Mechti, N., Zhang, X.G., Svenson, M., Bendtzen, K. and Klein, B. (1997). Cloning and expression of an alternatively spliced mRNA encoding a soluble form of the human interleukin-6 signal transducer gp130. *FEBS Lett.* **412**, 379-384

Dinarello, C.A. (2000). Proinflammatory cytokines. *Chest.* **118**, 503-508

Ding, H., Lin, H. and Feng, J. (2013). The rate of opening and closing of the DNA gate for topoisomerase II. *Theory Biosci.* **132**, 61-64

Dingemans, A.C., Witlox, A., Stallaert, R.A.L.M., van der Valk, P., Postmus, P.E. and Giaccone, G. (1999). Expression of DNA Topoisomerase II $\alpha$  and Topoisomerase II $\beta$  Genes Predicts Survival and Response to Chemotherapy in Patients with Small Cell Lung Cancer. *Clin Cancer Res.* **5**, 2048

Drake, F.H., Zimmerman, J.P., McCabe, F.L., Bartus, H.F., Per, S.R., Sullivan, D.M., Ross, W.E., Mattern, M.R., Johnson, R.K., Crooke, S.T. and Mirabelli, C.K. (1987). Purification of Topoisomerase II from Amsacrine-resistant P388 Leukemia Cells. *The Journal of Biological Chemistry.* **262**, 16739-16747

Durbecq, V., Paesmans, M., Cardoso, F., Desmedt, C., Di Leo, A., Chan, S., Friedrichs, K., Pinter, T., Van Belle, S., Murray, E., Bodrogi, I., Walpole, E., Lesperance, B., Korec, S., Crown, J., Simmonds, P., Perren, T.J., Leroy, J.Y., Rouas, G., Sotiriou, C., Piccart, M. and

- Larsimont, D. (2004). Topoisomerase-II $\alpha$  expression as a predictive marker in a population of advanced breast cancer patients randomly treated either with single-agent doxorubicin or single-agent docetaxel. *Mol Cancer Ther*, **3**, 1207-1214
- Dykhuizen, E.C., Hargreaves, D.C., Miller, E.L., Cui, K., Korshunov, A., Kool, M., Pfister, S., Cho, Y.J., Zhao, K. and Crabtree, G.R. (2013). BAF complexes facilitate decatenation of DNA by topoisomerase II $\alpha$ . *Nature*. **497**, 624-627
- Dziennis, S., Van Etten, R.A., Pahl, H.L., Morris, D.L., Rothstein, T.L., Bloch, C.M., Perlmutter, R.M. and Tenen, D.G. (1995). The CD11b promoter directs high-level expression of reporter genes in macrophages in transgenic mice. *Blood*. **85**, 319-329
- Eijdem, E.W., de Haas, M., Timmerman, A.J., Van der Schans, G.P., Kamst, E., de Noij, J., Astaldi-Ricotii, G.C., Borst, P. and Baas, F. (1995). Reduced topoisomerase II activity in multidrug-resistant human non-small cell lung cancer cell lines. *Br J Cancer*. **71**, 40-47
- Errington, F., Willmore, E., Tilby, M.J., Li, L., Li, G., Li, W., Baguley, B.C. and Austin, C.A. (1999). Murine transgenic cells lacking DNA topoisomerase II $\beta$  are resistant to acridines and mitoxantrone: analysis of cytotoxicity and cleavable complex formation. *Mol Pharmacol*, **56**, 1309-1316
- Errington, F., Willmore, E., Leontiou, C. Tilby, M.J., Austin, C.A. (2004). Differences in the longevity of topo II $\alpha$  and topo II $\beta$  drug-stabilized cleavable complexes and the relationship to drug sensitivity. *Cancer Chemother Pharmacol*. **53**, 155-162
- Faggad, A., Darb-Esfahano, S., Wirtz, R., Sinn, B., Sehouli, J., Konsgen, D., Lage, H., Weichert, W., Noske, A., Budczies, J., Muller, B.M., Buckendahl, A., Roske, A., Elwali, N. E., Dietel, M. and Denkert, C. (2009). Topoisomerase II $\alpha$  mRNA and protein expression in ovarian carcinoma: correlation with clinicopathological factors and prognosis. *Modern Pathology*. **22**, 579-588
- Fan, E., Shi, W. and Lowary, T.L. (2007). Synthesis of Daunorubicin Analogues Containing Truncated Aromatic Cores and Unnatural Monosaccharide Residues. *J Org Chem*. **72**, 2917-2928
- Fantuzzi, G. and Dinarello, C.A. (1999). Interleukin-18 and interleukin-1 $\beta$ : two cytokine substrates for ICE (caspase-1). *J Clin Immunol*. **19**, 1-11

- Fattman, C., Allan, W.P., Hasinoff, B.B. and Yalowich, J.C. (1996). Collateral sensitivity to the bisdioxopiperazine dexrazoxane (ICRF-187) in etoposide (VP-16) resistant human leukemia K562 cells. *Biochem Pharmacol.* **52**, 635-642
- Feldhoff, P.W., Mirski, S.E., Cole, S.P. and Sullivan, D.M. (1994). Altered subcellular distribution of topoisomerase II $\alpha$  in a drug-resistant human small cell lung cancer cell line. *Cancer Res.* **54**, 756-762
- Fernandes, D.J., Qiu, J. and Catapano, C.V. (1995). DNA topoisomerase II isozymes involved in anticancer drug action and resistance. *Adv Enzyme Regul.* **35**, 265-281
- Fernandez, X., Diaz-Ingelmo, O., Martinez-Garcia, B. and Roca, J. (2014). Chromatin regulates DNA torsional energy via topoisomerase II-mediated relaxation of positive supercoils. *EMBO.* **33**, 1492-1501
- Ferraro, C., Quemeneur, L., Fournel, S., Prigent, A., Revillard, J. and Bonnefoy-Berard, N. (2000). The topoisomerase inhibitor camptothecin and etoposide induce a CD95-independent apoptosis of activated peripheral lymphocytes. *Cell Death and Differentiation.* **7**, 197-206
- Fettelschoss, A., Kistowska, M., LeibundGut-Landmann, S., Beer, H.D., Johansen, P., Senti, G., Contassot, E., Bachmann, M.F., French, L.E., Oxenius, A. and Kündig, T.M. (2011). Inflammasome activation and IL-1 $\beta$  target IL-1 $\alpha$  for secretion as opposed to surface expression. *PNAS.* **108**, 18055-18060
- Flajnik, M.F. and Pasquier, L.D. (2004). Evolution of innate and adaptive immunity: can we draw a line? *Trends in Immunology.* **25**, 640-644
- Fortune, J.M. and Osheroff, N. (1998). Merbarone inhibits the catalytic activity of human topoisomerase II $\alpha$  by blocking DNA cleavage. *J Biol Chem.* **273**, 17643-17650
- Froelich-Ammon, S.J., Gale, K.C. and Osheroff, N. (1994). Site-specific cleavage of a DNA hairpin by topoisomerase II. DNA secondary structure as a determinant of enzyme recognition/cleavage. *J Biol Chem.* **269**, 7719-7725
- Frey, M.R., Saxon, M.L., Zhao, X., Rollins, A., Evans, S.S. and Black, J.D. (1997). Protein Kinase C Isozyme-mediated Cell Cycle Arrest Involves Induction of p21<sup>waf1/cip1</sup> and p27<sup>kip1</sup> and Hypophosphorylation of the Retinoblastoma Protein in Intestinal Epithelial Cells. *The Journal of Biological Chemistry.* **272**, 9424-9435

- Fujiwara, N. and Kobayashi, K. (2005). Macrophages in inflammation. *Curr Drug Targets Inflamm Allergy*. **4**, 281-286
- Gabay, C., Lamacchia, C., and Palmer, G. (2010). IL-1 pathways in inflammation and human diseases. *Nat Rev Rheumatol* **6**, 232-241.
- Gao, H., Yamasaki, E.F., Chan, K.K., Shen, L.L. and Snapka, R.M. (2003). DNA Sequence Specificity for Topoisomerase II Poisoning by the Quinoxaline Anticancer Drugs XK469 and CQS. *Molecular Pharmacology*. **63**, 1382-1388
- Garcia, A., Serrano, A., Abril, E., Jimenez, P., Real, L.M., Canton, J., Garrido, F. and Ruiz-Cabello, F. (1999). Differential effect on U937 cell differentiation by targeting transcription factors implicated in tissue- or stage-specific induced integrin expression. *Experimental Hematology*. **27**, 353-364
- Garcia-Rubio, M.L. and Aquilera, A. (2012). Topological constraints impair RNA polymerase II transcription and causes instability of plasmid-borne convergent genes. *Nucleic Acids Res.* **40**, 1050-1064
- Gentry, A.C., Juul, S., Veigaard, C., Knudsen, B. R. and Osheroff, N. (2011). The geometry of DNA supercoils modulates the DNA cleavage activity of human topoisomerase I. *Nucleic Acids Res.* **39**, 1014-1022
- Germe, T. and Hyrien, O. (2005). Topoisomerase II-DNA complexes trapped by ICRF-193 perturb chromatin structure. *EMBO*. **6**, 729-735
- Ghassabeh, G.H., De Baetselier, P., Brys, L., Noel, W., Van Ginderachter, J.A., Meerschaut, S., Beschin, A., Brombacher, F. and Raes, G. (2006). Identification of a common gene signature for type II cytokine-associated myeloid cells elicited in vivo in different pathologic conditions. *Blood*. **108**, 575-583
- Ghosh, C.C., Ramaswami, S., Juvekar, A., Vu, H.Y., Galdieri, L., Davidson, D. and Vancurova, I. (2010). Gene-specific repression of proinflammatory cytokines in stimulated human macrophages by nuclear I $\kappa$ B $\alpha$ . *J Immunol*. **185**, 3685-3693
- Gilbert, L.A., Larson, M.H., Morsut, L., Liu, Z., Bar, G.A., Torres, S.E., Stern-Ginossar, N., Brandman, O., Whitehead, E.H., Doudna, J.A., Lim, W.A., Weissman, J.S and Qi, L.S. (2013).

CRISPR-Mediated Modular RNA-Guided Regulation of Transcription in Eukaryotes. *Cell*. **154**, 442-451

Gilroy, K.L., Leontiou. C., Padget, K., Lakey, J. and Austin, C.A. (2006). mAMSA resistant human topoisomerase II $\beta$  mutation G465D has reduced ATP hydrolysis activity. *Nucleic Acids Res.* **34**, 1597-1607

Gilroy, K.L. and Austin, C.A. (2011). The Impact of the C-Terminal Domain on the Interaction of Human DNA Topoisomerase II  $\alpha$  and  $\beta$  with DNA. *PLOS ONE*. **6(2)**, e14693

Gla, E.M., Divjak, M., Bailey, M.J. and Walters, E.H. (2002).  $\beta$ -Actin and GAPDH housekeeping gene expression in asthmatic airways is variable and not suitable for normalising mRNA levels. *Thorax*. **57**, 765-70

Gomes, N.E., Brunialti, M.K.C., Mendes, M.E., Freudenberg, M., Galanos. C. and Salomao, R. (2010). Lipopolysaccharide-induced expression of cell surface receptors and cell activation of neutrophils and monocytes in whole human blood. *Braz J Med Biol Res.* **43**, 853-859

Gordon, S. (2003) .Alternative Activation of Macrophages. *Nature Reviews Immunology*. **3**,23-35

Gordon, S. and Taylor, P.R. (2005). Monocyte and Macrophage Heterogeneity. *Nature Reviews Immunology*. **5(12)**,953-964

Gosavi, S., Whitford, P.C., Jennings, P.A. and Onuchic, J.N. (2008). Extracting function from a  $\beta$ -trefoil folding motif. *PNAS*. **105**, 10384-10389

Goswami, P.C., Roti, J.L. and Hunt, C.R. (1996). The Cell Cycle-Coupled Expression of Topoisomerase II $\alpha$  during S Phase Is Regulated by mRNA Stability and Is Disrupted by Heat Shock or Ionizing Radiation. *Molecular and Cellular Biology*. **16**, 1500-1508

Grabowski, D.R., Holmes, K.A., Aoyama, M., Ye, Y., Rybicki, L.A., Bukowski, R.M., Ganapathi, M.K., Hickson, I.D. and Ganapathi, R. (1999). Altered Drug Interaction and Regulation of Topoisomerase II $\beta$ : Potential Mechanisms Governing Sensitivity of HI-60 Cells to Amsacrine and Etoposide. *Molecular Pharmacology*. **56**, 1340-1345

Grassl, C., Luckow, B., Schlöndorff, D. and Dendorfer, U. (1999). Transcriptional regulation of the interleukin-6 gene in mesangial cells. *J Am Soc Nephrol*. **10**, 1466-1477

- Grausland, M., Thougard, A.V., Fuchtbauer, A., Hofland, K.F., Hjorth, P.H., Jensen, P.B., Sehested, M., Fuchtbauer, E.M. and Jensen, L.H. (2007). A mouse model for studying the interaction of bisdioxopiperazines with topoisomerase II $\alpha$  in vivo. *Mol Pharmacol.* **72**, 1003-1014
- Greten, F.R., Arkan, M.C., Bollrath, J., Hsu, L., Goode, J., Miething, C., Goktune, S.I., Neuenhahn, M., Fierer, J., Paxian, S., Rooijen, N.V. Xu, Y., O'Cain, T., Jaffee, B.B., Busch, D.H., Duyster, J., Schmid, R.M., Eckmann, L. and Karin, M. (2007). NF- $\kappa$ B is a negative regulator of IL-1 $\beta$  secretion as revealed by genetic and pharmacological inhibition of IKK $\beta$ . *Cell.* **130**, 918-931
- Grigola, B., Mazzetti, I., Meliconi, R. Bazzi, S., Scorza, R., Candela, M., Gabrielli, A. and Facchini, A. (2000). Anti-topoisomerase II $\alpha$  autoantibodies in systemic sclerosis-association with pulmonary hypertension and HLA-B35. *Clin Exp Immunol.* **121**, 539-543
- Guinea-Viniegra, J., Zenz, R., Scheuch, H., Hnisz, D., Holcman, M., Bakiri, L., Schonhaler, H.B., Sibilio, M. and Wagner, E.F. (2009). TNF $\alpha$  shedding and epidermal inflammation are controlled by Jun proteins. *Genes and Development.* **23**, 2663-2674
- Hacham, M., Argov, S., White, R.M., Segal, S. and Apte, R.N. (2002). Different patterns of interleukin-1 $\alpha$  and interleukin-1 $\beta$  expression in organs of normal young and old mice. *Eur Cytokine Netw.* **13**, 55-65
- Hailey, K.L., Li, S., Andersen, M.D., Roy, M., Woods, V.L. and Jennings, P.A. (2009). Pro-interleukin (IL)-1 $\beta$  shares a core region of stability as compared with mature IL-1 $\beta$  while maintaining a distinctly different configurational landscape: a comparative hydrogen/deuterium exchange mass spectrophotometry study. *J Biol Chem.* **284**, 26137-26148
- Haldane, A., Finlay, G.J. and Baguley, B.C. (1993). A comparison of the effects of aphidicolin and other inhibitors on topoisomerase II-directed cytotoxic drugs. *Oncol Res.* **5**, 133-138
- Han, Z., Chatterjee, D., He, D.M., Early, J., Pantazis, P., Wyche, J.H. and Hendrickson, E.A. (1995). Evidence for a G2 checkpoint in p53-independent apoptosis induction by X-irradiation. *Mol Cell Biol.* **15**, 5849-5857

- Hansen, S.H., Behrendt, N., Dano, K. and Kristensen, P. (1990). Localization of urokinase-type plasminogen activator receptore on U937 cells: phorbol ester PMA induces heterogeneity. *Exp Cell Res.* **187**(2) 255-262
- Hande, K.R. (1998). Etoposide: four decades of development of a topoisomerase II inhibitor. *EJC.* **34**, 1514-1521
- Hashimoto, K., Otero, M., Imagawa, K., de Andres, M.C., Coico, J.M., Roach, H.I., Oreffo, R.O., Marcu, K.B. and Goldring, M.B. (2013). Regulated transcription of human matrix metalloproteinase 13 (MMP13) and interleukin-1 $\beta$  (IL1B) genes in chondrocytes depends on methylation of specific proximal promoter CpG sites. *J Biol Chem.* **288**, 10061-10072
- Hasinoff, B. B., Kuschak, T. I., Yalowich, J. C. and Creighton, A. M. (1995). A QSAR study comparing the cytotoxicity and DNA topoisomerase II inhibitory effects of bisdi- oxopiperazine analogs of ICRF-187 (dexrazoxane). *Biochem. Pharmacol.* **50**:953–958.
- Hasinoff, B.B., Kuschak, T.I., Creighton, A.M., Fattman, C.L., Allan, W.P., Thampatty, P. and Yalowich, J.C. (1997). Characterization of a Chinese hamster ovary cell line with acquired resistance to the bisdioxopiperazine dexazoxane (ICRF-187) catalytic inhibitor of topoisomerase II. *Biochem Pharmacol.* **53**, 1843-1853
- Hayden, M.S. and Ghosh, S. (2008). Shared principles in NF- $\kappa$ B signalling. *Cell.* **132**, 344-362
- Heming, T.A., Dave, S.K., Tuazon, D.M., Chopra, A.K., Peterson, J.W. and Bidani, A. (2001). Effects of extracellular pH on tumour necrosis factor  $\alpha$  production by resident alveolar macrophages. *Clinical Science.* **101**, 267-274
- Henkel, G.W., McKercher, S.R., Yamamoto, H., Anderson, K.L., Oshima, R.G. and Maki, R.A. (1996). PU.1 but not ets-1 is essential for macrophage development from embryonic stem cells. *Blood.* **88**, 2917-2926
- Hong, G., Kreuzer, K.N. (2003). Endonuclease cleavage of blocked replication forks: an indirect pathway of DNA damage from antitumor drug-topoisomerase complexes. *Proc Natl Acad Sci USA.* **100**, 5046–5051.
- Horiuchi, T., Mitoma, H., Harashima, S., Tsukamoto, H. and Shimoda, T. (2010). Transmembrane TNF- $\alpha$ : structure, function and interaction with anti-TNF agents. *Rheumatology (Oxford).* **49**, 1215-1228

- Hromas, R., Barlogie, B., Swartzendruber, D., and Drewinko, B. (1983). Potentiation of DNA-reactive antineoplastic agents and protection against S-phase-specific agents by anguidine in Chinese hamster ovary cells. *Cancer Res.* **43**, 3070-3073.
- Hsiang, Y.H., Lihou, M.G. and Liu, L.F. (1989). Arrest of replication forks by drug-stabilized topoisomerase I-DNA cleavable complexes as a mechanism of cell killing by camptothecin. *Cancer Res.* **49**, 5077-5082
- Hu, T., Sage, H. and Hsieh, T. (2002). ATPase Domain of Eukaryotic DNA Topoisomerase II: Inhibition of ATPase activity by the anti-cancer drug bisdioxopiperazine and ATP/ADP-induced dimerization. *J Biol Chem.* **277**, 5944-5951
- Huang, K., Gao, H., Yamasaki, E.F., Grabowski, D.R., Liu, S., Shen, L.L., Chan, K.K., Ganapathi, R. and Snapka, R.M. (2001). Topoisomerase II Poisoning by ICRF-193. *The Journal of Biological Chemistry.* **276**, 44488-44494
- Huang, H.S., Allen, J.A., Mabb, A.M., King, I.F., Miriyala, J., Taylor-Blake, B., Sciaky, N., Dutton, J.W., Lee, H.M., Chen, X., Bridges, A.S., Zylka, M.J., Roth, B.L. and Philpot, B.D. (2011). Topoisomerase inhibitors unsilenced the dormant allele of Ube3a in neurons. *Nature.* **481**, 185-189
- Huber, R., Pietsch, D., Gunther, J., Welz, B., Vogt, N. and Brand, K. (2014). Regulation of monocyte differentiation by specific signalling modules and associated transcription factor networks. *Cell. Mol. Life Sci.* **71**, 63-92
- Idris, H.T. and Naismith, J.H. (2000). TNF $\alpha$  and the TNF receptor superfamily: structure-function relationship. *Microsc Res Tech.* **50**, 184-195
- Infantino, V., Convertini, P., Cucci, L., Panaro, M.A., Di Noia, M. A., Calvello, R., Palmieri, F. and Iacobazzi, V. (2011). The mitochondrial citrate carrier: a new player in inflammation. *Biochem J.* **438**, 433-436
- Ishida, R., Sato, M., Narita, T., Utsumi, K.R., Nishimoto, T., Morita, T., Nagata, H. and Andoh, T. (1994). Inhibition of DNA Topoisomerase II by ICRF-193 Induces Polyploidization by Uncoupling Chromosome Dynamics from Other Cell Cycle Events. *The Journal of Cell Biology.* **126**, 1341-1351



- Ishimi, Y., Miyaura, C., Jin, C.H., Akatsu, T., Abe, E., Nakamura, Y., Yamaguchi, A., Yoshiki, S., Matsuda, T. and Hirano, T. (1990). IL-6 is produced by osteoblasts and induces bone resorption. *J Immunol.* **145**, 3297-3303
- Isik, S., Sano, K., Tsutsui, K., Seki, M., Enomoto, T., Saitoh, H. and Tsutsui, K. (2003). The SUMO pathway is required for selective degradation of DNA topoisomerase II $\beta$  induced by a catalytic inhibitor ICRF-193(1). *FEBS Lett.* **546**, 374-378
- Iwai, M., Hara, A., Andoh, T. and Ishida, R. (1997). ICRF-193, a catalytic inhibitor of DNA topoisomerase II, delays the cell cycle progression from metaphase, but not from anaphase to the G1 phase in mammalian cells. *FEBS Lett.* **406**, 267-270
- Janeway, C. A. (1989). Approaching the asymptote? Evolution and revolution in immunology. *Cold Spring Harb. Symp. Quant. Biol.* **54**, 1–13
- Janeway, C.A. and Medzhitov, R. (2002). Innate immune recognition. *Annu Rev Immuno.* **20**, 197-216
- Janssens, S. and Tschopp, J. (2006). Signals from within: the DNA-damage-induced NF- $\kappa$ B response. *Cell Death and Differentiation.* **13**, 773-784
- Jasek, E., Mirecka, J. and Litwin, J.A. (2008). Effect of differentiating agents (all-trans retinoic acid and phorbol 12-myristate 13-acetate) on drug sensitivity of HL60 and NB4 cells in vitro. *Folia Histochem Cytobiol.* **46**, 323-30
- Jensen, L.H., Dejligbjerg, M., Hansen, L.T., Grauslund, M., Jensen, P.B. and Sehested, M. (2004). Characterisation of cytotoxicity and DNA damage induced by the topoisomerase II-directed bisdioxopiperazine anti-cancer agent ICRF-187 (dexrazoxane) in yeast and mammalian cells. *BMC Pharmacol.* **2**, 31
- Jerke, U., Tkachuk, S., Kiyan, J., Stepanova, V., Kusch, A., Hinz, M., Dietz, R., Haller, H., Fuhrman, B. and Dumler, I. (2009). Stat1 Nuclear Translocation by Nucleolin upon Monocyte Differentiation. *PLoS One.* **e0008302**
- Johnson, C.A., Padget, K., Austin, C.A. and Turner, B.M. (2001). Deacetylase Activity Associates with topoisomerase II and Is Necessary for Etoposide-induced Apoptosis. *The Journal of Biological Chemistry.* **276**, 4539-4542.

- Johnson, K.R., Becker, K.P., Facchinetti, M.M., Hannun, Y.A. and Obeid, L.M. (2002). PKC-dependent activation of sphingosine kinase 1 and translocation to the plasma membrane. Extracellular release of sphingosine-1-phosphate induced by phorbol 12-myristate 13-acetate (PMA). *J Biol Chem.* **277**, 35257-35262
- Ju, B., Lunyak, V.V., Perissi, V., Gracia-Bassets, I., Rose, D. W., Glass, C.K. and Rosenfield, M.G. (2006). A Topoisomerase II $\beta$ -Mediated dsDNA break Required for Regulated Transcription. *Science*.**12**,1798-1802
- Kameda, K. and Sato, K. (1994). Regulation of IL-1 $\alpha$  expression in human keratinocytes: transcriptional activation of the IL-1 $\alpha$  gene by TNF- $\alpha$ , LPS, and IL-1 $\alpha$ . *Lymphokine Cytokine Res.* **13**, 29-35
- Karin, M., Lawrence, T. and Nizet, V. (2006). Innate Immunity Gone Awry: Linking Microbial Infections to Chronic Inflammation and Cancer. *Cell.* **124**, 823-835
- Kaufmann, S.H., McLaughlin, S.J., Kastan, M.B., Liu, L.F., Karp, J.E. and Burke, P.J. (1991). Topoisomerase II Levels during Granulocytic Maturation *in Vitro* and *in Vivo*. *Cancer Res.* **51**,3534
- Kawai, T. and Akira, S. (2007) Signaling to NF- $\kappa$ B by Toll-like receptors. *Trends Mol Med.* **13**, 460-469
- Kellner, U., Heidebrecht, H.J., Rudolph, P., Biersack, H. and Buck, F. (1997). Detection of human topoisomerase II $\alpha$  in cell lines and tissues: characterisation of five novel monoclonal antibodies. *J Histochem Cytochem.* **45**, 251-263
- Kim, M. Y., Zhang, T. and Kraus, W.L. (2005). Poly(ADP-ribosyl)ation by PARP-1: 'PAR-laying' NAD<sup>+</sup> into a nuclear signal. *Genes & Dev* **19**, 1951-1967
- Kimura, K., Saijo, M., Ui, M. and Enomoto, T. (1994). Growth State and Cell Cycle-dependent Fluctuation in the Expression of Two Forms of DNA Topoisomerase II and Possible Specific Modification of the Higher Molecular Weight Form in the M Phase. *The Journal of Biological Chemistry.* **269**, 1173-1176
- Kingston, H. and Mills, G. (2011). TLR-dependent T cell activation in autoimmunity. *Nature Reviews Immunology.* **11**, 807-822
- Kinne, R.W., Brauer, R., Stuhlmüller, B., Palomba-Kinne, E. and Burmester, G. (2000). Macrophages in rheumatoid arthritis. *Arthritis Research.* **2**, 189-202

- Klugewit, K., Ley, K., Schuppan, D., Nuck, R., Gaehtgens, P. and Walzog, B. (1997). Activation of the  $\beta 2$  integrin Mac-1 (CD11b/CD18) by an endogenous lipid mediator of human neutrophils and HL60 cells. *J Cell Sci.* **110**, 985-990
- Kobayashi, M., Adachi, N. and Koyama, H. (1998). Characterization of the 3' untranslated region of mouse DNA topoisomerase II $\alpha$  mRNA. *Gene.* **215**, 329-337
- Kohira, T., Matsumoto, K., Ichihara, A. and Nakamura, T. (1993). Identification of a biologically functional novel IL-1 $\beta$  -specific receptor on adult rat hepatocytes. *J Biochem.* **114**, 658-662
- Kosaka, C., Sasaguri, T., Ishida, A. and Ogata, J. (1996). Cell cycle arrest in the G2 phase induced by phorbol ester and diacylglycerol in vascular endothelial cells. *Am J Physiol.* **270**, C170-178
- Krah, R., Kozyavkin, S.A., Slesarev, A.I. and Gellert, M. (1996). A two-subunit type I DNA topoisomerase (reverse gyrase) from an extreme hyperthermophile. *Proc Natl Acad Sci.* **93**, 106-110
- Krämer, B., Wiegmann, K. and Krönke, M. (1995). Regulation of the Human TNF Promoter by the Transcription Factor Ets. *The Journal of Biological Chemistry.* **270**, 6577-6583
- Kramer, P.R., Kramer, S.F. and Guan, G. (2004). 17 $\beta$ -estradiol regulates cytokine release through modulation of CD16 expression in monocytes and monocyte-derived macrophages. *Arthritis Rheum.* **50**, 1967-1975
- Krappmann, D. and Scheidereit, C. (2005). A pervasive role of ubiquitin conjugation in activation and termination of I $\kappa$ B kinase pathways. *EMBO Rep.* **6**, 321-326
- Krause, S.W., RehLi, M., Heinz, S., Ebner, R. and Andreesen, R. (2000). Characterization of MAX.3 antigen, a glycoprotein expressed on mature macrophages, dendritic cells and blood platelets: identity with CD84. *Biochem J.* **346**, 729-736
- Krishnaraju, K., Hoffman, B. and Liebermann, D.A. (1998). The zinc finger transcription factor Egr-1 activates macrophage differentiation in M1 myeloblastic leukemia cells. *Blood.* **92**, 1957-1966

- Kroll, D.J., Sullivan, D.M., Gutierrez-Hartmann, A. and Hoeffler, J.P. (1993). Modification of DNA topoisomerase II activity via direct interactions with the cyclic adenosine-3', 5'-monophosphate response element-binding protein and related transcription factors. *Mol Endocrinol.* **3**, 305-318
- Kuwana, M., Okazaki, Y., Kodama, H., Izumi, K., Yasuoka, H., Ogawa, Y., Kawakami, Y. and Ikeda, Y. (2003). Human circulating CD14<sup>+</sup> monocytes as a source of progenitors that exhibit mesenchymal cell differentiation. *J Leukoc Biol.* **74**, 833-845
- Kumbrink, J., Kirsch, K.H. and Johnson, J.P. (2010). EGR1, EGR2, and EGR3 activate the expression of their coregulator NAB2 establishing a negative feedback loop in cells of neuroectodermal and epithelial origin. *J Chem Biochem.* **111**, 207-217
- Kunze, N., Yang, G.C., Dolberg, M., Sundarp, R., Knippers, R. and Richter, A. (1991). Structure of the human type I DNA topoisomerase gene. *The Journal of Biological Chemistry.* **266**, 9610-9616
- Larsen, A.K., Escargueil, A.E. and Skladanowski, A. (2003). Catalytic topoisomerase II inhibitors in cancer therapy. *Pharmacol Ther.* **99**, 167-181
- Lavoie, B.D., Hogan, E. and Koshland, D. (2002). In vivo dissection of the chromosome condensation machinery: reversibility of condensation distinguishes contributions of condensing and cohesion. *J Cell Biol.* **156**, 805-815
- Lawrence, T. (2009). The NF- $\kappa$ B pathway in inflammation. *Cold Spring Harb Perspect Biol.* **1**, a001651
- Lazdins, J.K., Matthias, G., Walker, M.R., Woods-Cook, K., Scheurich, P. and Pfizenmaier, K. (1997). Membrane Tumor Necrosis Factor (TNF) Induced Cooperative Signaling of TNFR60 and TNFR80 Favors Induction of Cell Death Rather Than Virus Production in HIV-infected T Cells. *JEM*, **185**, 81-90
- Lee, J.C., Laydon, J.T., McDonnell, P.C., Gallagher, T.F., Kumar, S., Green, D., McNulty, D., Blumethal, M.J., Heys, J. R., Landvatter, S.W., Strickler, J.E., McLaughlin, M.M., Siemems, I.R., Fisher, S.M., Li, G.P., White, J.R., Adams, J.L. and Young, P.R. (1999) A protein kinase involved in the regulation of inflammatory cytokine biosynthesis. *Nature.* **372**, 739-745

- Lee, K.C., Padget, K., Curtis, H., Cowell, I.G., Moiani, D., Sondka, Z., Morris, N.J., Jackson, G.H., Cockell, S.J., Tainer, J.A. and Austin, C.A. (2012). MRE11 facilitates the removal of human topoisomerase II complexes from genomic DNA. *Biol Open*. **1**, 863-873
- Lehtonen, A., Ahlfors, H., Veckman, V., Miettinen, M., Lahesmaa, R. and Julkunen, I. (2007). Gene expression profiling during differentiation of human monocytes to macrophages or dendritic cells. *Journal of Leukocyte Biology*. **82**, 710-720
- Leonardo, M.R., Silva, R.A., Assed, S. and Nelson-Filho, P. (2004). Importance of bacterial endotoxin (LPS) in endodontics. *J Appl Oral Sci*. **12**, 93-98
- Li, T.K. and Liu, L.F. (2001). Tumor cell death induced by topoisomerase-targeting drugs. *Annu Rev Pharmacol Toxicol*, **41**, 53–77.
- Li, L., Okino, S.T., Zhao, H., Pookot, D., Place, R.F., Urakami, S., Enokida, H. and Dahiya, R. (2006). Small dsRNAs induce transcriptional activation in human cells. *PNAS*. **103**, 17337-17342
- Li, M. and Yu, X. (2013). Function of BRCA1 in the DNA damage response is mediated by ADP-ribosylation. *Cancer Cell*. **23**, 693-704
- Lichte, P., Grigoleit, J.S., Steiner, E.M., Kullmann, J.S., Schedlowski, M., Oberback, R. and Kobbe, P. (2013). Low dose LPS does not increase TLR4 expression on monocytes in a human in vivo model. *Cytokine*. **63(1)**, 74-80
- Lim, K., Lee, J.I., Yun, K.A., Son, M.Y., Park, J.I., Yoon, W.H. and Hwang, B.D. (1998). Reduced level of ATF is correlated with transcriptional repression of DNA topoisomerase II $\alpha$  gene during TPA-induced differentiation of HL-60 cells. *Biochem Mol Biol Int*. **46**, 35-42
- Lindsley, J.E. and Wang, J.C. (1991). Proteolysis patterns of eptopically labelled yeast DNA topoisomerase II suggest an allosteric transition in the enzyme induced by ATP binding. *Proc Natl Acad Sci*. **88**, 10485-10489
- Liu, L.F., Liu, C.C. and Alberts. B.M. (1980). Type II DNA topoisomerases: enzymes that can unknot a topologically knotted DNA molecule via a reversible double-strand break. *Cell*. **19**, 697-707
- Liu, L. F. and Wang, J.C. (1987). Supercoiling of the DNA template during transcription. *Proc. Natl. Acad. Sci*. **84**, 7024-7027

- Liu, H., Sidiropoulos, P., Song, G., Pagliari, L.J., Birrer, M.J., Stein, B., Anrather, J. and Pope. R.M. (2000). TNF- $\alpha$  Gene Expression in Macrophages: Regulation by NF- $\kappa$ B is Independent of c-Jun or C/EBP $\beta$ . *The Journal of Immunology*. **164**, 4277-4285
- Liu, Z., Deibler, R.W., Chan, H.S., Zechiedrich, L. (2009). The why and how of DNA unlinking. *Nucl. Acids Res.* **33**, 661-671
- Loflin, P.T., Altschuler, E., Hochhauser, D., Hickson, I.D. and Zwelling, L.A. (1996). Phorbol ester-induced down-regulation of topoisomerase II $\alpha$  mRNA in a human erythroleukemia cell line. Evidence for a post-transcriptional mechanism. *Biochem Pharmacol.* **52**, 1065-1072
- Loike, J.D. and Horwitz, S.B. (1976). Effect of VP-16-213 on the intracellular degradation of DNA in HeLa cells. *Biochemistry*. **15**, 5443-5448
- Lopez-Castejon, G. and Brough, D. (2011). Understanding the mechanism of IL-1 $\beta$  secretion. *Cytokine and Growth factors Reviews*. **22**, 189-195
- Lucas, I., Germe, T., Chevrier-Miller, M. and Hyrien, O. (2001) Topoisomerase II can unlink replicating DNA by precatenane removal. *EMBO J.* **20**, 6509-6519
- Luo, K., Yuan, J., Chen, J. and Lou, Z. (2009). Topoisomerase II $\alpha$  controls the decatenation checkpoint. *Nat Cell Biol.* **11**, 204-210
- Luster, A.D. (1998). Chemokines-Chemotactic Cytokines that Mediate Inflammation. *N Engl J Med.* **338**, 436-445
- Lust, J.A., Donovan, K.A., Kline, M.P., Greipp, P.R., Kyle, R.A. and Maihle, N.J. (1992). Isolation of an mRNA encoding a soluble form of the human interleukin-6 receptor. *Cytokine*. **4**, 96-100
- Lyu, Y.L. and Wang, J.C. (2003). Aberrant lamination in the cerebral cortex of mouse embryos lacking DNA Topoisomerase II $\beta$ . *PNAS*. **100**, 7123-7128.
- Lyu, Y.L., Lin, C., Azarova, A.M., Cai, L., Wang, J.C. and Liu, L.F. (2006). Role of Topoisomerase II $\beta$  in the Expression of Developmentally Regulated Genes. *Molecular and Cellular Biology*. **26**, 7929-7941.

- MacMicking, J., Xie, Q.W. and Nathan, C. (1997). Nitric oxide and macrophage function. *Annu Rev Immunol.* **15**, 323-350
- Malik, M. and Nitiss, J.L. (2004). DNA repair functions that control sensitivity to topoisomerase-targeting drugs. *Eukaryot Cell.* **3**, 82-90
- Malo, M.S., Biswas, S., Abedrapo, M.A., Yeh, L., Chen, A. and Hodin, R.A. (2006). The pro-inflammatory cytokines, IL-1 $\beta$  and TNF-  $\alpha$ , inhibit intestinal alkaline phosphatase gene expression. *DNA Cell Biol.* **25**, 684-695
- Mantovani, A. (2006). Macrophage diversity and polarization: in vivo veritas. *Blood.* **108**, 408-409
- Mao, Y., Desai, S.D. and Liu, L.F. (2000). SUMO-1 conjugation to human DNA topoisomerase II isozymes. *J Biol Chem.* **275**, 26066-26073
- Mao, Y., Desai, S. D., Ting, C., Hwang, J. and Liu, L.F. (2001). 26 S Proteasome –mediated Degradation of Topoisomerase II Cleavable Complexes. *The Journal of Biological Chemistry*, **276**, 40652-40658
- Marsh, K.L., Willmore, E., Tinelli, S., Cornarotti, M., Meczes, E.L., Capranico, G., Fisher, M. and Austin, C.A. (1996). Amascrine-Promoted DNA Cleavage Site Determinants for the Two Human DNA Topoisomerase II Isoforms  $\alpha$  and  $\beta$ . *Biochemical Pharmacology.* **52**, 1675-1685
- Martinez, F. O., Gordon, S., Locati, M. and Mantovani, A. (2006). Transcriptional Profiling of the Human Monocyte-to-Macrophage Differentiation and Polarization: New Molecules and Patterns of Gene Expression. *The Journal of Immunology.* **177**, 7307-7311
- Matthews, V., Schuster, B., Schutze, S., Bussmeyer, I., Ludwig, A., Hundhausen, C., Sadowski, T., Saftig, P., Hartmann, D., Kallen, K.J. and Rose-John, S. (2003). Cellular cholesterol depletion triggers shedding of the human interleukin-6 receptor by ADAM10 and ADAM17 (TACE). *J Biol Chem.* **278**, 38829-38839
- Mauviel, A., Temime, N., Charron, D., Loyau, G. and Pujol, J.P. (1988). Interleukin-1 $\alpha$  and  $\beta$  induce interleukin-1 $\beta$  gene expression in human dermal fibroblasts. *Biochem Biophys Res Commun.* **156**, 1209-1214
- McClendon, A.K., Rodriguez, A.C. and Osheroff, N. (2005). Human topoisomerase II $\alpha$  rapidly relaxes positively supercoiled DNA: implications for enzyme action ahead of replication forks. *J Biol Chem.* **280**, 39337-45.

- McCool, K.W. and Miyamoto, S. (2012). DNA damage-dependent NF- $\kappa$ B activation: NEMO turns nuclear signalling inside out. *Immunol Rev.* **246**, 311-326
- McInnes, I.B. and Schett, G. (2007). Cytokines in the pathogenesis of rheumatoid arthritis. *Nature Reviews Immunology.* **7**, 429-442
- McInti, R.H., Morales, P.J., Petroff, M.G., Colonna, M. and Hunt, J.S. (2004). Recombinant HLA-G5 and -G6 drive U937 myelomonocytic cell production of TGF- $\beta$ 1. *J Leukoc Biol.* **76**, 1220-1228
- McNamara, S., Wang, H., Hanna, N. and Miller Jr, W. H. (2008). Topoisomerase II $\beta$  Negatively Modulates Retinoic Acid Receptor  $\alpha$  Function: a Novel Mechanism of Retinoic Acid Resistance. *Molecular and Cellular Biology.* **28**, 2066-2077.
- McNamara, S., Nichol, J.N., Wang, H. and Miller Jr, W.H. (2010). Targeting PKC  $\delta$ -mediated topoisomerase II $\beta$  overexpression subverts the differentiation block in a retinoic acid-resistant APL cell line. *Leukemia.* **24**, 729-739
- Means, T.K., Pavlovich, R.P., Roca, D., Vermeulen, M.W. and Fenton, M.J. (2000) Activation of TNF- $\alpha$  transcription utilizes distinct MAP kinase pathways in different macrophage populations. *J Leukoc Biol.* **67**, 885-893
- Melhelm, R.F., Strahler, J.R., Hailat, N., Zhu, X.X. and Hanash, S.M. (1991). Involvement of OP18 in cell proliferation. *Biochemical and Biophysical Research Communications.* **179**, 1649-1655
- Milavetz, B. I. (2002). SP1 and AP-1 Elements Direct Chromatin Remodeling in Chromosomes during the First 6 H of Infection. *Virology.* **294**, 170-179
- Miller, K.G., Liu, L.F. and England, P.T. (1981). A homogenous type II DNA topoisomerase from HeLa cell nuclei. *The Journal of Biological Chemistry.* **256**, 9334-9339
- Mirski, S.E., Sparks, K.E., Yu, Q., Lang, A.J., Jain, N., Campling, B.G. and Cole, S.P. (2000). A truncated cytoplasmic topoisomerase II $\alpha$  in a drug-resistant lung cancer cell line is encoded by a TOP2A allele with a partial deletion of exon 34. *Int J Cancer.* **85**, 534-539
- Mitchell, R.A., Liao, H., Chesney, J., Figerle-Rowson, G., Baugh, J., David, J. and Bucala, R. (2002). Macrophage migration inhibitory factor (MIF) sustains macrophage proinflammatory function by inhibiting p53: Regulatory role in the innate immune response. *PNAS.* **99**, 345-350



- Moelants, E.A.V., Mortier, A., Van Damme, J. and Proost, P. (2013). Regulation of TNF $\alpha$  with a focus on rheumatoid arthritis. *Immunology and Cell Biology*. 1-9
- Mogensen, T.H. (2009). Pathogen recognition and inflammatory signalling in innate immune defences. *Clin Microbiol Rev*. **22**, 240-273
- Monaco, G., Vigneti, E., Lancieri, M., Cornaglia-Ferraris, P., Lambertenghi-Delilieri, G. and Revoltella, R. (1982). Induction of Monocyte-Macrophage Differentia of Human Hematopoietic Cells (CM-S) by Phorbol Esters. *Cancer Research*. **42**, 4182
- Moo, A.L. and Wang, T.S. (1994). Down-regulation of genes encoding DNA replication proteins during cell cycle exit. *Cell Growth and Differentiation*. **5**, 485-494
- Montaudon, D., Pourquier, P., Denis, F., de Tinguy-Moreaud, E., Lagarde, P. and Robert, J. (1997). Differential stabilization of topoisomerase-II-DNA cleavable complexes by doxorubicin and etoposide in doxorubicin-resistant rat glioblastoma cell. *Eur J Biochem*. **245**, 307-315
- Moreland, J.G., Fuhrman, R.M., Pruessner, J.A. and Schwartz, D.A. (2002). CD11b and intercellular adhesion molecule-1 are involved in pulmonary neutrophil recruitment in lipopolysaccharide-induced airway disease. *Am J Respir Cell Mol Biol*. **27**, 474-480
- Moresco, E.M.Y., LaVine, D. and Beutler, B. (2011). Toll-lie receptors. *Current Biology*. **21**, R488-R493
- Morgan, S.E., Cadena, R.S., Raimondi, S.C. and Beck, W.T. (2000). Selection of Human Leukemic CEM Cells for Resistance to the DNA Topoisomerase II Catalytic Inhibitor ICRF-187 Results in Increased Levels of Topoisomerase II $\alpha$  and Altered G<sub>2</sub>/M Checkpoint and Apoptotic Responses. *Molecular Pharmacology*. **57**, 296-307
- Mosser, D. M. (2003). The many faces of macrophage activation. *Journal of Leukocyte Biology*. **73**,209-212
- Mosser, D.M. and Edwards, J.P. (2008). Exploring the full spectrum of macrophage activation. *Nat Rev Immunol*. **12**, 958-869

- Mullberg, J., Oberthur, W., Lottspeich, F., Mehl, E., Dittrich, E. and Graeve, L. (1994). The soluble human IL-6 receptor. Mutational characterization of the proteolytic cleavage site. *J Immunol.* **152**, 4958-4968
- Muñoz-Cánoves, P., Scheele, C., Pederson, B.K. and Serrano, A.L. (2013). Interleukin-6 myokine signaling in skeletal muscle: a double-edged sword, *FEBS J.* **280**, 4131-4148
- Murphy, A.J., Woollard, K.J., Hoang, A., Mukhamedova, N., Stirzaker, R.A., McCormick, S.P.A., Remaley, A.T., Sviridov, D. and Chin-Dusting, J. (2008). High-Density Lipoprotein Reduces the Human Monocyte Inflammatory Response. *Arteriosclerosis, Thrombosis, and Vascular Biology.* **28**, 2071-2077
- Muslimovic. A., Ismail, I.H., Gao, Y. and Hammarsten, O. (2008). An optimized method for measurement of  $\gamma$ -H2AX in blood mononuclear and cultured cells. *Nat Protoc.* **3**, 1187-1193
- Nakano, H., Yamazaki, T., Miyatake, S., Nozaki, N., Kikuchi, A. and Saito, T. (1996). Specific interaction of topoisomerase II $\beta$  and the CD3 epsilon chain of the T cell receptor complex. *J Biol Chem.* **271**, 6483-6489
- Namangala, B., De Baetselier, P., Noel, W., Brys, L. and Beschin, A. (2001). Alternative versus classical macrophage activation during experimental African trypanosomosis. *J Leukoc Biol.* **69**, 387-396
- Nelson, W.G., Liu, L.F. and Coffey, D.S. (1986). Newly replicated DNA is associated with DNA topoisomerase II in cultured rat prostatic adenocarcinoma cells. *Nature.* **322**, 187-189
- Neuner, P., Urbanski, A., Trautinger, F., Möller, A., Kirnbauer, R., Kapp, A., Schöpf, E., Schwarz, T. and Luger, T.A. (1991). Increased IL-6 production by monocytes and keratinocytes in patients with psoriasis. *J Invest Dermatol.* **97**, 27-33
- Newton, K. and Dixit, V.M. (2012). Signaling in Innate Immunity and Inflammation. *Cold Spring Harb Perspect Biol.* **4**, a006049
- Ngkelo, A., Meja, K., Yeadon, M., Adcock, I. and Kirkham, P.A. (2012). LPS induced inflammatory responses in human peripheral blood mononuclear cells is mediated through NOX4 and  $G_{i\alpha}$  dependent PI-3kinase signalling. *Journal of Inflammation.* **9**, doi: 10.1186/1476-9255-9-1

- Nishida, K., Seto, M. and Ishida, R. (2001). Different Susceptibilities of Postmitotic Checkpoint-proficient and –deficient Balb/3T3 Cells to ICRF-193, a Catalytic Inhibitor of DNA Topoisomerase II. *Jpn. J. Cancer Res.*, **92**, 193-202
- Nitiss, J.L. (2009). DNA topoisomerase II and its growing repertoire of biological functions. *Nature Reviews Cancer*. **9**(5), 327-337
- Nitiss, J.L. (2009). Targeting DNA topoisomerase II in cancer chemotherapy. *Nature Reviews Cancer*. **9**, 338-350
- Oeckinghaus, A. and Ghosh, S. (2009). The NF- $\kappa$ B family of transcription factors and its regulation. *Cold Spring Harb Perspect Biol*. **1**, a000034
- Oestergaard, V.H., Knudsen, B.R. and Andersen, A.H. (2004). Dissecting the cell-killing mechanism of the topoisomerase II-targeting drug ICRF-193. *J Biol Chem*. **279**, 28100-28105
- Okabe, T. and Yasukawa, K. (1990). A Human Monocyte Growth Factor Produced by Lung Cancer Cells. *Cancer Res*. **50**, 3863-3865
- Oliva, J.L., Caino, M.C., Senderowicz, A.M. and Kazanietz, M.G. (2008). S-Phase-specific activation of PKC $\alpha$  induces senescence in non-small cell lung cancer cells. *J Biol Chem*. **283**, 5466-5476
- O'Neill, L.A.J., Golenbock, D. and Bowie, A.G. (2013). The history of Toll-like receptors – redefining innate immunity. *Nat Rev Immunology*. **13**, 453 -460
- Oprea, A. and Kress, M. (2000). Involvement of the pro-inflammatory cytokines tumor necrosis factor- $\alpha$ , IL-1 $\beta$ , and IL-6 but not IL-8 in the development of heat hyperalgesia effects on heat evoked calcitonin gene-related peptide release from rat skin, *J Neurosci*. **20**, 6289-6293
- Ostuni, R. and Natoli, G. (2011). Transcriptional control of macrophage diversity and specialization. *Eur. J. Immunol*. **41**, 2470-2525
- Otte, A., Mandel, K., Reinstrom, G. and Hass, H. (2011). Abolished adherence alters signalling pathways in phorbol ester-induced human U937 cells. *Cell Communication and Signaling*. **9**, doi: 10.1186/1478-811X-9-20

Padget, K., Carr, R., Pearson, A.D., Tilby, M.J. and Austin, C.A. (2000). Camptothecin-stabilised topoisomerase I-DNA complexes in leukaemia cells visualised and quantified in situ by the TARDIS assay (trapped in agarose DNA immunostaining). *Biochem Pharmacol.* **59**, 629-638

Padget, K., Pearson, A.D. and Austin, C.A. (2000). Quantitation of DNA topoisomerase II $\alpha$  and  $\beta$  in human leukaemia cells by immunoblotting. *Leukemia*. **14**, 1997-2005

Padilla, P.I., Wada, A., Yahiro, K., Kimura, M., Niidome, T., Aoyagi, H., Kumatori, A., Anami, M., Hayashi, T., Fujisawa, J., Saito, H., Moss, J. and Hirayama, T. (2000). Morphologic Differentiation of HL-60 Cells Is Associated with Appearance of RPTP $\beta$  and Induction of *Helicobacter pylori* VacA Sensitivity. *J Biol Chem*. **275**, 15200-15206

Pahl, H.L., Rosmarin, A.G. and Tenen, D.G. (1992). Characterization of the myeloid-specific CD11b promoter. *Blood*. **79**, 865-870

Pahl, H.L., Scheibe, R.J., Zhang, D.E., Chen, H.M., Galson, D.L., Maki, R.A. and Tenen, D.G. (1993). The proto-oncogene PU.1 regulates expression of the myeloid specific CD11b promoter. *J Biol Chem*. **268**, 5014-5020

Papillon, J., Menetret, J.F., Batisse, C., Helye, R., Schultz, P., Potier, N. and Lamour, V. (2013). Structural insight into negative DNA supercoiling by DNA gyrase, a bacterial type 2A DNA topoisomerase. *Nucleic Acids Res*. **41**, 7815-7827

Park, I. and Avraham, H.K. (2006). Cell cycle-dependent DNA damage signalling induced by ICRF-193 involved ATM, ATR, CHK2, and BRCA1. *Exp Cell Res*. **312**, 1996-2008

Pastor, N., Dominguez, I., Orta, M.L., Campanella, C., Mateos, S. and Cortes, F. (2012). The DNA topoisomerase II catalytic inhibitor merbarone is genotoxic and induces endoreduplication. *Mutat Res*. doi: 10.1016/j.mrfmmm.2012.07.005

Patel, S., Jazrawi, E., Creighton, A.M., Austin, C.A. and Fisher, L.M. (2000). Probing the interaction of the cytotoxic bisdioxopiperazine ICRF-193 with the closed enzyme clamp of human topoisomerase II $\alpha$ . *Mol Pharmacol*. **58**, 560-568

Patel, J.R. and Brewer, G.J. (2008) Age-related differences in NF- $\kappa$ B translocation and Bcl/Bax ration caused by TNF $\alpha$  and A $\beta$ 42 promote survival in middle-age neurons and death in old neurons. *Exp Neurol*. **213**, 93-100

- Pederson, B.K. (2006). The anti-inflammatory effect of exercise: its role in diabetes and cardiovascular disease control. *Essays Biochem.* **42**, 105-117
- Per, S.R., Matte, M.R., Mirabelli, C.K., Drake, F.H., Johnson, R.K. and Crooke, S.T. (1987). Characterization of a subline of P388 leukemia resistant to amsacrine: evidence of altered topoisomerase II function. *Molecular Pharmacology.* **32**, 17-25
- Perez, C., Vilaboa, N.E., Garcia-Bermejo, L., de Blas, E., Creighton, A. and Aller, P. (1997). Differentiation of U-937 promonocytic cells by etoposide and ICRF-193, two antitumour DNA topoisomerase II inhibitors with different mechanisms of action. *Journal of Cell Science.* **110**, 337-343
- Perry, S.E., Mostafa, S.M., Wenstone, R., Shenkin, A. and McLaughlin, P.J. (2004). HLA-DR regulation and the influence of GM-CSF on transcription, surface expression and shedding. *Int J Med Sci.* **1**, 126-136
- Peterson, A.M.W. and Pederson, B.K. (2006). The Role of IL-6 in Mediating the Anti-Inflammatory Effects of Exercise. *Journal of Physiology and Pharmacology.* **57**, 43-51
- Petrov, P., Drake, F.H., Loranger, A., Huang, W. and Hancock, R. (1993). Localization of DNA Topoisomerase II in Chinese Hamster Fibroblasts by Confocal and Electron Microscopy. *Experimental Cell Research.* **204**, 73-81
- Pickup, J.C. (2004). Inflammation and activated innate immunity in the pathogenesis of type II diabetes. *Diabetes Care.* **27**, 813-823
- Polhaus, J.R., Kreuzer, K.N. (2005). Norfloxacin-induced DNA gyrase cleavage complexes block *Escherichia coli* replication forks, causing double-stranded breaks *in vivo*. *Mol Microbiol.* **56**, 1416-1429
- Pommier, Y., Orr, A., Kohn, K.W. and Riou, J. (1992). Differential Effects of Amsacrine and Epipodophyllotoxins on Topoisomerase II Cleavage in the Human *c-myc* Protooncogene. *Cancer Research.* **52**, 3125
- Pommier, Y., Capranico, G., Orr, A. and Kohn, K.W. (1991). Local base sequence preferences for DNA cleavage by mammalian topoisomerase II in the presence of amsacrine or teniposide. *Nucleic Acids Research.* **19**, 5973-5980

Pope, R., Mung, S., Liu, H. and Thimmapaya, B. (2000). Regulation of TNF $\alpha$  Expression in Normal Macrophages: The Role of C/EBP $\beta$ . *Cytokine*. **12**, 1171-1181

Potapova, O., Basu, S., Mercola, D. and Holbrook, N.J. (2001). Protective role for c-Jun in the cellular response to DNA damage. *J Biol Chem*. 276, 28546-28553

Poyet, J., Srinivasula, S.M., Lin, J., Fernandes-Alnemri, T., Yamaoka, S., Tsichlis, P.N. and Alnemri, E.S. (2000). Activation of the I $\kappa$ B Kinases by RIP via IKK $\gamma$ / NEMO-mediated Oligomerization. *The Journal of Biological Chemistry*. 275, 37966-37977

Punchard, N.A., Whelan, C.J. and Adcock, I. (2004). The Journal of Inflammation. *J Inflamm (Lond)*. **1**,1

Qi, X., Hou, S., Lepp, A., Li, R., Basirs, Z., Lou, Z. and Chen, G. (2011). Phosphorylation and stabilization of topoisomerase II $\alpha$  protein by p38 $\gamma$  mitogen-activated protein kinase sensitize breast cancer cells to its poisons. *J Biol Chem*. **286**, 35883-35890

Ramamoorthy, M., Tadokoro, T., Rybanska, I., Ghosh, A.K., Wersto, R., May, A., Kulikowicz, T., Sykora, P., Croteau D.L. and Bohr, V.A. (2012). RECQL5 cooperates with Topoisomerase II $\alpha$  in DNA decatenation and cell cycle progression. *Nucleic Acids Res*. 40, 1621-1635

Ramirez-Carrozzi, V.R., Nazarian, A.A., Li, C.C., Gore, S.L., Sridharan, R., Imbalzano, A.N. and Smale, S.T. (2006). Selective and antagonistic functions of SWI/SNF and Mi-2 $\beta$  nucleosome remodeling complexes during an inflammatory response. *Genes Dev*. **20**, 282–296

Rattner, J.B., Hendzel, M.J., Furbee, C.S., Muller, M.T. and Bazett-Jones, D.P. (1996). Topoisomerase II $\alpha$  Is Associated with the Mammalian Centromere in a Cell Cycle- and Species-specific Manner and Is Required for Proper Centromere/Kinetochore Structure. *The Journal of Cell Biology*. **134**, 1097-1107

Reimann, T., Büscher, D., Hipskind, R.A., Krautwald, S., Lohmann-Matthes, M.L. and Baccarini, M. (1994). Lipopolysaccharide induces activation of the Raf-1/MAP kinase pathway. A putative role for Raf-1 in the induction of the IL-1 $\beta$  and the TNF- $\alpha$  genes. *The Journal of Immunology*. **153**, 5740-5749

- Reith, W., LeibundGut-landmann, S. and Waldburger, J.-M. (2005) .Regulation of MHC class II gene expression by the class II transactivator. *Nat. Rev.* **5**, 793–806
- Reitman, M. and Felsenfeld, G. (1990). Developmental Regulation of Topoisomerase II Sites and Dnase I-Hypersensitive Sites in the Chicken  $\beta$ -Globin Locus. *Mol Cell Biol.* **10**, 2774-2786
- Rey-Giraud, F., Hafner, M. and Ries, C.H (2012). In Vitro Genreation of Monocyte-Derived Macrophages under Serum-Free Conditions Improves Their Tumor Promoting Functions. *PLoS One.* **7**, e42656
- Rich, A. and Zhang, S. (2003). Z-DNA: the long road to biological function. *Nature Reviews Genetics.* **4**, 566-572
- Rider, P., Carmi, Y., Voronoc, E. and Apte, R.N. (2013). Interleukin-1 $\alpha$ . *Semin Immunol.* **25**, 430-8
- Ritke, M.K., Allan, W.P., Fattman, C., Gunduz, N.N. and Yalowich, J.C. (1994). Reduced phosphorylation of topoisomerase II in etoposide-resistant human leukemia K562 cells. *Mol Pharamcol.* **46**, 58-66
- Roca, J. and Wang, J.C. (1992). The capture of a DNA double helix by an ATP-dependent protein clamp: a key step in DNA transport by type II DNA topoisomerases. *Cell.* **71**, 833-840
- Roca, J., Berger, J.M. and Wang, J.C. (1993). On the simultaneous binding of eukaryotiv DNA topoisomerase II to a pair of double-stranded DNA helices. *J Biol Chem.* **268**, 14250-14255
- Roca, J., Ishida, R., Berger, J.M., Andoh, T. and Wang, J.C. (1994). Antitumor bisdioxopiperazines inhibit yeast DNA topoisomerase II by trapping the enzyme in the form of a closed protein clamp. *Proc Natl Acad Sci USA.* **91**,1781–1785
- Roca, J., Berger, J.M., Harrison, S.C. and Wang, J.C. (1996). DNA transport by a type II topoisomerase: direct evidence for a two-gate mechanism. *Proc Natl Acad Sci.* **93**, 4057-4062
- Rodriguez, A.A., Makris, A., Wu, M.F., Rimawi, M., Froehlich, A., Dave, B., Hilsenbeck, S.G., Chamness, G.C., Lewis, M.T., Dobrolecki, L.E., Jain, D., Sahoo, S., Osborne, C.K. and Chang, J.C. (2010). DNA repair signature is associated with anthracycline response in triple negative breast cancer patients. *Breast Cancer Res Treat.* **123**, 189-196

- Rogers, A. and Eastell, R. (2001). The effect of 17 $\beta$ -estradiol on production of cytokines in cultures of peripheral blood. *Bone*. **29**, 30-34
- Roger, T., Miconnet, I., Schiesser, A., Kai, H., Miyake, K. and Calandra, T. (2005). Critical role for Ets, AP-1 and GATA-like transcription factors in regulating mouse Toll-like receptor 4 (*Tlr4*) gene expression. *Biochem J*. **387**, 355-365
- Roman, J., Ritzenthaler, J.D., Fenton, M.J., Roser, S. and Schuyler, W. (2000). Transcriptional regulation of the human interleukin-1 $\beta$  gene by fibronectin: role of protein kinase C and activator protein 1 (AP-1). *Cytokine*. **12**, 1581-1596
- Rose-John, S., Waetzig, G.H. and Scheller, J., Grotzinger, J., Seegert, D. (2007). The IL-6/sIL-6R as a novel target for therapeutic approaches. *Expert Opin Ther Targets*. **11**, 613-624
- Rose-John, S. (2012). The biology of interleukin-6 in the 21<sup>st</sup> century. *Semin Immunol*. **26**, 1
- Rosenbloom, K.R., Sloan, C.A., Malladi, V.S., Dreszer, T.R., Learned, K., Kirkup, V.M., Wong, M.C., Maddren, M., Fang, R., Heitner, S.G., Lee, B.T., Barber, G.P., Harte, R.A., Diekhans, M., Long, J.C., Wilder, S.P., Zweig, A.S., Karolchik, D., Kuhn, R.M., Haussler, D., Kent, W.J. (2013) [ENCODE data in the UCSC Genome Browser: year 5 update](#). *Nucleic Acids Res*. **41**(Database issue), D56-63
- Rutledge, R.G. and Cote, C., (2003). Mathematics of quantitative kinetic PCR and the application of standard curves. *Nucleic Acids Research*. **31**, e93
- Saccani, S., Panyano, S. and Natoli, G. (2001). Two waves of Nuclear Factor  $\kappa$ B Recruitment to Target Promoters. *The Journal of Experimental Medicine*. **193**, 1351-1360
- Sancéau, J., Kaisho, T., Hirano, T. and Wietzerbin, J. (1995). Triggering of the human interleukin-6 gene by interferon- $\gamma$  and tumor necrosis factor- $\alpha$  in monocytic cells involves cooperation between interferon regulatory factor-1, NF- $\kappa$ B, and Sp1 transcription factors. *J Biol Chem*. **270**, 27920-27931
- Sano, K., Miyaji-Yamaguchi, M., Tsutsui, K.M. and Tsutsui, K. (2008). Topoisomerase II $\beta$  Activates a Subset of Neuronal Genes that Are Repressed In AT-Rich Genomic Environment. *PLoS One*, **3**, e4103



- Sauter, K.A.D., Wood, L.J., Wong, J., Iordanoc, M. and Magun, B.E. (2011). Doxorubicin and daunorubicin induce processing and release of interleukin-1 $\beta$  through activation of the NLRP3 inflammasome. *Cancer Biol Ther.* **11**, 1008-1016
- Scheller, J. and Rose-John, S. Interleukin-6 and its receptor: from bench to bedside. *Med Microbio Immunol.***195**, 173-183
- Scheller, J., Chalaris, A., Schmidt-Arras, D. and Rose-John, S. (2011). The pro- and anti-inflammatory properties of the cytokine interleukin-6. *Biochimica et Biophysica Acta-Molecular Cell Research.* **1813**, 878-888
- Schilling, D., Beissert, T., Fenton, M.J. and Nixdorff, K. (2001). Negative regulation of IL-1 $\beta$  production at the level of transcription in macrophages stimulated with LPS. *Cytokine.* **16**, 51-61
- Schindlbeack, C., Mayr, D., Olivier, C., Rack, B., Engelstaedter, V., Jueckstock, J., Jenderek, C., Andergassen, U., Jeschke, U. and Friese, K. (2010). Topoisomerase II $\alpha$  expression rather than gene amplification predicts responsiveness of adjuvant anthracycline-based chemotherapy in women with primary breast cancer. *J Cancer Res Clin Oncol.* **136**, 1029-1037
- Schneider, E., Hutchins, A.M., Darkin, S.J., Lawson, P.A., Ralph, R.K. (1988). Relationship between sensitivity to 4'-(9-acridinylamino)methanesulfon-m-anisidide and DNA topoisomerase II in a cold-sensitive cell-cycle mutant of a murine mastocytoma cell line. *Biochim Biophys Acta.* **951**, 85-97
- Schneider, T.D., Lawson, P.A., Ralph, R.K. (1989). Inhibition of protein synthesis reduces the cytotoxicity of 4'-(9-acridinylamino)methanesulfon-m-anisidide without affecting DNA breakage and DNA topoisomerase II in a murine mastocytoma cell line. *Biochem Pharmacol.* **38**, 263-269
- Schoeffler, A.J. and Berger, J.M. (2008). DNA topoisomerases: harnessing and constraining energy to govern chromosome topology. *Q Rev Biophys.* **41**, 41-101
- Scott, A.J., O'Dea, K.P., O'Callaghan, D., Williams, L., Dokpesi, J.O., Tatton, L., Handy, J.M., Hogg, P.J. and Takata, M. (2011). Reactive Oxygen Species and p38 Mitogen-activated Protein Kinase Mediate Tumor Necrosis Factor  $\alpha$  -Converting Enzyme (TACE/ADAM-17) Activation in Primary Human Monocytes. *J Biol Chem.* **286**, 35466-35476

- Sehested, M., Wessel, I., Jensen, L.H., Holm, B., Oliveri, R.S., Kenwrick, S., Creighton, A.M., Nitiss, J.L. and Jensen, P.B. (1998). Chinese hamster ovary cells resistant to the topoisomerase II catalytic inhibitor ICRF-159: a Tyr49Phe mutation confers high-level resistance to bisdioxopiperazines. *Cancer Res.* **58**, 1460-1468
- Seong, S. and Matzinger, P. (2004). Hydrophobicity: an ancient damage-associated molecular pattern that initiates innate immune responses. *Nature Reviews Immunology.* **4**, 469–478
- Shapiro, P.S., Whalen, A.M., Tolwinski, N.S., Wilsbacher, J., Froelich-Ammon, S.J., Garcia, M., Osheroff, N. and Ahn, N.G. (1999). Extracellular Signal-Regulated Kinase Activates Topoisomerase II $\alpha$  through a Mechanism Independent of Phosphorylation. *Mol Cell Biol.* **19**, 3551-3560
- Sharif, O., Bolshakov, V.N., Raines, S., Newham, P. and Perkins, N.D. (2007). Transcriptional profiling of the LPS induced NF- $\kappa$ B response in macrophages. *BMC Immunology.* **8**, doi:10.1186/1471-2172-8-1
- Shelley, C.S., Teodoridis, J.M., Park, H., Farokhzad, O.C., Bottinger, E.P. and Arnaout, M.A. (2002). During differentiation of the monocytic cell line U937, Pur  $\alpha$  mediates induction of the CD11c  $\beta$ 2 integrin gene promoter. *J Immunol.* **168**, 3887-3893
- Shen, H. and Pervaiz, S. (2006). TNF receptor superfamily-induced cell death: redox-dependent execution. *The FASEB Journal.* **20**, 1589-1598
- Shibolet, O. and Podolsky, D.K. (2007). TLRs in the Gut. IV. Negative regulation of Toll-like receptors and intestinal homeostasis: addition by subtraction. *Am J Physiol Gastrointest Liver Physiol.* **292**, G1469-1473
- Siddiqui, H., Solomon, D.A., Gunawardena, R.W., Wang, Y. and Knudsen, E.S. (2003). Histone deacetylation of RB-responsive promoters: requisite for specific gene repression but dispensable for cell cycle inhibition. *Mol Cell Biol.* **23**, 7719-7731
- Smith, P.K., Krohn, R.I., Hermanson, G.T., Mallia, A.K., Gartner, F.H., Provenzano, M.D., Fujimoto, E.K., Goeke, N.M., Olson, B.J., Klenk, D.C (1985). Measurement of protein using bichinchoninic acid. *Anal Biochem.* **150**, 76-85

- Solovyan, V.T., Bezvenyuk, Z.A., Salminen, A., Austin, C.A., Courtney, M.J. (2002) The Role of Topoisomerase II in the Excision of DNA Loop Domains during Apoptosis. *The Journal of Biological Chemistry*. **277**, 21458-21467
- Song, L., Zhang, Z., Gräsfeder, L.L., Boyle, A.P., Giresi, P.G., Lee, B.K., Sheffield, N.C., Gräf, S., Huss, M., Keefe, D., Liu, Z., London, D., McDaniel, R.M., Shibata, Y., Showers, K.A., Simon, J.M., Vales, T., Wang, T., Winter, D., Zhang, Z., Clarke, N.D., Birney, E., Iyer, V.R., Crawford, G.E., Lieb, J.D. and Furey, T.S. (2011). Open chromatin defined by DNaseI and FAIRE identifies regulatory elements that shape cell-type identity. *Genome Res*. **21**, 1757-1767
- Song, J.H., Kweon, S.H. and Kim, T.S. (2012). High TOP2B/TOP2A expression ratio at diagnosis correlates with favourable outcome for standard chemotherapy in acute myeloid leukaemia. *British Journal of Cancer*. **107**, 108-115
- Spooren, A., Kolmus, K., Laureys, G., Clinckens, R., De Keyser, J., Haegeman, G. and Gerlo, S. (2011). Interleukin-6, a mental cytokine. *Brain Research Reviews*. **67**, 157-183
- Stanley, A.C. and Lacy, P. (2010) Pathways for cytokine secretion. *Physiology*. **25**, 218-229
- Stewart, L., Redinbo, M.R., Qiu, X., Hol, W.G. and Champoux, J.J. (1998). A Model for the Mechanism of Human Topoisomerase I. *Science*. **279**, 1534-1541
- Stewart, G.S., Wang, B., Bignell, C.R., Taylor, A.M. and Elledge, S.J. (2003). MDC1 is a mediator of the mammalian DNA damage checkpoint. *Nature*. **421**, 961-966
- Stivers, J.T. (1997). Vaccinia DNA Topoisomerase I: Evidence Supporting a Free Rotation Mechanism for DNA Supercoil Relaxation. *Biochemistry*. **36**, 5212-5222
- Sundstrom, C and Nilsson, K. (1976). Establishment and characterization of a human histiocytic lymphoma *Int. J. Cancer* **17**, 565-577.
- Suzan, M., Salaun, D., Neuveut, C., Spi B., Hirsch, I., Le Bouteiller, P., Querat, G. and Si, J. (1991). Induction of NF- $\kappa$ B during monocyte differentiation by HIV type 1 infection. *J Immunol*. **146**, 377-383
- Suzuki, T., Hashimoto, S., Toyoda, N., Nagai, S., Yamazaki, N., Dong, H.Y., Sakai, J., Yamashita, T., Nukiwa, T. and Matsushima, K. (2000). Comprehensive gene expression profile of LPS-stimulated human monocytes by SAGE. *Blood*. **7**, 2584-2591

- Takashiba, S., Van Dyke, T.E., Amar, S., Murayama, Y., Soskolne, A.W. and Shapira, L. (1999). Differentiation of Monocytes to Macrophages Primes Cells for Lipopolysaccharide Stimulation via Accumulation of Cytoplasmic Nuclear Factor  $\kappa$ B. *Infect Immun.* **67**, 5573-5578
- Takeda, K., Kaisho, T. and Akira, S. (2003). Toll-like receptors. *Annu Rev Immunol.* **21**, 335-376
- Takemori, H., Kajimura, J. and Okamoto, M. (2007). TORC-SIK cascade regulated CREB activity through the basic leucine zipper domain. *FEBS Journal.* **274**, 3202-3209
- Tammaro, M., Barr, P., Ricci, B. and Yan, H. (2013). Replication-Dependent and Transcription-Dependent Mechanisms of DNA Double-Strand Break Induction by the Topoisomerase 2-Targeting Drug Etoposide, *PLoS ONE.* **8**, e79202
- Tan, K.B., Dorman, T.E., Falls, K.M., Chung, T.D., Mirabelli, C.K., Crooke, S.T. and Mao, J. (1992). Topoisomerase II $\alpha$  and topoisomerase II $\beta$  genes: characterization and mapping to human chromosomes 17 and 3, respectively. *Cancer Res.* **52**, 231-234
- Tang, D., Kang, R., Coyne, C.B., Zeh, H.J. and Lotze, M.T. (2012). PAMPs and DAMPs: signals that spur autophagy and immunity. *Immunol Rev.* **249**, 158-175
- Teixeira, C., Stang, S. L., Zheng, Y., Beswick, N.S. and Stone, J.C. (2003). Interfration of DAG signalling systems mediated by PKC dependent phosphorylation of RasGRP3. *Blood.* **102**, 1414-1420
- Thakurela, S., Garding, A., Jung, J., Schubeler, D., Burger, L. and Tiwari, V.K. (2013). Gene regulation and priming by topoisomerase II $\alpha$  in embryonic stem cells. *Nat Commun.* **4**, 2478
- Thurman, R.E., Rynes, E., Humbert, R., Vierstra, J., Maurano, M.T., Haugen, E., Sheffield, N.C., Stergachis, A.B., Wang, L., Vernot, B., Garg, K., John, S., Sandstrom, R., Bates, D., Boatman, L., Canfield, T.K., Diegel, M., Dunn, D., Ebersol, A.K., Frum, T., Giste, E., Johnson, A.K., Johnson, E.M., Kutayavin, T., Lajoie, B., Lee, B.K., Lee, K., London, D., Lotakis, D., Neph, S., Neri, F., Nguyen, E.D., Qu, H., Reynolds, A.P., Roach, V., Safi, A., Sanchez, M.E., Sanyal, A., Shafer, A., Simon, J.M., Song, L., Vong, S., Weaver, M., Yan, J., Zhang, Z., Zhang, Z., Lenhard, B., Tewari, M., Dorschner, M.O., Hansen, R.S., Navas, P.A., Stamatoyannopoulos, G., Iyer, V.R., Lieb, J.D., Sunyaev, S.R., Akey, J.M., Sabo, P.J., Kaul, R., Furey, T.S., Dekker, J., Crawford, G.E., and Stamatoyannopoulos, J.A. (2012). The accessible chromatin landscape

of the human genome. *Nature*. **489**, 75-82.

Tiwari, V.K., Burger, L., Nikolettou, V., Deogracias, R., Thakurela, S., Wirbelauer, C., Kaut, J., Terranova, R., Hoerner, L., Mielke, C., Boege, F., Murr, R., Peters, A.H. Barde, Y.A. and Schubeler, D. (2012). Target genes of Topoisomerase II $\beta$  regulate neuronal survival and are defined by their chromatin state. *Proc Natl Acad Sci*. **109**, E934-943

To, K.K.W., Polgar, O., Huff, L.M., Morsaki, K. and Bates, S.E. (2008). Histone Modifications at the ABCG2 Promoter following Treatment with Histone Deacetylase Inhibitor Mirror Those in Multidrug-Resistant Cells. *Mol Cance Res*. **6**, 151-164

Tominaga, K., Kirikae, T. and Nakano, M. (1997). Lipopolysaccharide (LPS)-induced IL-6 production by embryonic fibroblasts isolated from LPS-responsive and LPS-hyporesponsive mice. *Mol Immunol*. **34**, 1147-1156

Toyoda, E., Kagaya, S., Cowell, I.G., Kurosaw, A., Kanmohita, K., Nishikawa, K., Iizumi, S., Koyama, H., Austin, C.A. & Adachi, N. (2008). NK314, a topoisomerase II inhibitor that specifically targets the  $\alpha$  isoform. *J Biol Chem*. **283**, 23711-23720

Trao K., Zirkin, B., Thimmulappa, R.K., Biswal, S. and Trush, M.A. (2012). Upregulation of TLR1, TLR2, TLR4, and IRAK-2 expression during ML-1 Cell Differentiation to Macrophages: Role in the Potentiation of Cellular Responses to LPS and LTA. *IRN Oncology*. **2012**, 1-10

Trede, N.S., Tsytsykova, A.V., Chatila, T., Goldfeld, A.E. and Geha, R.S. (1995) Transcriptional activation of the human TNF- $\alpha$  promoter by superantigen in human monocytic cells: role of NF- $\kappa$ B. *J Immunol*. **155**, 902-908

Triantafyllou, M. and Triantafyllou, K. (2004). heat-shock protein 70 and heat-shock protein 90 associate with Toll-like receptor 4 in response to bacterial lipopolysaccharide. *Biochem Soc Trans*. **32**, 636-639

Tsai, S., Valkov, N., Yang, W., Gump, J., Sullivan, D. and Seto, E. (2000). Histone deacetylase interacts directly with DNA topoisomerase II. *Nature Genetics*. **26**, 349-353.

Tsujioka, H., Imanishi, T., Ikejima, H., Kuroi, A., Takarada, S., Tanimoto, T., Kitabata, H., Okochi, K., Arita, Y., Ishibashi, K., Komukai, K., Kataiwa, H., Nakamura, N., Hirata, K., Tanaka, A. and Akasaka, T. (2009). Impact of heterogeneity of human peripheral blood monocyte subsets on myocardial salvage in patients with primary acute myocardial infarction. *J Am Coll Cardiol*. **54**, 130-138

- Tsutsui, K., Tsutsui, K., Sano, K., Kikuchi, A. and Tokunaga, A. (2001). Involvement of DNA Topoisomerase II $\beta$  in Neuronal Differentiation. *The Journal of Biological Chemistry*. **276**, 5769-5778.
- Uemura, T., Ohkura, H., Adachi, Y., Morino, K., Shizaki, K. and Yanagida, M. (1987). DNA topoisomerase II is required for condensation and separation of mitotic chromosomes in *S.pombe*. *Cell*. **50**, 917-925
- Valledor, A.F., Borrás, F.E., Culléll-Young, M. and Celada, A. (1998). Transcription factors that regulate monocyte/macrophage differentiation. *J Leukoc Biol*. **63**, 405-417
- Valledor, A.F., Xaus, J., Marques, L. and Celada, A. (1999). Macrophage colony-stimulating factor induces the expression of mitogen-activated protein kinase phosphatase-1 through a protein kinase C-dependent pathway. *J Immunol*. **163**, 2452-2462
- van Furth, R., Raeburn, J.A. and van Zwet, T.L. (1979). Characteristics of human mononuclear phagocytes. *Blood*. **54**, 485-500
- Varecha, M., Potesilova, M., Matula, P. and Kozubek, M. (2012). Endonuclease G interacts with histone H2B and DNA topoisomerase II $\alpha$  during apoptosis. *Mol Cell Biochem*. **363**, 301-307
- Vasselon, T. and Detmers, P.A. (2002). Toll Receptors: a Central Element in Innate Immune Responses. *Infect Immun*. **70**, 1033-1041
- Vejpongsa, P. and Yeh, E.T. (2014). Topoisomerase 2 $\beta$ : a promising molecular target for primary prevention of anthracycline-induced cardiotoxicity. *Clin Pharmacol Ther*. **95**, 45-52
- Verdrengh, M., Isaksson, O. and Tarkowski, A. (2005). Topoisomerase II inhibitors, irrespective of their chemical composition, ameliorate experimental arthritis. *Rheumatology*. **44**, 183-186
- Volkova, M. and Russell, R. (2011). Anthracycline cardiotoxicity: prevalence, pathogenesis and treatment. *Curr Cardiol Rev*. **7**, 214-220
- Wajant, H., Pfizenmaier, K. and Scheurich, P. (2003). Tumor necrosis factor signalling. *Cell Death Differ*. **10**, 45-65

- Wall, M. K., Mitchenall, L. A. and Maxwell, A. (2004). Arabidopsis thaliana DNA gyrase is targeted to chloroplasts and mitochondria. *Proc Natl Acad Sci.* **101**, 7821-7826
- Wang, Q., Zambetti, G.P. and Suttle, D.P. (1997). Inhibition of DNA topoisomerase II $\alpha$  gene expression by the p53 tumor suppressor. *Mol Cell Biol.* **17**, 389-397
- Wang, Y., Guo, H., Chen, C. and Ho, S. (2006). Staurosporine Modulates Radiosensitivity and Radiation-Induced Apoptosis in U937 cells. *International Journal of Radiation Biology.* **82**, 97-109
- West, K.L. and Austin, C.A. (1999). Human DNA topoisomerase II $\beta$  binds and cleaves four-way junction DNA *in vitro*. *Nucleic Acids Res.* **27**, 984-992
- Willmore, E., Frank, A.J., Padget, K., Tilby, M.J. and Austin, C.A. (1998). Etoposide Targets Topoisomerase II $\alpha$  and II $\beta$  in Leukemic Cells: Isoform-Specific Cleavable Complexes Visualized and Quantified *In Situ* by a Novel Immunofluorescence Technique. *Molecular Pharmacology.* **54**, 78-85
- Woessner, R.D., Mattern, M.R., MirabelLi, C.K., Johnson, R.K. and Drake, F.H. (1991). Proliferation- and cell cycle-dependent differences in expression of the 170 kilodalton and 180 kilodalton forms of topoisomerase II in NIH-3T3 cells. *Cell Growth Differ.* **4**, 209-214
- Wongchana, W. and Palaga, T. (2012). Direct regulation of interleukin-6 expression by Notch signaling in macrophages. *Cell Mol Immunol.* **9**, 155-162
- Wozniak, A.J. and Ross, W.E. (1983). DNA damage as a basis for 4'-demethylepipodophyllotoxin-9-(4,6-O-ethylidene- $\beta$ -D-glucopyranoside) (etoposide) cytotoxicity. *Cancer Res.* **43**, 120-124
- Wu, J. and Liu, L.F. (1997). Processing of topoisomerase I cleavable complexes into DNA damage by transcription. *Nucleic Acids Res.* **2**, 4181-4186.
- Wu, C., Li, T., Farh, L., Lin, L., Lin, T., Yu, Y., Yen, T., Chiang, C., Chan, N. (2011). Structural Basis of Type II Topoisomerase Inhibition by the Anticancer Drug Etoposide. *Science.* **333**, 459-462
- Willmore, E., Frank, A.J., Padget, K., Tilby, M.J. and Austin, C.A., (1998) Etoposide Targets Topoisomerase II $\alpha$  and II $\beta$  in Leukemic Cells: Isoform-Specific Cleavable Complexes

Visualized and Quantified In Situ by a Novel Immunofluorescence Technique. *Molecular Pharmacology*. **54**, 78-85

Woessner, R.D., Chung, T.D., Hofmann, G.A., Mattern, M.R., Mirabelli, C.K., Drake, F.H. and Johnson, R.K. (1990). Differences between normal and ras-transformed NIH-3T3 cells in expression of the 170kD and 180kD forms of topoisomerase II. *Cancer Res.* **50**, 2901-2908

Woessner, R.D., Mattern, M.R., Mirabelli, C.K., Johnson, R.K. and Drake, F.H. (1991). Proliferation- and cell cycle-dependent differences in expression of the 170 kilo Dalton and 180 kilo Dalton forms of topoisomerase II in NIH-3T3 cells. *Cell Growth Differ.* **2**, 209-14.

Xiao, H., Mao, Y., Desai, S.D., Zhou, N., Ting, C.Y., Hwang, J. and Liu, L.F. (2003). The topoisomerase II $\beta$  circular clamp arrests transcription and signals a 26S proteasome pathway. *Proc Natl Acad Sci.* **100**, 3239-3244

Xiao, W., Hodge, D.R., Wang, L., Yang, X., Zhang, X. and Farrar, W.L. (2004). Co-operative functions between nuclear factors NF- $\kappa$ B and CCAT/enhancer-binding protein-  $\beta$  (C/EBP- $\beta$ ) regulate the IL-6 promoter in autocrine human prostate cancer cells. *Prostate.* **61**, 354-370

Xie, W., Shao, N., Ma, X., Ling, B., Wei, Y., Ding, Q., Yang, G., Liu, N., Wang, H. and Chen, K. (2006). Bacterial endotoxin lipopolysaccharide induces up-regulation of glyceraldehyde-3-phosphate dehydrogenase in rat liver and lungs. *Life Sci.* **79**, 1820-1827

Yamazaki, S., Muta, T. and Takeshige, K. (2001). A novel I $\kappa$ B protein, I $\kappa$ B-zeta, induced by proinflammatory stimuli, negatively regulates nuclear factor  $\kappa$ B in the nuclei, *J Biol Chem.* **276**, 27657-27662

Yan, Z. (2006). Regulation of TLR4 is a Tale About Tail. *Arteriosclerosis, Thrombosis, and Vascular Biology.* **26**, 2582-2584

Yang, L., Wold, M.S., Li, J.J., Kelly, T.J. and Liu, L.F. (1987). Roles of DNA topoisomerases in simian virus 40 DNA replication in vitro. *Proc Natl Acad Sci.* **84**, 950-954

Yang, X., Li, W., Prescott, E.D., Burden, S.J. and Wang, J.C. (2000). DNA topoisomerase II $\beta$  and neural development. *Science.* **287**, 131-134



- Yoshida, K., Yamaguchi, T., Shinagawa, H., Taira, N., Nakayama, K.I. and Miki, Y. (2006). Protein kinase C delta activates topoisomerase II $\alpha$  to induce apoptotic cell death in response to DNA damage. *Mol Cell Biol.* **26**, 3414-3431
- Zaman, G., Sunter, A., Galea, G.L., Javaheri, B., Saxon, L.K., Moustafa, A., Armstrong, V.J., Price, J.S. and Lanyon, L.E. (2012). Loading-related regulation of transcription factor EGR2/Krox-20 in bone cells is ERK1/2 protein-mediated and prostaglandin, Wnt signalling pathway -, and insulin-like growth factor-I axis-dependent. *J Biol Chem.* **287**, 3946-3962
- Zarembek, K.A. and Godowski, P.J. (2002). Tissue expression of human Toll-like receptors and differential regulation of Toll-like receptor mRNAs in leukocytes in response to microbes, their products, and cytokines. *J Immunol.* **168**, 554-561
- Zechiedrich, E.L. and Osheroff, N. (1990). Eukaryotic topoisomerases recognize nucleic acid topology by preferentially interacting with DNA crossovers. *EMBO J.* **9**, 4555-4562
- Zhang, G. and Ghosh, S. (2001). Toll-like receptor-mediated NF- $\kappa$ B activation: a phylogenetically conserved paradigm in innate immunity. *J Clin Invest.* **107**, 13-19
- Zhang, J.M. and An, J. (2007). Cytokines, Inflammation and Pain. *Int Anesthesiol Clin.* **45**, 27-37
- Zhang, J., Cho, S., Shu, L., Yan, W., Guerrero, T., Kent, M., Skorupski, K., Chen, H. and Chen, X. (2011). Translational repression of p53 by RNPC1 a p53 target overexpressed in lymphomas. *Genes & Dev.* **25**, 1528-1543
- Zhang, Y., Guo, F., Yingdong, N. and Zhao, R. (2013). LPS-induced inflammation in the chicken is associated with CCAAT/enhancer binding protein  $\beta$ -mediated fat mass and obesity associated gene down-regulation in the liver but not hypothalamus. *BMC Vet Res.* **9**, 257
- Zhao, K., Li, X., Zhao, Q., Huang, Y., Li, D., Peng, Z., Shen, W., Zhao, J., Zhou, Q., Chen, Z., Sims, P.J., Wiedmer, T. and Chen, G. (2004). Protein Kinase C delta mediates retinoic acid and phorbol myristate acetate-induced phospholipid scramblase 1 gene expression: its role in leukemic cell differentiation. *Blood.* **104**, 3731-3738

Zhao, L., Ye, P. and Gonda, T.J. (2013). The MYB proto-oncogene suppresses monocytic differentiation of acute myeloid leukemia cells via transcriptional activation of its target gene GFI1. *Oncogene*. doi:10.1038/onc.2013.419

Zhou, H., Liao, J., Aloor, J., Nie, H., Wilson, B.C., Fessler, M.B., Gao, H.M. and Hong, J.S. (2013). Cd11b/CD18 (Mac-1) is a novel surface receptor for extracellular double-stranded RNA to mediate cellular inflammatory responses. *J Immunol*. **190**, 115-125

Zhu, J., Zhang, J., Xiang, D., Zhang, Z., Zhang, L., Wu, M., Zhu, S., Zhang, R. and Han, W. (2010). Recombinant human interleukin-1 receptor antagonist protects mice against acute doxorubicin-induced cardiotoxicity. *Eur J Pharmacol*. **643**, 247-253

Zini, N., Santi, S., Ognibene, A., Bavelloni, A., Neri, L.M., Valmori, A., Mariani, E., Negri, C., Astaldi-Ricotti, G.C. and Maraldi, N.M. (1994). Discrete Localization of Different DNA Topoisomerases in HeLa and K562 Cell Nuclei and Subnuclear Fractions. *Experimental Cell Research*. **210**, 336-348

Zuklys, K.L., Szer, I.S. and Szer, W. (1991). Autoantibodies to DNA topoisomerase II in juvenile rheumatoid arthritis. *Clin Exp Immunol*. **84**, 245-249

Zwelling, L.A., Chan, D., Hinds, M., Mayes, J., Silberman, L.E. and Blick, M. (1988). Effect of phorbol ester treatment on drug-induced, topoisomerase II-mediated DNA cleavage in human leukemia cells. *Cancer Res*. **48**, 6625-6633

Zwelling, L.A., Hinds, M., Chan, D., Altschuler, E., Mayes, J. and Zipf, T.F. (1990). Phorbol ester effects on topoisomerase II activity and gene expression in HL-60 human leukemia cells with different proclivities toward monocytoid differentiation. *Cancer Res*. **50**, 7116-7122

## Appendix A

---

$$\text{Efficiency} = 10^{-(1/\text{slope})}$$

$$\text{For example, efficiency of Topo II}\alpha \text{ (Fig 4.4a)} = 10^{-(1/-3.335)}$$

$$= 1/-3.335 = -0.2999$$

$$= 10^{(0.299)}$$

$$= 1.991$$

$$= (1.991 - 1) \times 100 = 99.1\% \text{ (Efficiency of Primer)}$$

### **Figure A.1 Calculating the Efficiency of Primers.**

The calculations used in this flow diagram are based on the published method of efficiency calculation by Rutledge & Côté (2003).

Table A.1 p values from Figure 4.3

<b>Isoform</b>	<b>p value</b>
<b><math>\alpha</math></b>	0.0002 ***
<b><math>\beta</math></b>	0.0008 ***

Table A.2 p values from Figure 4.4

<b>Isoform</b>	<b>p value</b>
<b><math>\alpha</math></b>	0.049 *
<b><math>\beta</math></b>	0.0018 **

Table A.3 p values from Figure 4.7

<b>Isoform</b>	<b>p value</b>
<b><math>\alpha</math></b>	-
<b><math>\beta</math></b>	0.016 *

Table A.4 p values from Figure 4.8

<b>Treatment</b>	<b>p value</b>
<b>No PMA</b>	0.084
<b>PMA</b>	0.015 *

Table A.5 p values from Figure 4.12

<b>Isoform</b>	<b>p value</b>
<b><math>\alpha</math></b>	0.047 *
<b><math>\beta</math></b>	0.11

Table A.6 p values from Figure 4.13

<b>Isoform</b>	<b>p value</b>
<b><math>\alpha</math></b>	0.0005 ***
<b><math>\beta</math></b>	0.005 **



Table A.7 p values from  
Figure 4.14

VP-16 concentration (uM)	p value
0.01	0.39
0.1	0.91
1	0.007**
2.5	0.015**
5	<0.0001** *
7.5	<0.0001** *
10	<0.0001** *

Table A.8 p values from  
Figure 4.15

VP-16 concentration (uM)	p value
0.01	0.6
0.1	0.1
1	0.0001** *
2.5	0.005**
5	0.005**
7.5	0.02*
10	0.007**

Table A.9 p values from  
Figure 4.16a Co-treat vs  
non-PMA

VP-16 concentration (uM)	p value
0.01	0.26
0.1	0.55
1	0.84
2.5	0.26
5	0.15
7.5	0.26
10	0.11

Table A.10 p values from  
Figure 4.16a Co-treat vs  
PMA

VP-16 concentration (uM)	p value
0.01	0.17
0.1	0.63
1	0.05*
2.5	0.07
5	0.004**
7.5	0.016*
10	0.005**

Table A.11 p values from  
Figure 4.16b Co-treat vs  
non-PMA

VP-16 concentration (uM)	p value
0.01	0.89
0.1	0.69
1	0.0001** *
2.5	0.005**
5	0.005**
7.5	0.024*
10	0.007**

Table A.12 p values from  
Figure 4.16b Co-treat vs  
PMA

VP-16 concentration (uM)	p value
0.01	0.74
0.1	0.11
1	0.001**
2.5	0.005**
5	0.01**
7.5	0.04*
10	0.066

Table A.13 p values from Figure 4.17	
ICRF-193 concentration (uM)	p value
0.001	0.85
0.01	0.42
0.02	0.43
0.04	0.27
0.06	0.27
0.08	0.23
0.1	0.16
1	0.04
2.5	0.001**
5	0.003**
7.5	0.01**

Table A.14 p values from Figure 4.18	
ICRF-193 concentration (uM)	p value
0.001	0.17
0.01	0.01**
0.02	0.32
0.04	0.15
0.06	0.23
0.08	0.2
0.1	0.5
1	<0.0001***
2.5	0.0001***
5	0.0003**
7.5	0.006**

Table A.15 p values from Figure 4.19	
ICRF-187 concentration (ug/ml)	p value
0.0001	0.52
0.001	0.36
0.01	0.37
0.1	0.23
1	0.1
5	0.005**
10	0.05*
20	0.006**

Table A.16 p values from Figure 4.20	
ICRF-187 concentration (ug/ml)	p value
0.0001	0.06
0.001	0.49
0.01	0.004**
0.1	0.07
1	0.006**
5	0.0006**
10	0.006**
20	0.005**



**Figure A.2 Western blot probed for GAPDH as loading control – Figure 4.11a.**

The nitrocellulose blot presented in Figure 4.11a was stripped as described in material and methods Section 2.16 and probed with an antibody raised to GAPDH. See Table 2.2 for antibody details and Section 2.16.7 for probing method. The samples are in the same position as indicated in Figure 4.11a.



**Figure A.3 Western blot probed for GAPDH as loading control – Figure 4.11b.**

The nitrocellulose blot presented in Figure 4.11b was stripped as described in material and methods Section 2.16 and probed with an antibody raised to GAPDH. See Table 2.2 for antibody details and Section 2.16.7 for probing method. The samples are in the same position as indicated in Figure 4.11b.



**Figure A.4 Western blot probed for GAPDH as loading control – Figure 4.12a.**

The nitrocellulose blot presented in Figure 4.12a was stripped as described in material and methods Section 2.16 and probed with an antibody raised to GAPDH. See Table 2.2 for antibody details and Section 2.16.7 for probing method. The samples are in the same position as indicated in Figure 4.12a.



**Figure A.5 Western blot probed for GAPDH as loading control – Figure 4.12b.**

The nitrocellulose blot presented in Figure 4.12b was stripped as described in material and methods Section 2.16 and probed with an antibody raised to GAPDH. See Table 2.2 for antibody details and Section 2.16.7 for probing method. The samples are in the same position as indicated in Figure 4.12b.



## Appendix B

Table B.1 p values for Figure 5.3		Table B.2 p values for Figure 5.4		Table B.3 p values for Figure 5.5		Table B.4 values for Figure 5.13	
ICRF-193 pre-treatment (h)	p value	ICRF-193 pre-treatment (h)	p value	ICRF-193 pre-treatment (h)	p value	ICRF-193 pre-treatment (h)	p value
2	0.566	2	0.02*	2	0.15	2	0.15
4	0.32	4	0.53	4	0.97	4	0.92
6	0.3	6	0.76	6	0.94	6	0.49
24	0.78	24	0.76	24	0.5	24	0.56
48	0.37	48	0.42	48	0.11	48	0.02*
72	0.7	72	0.94	72	0.01	72	0.015*

Table B.5 p value from Figure 5.6		Table B.6 p value from Figure 5.7		Table B.7 p value from Figure 5.8		Table B.8 p value from Figure 5.9	
ICRF-193 treatment (h)	p value	ICRF-193 treatment (h)	p value	ICRF-193 treatment (h)	p value	ICRF-193 treatment (h)	p value
6	0.79	6	0.16	6	0.38	6	0.47
72	0.12	72	0.29	72	0.85	72	0.85
Table B.9 p value from Figure 5.10a		Table B.10 p value from Figure 5.10b		Table B.11 p value from Figure 5.11		Table B.12 p value from Figure 5.16	
ICRF-193 treatment (h)	p value	ICRF-193 treatment (h)	p value	ICRF-193 treatment (h)	p value	ICRF-193 concentration (uM)	p value
6	0.46	6	0.38	6	0.1	1	0.37
72	0.77	72	0.42	72	0.8	150	0.47
Table B.13 p value from Figure 5.17		Table B.14 p value from Figure 5.18		Table B.15 p value from Figure 5.19			
ICRF-193 concentration (uM)	p value	ICRF-193 concentration (uM)	p value	ICRF-193 concentration (uM)	p value		
1	0.36	1	0.71	1	0.09		
150	0.48	150	0.47	150	0.02		

Table B.16 p values from  
Figure 5.20a

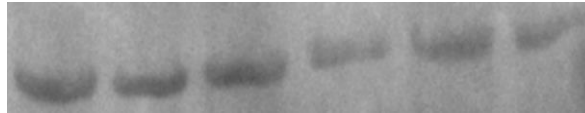
LPS concentration (ng/ml)	p value
0.1	0.95
1	0.08
5	<0.0001

Table B.17 p values from  
Figure 5.20b

LPS concentration (ng/ml)	p value
0.1	0.69
1	0.62
5	0.36



**Figure B.1 Western blot probed for GAPDH as loading control- Figure 5.1a.** The nitrocellulose blot presented in Figure 5.1a was stripped as described in material and methods Section 2.16 and probed with an antibody raised to GAPDH. See Table 2.2 for antibody details and Section 2.16.7 for probing method. The samples are in the same position as indicated in Figure 5.1a.



**Figure B.2 Western blot probed for GAPDH as loading control- Figure 5.1b.** The nitrocellulose blot presented in Figure 5.1b was stripped as described in material and methods Section 2.16 and probed with an antibody raised to GAPDH. See Table 2.2 for antibody details and Section 2.16.7 for probing method. The samples are in the same position as indicated in Figure 5.1b.

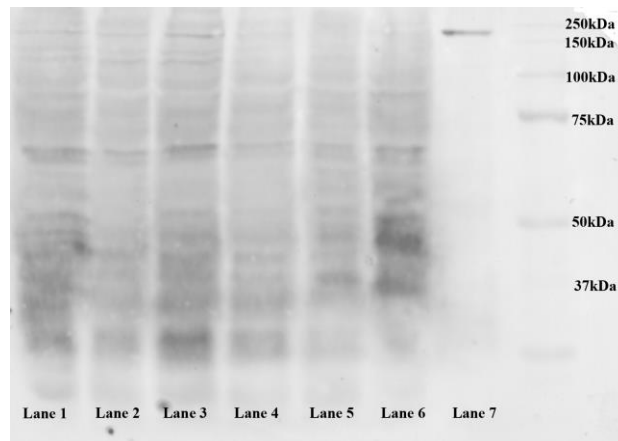


**Figure B.3 Western blot probed for Topoisomerase II $\beta$**  Samples prepared for this blot are as follows, Lane 1; 6 h pre-treatment with 0.1% DMSO (v/v), followed by 72 h treatment with 0.1% DMSO (v/v). Lane 2; 6 h pre-treatment with 0.1% DMSO (v/v) followed by 72 h treatment with 5 ng/ml PMA and 10 ng/ml LPS. Lane 3; 6 h pre-treatment with 1 nM ICRF-193 followed by 72 h treatment with 0.1% DMSO (v/v). Lane 4; 6 h pre-treatment with 1 nM ICRF-193 followed by 72h treatment with 5 ng/ml PMA and 10 ng/ml LPS. Lane 5; 72 h co-treatment 150 nM ICRF-193, 5 ng/ml PMA and 10 ng/ml LPS. Lane 6; 72 h co-treatment 0.1% DMSO (v/v), 5 ng/ml PMA and 10 ng/ml LPS. Lane 7; Recombinant topo II $\beta$ . Cells were harvested by cell scraping and whole cell lysates were prepared as described in Section 2.16.1. 31.9 $\mu$ g of whole protein was loaded onto a 10% SDS-PAGE gel, electrophoresis, western blotting and probing was performed as described in Section 2.16.

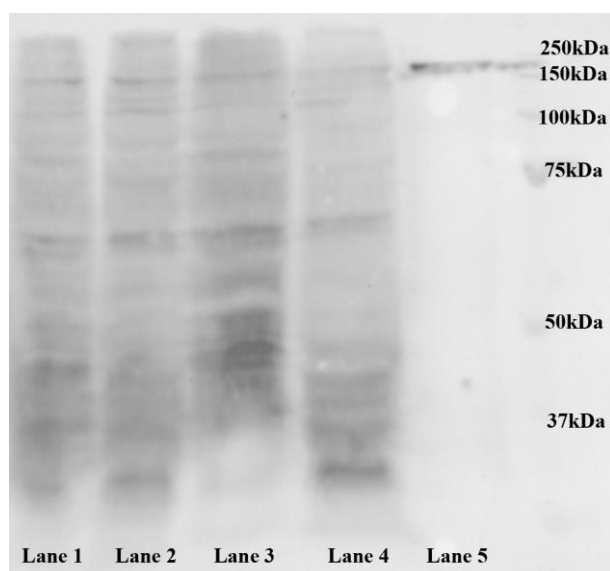


**Figure B.4 Western blot probed for Topoisomerase II $\beta$  – 72 h 1 nM ICRF-193 pre-treatment.**

Samples prepared for this blot were as followed; Lane 1; 72 hour pre-treatment with 0.1% DMSO (v/v) followed by 72 h treatment with 0.1% DMSO (v/v). Lane 2; 72 h pre-treatment with 0.1% DMSO (v/v) followed by 72 h treatment with 5 ng/ml PMA and 10 ng/ml LPS. Lane 3; 72 h pre-treatment with 1 nM ICRF-193 followed by 72 h treatment with 0.1% DMSO (v/v). Lane 4; 72 h pre-treatment with 1 nM ICRF-193 followed by 72 h treatment with 5 ng/ml PMA and 10ng/LPS. Lane 5; Recombinant topo II $\beta$ . Cells were harvested by cell scraping and whole cell lysates were prepared as described in Section 2.16.1. 31.9 $\mu$ g of whole protein was loaded onto a 10% SDS-PAGE gel, electrophoresis, western blotting and probing was performed as described in Section 2.16.



**Figure B.5 Western blot probed for GAPDH as loading control- Figure 5.14.**

The nitrocellulose blot presented in Figure 5.14 was stripped as described in material and methods Section 2.16 and probed with an antibody raised to GAPDH. See Table 2.2 for antibody details and Section 2.16.7 for probing method. The samples are in the same position as indicated in Figure 5.14.



**Figure B.6 Western blot probed for GAPDH as loading control- Figure 5.21.**

The nitrocellulose blot presented in Figure 5.21 was stripped as described in material and methods Section 2.16 and probed with an antibody raised to GAPDH. See Table 2.2 for antibody details and Section 2.16.7 for probing method. The samples are in the same position as indicated in Figure 5.21



**Figure B.7 Western blot probed for GAPDH as loading control- Figure 5.22a.** The nitrocellulose blot presented in Figure 5.22a was stripped as described in material and methods Section 2.16 and probed with an antibody raised to GAPDH. See Table 2.2 for antibody details and section 2.16.7 for probing method. The samples are in the same position as indicated in Figure 5.22a.



**Figure B.8 Western blot probed for GAPDH as loading control- Figure 5.22b.** The nitrocellulose blot presented in Figure 5.22b was stripped as described in material and methods Section 2.16 and probed with an antibody raised to GAPDH. See Table 2.2 for antibody details and Section 2.16.7 for probing method. The samples are in the same position as indicated in Figure 5.22b.

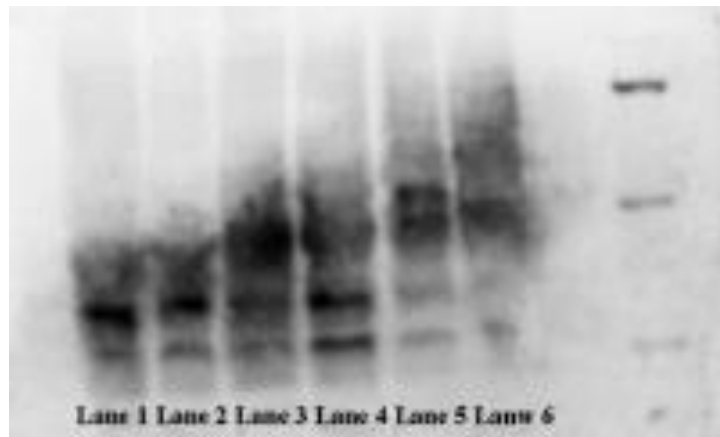


**Figure B.9 Western blot probed for TNF $\alpha$  (whole blot from Figure 5.14)** Samples prepared for this blot are as follows, Lane 1; 6 h pre-treatment with 0.1% DMSO (v/v), followed by 72 h treatment with 0.1% DMSO (v/v). Lane 2; 6 h pre-treatment with 0.1% DMSO (v/v) followed by 72 h treatment with 5 ng/ml PMA and 10 ng/ml LPS. Lane 3; 6 h pre-treatment with 1 nM ICRF-193 followed by 72 h treatment with 0.1% DMSO (v/v). Lane 4; 6 h pre-treatment with 1 nM ICRF-193 followed by 72h treatment with 5 ng/ml PMA and 10 ng/ml LPS. Lane 5; 72 h co-treatment 150 nM ICRF-193, 5 ng/ml PMA and 10 ng/ml LPS. Lane 6; 72 h co-treatment 0.1% DMSO (v/v), 5 ng/ml PMA and 10 ng/ml LPS. Please note Lanes 3 & 4 are denoted as Lanes 1 and 2 in Figure 5.14.

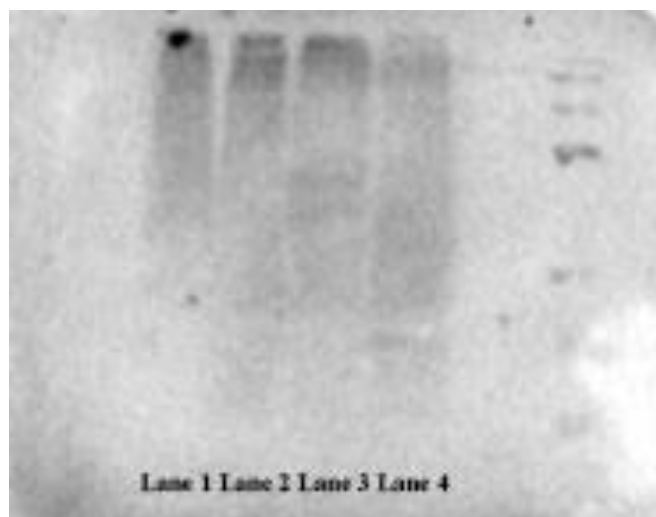


**Figure B.10 Western blot probed for TNF $\alpha$  – 72 h 1 nM ICRF-193 pre-treatment**  
 Samples prepared for this blot were as followed; Lane 1; 72 hour pre-treatment with 0.1% DMSO (v/v) followed by 72 h treatment with 0.1% DMSO (v/v). Lane 2; 72 h pre-treatment with 0.1% DMSO (v/v) followed by 72 h treatment with 5 ng/ml PMA and 10 ng/ml LPS. Lane 3; 72 h pre-treatment with 1 nM ICRF-193 followed by 72 h treatment with 0.1% DMSO (v/v). Lane 4; 72 h pre-treatment with 1 nM ICRF-193 followed by 72 h treatment with 5 ng/ml PMA and 10ng/LPS. Cells were harvested by cell scraping and whole cell lysates were prepared as described in Section 2.16.1. 31.9 $\mu$ g of whole protein was loaded onto a 10% SDS-PAGE gel, electrophoresis, western blotting and probing was performed as described in Section 2.16.



**Figure B.11 Western blot probed for GAPDH as loading control- Figure B.8.**  
 The nitrocellulose blot presented in Figure B.12 was stripped as described in material and methods Section 2.16 and probed with an antibody raised to GAPDH. See Table 2.2 for antibody details and Section 2.16.7 for probing method. The samples are in the same position as indicated in Figure B.12.



**Figure B.12 Western blot probed for topoisomerase II $\beta$**   
 Wild type and topo II $\beta$  -/- mouse embryonic fibroblasts were grown to confluency and harvested using trypsin (Section 2.9). Whole cell lysates were prepared as described in Section 2.16.7 25.7 $\mu$ g of whole protein was then loaded onto a SDS-PAGE gel, electrophoresis, western blotting and probing were performed as described in section 2.16. The band on the left is wild type sample and the lack of band on the right is the topo II $\beta$  -/- sample.

## Appendix C

Table C.1 p values from Figure 6.5

No LPS vs LPS	p value (Primer pair 1)	p value (Primer pair 2)	p value (Primer pair 3)	p value (Primer pair 4)
3535	0.8	0.45	0.38	0.43
AcH <sub>3</sub>	0.11	0.11	0.08	-

Table C.2 p values from Figure 6.6

3535 vs GFP	p value (Primer pair 1)	p value (Primer pair 2)	p value (Primer pair 3)	p value (Primer pair 4)
No LPS	0.74	0.48	0.49	0.98
LPS	0.76	0.98	0.13	0.21

Table C.3 p values from Figure 6.6

GFP vs AcH <sub>3</sub>	p value (Primer pair 1)	p value (Primer pair 2)	p value (Primer pair 3)	p value (Primer pair 4)
No LPS	0.09	0.17	0.09	0.32
LPS	0.01	0.02	0.007	-

Table C.4 p values from Figure 6.5

3535 vs AcH <sub>3</sub>	p value (Primer pair 1)	p value (Primer pair 2)	p value (Primer pair 3)	p value (Primer pair 4)
No LPS	0.06	0.69	0.92	0.29
LPS	0.012	0.019	0.0075	-



Table C.5 p values from Figure 6.6

3535 vs GFP	p value (Primer pair 1)	p value (Primer pair 2)	p value (Primer pair 3)	p value (Primer pair 4)
No LPS	0.74	0.72	0.54	0.45
LPS	0.28	0.015	0.24	0.36

Table C.7 p values from Figure 6.6

GFP vs AcH <sub>3</sub>	p value (Primer pair 1)	p value (Primer pair 2)	p value (Primer pair 3)	p value (Primer pair 4)
No LPS	0.14	0.09	0.36	0.23
LPS	0.14	0.09	0.36	0.23

Table C.6 p values from Figure 6.6

No LPS vs LPS	p value (Primer pair 1)	p value (Primer pair 2)	p value (Primer pair 3)	p value (Primer pair 4)
3535	0.36	0.38	0.38	0.68
AcH <sub>3</sub>	0.04	0.13	0.25	0.37

Table C.8 p values from Figure 6.6

3535 vs AcH <sub>3</sub>	p value (Primer pair 1)	p value (Primer pair 2)	p value (Primer pair 3)	p value (Primer pair 4)
No LPS	0.34	0.3	0.84	0.91
LPS	0.002	0.01	0.048	0.25

## Appendix D

### ELSEVIER LICENSE TERMS AND CONDITIONS

Aug 29, 2014

This is a License Agreement between Ashleigh Roythorne ("You") and Elsevier ("Elsevier") provided by Copyright Clearance Center ("CCC"). The license consists of your order details, the terms and conditions provided by Elsevier, and the payment terms and conditions.

**All payments must be made in full to CCC. For payment instructions, please see information listed at the bottom of this form.**

Supplier	Elsevier Limited The Boulevard, Langford Lane Kidlington, Oxford, OX5 1GB, UK
Registered Company Number	1982084
Customer name	Ashleigh Roythorne
Customer address	60 East View Newcastle Upon Tyne, NE13 6EE
License number	3456080786119
License date	Aug 25, 2014
Licensed content publisher	Elsevier
Licensed content publication	Trends in Molecular Medicine
Licensed content title	Signaling to NF- $\kappa$ B by Toll-like receptors
Licensed content author	Taro Kawai, Shizuo Akira
Licensed content date	November 2007
Licensed content volume number	13
Licensed content issue number	11
Number of pages	10
Start Page	460
End Page	469
Type of Use	reuse in a thesis/dissertation
Portion	figures/tables/illustrations
Number of figures/tables/illustrations	1
Format	both print and electronic
Are you the author of this Elsevier article?	No
Will you be translating?	No
Title of your thesis/dissertation	Exploring the role of topoisomerase II beta in macrophage maturation and pro-inflammatory cytokine production

Expected completion date	Sep 2014
Estimated size (number of pages)	300
Elsevier VAT number	GB 494 6272 12
Permissions price	0.00 GBP
VAT/Local Sales Tax	0.00 GBP / 0.00 GBP
Total	0.00 GBP

## OXFORD UNIVERSITY PRESS LICENSE TERMS AND CONDITIONS

Aug 29, 2014

---

This is a License Agreement between Ashleigh Roythorne ("You") and Oxford University Press ("Oxford University Press") provided by Copyright Clearance Center ("CCC"). The license consists of your order details, the terms and conditions provided by Oxford University Press, and the payment terms and conditions.

**All payments must be made in full to CCC. For payment instructions, please see information listed at the bottom of this form.**

License Number	3456081217273
License date	Aug 25, 2014
Licensed content publisher	Oxford University Press
Licensed content publication	Nucleic Acids Research
Licensed content title	The why and how of DNA unlinking:
Licensed content author	Zhirong Liu, Richard W. Deibler, Hue Sun Chan, Lynn Zechiedrich
Licensed content date	02/01/2009
Type of Use	Thesis/Dissertation
Institution name	None
Title of your work	Exploring the role of topoisomerase II beta in macrophage maturation and pro-inflammatory cytokine production
Publisher of your work	n/a
Expected publication date	Sep 2014
Permissions cost	0.00 GBP
Value added tax	0.00 GBP
Total	0.00 GBP
Total	0.00 GBP

## NATURE PUBLISHING GROUP LICENSE TERMS AND CONDITIONS

Aug 29, 2014

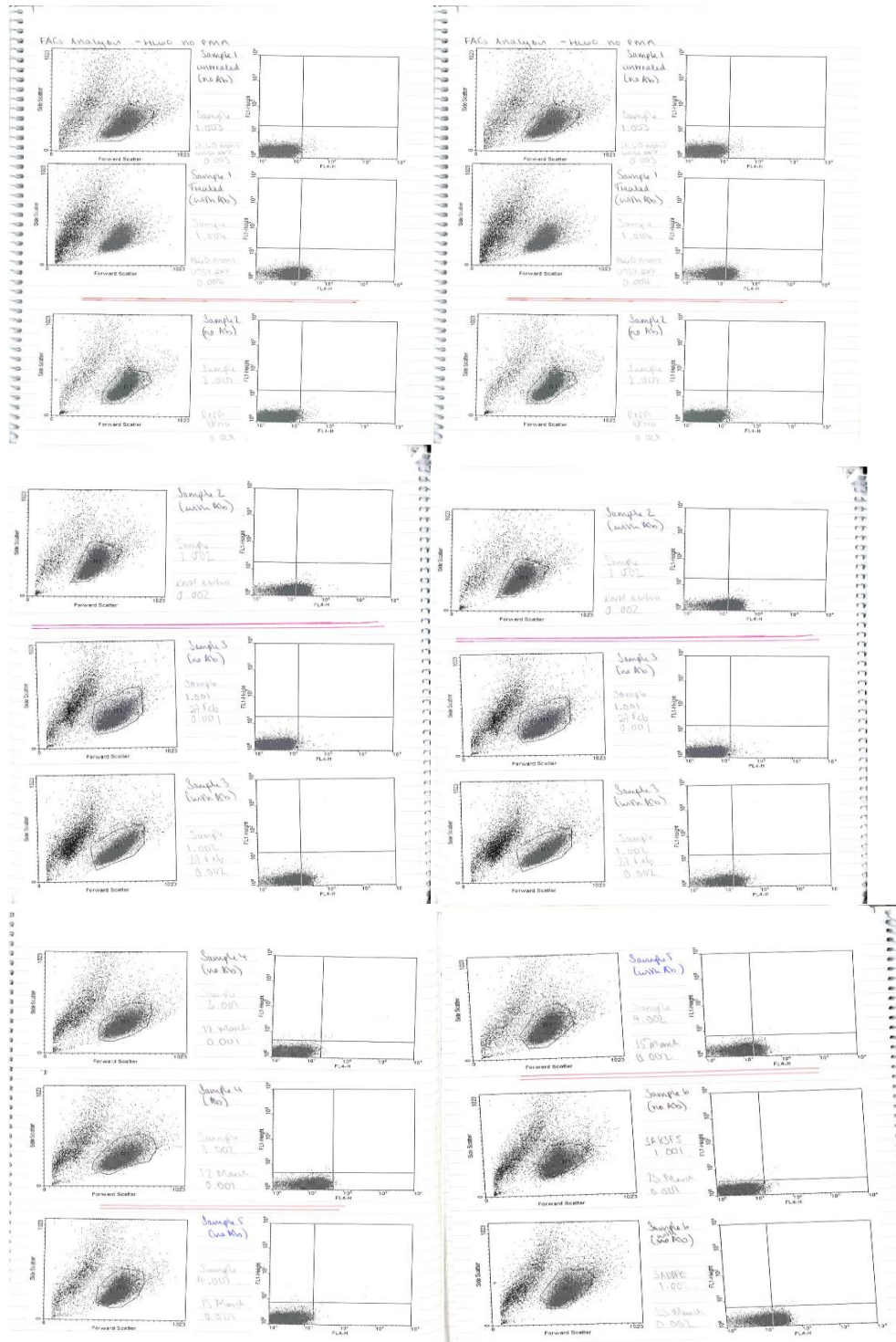
---

This is a License Agreement between Ashleigh Roythorne ("You") and Nature Publishing Group ("Nature Publishing Group") provided by Copyright Clearance Center ("CCC"). The license consists of your order details, the terms and conditions provided by Nature Publishing Group, and the payment terms and conditions.

**All payments must be made in full to CCC. For payment instructions, please see information listed at the bottom of this form.**

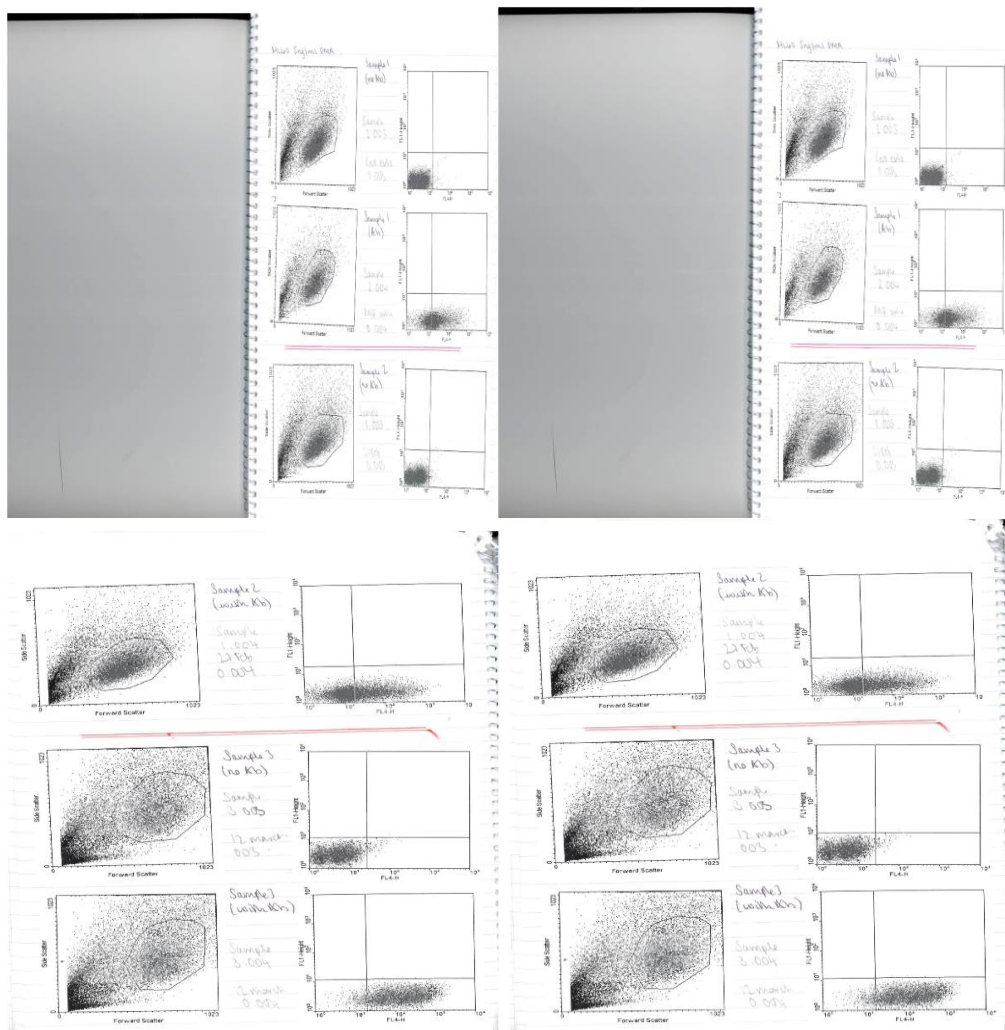
License Number	3456081468226
License date	Aug 25, 2014
Licensed content publisher	Nature Publishing Group
Licensed content publication	Nature Reviews Cancer
Licensed content title	DNA topoisomerase II and its growing repertoire of biological functions
Licensed content author	John L. Nitiss
Licensed content date	Apr 20, 2009
Volume number	9
Issue number	5
Type of Use	reuse in a dissertation / thesis
Requestor type	academic/educational
Format	print and electronic
Portion	figures/tables/illustrations
Number of figures/tables/illustrations	2
High-res required	no
Figures	Figure 1 and 2
Author of this NPG article	no
Your reference number	None
Title of your thesis / dissertation	Exploring the role of topoisomerase II beta in macrophage maturation and pro-inflammatory cytokine production
Expected completion date	Sep 2014
Estimated size (number of pages)	300

0.00 GBP



# **Figure D.1 Scatter graphs for HL-60 cells (non-PMA treated) after flow cytometry using and antibody to CD11b**

Cells were seeded at  $3 \times 10^5$  cells/ml and treated with 0.1% DMSO for 72 h. Cells were then harvested and washed before being probed with an antibody to CD11b – conjugated to APC. Flow cytometry was then performed, and the resulting scatter graphs (FL4-H is the channel of the flow cytometer capable of detecting and APC signal) are shown in this figure. The top left scatter graph is the control set of cells that were not treated with antibody. The other five scatter graphs depict the results of non-PMA treated HL-60 cells when probed with an antibody to CD11b.



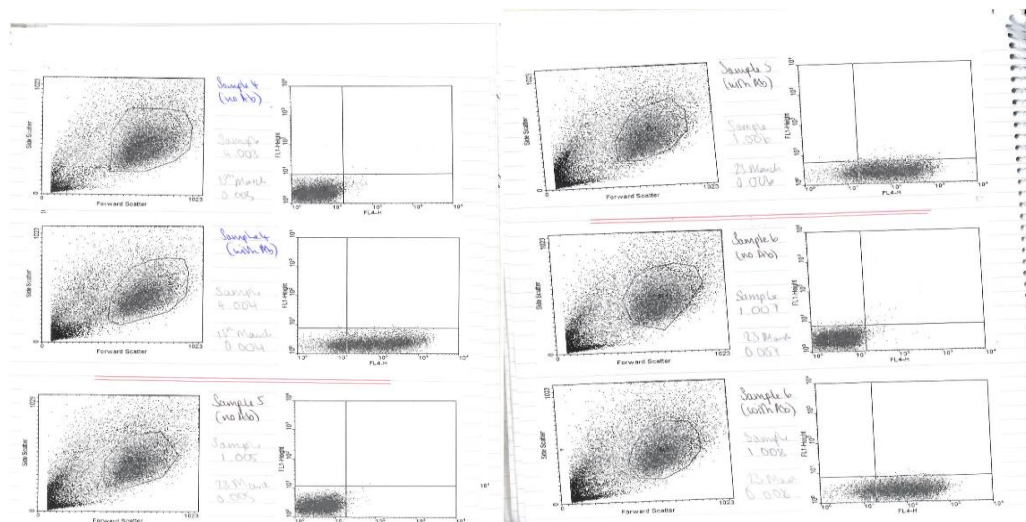


**Figure D.2 Scatter graphs for HL-60 cells (PMA treated) after flow cytometry using and antibody to CD11b.**

Cells were seeded at  $3 \times 10^5$  cells/ml and treated with 5ng/ml PMA for 72 h. Cells were then harvested and washed before being probed with an antibody to CD11b – conjugated to APC. Flow cytometry was then performed, and the resulting scatter graphs (FL4-H is the channel of the flow cytometer capable of detecting and APC signal) are shown in this figure. The top left scatter graph is the control set of cells that were not treated with antibody. The other five scatter graphs depict the results of PMA treated HL-60 cells when probed with an antibody to CD11b.